Ukrainian Food Journal

Volume 14, Issue 3 2025

Куіv Київ 2025 Ukrainian Food Journal is an international scientific periodical journal that publishes articles by specialists in the field of food science, engineering and technology, chemistry, economics and management.

Ukrainian Food Journal — міжнародне наукове періодичне видання для публікації результатів досліджень фахівців у галузі харчової науки, техніки та технології, хімії, економіки і управління.

Ukrainian Food Journal is abstracted and indexed by scientometric databases:

Ukrainian Food Journal індексується наукометричними базами:

Index Copernicus (2012) EBSCO (2013) Google Scholar (2013) UlrichsWeb (2013) CABI full text (2014)

Online Library of University of Southern Denmark (2014)
Directory of Open Access scholarly Resources (ROAD) (2014)
European Reference Index for the Humanities and the Social Sciences (ERIH PLUS)
(2014)

Directory of Open Access Journals (DOAJ) (2015) InfoBase Index (2015)

Chemical Abstracts Service Source Index (CASSI) (2016) FSTA (Food Science and Technology Abstracts) (2018) Web of Science (Emerging Sourses Citaton Index) (2018) Scopus (2022)

Ukrainian Food Journal включено у перелік наукових фахових видань України з технічних наук, категорія А (Наказ Міністерства освіти і науки України № 358 від 15.03.2019)

Editorial office address:

National University of Food Technologies 68 Volodymyrska str. Kyiv 01601, Ukraine

Адреса редакції:

Національний університет харчових технологій вул. Володимирська, 68 Київ 01601, Україна

e-mail: ufj_nuft@meta.ua

© NUFT, 2025

© HYXT, 2025

Ukrainian Food Journal is an open-access, peer-reviewed scientific journal published by the National University of Food Technologies (Kyiv, Ukraine). The journal accepts original research articles, short communications, review papers, news, and literature reviews across all areas of food science, including food technology, engineering, nutrition, food chemistry, economics, and management.

Manuscripts must present novel findings, demonstrate a clear connection to food science, and be of broad interest to the international scientific community.

Topics covered by the journal include:

- Food engineering
- Food chemistry
- Food microbiology
- Food quality and safety
- Food processes
- Automation of food processes
- Food packaging
- Economics
- Food nanotechnologies
- Economics and management

Please note that the journal does not consider the following types of submissions:

Articles containing medical claims or involving studies on humans or animals, as these topics fall outside the journal's scope.

Articles lacking scientific novelty or significance, including those focused solely on solving routine practical or engineering problems.

Ukrainian Food Journal is published quarterly, with four issues released each year in March, June, September, and December.

Reviewing a Manuscript for Publication

Upon receiving a manuscript, the Editor-in-Chief first evaluates its content to ensure it aligns with the journal's scope. The Editor-in-Chief also reviews the article's formatting, style, and illustrative materials, may offer recommendations for improvement, and decides whether to forward the manuscript for peer review.

All manuscripts submitted to the Ukrainian Food Journal undergo a double-blind peer review process. Each submission is reviewed by at least two independent experts: one member of the Editorial Board and one reviewer who is external to both the Editorial Board and the publisher. This ensures an objective and balanced evaluation of the manuscript's scientific quality.

The full Guide for Authors is available on our website:

http://ufj.nuft.edu.ua

International Editorial Board

Editor-in-Chief:

Olena Stabnikova, Dr., National University of Food Technologies, Ukraine

Members of Editorial Board:

Sonia Amariei, PhD, Prof., University "Ştefan cel Mare" of Suceava, Romania Eirin Marie Skjøndal Bar, PhD, Assoc. Prof., Norwegian University of Science and Technology, Trondheim, Norway

Yurii Bilan, PhD, Prof., Tomas Bata University in Zlin, Czech Republic

Kirsten Brandt, PhD, Newcastle University, United Kingdom

Moisés Burachik, PhD, *Institute of Agricultural Biotechnology of Rosario (INDEAR)*, *Bioceres Group, Rosario, Argentina*

Stanka Damianova, PhD, Prof., Ruse University "Angel Kanchev", branch Razgrad, Bulgaria **Yuliya Dzyazko**, PhD, Prof., Institute of General and Inorganic Chemistry of the National Academy of Sciences of Ukraine

Yun-Hwa Peggy Hsieh, PhD, Prof. Emerita, Florida State University, USA

Lelieveld Huub, PhD, Global Harmonization Initiative Association, The Netherlands

Sheila Kilonzi, PhD, Karatina University, Kenya

Jasmina Lukinac, PhD, Assoc. Prof., University of Osijek, Croatia

Dora Marinova, PhD, Prof., Curtin University Sustainability Policy Institute, Curtin University, Australia

Rana Mustafa, PhD, Global Institute for Food Security, University of Saskatchewan, Canada Godwin D. Ndossi, PhD, Prof., Hubert Kairuki Memorial University, Dar es Salaam, Tanzania Umezuruike Linus Opara, PhD, Prof., Stellenbosch University, Cape Town, South Africa Semih Otles, PhD, Prof., Ege University, Turkey

Octavio Paredes-López, PhD, Prof., *The Center for Research and Advanced Studies of the National Polytechnic Institute, Guanajuato, Mexico*

Tetiana Pirog, PhD, Prof., National University of Food Technologies, Ukraine

Cristina Popovici, PhD, Assoc. Prof., Technical University of Moldova

Agota Giedrė Raišienė, PhD, Lithuanian Institute of Agrarian Economics, Lithuania

Egon Schnitzler, PhD, Prof., State University of Ponta Grossa, Ponta Grossa, Brazil

Oleksandr Shevchenko, PhD, Prof., National University for Food Technologies, Ukraine Cristina Luisa Miranda Silva, PhD, Assoc. Prof., Portuguese Catholic University – College of Biotechnology, Portugal

Stefan Stefanov, PhD, Prof., University of Food Technologies, Bulgaria

Yordanka Stefanova, PhD, Assist. Prof., University of Plovdiv "Paisii Hilendarski", Bulgaria María S. Tapia, PhD, Prof., Central University of Venezuela, Caracas, Venezuela; COR MEM of the Academy of Physical, Mathematical and Natural Sciences of Venezuela

Bảo Thy Vương, PhD, Mekong University, Vietnam

Managing Editor:

Oleksii Gubenia, PhD, Assoc. Prof., National University of Food Technologies, Ukraine

Contents

Food Technology	393
Rosen Chochkov, Petya Ivanova, Denka Zlateva, Mariela Bogdanova Rheological and sensory properties and bioactive compounds of wheat dough and bread enriched with nettle (<i>Urtica dioica</i> L.) flour	393
Simone Salomão Jezzini dos Santos, Camila Delinski Bet, Radla Bassetto Zabian Bisinella, Stéphanie Schiavo Romko, Egon Schnitzler Ultrasound-assisted modification and multianalytical characterization of organic Arracacia xanthorrhiza starch	406
Oleksandra Kunyk, Walter Leal, Vasyl Pasichniy, Andrii Marynin, Olena Stabnikova Impact of tocopheryl and retinyl acetates on oxidative stability of Hypericum perforatum L. and Matricaria recutita L. macerates in corn oil during storage	420
Dimitar Dimitrov, Iliyan Simeonov, Simeon Krumov Volatile profile of white wines produced from grape varieties cultivated under the soil-climatic conditions of Kyustendil, Southwestern Bulgaria	433
Mykola Vorontsov, Oleg Galenko, Oksana Topchii Thermal stability and technological performance of fibre-fortified protein- fat emulsions for meat and fish products	448
Roman Mukoid, Yurii Bulii, Serhii Kiriienko Oxygen-driven 2-furfural accumulation and its influence on beer sensory stability	464
Processes and Equipment	478
Oleksandr Gavva, Lyudmila Kryvoplias-Volodina, Yuriy Dolomakin, Anton Kokhan, Nataliya Kulyk Effect of bulk material mechanics on optimal packaging geometry in adaptronic dosing systems	478

Economics and Management	507
Tímea Juhasz	
Basic food purchasing habits of young people in dimension of price inflation	507
Microbiology, Biotechnology	521
Viktor Stabnikov, Iryna Kovshar, Dmytro Stabnikov Biotechnology approaches and improvement strategies in biocement	
production	521
Education and Science News	554
"Wild edible plants: Improving foods nutritional value and human health through biotechnology": International publication of Ukrainian scientists	
research studies	554
Instructions for authors	556

Rheological and sensory properties and bioactive compounds of wheat dough and bread enriched with nettle (*Urtica dioica* L.) flour

Rosen Chochkov¹, Petya Ivanova¹, Denka Zlateva², Mariela Bogdanova¹

- 1 University of Food Technologies, Plovdiv, Bulgaria
- 2 University of Economics, Varna, Bulgaria

Abstract

Keywords:

Nettle flour Wheat dough Bread Rheological Sensory Bioactive

Article history:

Received 23.04.2025 Received in revised form 1.06.2025 Accepted 30.09.2025

Corresponding author:

Rosen Chochkov E-mail: rosen4o4kov@ abv.bg

DOI: 10.24263/2304-974X-2025-14-3-3

Introduction. The aim of this study was to analyse the effect of nettle (*Urtica dioica* L.) flour on the rheological and sensory properties, as well as the bioactive compound content, of wheat dough and bread.

Materials and methods. The bread was made by type 500 wheat flour with the addition of nettle flour. Wheat dough rheological properties were determined by measuring the water absorption, consistency, dough development time, stability and dough softening on farinograph Brabender. The antioxidant activity of ethanolic extracts was evaluated by FRAP (ferric reducing antioxidant power) and DPPH (2,2-diphenyl-1-picrylhydrazyl) radical scavenging methods.

Results and discussion. In the bread formulation, nettle flour was used as a partial substitute for wheat flour at levels of 2, 4, and 6%. The highest dough consistency was observed in the control sample, while all enriched samples showed lower values. However, with increasing substitution levels, consistency values gradually increased. The addition of nettle flour did not affect dough development time. A slight increase (up to 1.3%) in baking loss was observed in breads containing the lowest level of nettle flour compared to the control.

All breads enriched with nettle flour showed a less uniform crumb structure and a more irregular overall appearance relative to the control. The visual quality scores of breads containing nettle flour were lower, and a significant difference in crust coloration was observed. The crumb of the control sample had a typical yellowish hue characteristic of wheat bread, while the addition of nettle flour produced progressively darker coloration. Furthermore, the content of bioactive compounds increased significantly with higher nettle flour content.

Conclusions. As the proportion of nettle flour increased, the dough formation time remained unchanged, while water absorption and dough development time increased compared with the control sample. The incorporation of 2% nettle flour produced the highest bread volume and specific volume. Increasing the nettle flour content enhanced the porosity of the bread crumb but negatively affected its taste quality. The antioxidant activity of the wheat bread increased proportionally with the level of nettle flour substitution.

Introduction

There has been a global trend towards the use of the natural substances present in the food as a source of antioxidant and functional ingredients (Dziki et al., 2014; Kuzmin et al., 2020; Paredes-López et al., 2022; Stabnikova et al., 2021, 2024).

Due to their widespread consumption, cereal-based food products (e.g., bread), which provide more than 50% of the total energy intake in developed societies, are considered excellent vehicles for functional supplementation (Akhtar et al., 2011). Consumption of the wheat-based products, especially bread, is rapidly growing in Europe (Cauvain, 2015). Indeed, bread is consumed every day all over the world. Due to its popularity, bread is often enriched with functional products of natural origin (Ibrahim et al., 2015). To enhance the nutritional value of bread, the upward trend of incorporating plant's seeds, leaves and/or their extracts as a source of phytonutrients is increased (Đurović et al., 2020; Gubsky et al., 2025).

With a history dating back more than 2000 years, stinging nettle has been used as a food and natural medicine for centuries (Said et al., 2015). Due to its balanced protein composition and relatively high content of minerals and vitamins, stinging nettle is often used as a natural supplement that increases the content of biologically active substances in foods. Protein constitutes about 30% of the dry mass and contains numerous amino acids essential for human nutrition. Minerals make up approximately 20% of the dry mass (Said et al., 2015). Nettle is also rich in vitamin C (Guil-Guerrero et al., 2003), chlorophylls, carotenoids, and phenolic compounds, and exhibits significant antioxidant activity (Mannila et al., 2023). Due to its seasonal availability, the consumption of fresh nettle is limited; therefore, it can be utilized in dried form as an additive in various food products.

Nettle leaf flour contains on average about 30% protein, 4% fat, 10% fiber, and 15% ash (Man et al., 2019). Therefore, it can be used as a high-protein supplement and has been incorporated into various food products, including bread (Adhikari et al., 2016). The addition of nettle to bread significantly increases the levels of nutrients such as fiber, calcium, copper, and iron (Maietti et al., 2021). Man et al. (2019) also reported that supplementation of wheat flour with nettle powder enhances the protein, fiber, and mineral content of bread. Sensory evaluation of the enriched breads indicated acceptable organoleptic properties in samples containing up to 4% nettle flour. On the other hand, Saidov et al. (2022) confirmed an increase in protein and fiber content but reported that the specific volume of bread decreased with higher levels of nettle leaf powder. This reduction was attributed to the lower gluten content of the mixture and the interactions between dietary fiber components, water, and gluten. Krawecka et al. (2021) investigated the effect of Urtica dioica L. addition on the nutritional and quality characteristics of wheat pasta. Their results showed that nettle supplementation significantly increased the contents of calcium, iron, potassium, and magnesium. Moreover, as the proportion of nettle increased, a statistically significant ($p \le 0.05$) rise was observed in total dietary fiber, particularly in the insoluble fraction, as well as in the levels of pigments such as chlorophylls and carotenoids.

Neveen and Shaimaa (2023) found that water absorption gradually increased with the addition of dry nettle leaves in biscuit formulation. Likewise, dough development time increased as compared to the corresponding control. On the other hand, dough stability time was shortened because the existence of fiber particles resulted in a disruption of the starchgluten network and thus – in a decrease of dough stability time.

Stinging nettle is undoubtedly a raw material worth attention in the context of functional food design. The aim of this study is to investigate the rheological, sensory and antioxidant properties of wheat dough and bread fortified with nettle (*Urtica dioica* L.) flour (added in an amount of 2, 4 and 6% to replace the equal amount of the wheat flour in bread formulation).

Materials and methods

Materials

For the preparation of the bread samples, the following raw materials were used: commercial wheat flour (type 500, Sheri 61 LCOO) with the average chemical composition, g/100 g: fat 0.9 (of which saturated 0.3), carbohydrates 70.3 (of which sugars 3.4), fiber 4.0, protein 10.8, and moisture 10.6; commercial nettle flour (Viki Nuts Ltd) with the average chemical composition, g/100 g: fat 0.85 (of which saturated 0.07), carbohydrates 3.42 (of which sugars 2.56), fiber 40.00, protein 31.66, and moisture 5.40. Additional ingredients included water (ISO 6107-1:2004), compressed yeast (Lesaffre Bulgaria Ltd), and salt compliant with the Codex Standard for Food Grade Salt (CX STAN 150-1985).

Methods

Preparation of dough and bread samples

Kneading was carried out using a one-phase dough preparation process to obtain a homogeneous dough mass at an initial temperature of 26–27 °C. The mixture of flour (wheat and/or nettle), yeast, salt, and water was kneaded in a laboratory kneading machine (Labomix 1000, Hungary).

The control sample (CS) was prepared using only wheat flour (WF), while the experimental bread samples were produced by substituting wheat flour with nettle flour (NF): NF2 (NF 2%: WF 98%), NF4 (NF 4%: WF 96%), and NF6 (NF 6%: WF 94%). For each formulation, the following ingredients were added: water 56%, yeast 2%, and salt 1.5%.

The prepared doughs were allowed to mature for 30 min at 30 °C. Subsequently, the dough was divided into portions of 230 g for flat bread and 440 g for pan bread. After shaping, the dough pieces were subjected to final fermentation at 33–34 °C for 60 min in a fermentation chamber (Tecnopast CRN 45-12, Novacel Rovimpex, Novaledo Trento, Italy).

The doughs were then baked in an electric floor oven Salva E-25 (Salva Industrial S.L.U., Lezo, Spain), preheated to a temperature of 220–230 °C, for 22–24 min. After baking, the breads were allowed to cool for 3 h at room temperature.

Rheological properties of the dough

The following dough properties were determined by a farinograph (Brabender GmbH&Co KG, Duisburg, Germany): water absorption (%), development time (min), stability (min), degree of softening (farinograph units (FU)) and consistency (FU), according AACC Method 54-21.02 (AACC International. AACC Approved Methods of Analysis, 11th ed.; AACC International: St. Paul, MN, USA, 2010).

Physical properties of bread

The quality of the bread samples was assessed as followed: bread loaf volume was determined after baking and cooling for 3 h at room temperature by a rapeseed displacement method (AACC, 2010).

The specific volume was calculated by the ratio between volume (ml) and mass (g) of each sample. Bread height and diameter were measured by a calliper, and the shape stability (Height/Diameter) was calculated (Novotni et al., 2012). Bake loss (%) was determined by weighing each loaf before and after baking (Kim et al., 2015). The bread loaves were wrapped in plastic bags and stored at room temperature (27 ± 2 °C) to determine the storage time (in days) until visible mold growth occurred.

Sensory evaluation

Sensory evaluation of the obtained breads was performed by a descriptive panel consisting of 25 panellists (52% women and 48% men) aged 22 – 60 years, who were familiar with sensory analysis of food but not specifically trained in the evaluation of bread. The analysis was carried out according to ISO 6658:2017. The panellists were asked to score seven parameters, namely appearance, crust color, crumb color, porosity, chewability, aroma and taste. They expressed the intensity of each attribute on a 9-point hedonic scale (9 – extremely good; 1 – extremely bad).

Bioactive compound content

The extraction of bioactive compounds from dry breads was carried out with 70% ethanol as described by Vasileva et al. (2018). Bread samples were sliced (about 1.5 cm thick), dried (40 °C, 24 h), ground in a mill, and sieved (0.5 mm sieve). Ethanol extracts from breads were obtained with 70% ethanol (solid to liquid ratio 1:20) in an ultrasonic bath (VWR, Malaysia; 45 kHz, 30 W) at 45 °C for 15 min. Samples were then centrifuged at 1800xg for 15 min (MPW-251, Med. Instruments, Poland). The supernatants were used for further studies.

Analytical methods

Total polyphenols were quantified by using Folin-Ciocalteu's reagent (Ainsworth and Gillespie, 2007). Gallic acid was employed as calibration standard and the results were expressed as mg equivalents gallic acid (GAE) per gram dry weight (DW).

Total flavonoids were determined using Al(NO₃)₃ reagent and measuring the absorbance at 415 nm according to Kivrak et al. (2019). The results were expressed as mg equivalents quercetin (QE) per gram DW.

The antioxidant activity of ethanolic extracts was evaluated by two methods: FRAP (ferric reducing antioxidant power) and DPPH (2,2-diphenyl-1-picrylhydrazyl) radical scavenging methods.

The FRAP method is based only on single electron transfer mechanism and was measured according to the method of Dimov et al. (2018) with some modification. Three ml freshly prepared FRAP reagent (10 parts 0.3 M acetate buffer (pH 3.6), 1 part 10 mM 2,4,6-tripyridyl-s-triazine (TPTZ) in 40 mM HCl and 1 part 20 mM FeCl3.6H2O in d. H₂O) were mixed with 0.1 ml of investigated ethanolic extract. The reaction time was 10 min at 37 °C in darkness and the absorbance was measured at 593 nm against blank prepared with 70% ethanol. A standard curve was built with FeSO₄.7H₂O. The results of FRAP analysis were expressed as μmol Fe²⁺ equivalents per gram DW (Irshad et al., 2012).

The DPPH radical method is based on mixed hydrogen atom transfer and single electron transfer mechanisms. DPPH radical scavenging activity was estimated according to Dimov et al. (2018) with some modification. Briefly, 0.15 ml of ethanolic extract was

mixed with 2.85 ml 0.06 mM DPPH fresh solution in 96% ethanol. The mixture was left for 30 min (kept in the dark at room temperature) so that a reaction could take place, and then the absorbance at 517 nm was measured by spectrophotometer in comparison to the blank containing 70% ethanol. The results of DPPH analysis were expressed as mmol Trolox equivalents (TE) per gr DW.

Statistical analysis

Results are presented as means of at least three independent determinations \pm standard deviation (SD). Statistical evaluation was performed by using one-way analysis of variance (ANOVA) of the IBM SPSS Statistics program (Somers, NY, USA). Mean differences were established by Fisher's least significant difference test for paired comparison with a significance level $\alpha=0.05$.

Results and discussion

Effect of nettle flour on the rheological properties of dough

The dough rheological properties are decisive for its behaviour during technological operations. The results are presented in Table 1.

Table 1
Effect of nettle flour on rheological properties of wheat dough

Bread	Water absorption,%	Consistency, F.U.	Time of dough development, min	Stability, min	Dough softening, F.U.
CS	62.4	520	1.5	7	170
NF2	63.3	490	1.5	10	170
NF4	63.3	480	1.5	8.5	140
NF6	63.3	500	1.5	6.5	140

Note: F.U. - Farinograph Units.

As can be seen, the water absorption of the control and test samples was almost identical. However, the results obtained by other researchers differ from our findings. According to Neveen et al. (2023), the water absorption of enriched samples gradually increased with the addition of dry nettle leaves at 5%, 10%, and 15% substitution levels. This discrepancy is likely due to the different forms of nettle used, as the physical characteristics of nettle flour and dry leaves can influence dough hydration behavior.

The highest consistency score was measured for the control sample. All enriched samples had lower scores, with increasing degree of substitution of wheat flour with nettle flour the values increased. The use of nettle flour did not change dough development time. The stability of the samples with nettle flour for samples NF2 and NF4 increased compared to the control, while for sample NF6 decreased. Compared with the control, dough softening progressively decreased as the proportion of nettle flour increased.

Quality assessment of wheat bread enriched with nettle flour

To assess the baking characteristics of the wheat bread enriched with nettle flour – pan bread was prepared from each formulation (Figure 1). Fermentation and baking of all the samples were carried out under equal conditions, according to the adopted technology.



Figure 1. Cross-section of wheat bread enriched with nettle flour (from left to right: CS; NF2; NF4; NF6)

Results from the assessment of the baking characteristics are presented in Table 2.

Volume of wheat bread enriched with nettle flour

Table 2

Duord comples	Volume, ml			
Bread samples	Floor bread	Pan bread		
CS	820	1512		
NF2	686	1332		
NF4	523	1060		
NF6	490	1030		

The results show that the volume of wheat bread samples with added nettle flour decreases. With increasing the quantity of nettle flour, respectively, the values decrease. The results obtained for the highest added amount – sample NF6, show a significant decrease in the volume of the floor bread, by 40%, compared to the control sample. This confirms the conclusions drawn from the dough rheological characteristics, that the highest amount of nettle flour leads to a deterioration in the rheology of the dough, and hence the quality of bread. The results for the pan bread are similar to those for the floor bread.

According to the literature, the addition of fiber-rich materials up to 7% leads to a proportional decrease in bread volume, corresponding to the reduction in gluten content within the blend. Laurikainen et al. (1998) reported that when this level is exceeded, bread volume decreases more rapidly than theoretically expected, which they attributed to a reduced gluten protein content.

The specific volume of bread, defined as the ratio of its volume to its weight, provides a more comprehensive characteristic of bread quality. The results for the specific volume of wheat bread supplemented with nettle flour are presented in Figure 2.

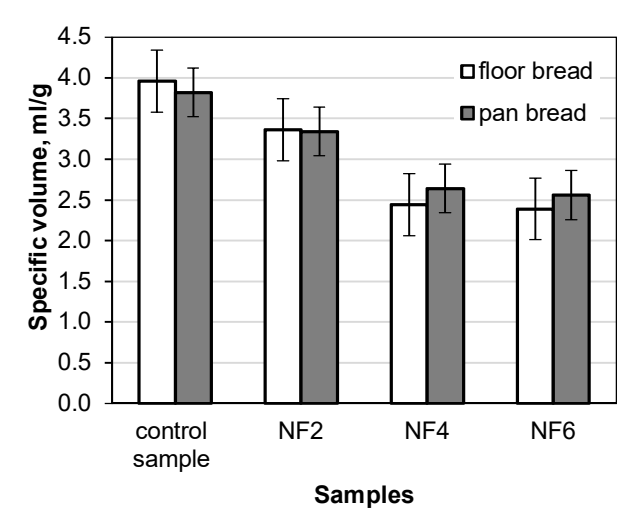


Figure 2. Specific volume of floor and pan wheat bread enriched with nettle flour

Regardless of the method of baking the bread (flat or pan bread), a decrease in the specific volume is observed with increasing the amount of added nettle flour. Man et al. (2019) also reported similar results. They pointed out that the specific volume of the breads decreased as the level of nettle leaves powder increased due the dilution of gluten content in the blend and due to the interactions among fiber components, water and gluten. In this regard, Đurović and co-authors (2020) pointed out that the form in which the nettle is added matters. They added nettle leaves and extract (in equal amounts) to the wheat bread formulation. When using nettle leaves, the reduction in the volume of the loaves of bread was much more pronounced. Some authors, however, do not support this opinion. Hung et al. (2007) argued that the existence of dietary fiber diluted the protein and interfered with the optimal gluten matrix formation during dough mixing.

The shape stability of bread is denoted H/D and is determined by the ratio between the height and diameter of the floor bread. Figure 3 presents the shape stability (H/D) of the control sample and test samples of wheat floor bread supplemented with nettle flour.

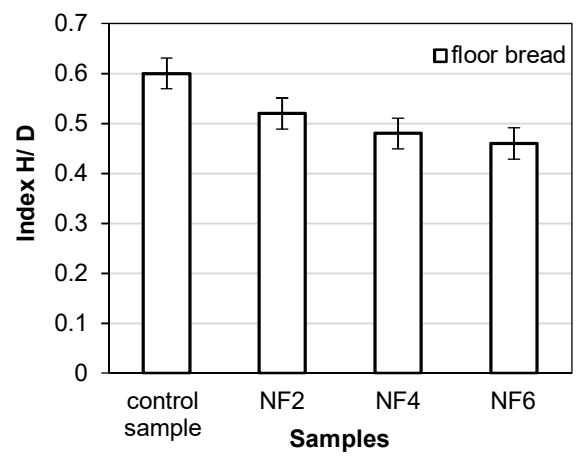


Figure 3. Shape stability of wheat bread enriched with nettle flour

In terms of shape stability (H/D), the samples with nettle flour have lower values compared to the control sample (0.6). The closest to the control sample are the results obtained about sample NF2 - (0.52). The other samples (NF4 and NF6) have almost identical values for H/D much lower than the obtained for the bread prepared from wheat flour.

The baking loss of flour and pan wheat-nettle bread is shown in Table 3.

Table 3 Baking loss of floor and pan wheat bread enriched with nettle flour

Duord comples	Baking loss,%		
Bread samples	Floor bread	Pan bread	
CS	10.00	10.22	
NF2	11.30	9.54	
NF4	10.40	8.87	
NF6	10.86	8.64	

With addition of a lowest quantity of nettle flour, baking loss (floor bread) increase by up to 1.3% compared to the control sample. It is interesting to note that the floor bread with nettle flour had lower baking loss compared to the control sample (up to 1.58%). For the pan bread, the difference between control sample and lowest quantity of nettle flour is 0.68%. In the case of pan bread, increasing the amount of added nettle flour has been found to reduce baking loss. Wójcik et al. (2021) conducted similar studies, but they enriched wheat bread with nettle infusion, added in amount of 10, 20, 30 and 40 mg/ml. The authors concluded that the increasing addition of nettle infusion caused a decrease in baking loss and the volume of the obtained loaves. This pattern does not occur in the case of floor bread.

Sensory profile of wheat breads enriched with nettle flour

Overall, the use of nettle flour can change the quality of wheat bread in terms of sensory properties. The results obtained are presented in Figure 4.

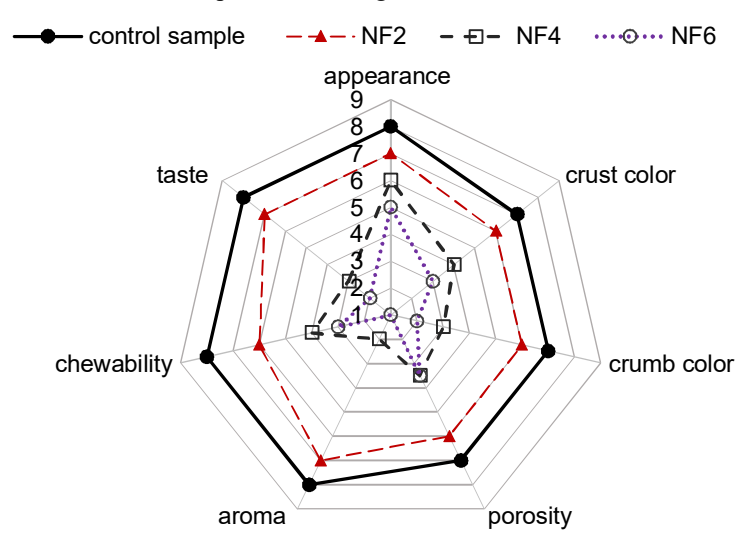


Figure 4. Sensory profile of wheat breads enriched with nettle flour

The present study indicated that the scores for all sensory properties decreased with the increasing the proportion of nettle flour. When cutting, the control sample exhibits a lower tendency to crush, unlike the test samples. All test samples have a more atypical development and a more uneven crumb structure, compared to the control sample. The appearance values of the enriched sample NF2 compared to CS decrease by 12.50%, while for the enriched sample NF6 compared to CS there is a decrease by 37.50%. Significant difference in the coloration of the crust is observed. The color of the bread crumb of the control sample is yellowish, typical for wheat flour bread. In the test samples, the color shade is more saturated and belongs to the green range. The color of the crust and the crumb for CS and NF2 have the higher data values. Diddana et al. (2021) investigated the nutritional composition and sensory acceptability of unleavened flatbread (Kitta) developed from stinging nettle (Urtica simensis L.) leaf and maize (Zea mays L.) flour. The authors concluded that color acceptability of flatbread was significantly (p < 0.05) reduced with increasing the proportion of nettle leaf flour. Sample NF2 exhibits higher porosity compared to samples NF4 and NF6. The results indicated the the control bread and the bread NF2 have the higher values (8 and 6) for chewability compared to the bread NF4 and NF6. For the taste the results were almost similar – the control sample and the sample NF2 have achieved higher scores (8 and 7) compared to the samples NF4 and NF6 (3 and 2). Rădulescu et al. (2024) reported that the addition of nettle powder to the bread dough gives a specific taste and texture to the bread.

The control sample has a well pronounced, typical for wheat bread aroma. In the enriched samples NF4 and NF6, a much more intensive nettle aroma is detected, but it slightly differs from the aroma of fresh nettle. However drying changes the aroma of food products through losses in volatile compounds or the formation of new volatile compounds as a result of oxidation and esterification reactions (Diaz-Maroto et al., 2002; Orphanides et al., 2013). Man et al. (2019) reported almost the same results – bread prepared with 100% of wheat flour scored maximum than the rest of the samples. Evaluating the samples enriched with nettle powder, the highest score was observed in the bread containing 2% NF, while the lowest was recorded for the bread with 6% NF. The enriched breads showed reduced volume and porosity, which resulted in lower overall sensory scores.

Bioactive compounds in wheat bread with nettle flour

The antioxidant activity, dry matter content, total phenols and flavonoids of the bread samples are presented in Table 4.

Bioactive compounds in wheat bread with nettle flour

Total Total DPPH, FRAP, Bread Drv flavonoids, phenols, μmol Fe²⁺/g mM TE/g samples substance,% mg QE/g mg GAE/g DM DM DM **DM** CS 90.11±0.06a 0.12 ± 0.00^{d} 0.63 ± 0.03^{d} 0.42 ± 0.00^{d} 3.20 ± 0.06^{d} NF2 90.12±0.12a 0.16 ± 0.00^{c} 0.78 ± 0.03^{c} 0.77 ± 0.05^{c} 4.22±0.05° NF4 90.12±0.07a 0.21 ± 0.00^{b} 0.96 ± 0.02^{b} 0.86 ± 0.02^{b} 4.68 ± 0.05^{b} NF6 90.02±0.25a 0.23±0.00a 1.18±0.02a 1.02±0.02a 5.03±0.08a

Table 4

^{*}DM – dry matter

 $^{^{}a-d}$ Means in a column without a common letter differ significantly (p < 0.05).

The study found that increasing the proportion of nettle flour (2, 4, and 6%) did not affect the dry matter content of the resulting bread samples. However, the total flavonoid content increased with higher levels of nettle flour, with the most pronounced increase observed in the sample containing 6% nettle flour, where the quercetin equivalent (QE) content was nearly double that of the control. According to Fattahi et al. (2014), stinging nettle is rich in polyphenols and flavonoids and exhibits strong antioxidant activity, contributing to various protective and disease-preventing properties.

The total phenols also increased and the difference between the control and the sample with 6% nettle flour was 0.55 mg, which is 87.30%. Hudec et al. (2007) studied total phenolic content of different nettle parts (root, stalk, and leaves). It was found that the result for nettle leaves was 7.62 mg GAE/g DM. The DPPH radical scavenging and iron-reducing antioxidant capacity increased with increasing of nettle flour. According to the DPPH method, bread with 6% nettle flour showed 2.4 times higher radical scavenging activity, and the iron-reducing ability increased by 1.6 times.

Others studies also demonstrated that the antioxidant activity of wheat bread and bread enriched with nettle flour was higher in the total phenols in nettle flour bread were 0.3 mg more than in wheat bread, which is 36.14%. Lutein in wheat bread is 2.51 mg less than in nettle flour bread, and beta-carotene was 0.31 mg more in nettle flour bread. Maietti et al. (2021) demonstrated that the amount of total phenolic compounds increased from 372 µg GAE/g of fresh weight (FW) in wheat bread to 597 µg GAE/g FW in bread enriched with nettle flour. Furthermore, antioxidant activity was also higher in enriched bread compared to wheat bread (0.83 vs. 0.53 mg TE/g FW, respectively). Đurović et al. (2020) also found that bread prepared with nettle leaf flour showed significant antioxidant activity against the DPPH radical.

In summary, it can be concluded that increasing the amount of nettle flour enhances the antioxidant activity of bread. The results indicate that the NF6 sample exhibits the highest antioxidant levels compared to the control, demonstrating that higher additions of nettle flour significantly increase the content of antioxidant compounds. According to Joshi et al. (2014), stinging nettle (*Urtica dioica*) leaves are rich in phytoconstituents, including polyphenols, flavonoids (kaempferol, isorhamnetin, quercetin, isoquercitrin, and rutin), phenolic acids (caffeic acid and chlorogenic acid), and carotenoids (β -carotene, hydroxyl- β -carotene, luteoxanthin, lutein epoxide, and violaxanthin), as well as essential oils, fatty acids, minerals, and vitamins.

Conclusions

The study found that increasing the amount of nettle (*Urtica dioica*) flour did not affect dough development time, while dough stability increased and dough softening decreased. Incorporating 2% nettle flour resulted in the best bread volume and specific volume compared to the other enriched samples. Sensory analysis showed that higher levels of nettle flour negatively affected the bread's appearance, porosity, and taste. The sample with 2% nettle flour had sensory properties closest to the control. Overall, the study demonstrated that partially replacing wheat flour with nettle flour is an effective strategy to enhance the bread's bioactive potential and boost its antioxidant activity.

References

- AACC (2010). AACC Approved Methods of Analysis, 11th ed.; AACC International: St. Paul, MN, USA.
- Adhikari B.M., Bajracharya A., Shrestha A.K. (2016), Comparison of nutritional properties of stinging nettle (*Urtica dioica* L.) flour with wheat and barley flours, *Food Science and Nutrition*, 4(1), pp. 119–124, https://doi.org/10.1002/fsn3.259
- Ahmad A.M.R., Waqas A., Sanaullah I., Mavra J., Summer R., Iahtisham-ul-Haq. (2021), Prebiotics and iron bioavailability? Unveiling the hidden association A review, *Trends in Food Science & Technology*, 110, pp. 584–590, https://doi.org/10.1016/j.tifs.2021.01.085
- Ainsworth E.A., Gillespie K.M. (2007), Estimation of total phenolic content and other oxidation substrates in plant tissues using Folin-Ciocalteu reagent, *Nature Protocols*, 2, pp. 875–877, https://doi.org/10.1038/nprot.2007.102
- Akhtar S., Anjum F.M., Anjum M.A.A. (2011), Micronutrient fortification of wheat flour: Recent development and strategies, *Food Research International*, 44, pp. 652–659, https://doi.org/10.1016/j.foodres.2010.12.033
- Cauvain S. (2015), *Technology of Breadmaking*, Springer International Publishing, Cham, https://doi.org/10.1007/978-3-319-14687-4
- Das L., Raychaudhuri U., Chakraborty R. (2012), Supplementation of common white bread by coriander leaf powder, *Food Science and Biotechnology*, 21, pp. 425–433, https://doi.org/10.1007/s10068-012-0054-9
- Diaz-Maroto M.C., Pérez-Coello M.S., Cabezudo M.D., (2002), Effect of drying method on the volatiles in bay leaf (*Laurus nobilis* L.), *Journal of Agricultural and Food Chemistry*, 50(16), pp. 4520–4524, https://doi.org/10.1007/s10068-012-0054-9
- Diddana T.Z., Kelkay G.N., Tescha E.E. (2021), Nutritional composition and sensory acceptability of stinging nettle (*Urtica simensis*) flour-supplemented unleavened maize (*Zea mays* L.) flatbread (Kitta), *International Journal of Food Science*, 2021, 6666358, https://doi.org/10.1155/2021/6666358
- Dimov I., Petkova N., Nakov G., Taneva I., Ivanov I., Stamatovska V. (2018), Improvement of antioxidant potential of wheat flours and breads by addition of medicinal plants, *Ukrainian Food Journal*, 7(4), pp. 671–681, https://doi.org/10.24263/2304-974X-2018-7-4-11
- Đurović S., Vujanović M., Radojković M., Filipović J., Filipović V., Gašić U., Tešić Ž., Mašković P., Zeković Z. (2020), The functional food production: Application of stinging nettle leaves and its extracts in the baking of a bread, Food Chemistry, 312, 126091, https://doi.org/10.1016/j.foodchem.2019.126091
- Dziki D., Różyło R., Gawlik-Dziki U., Świeca M. (2014), Current trends in the enhancement of antioxidant activity of wheat bread by the addition of plant materials rich in phenolic compounds, *Trends in Food Science & Technology*, 40(1), pp. 48–61, https://doi.org/10.1016/j.tifs.2014.07.010
- Fattahi S., Zabihi E., Abedian Z., Pourbagher R., Ardekani A.M., Mostafazadeh A., Akhavan-Niaki H. (2014), Total phenolic and flavonoid contents of aqueous extract of stinging nettle and in vitro antiproliferative effect on hela and BT-474 cell lines, *International Journal of Molecular and Cellular Medicine*, 3(2), pp. 102–107.
- Hudec J., Burdová M., Kobida L., Komora L., Macho V., Kogan G., Turianica I., Kochanová R., Ložek O., Habán M., Chlebo P. (2007), Antioxidant capacity changes and phenolic profile of Echinacea purpurea, nettle (Urtica dioica L.), and dandelion (Taraxacum officinale) after application of polyamine and phenolic biosynthesis regulators, Journal of Agricultural and Food Chemistry, 55(14), pp. 5689–5696, https://doi.org/10.1021/jf070777c
- Hung P.V., Maeda T., Morita N. (2007), Dough and bread qualities of flours with whole waxy wheat flour substitution, *Food Research International*, 40(2), pp. 273–279, https://doi.org/10.1016/j.foodres.2006.10.007
- Gubsky S., Stabnikova O., Stabnikov V., Paredes-López O. (Eds.), *Wild Edible Plants: Improving Foods Nutritional Value and Human Health through Biotechnology*, CRC Press, Boca Raton, https://doi.org/10.1201/9781003486794

- Guil-Guerrero J.L., Rebolloso-Fuentes M.M., Isasa M.T. (2003), Fatty acids and carotenoids from stinging nettle (*Urtica dioica* L.), *Journal of Food Composition and Analysis*, 16(2), pp. 111–119, https://doi.org/10.1016/S0889-1575(02)00172-2
- Ibrahim U.K., Salleh R.M., Maqsood-ul-Haque S.N.S. (2015), Bread towards functional food: An overview, *International Journal of Food Engineering*, 1(1), pp. 39–43, https://doi.org/10.18178/ijfe.1.1.39-43
- Irshad Md., Zafaryab Md., Singh M., Moshahid M.A.R. (2012), Comparative analysis of the antioxidant activity of Cassia fistula extracts, International Journal of Medicinal Chemistry, 2012, 157125, https://doi.org/10.1155/2012/157125
- ISO 6658:2017, Sensory Analysis Methodology General Guidance.
- Jin M., Cai Y.X., Li J.H., Zhao H. (1996), 1, 10-phenanthroline- Fe²⁺ oxidative assay of hydroxyl radical produced by H₂O₂/Fe²⁺, *Progress in Biochemistry and Biophysics*, 23, pp. 553–555.
- Joshi B.C., Mukhija M., Kalia A.N. (2014), Pharmacognostical review of *Urtica dioica* L., *International Journal of Green Pharmacy*, 8, pp. 201–209, https://doi.org/10.22377/ijgp.v8i4.414
- Kim W.M., Lee G.H. (2015), Comparison of imported wheat flour bread making properties and Korean wheat flour bread making properties made by various bread making methods, *Journal of Korean Society of Food Science and Nutrition*, 44(3), pp. 434–441.
- Kivrak Ş., Göktürk T., Kivrak I., Kaya E., Karababa E. (2019), Investigation of phenolic profiles and antioxidant activities of some Salvia species commonly grown in Southwest Anatolia using UPLC-ESI-MS/MS, *Food Science and Technology, Campinas*, 39(2), pp. 423–431, https://doi.org/10.1590/fst.3201
- Krawęcka A., Sobota A., Pankiewicz U., Zielińska E., Zarzycki P. (2021), Stinging nettle (*Urtica dioica L.*) as a functional component in durum wheat pasta production: Impact on chemical composition, in vitro glycemic index, and quality properties, *Molecules*, 26(22), 6909, https://doi.org/10.3390/molecules26226909
- Kuzmin O., Kucherenko V., Stukalska N., Kuts A., Oliynyk S., Rakhmetov D. (2020), Antioxidant ability of alcoholic infusions from vegetable raw materials, *Ukrainian Food Journal*, 9(4), pp. 795–808, https://doi.org/10.24263/2304-974X-2020-9-4-6
- Laurikainen T., Harkonen H., Autio K., Poutanen K. (1998), Effects of enzymes in fiber-enriched baking, *Journal of the Science of Food and Agriculture*, 76(2), pp. 239–249, https://doi.org/10.1002/(SICI)1097-0010(199802)76:2<239::AID-JSFA942>3.0.CO;2-L
- Maietti A., Tedeschi P., Catani M., Stevanin C., Pasti L., Cavazzini A., Marchetti N. (2021), Nutrient composition and antioxidant performances of bread-making products enriched with stinging nettle (*Urtica dioica* L.) leaves, *Foods*, 10(5), 938, https://doi.org/10.3390/foods10050938
- Man S.M., Paucean A., Chis M.S., Muste S., Pop A., Muresan A.E., Martis G. (2019), Effect of nettle leaves powder (*Urtica dioica* L.) addition on the quality of bread, *Hop and Medicinal Plants*, 27(1–2), pp. 104–112, https://doi.org/10.15835/hpm.v27i1-2.13590
- Mannila E., Marti-Quijal F.J., Selma-Royo M., Calatayud M., Falcó I., de la Fuente B., Barba F.J., Collado M.C., Linderborg K.M. (2023), In vitro bioactivities of food grade extracts from yarrow (*Achillea millefolium* L.) and stinging nettle (*Urtica dioica* L.) leaves, *Plant Foods for Human Nutrition*, 78(1), pp. 132-138, https://doi.org/10.1007/s11130-022-01020-y
- Neveen A.M.A., Shaimaa M.H. (2023), Effect of bioactive compounds of sting nettle (*Urtica diocia* L.) leaves on shelf life of the salty biscuits, *Food Technology Research Journal*, 2(2), pp. 73–85.
- Novotni D., Curić D., Bituh M., Colić Barić I., Skevin D., Cukelj N. (2011), Glycemic index and phenolics of partially-baked frozen bread with sourdough, *International Journal of Food Science and Nutrition*, 62(1), pp. 26–33, https://doi.org/10.3109/09637486.2010.506432
- Orphanides A., Goulas V., Gekas V. (2013), Effect of drying method on the phenolic content and antioxidant capacity of spearmint, *Czech Journal of Food Science*, 31(5), pp. 509–513, https://doi.org/10.17221/526/2012-CJFS
- Paredes-López O., Shevchenko O., Stabnikov V., Ivanov V. (Eds.), (2022), *Bioenhancement and Fortification of Foods for a Healthy Diet*, CRC Press, Boca Raton, https://doi.org/10.1201/9781003225287

—— Processes and Equipment——

- Rădulescu L., Tarkanyi P., Velciov A.B., Alda L.M., Alda S., Bordean D.M. (2024), Nettle bread, a potential functional product, scientific papers, *Scientific Papers, Series A. Agronomy*, 67(1), pp. 591–595.
- Said A.A.H., Otmani I.S.E., Derfoufi S., Benmoussa A. (2015), Highlights on nutritional and therapeutic value of stinging nettle (*Urtica dioica* L.). *International Journal of Pharmacy and Pharmaceutical Science*, 7(10), pp. 8–14.
- Saidov A.M., Balguzhinova Z.E., Zhangabylova N.D., Alseitov K.S., Iskakov K.E. (2022), Influence of nettle powder addition on bread quality indicators, *The Journal of Almaty Technological University*, 3, pp. 108–114.
- Stabnikova O., Marinin A., Stabnikov V. (2021), Main trends in application of novel natural additives for food production, *Ukrainian Food Journal*, 10(3), pp. 524–551, https://doi.org/10.24263/2304-974X-2021-10-3-8
- Stabnikova O., Stabnikov V., Paredes-López O. (2024), Fruits of wild-grown shrubs for health nutrition, *Plant Foods for Human Nutrition*, 79(1), pp. 20-37, https://doi.org/10.1007/s11130-024-01144-3
- Vasileva I., Denkova R., Chochkov R., Teneva D., Denkova Z., Dessev T., Denev P., Slavov A. (2018), Effect of lavender (*Lavandula angustifolia*) and melissa (*Melissa officinalis*) waste on quality and shelf life of bread, *Food Chemistry*, 253, pp. 13–21, https://doi.org/10.1016/j.foodchem.2018.01.131
- Wójcik M., Różyło R., Łysiak G., Kulig R., Cacak-Pietrzak G. (2021), Textural and sensory properties of wheat bread fortified with nettle (*Urtica dioica* L.) produced by the scalded flour method, *Journal of Food Processing and Preservation*, 45(10), e15851, https://doi.org/10.1111/jfpp.15851

Cite:

UFJ Style

Chochkov R., Ivanova P., Zlateva D., Bogdanova M. (2025), Rheological and sensory properties and bioactive compounds of wheat dough and bread enriched with nettle (*Urtica dioica* L.) flour, *Ukrainian Food Journal*, 14(3), pp. 393–405, https://doi.org/10.24263/2304-974X-2025-14-3-3

APA Style

Chochkov, R., Ivanova, P., Zlateva, D., & Bogdanova M. (2025). Rheological and sensory properties and bioactive compounds of wheat dough and bread enriched with nettle (*Urtica dioica* L.) flour. *Ukrainian Food Journal*, 14(3), 393–405. https://doi.org/10.24263/2304-974X-2025-14-3-3

Ultrasound-assisted modification and multianalytical characterization of organic *Arracacia xanthorrhiza* starch

Simone Salomão Jezzini dos Santos, Camila Delinski Bet, Radla Bassetto Zabian Bisinella, Stéphanie Schiavo Romko, Egon Schnitzler

State University of Ponta Grossa, Brazil

Abstract

Keywords:

Starch
Arracacia
xanthorrhiza
Ultrasound
Modification
Thermal
stability

Article history:

Received 25.06.2025 Received in revised form 23.09.2025 Accepted 30.09.2025

Corresponding author:

Egon Schnitzler E-mail: egons@uepg.br

DOI: 10.24263/2304-974X-2025-14-3-

Introduction. Native starches have certain industrial limitations, making it necessary to apply physical modification methods such as ultrasound treatment. This study investigates the effects of ultrasound on the structural, thermal, and physicochemical properties of organic starch extracted from *Arracacia xanthorrhiza*.

Materials and methods. The *Arracacia xanthorrhiza* roots were obtained from a small-scale producer in Curitiba, Paraná, Brazil. Starch was extracted using an aqueous method, modified by ultrasound, and subsequently characterized in terms of thermal, pasting, morphological, structural, and physicochemical properties.

and discussion. The aqueous extraction of mandioquinha-salsa starch yielded 34.64% based on raw material and 48.18% on processed mass, showing values consistent with previous studies. The application of ultrasound at different amplitudes (40%. 50%, 60%, and 70%) resulted in notable structural and functional changes in the starch. Rapid Visco Analysis revealed that the 40% amplitude treatment improved shear resistance and reduced breakdown and retrogradation, while higher amplitudes increased peak and final viscosities. Thermogravimetric (TG) and derivative thermogravimetric (DTG) analyses showed that the 50% amplitude treatment resulted in the highest degradation temperature, while the 60% treatment exhibited the widest range of thermal stability. Differential Scanning Calorimetry (DSC) analysis confirmed lower gelatinization enthalpy for the 40% treated starch, indicating reduced energy demand during gelatinization. FEG-SEM (Field Emission Gun – Scanning Electron Microscope) images demonstrated changes in granule morphology, with increased particle size up to 50% amplitude, followed by a reduction at higher intensities, without evidence of granule agglomeration. X-ray diffraction showed a gradual increase in crystallinity with ultrasound treatment, although all modified samples had lower crystallinity than the native starch. These results demonstrate that ultrasound is an effective and clean modification method, capable of enhancing the thermal stability, viscosity behavior, and structural organization of starch from Arracacia xanthorrhiza, making it suitable for food and packaging applications.

Conclusions. Ultrasound-modified starches from *Arracacia xanthorrhiza* showed improved functional and thermal properties compared to native starch.

Introduction

Starches, like cellulose, are among the most abundant carbohydrates in nature, and their structural and functional properties vary widely depending on their botanical origin. These differences are related to the amylose-to-amylopectin ratio, granule size, and morphology, directly affecting their applications in the food, pharmaceutical, and packaging industries (Zhang et al., 2023). Industrial interest in native and functional starches has grown, particularly due to the technological properties of resistant starch, which is associated with glycemic modulation, gut health, and beneficial effects on the microbiota (Bojarczuk et al., 2022; Li, 2022).

However, native starches present technological limitations such as retrogradation, syneresis, and low thermal stability, which compromise their industrial use. To overcome these limitations, various modification methods have been applied, including chemical, enzymatic, and physical modifications (Giacomozzi et al., 2021; Wang et al., 2023).

Among physical methods, ultrasound application stands out as a clean and environmentally friendly approach, promoting structural changes in starch granules through acoustic cavitation. This technique produces granules that are more porous, with reduced particle size, altered crystallinity, and improved solubility, all without using toxic reagents or harsh processes (Zhu, 2015). Ultrasonic modification has been widely studied across various starch sources, proving effective in enhancing functional properties.

Mandioquinha-salsa (*Arracacia xanthorrhiza*) is an Andean tuber widely cultivated in Brazil, especially in the South and Southeast regions. Its starch is characterized by high digestibility, fine granular morphology, and a high amylopectin content, making it a good candidate for structural modifications aimed at greater stability and functionality.

Therefore, this study aims to evaluate the effects of ultrasonic treatment on organic mandioquinha-salsa starch using different amplitudes and exposure times. The samples were characterized by thermal analyses (DSC/TG), pasting properties (RVA), electron microscopy, and physicochemical evaluation, seeking to demonstrate the viability of this technique as a tool to generate functional starches with high technological potential.

Materials and methods

Starch extraction

Organic *Arracacia xanthorrhiza* roots (yellow common variety) were obtained from a local producer in Curitiba (Paraná, Brazil). The roots were washed, peeled, sliced into 3–5 mm pieces, and stored under refrigeration (5 °C) until use.

Starch extraction was performed using an aqueous method. Enzymatic inactivation was carried out by immersing the sliced material in a sodium metabisulfite solution ($Na_2S_2O_5$) for 30 minutes, followed by rinsing in running water.

The aqueous grinding was performed in an industrial blender using a fixed proportion of root to water. The homogenized suspension was sieved (270 mesh), centrifuged, and the resulting starch was dried in a forced-air oven at 35 °C for 24 hours. The dried starch was then manually ground with a mortar and pestle.

The native starch was stored in a desiccator containing anhydrous calcium chloride until further modification and analysis.

Starch modification

The starch granules were modified by ultrasound treatment using a Vibra-Cell 500 W device (Sonics & Materials Inc., USA) operating at a frequency of 20 kHz. A 10% (w/v) starch suspension in deionized water was subjected to ultrasonic waves while being kept in an ice bath to prevent starch gelatinization during the process. The total ultrasound exposure time was 30 minutes, as described by Liu et al. (2023).

Analysis

Thermogravimetric analysis (TG) was performed using a TGA-50 instrument (Shimadzu, Japan) under the following conditions: sample mass of approximately 7.0 mg; air atmosphere with a flow rate of 150 mL min⁻¹; heating rate of 10 °C min⁻¹ from 30 °C to 650 °C. Mass losses were calculated using the TA-60 analysis software.

Differential scanning calorimetry (DSC) analyses were performed using a DSC-Q200 instrument (TA Instruments, USA), previously calibrated. The experimental conditions were as follows: air flow rate of 50 mL min $^{-1}$, heating range from 20 °C to 100 °C, and heating rate of 10 °C min $^{-1}$. Approximately 2.5 mg of each sample was weighed and mixed with 10 μ L of distilled water (1:4, w/v) in aluminum pans, which were then hermetically sealed. The pans were allowed to stand for 1 hour before analysis to ensure moisture equilibrium and starch granule swelling.

X-ray diffraction (XRD) analysis was carried out using an Ultima IV diffractometer (Rigaku, Japan), located at the Multiuser Laboratory Complex (C-LABMU) of the State University of Ponta Grossa (UEPG). The measurements were performed using CuK α radiation ($\lambda=1.541~\mbox{Å}$), with the equipment set to 40 kV and 20 mA. The scattered radiation was recorded over a 20 range from 3° to 40°, with a scanning speed of 2° min $^{-1}$ and a step size of 0.06° (Kubiaki et al., 2016).

Pasting properties were evaluated using a Rapid Visco Analyzer (RVA), model RVA-4 (Newport Scientific, Australia). Native and ultrasound-modified starch suspensions were prepared at 8% (w/w, dry basis) in deionized water, with a final mass of 28 g. The controlled heating and cooling cycle consisted of constant stirring at 50 °C for 2 minutes, followed by heating from 50 °C to 95 °C at a rate of 6 °C min⁻¹. The sample was then held at 95 °C for 5 minutes, cooled back to 50 °C at the same rate, and held at 50 °C for an additional 2 minutes, according to the method described by Balet et al. (2019).

The diameter and shape of the mandioquinha-salsa starch granules were observed using Field Emission Gun – Scanning Electron Microscope (FEG-SEM) model MIRA 3 (Tescan, Czech Republic). Samples were mounted on carbon tapes and coated with gold plasma to ensure electron conductivity. Analysis was conducted at an accelerating voltage of 20 kV with magnifications of 1000x and 2000x, as described by Cremasco (2023).

Statistical analysis

The results of the analyses were expressed as mean followed by standard deviation. Analysis of variance (ANOVA) and Tukey's test were used to compare the means between the samples with 95% confidence (p < 0.05).

Results and discussion

The starch extraction process from *Arracacia xanthorrhiza* roots began with 4,980 g of raw material, previously selected and cleaned to remove surface impurities, peels, and fibrous residues. After this preparation, 3,580 g of usable fresh matter were obtained, indicating a pre-processing loss of approximately 28.11%. Following all extraction steps, 1,725 g of native starch were recovered. This corresponds to a yield of 48.18% based on the usable fresh mass, and 34.64% relative to the total raw material.

These values are lower than those reported by Leonel and Sarmento (2008), who observed a starch yield of 53.4% using the aqueous extraction method for *A. xanthorrhiza*. The reduced efficiency observed in the present study may be attributed to several factors, including variations in tuber, post-harvest storage conditions, and differences in the mechanical and operational parameters of the extraction process, as highlighted by Daiuto et al. (2005) and more recently by Kaur et al. (2023) and Nayak et al. (2022). These authors emphasize that starch recovery is strongly influenced by the botanical source, enzyme activity, and mechanical cell disruption efficiency, all of which can affect starch liberation and purity during wet extraction.

Pasting properties

The pasting properties of native and ultrasound-modified arracacha starches (at 40%, 50%, 60%, and 70% amplitudes) were evaluated using a Rapid Visco Analyzer (RVA). Significant changes were observed in viscosity and gelatinization behavior during heating and shear (Figure 1, Table 1). Granule swelling and rupture led to paste formation, with increasing viscosity proportional to the applied amplitude.

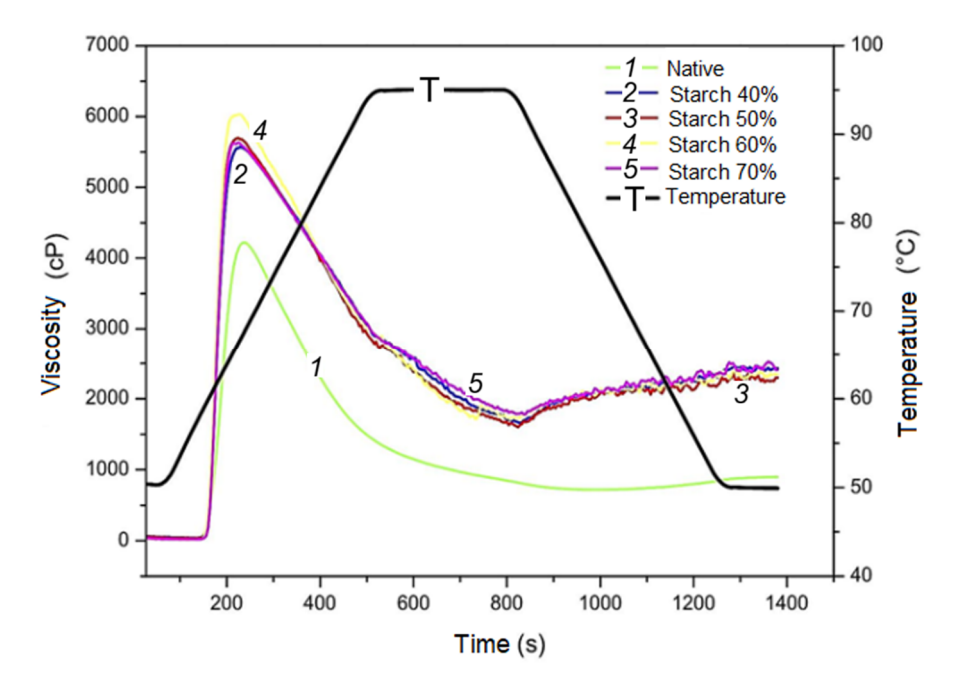


Figure 1. Viscoamylogram of native and ultrasound-treated arracacha starch

Native starch presented a pasting temperature of 78 °C and a peak viscosity (PV) of 4,000 cP. Ultrasound-treated samples showed higher pasting temperatures and PVs: 88 °C/5,500 cP (US40%), 90 °C/5,600 cP (US50%), 94 °C/6,000 cP (US60%), and 89 °C/5,550 cP (US70%). These results suggest improved thermal stability and water retention capacity, particularly at 50% and 60% amplitudes.

Table 1
Rapid Visco Analyzer (RVA) pasting properties of native and ultrasound-treated
arracacha starches

Starch	Pasting temperature, °C	Peak viscosity, cP	Breakdown, cP	Retrogradation	Final viscosity, cP
Native	59.83± 0.01ª	4284±3.51°	3570±1.52e	185±2.51 ^d	904±4.00°
Starch 40%	58.60±0.01 ^b	5568±3.51 ^d	3908±1.17°	771±7.02ª	2429±4.16 ^a
Starch 50%	59.01±0.60 b	5692±3.00 ^b	4092±2.51 ^b	698±3.00 ^b	2294±3.51 ^d
Starch 60%	58.61±0.01 b	6029±4.04ª	4322±3.00 ^a	636±4.04°	2345±1.52°
Starch 70%	58.94±0.04 b	5630±1.52°	3849±2.51 ^d	630±4.01 °	2414±4.50 ^b

^{abc}Different letters in the same column represent significant differences according to Tukey's Test (p<0.05)

Final viscosities (FV) were higher than their respective PVs in all modified samples, indicating enhanced molecular rearrangement during cooling. The US40% sample showed the lowest breakdown, suggesting greater resistance to thermal shear.

Reduced retrogradation tendency was observed in the ultrasound-treated samples, especially US40%, likely due to partial disruption of amorphous regions and preservation of crystalline domains (Zhang et al., 2021). Wang et al. (2022) reported similar findings in ultrasound-treated rice starches, which showed increased thermal stability and reduced setback. During RVA analysis, the sample was maintained at 90 °C for 6 minutes, followed by cooling at 5 °C/min to 50 °C, enabling setback evaluation. Gel formation and retrogradation behavior are directly influenced by amylose content, as shown by Li et al. (2023).

Thermogravimetric analysis (TGA)

The thermal degradation behavior of native and ultrasound-modified arracacha starches was evaluated by thermogravimetric analysis (TGA) and derivative thermogravimetry (DTG) (Figure 2, Table 2). Starch depolymerization typically begins above 300 °C and can be confirmed by the DTG peak temperature (Tp), corresponding to the second mass loss event (Zhang et al., 2020).

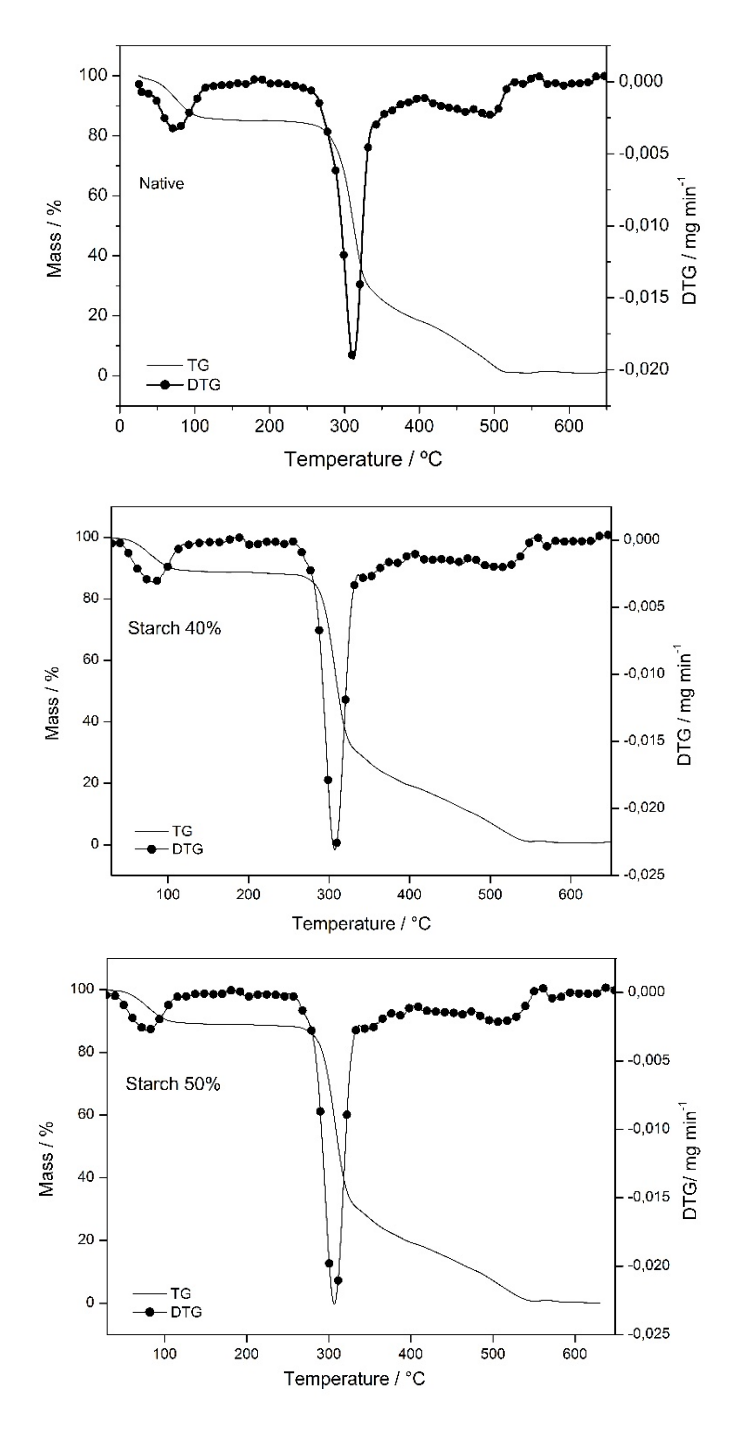


Figure 2. Thermogravimetry (TG) and Derivative Thermogravimetry (DTG) curves for the native starch, 40, 50, 60 and 70% modified starches

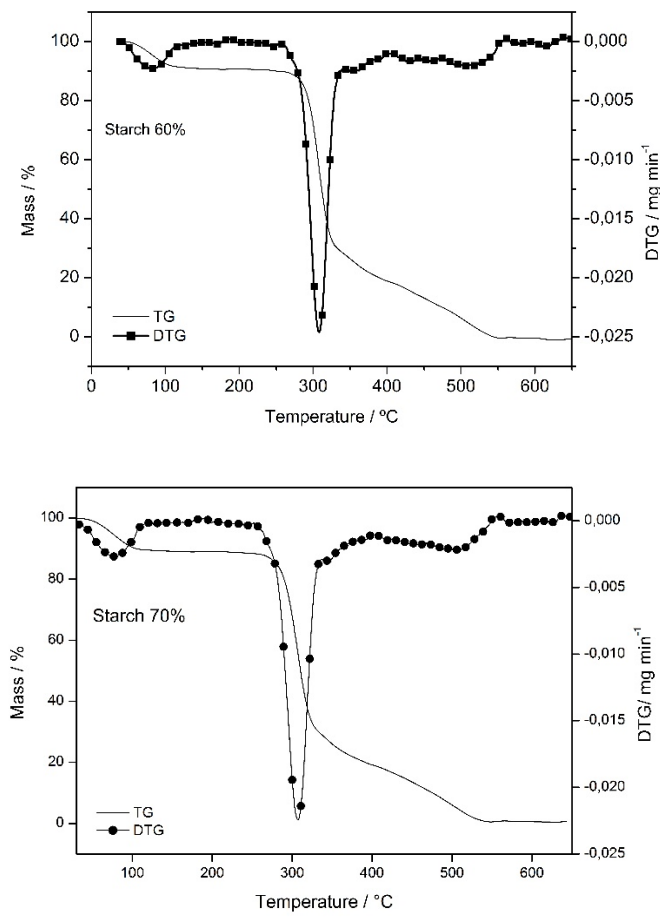


Figure 2 (continue). Thermogravimetry (TG) and Derivative Thermogravimetry (DTG) curves for the native starch, 40, 50, 60 and 70% modified starches

In the first mass loss event, attributed to moisture evaporation, all samples exhibited an initial temperature (Ti) of 30 °C. However, the samples treated at 40% and 50% amplitude showed the highest final temperatures (Tf), reaching 139.77 °C and 139.28 °C, respectively, indicating greater moisture retention.

In the second event, related to starch decomposition, the native starch showed the lowest Ti (248.59 °C), while the sample treated at 60% amplitude had the highest (254.76 °C), suggesting enhanced thermal resistance. In the third degradation step, the US40% sample exhibited the highest Ti (382.38 °C), while the US50% sample reached the highest Tf (596.44 °C).

The widest thermal stability range was observed for the US60% sample (137.12–254.76 °C), indicating that moderate ultrasound treatment may enhance structural reorganization. Ultrasonic cavitation likely disrupts covalent bonds in amylose and amylopectin chains and promotes new interactions, resulting in increased thermal resistance (Kumar et al., 2023).

Table 2
Thermogravimetric Analysis (TGA) and Derivative Thermogravimetry (DTG) results of native and ultrasound-modified starches

Starch	T, °C	1°	Stability	2°	3°
Native	Ti-Tf, °C	30-137.19	137.19–248.59	248.59-386.10	386.10- 585.22
	Tp, °C	74.78		311.88	486.96
	Δ m,%	14.10		66.15	18.85
Starch 40%	Ti-Tf, °C	30–139.77	139.77–254.24	254.24 –382.38	382.38 - 589.47
	Tp, °C	82.90		306.99	506.83
	Δ m,%	10.60		68.10	20.80
Starch 50%	Ti-Tf, °C	30–139.28	139.28–253.87	253.87–356.92	356.92–596.44
	Tp, °C	77.53		307.67	562.56
	Δ m,%	10.30		63.80	25.60
Starch 60%	Ti-Tf ,°C	30–137.12	137.12–254.76	254.76–380.42	380.42-571.44
	Tp, °C	84.14		308.10	507.34
	Δ m,%	9.13		69.42	21.12
Starch 70%	Ti-Tf, °C	30–137.61	137.61–250.99	250.99–351.50	351.50-572.16
	Tp, °C	77.82		307.35	559.85
	Δ m,%	10.90		65.20	23.60

 Δm , mass loss (%); Ti, initial temperature; Tf, final temperature; ΔT , temperature difference (°C); Tp, peak temperature (°C). Values followed by the same letter in the same column do not differ significantly according to Tukey's test (p < 0.05).

The greatest initial degradation (lowest Ti) and highest mass loss ($\Delta m = 18.76\%$) were observed in the native starch, while ultrasound-treated samples exhibited greater thermal stability. Ash content decreased in modified samples: native (0.90%), US40% (0.50%), US50% (0.35%), US60% (0.33%), and US70% (0.30%).

Instrumental and sample-related factors, such as furnace heating rate, atmosphere, crucible geometry, particle size, and thermal conductivity, can influence TGA results (Ionashiro et al., 2012). DTG, based on the first derivative of the TGA curve over time, enhances resolution of mass loss steps, enabling precise identification of decomposition stages and thermal stability profiles in starch-based biopolymers (Aggarwal and Dollimore, 1998).

Differential Scanning Calorimetry (DSC)

Differential Scanning Calorimetry (DSC) is a thermoanalytical technique used to evaluate heat-induced physical and chemical transitions by measuring enthalpy variation (Δ H) between a sample and a reference under a programmed temperature increase (Chakraborty et al., 2022). The onset (To), peak (Tp), and conclusion (Tc) temperatures are directly related to starch granule crystallinity, X-ray diffraction patterns, and the amylose-to-amylopectin ratio, which vary significantly in modified starches (Li, 2022).

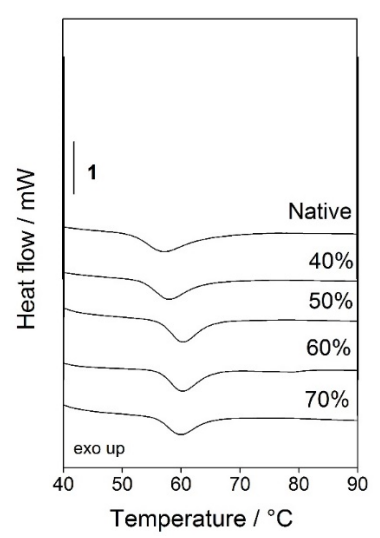


Figure 3. Differential Scanning Calorimetry (DSC) results of arracacha starch curves for the native starch, 40%, 50%, 60% and 70% modified starches

Starch gelatinization generally occurs in the presence of sufficient water and under heat (Figure 3). Table 3 reports the thermal properties during gelatinization of arracacha starch. Although the gelatinization enthalpies (ΔH_{gel}) did not differ significantly between samples (Tukey's test, p < 0.05), the starch treated with 40% ultrasound amplitude enthalpy exhibited the lowest $(12.61 \pm 0.07 \text{ J/g})$, indicating lower energy consumption. In contrast, the sample treated at 50% amplitude had the highest value $(14.80 \pm 0.19 \text{ J/g}).$

Wei et al. (2023a) observed similar trends in quinoa and maize starches subjected to ultrasound treatment, where prolonged exposure led to reduced gelatinization temperatures and ΔH values. These effects are attributed to cavitation-induced microjets that alter non-starch matrix components and affect starch—water interactions.

Table 3

Differential Scanning Calorimetry (DSC) results of arracacha starch

Starch	To, °C	Tp, °C	Tc, °C	ΔH, J/g
Native	59.04±0.13 ^a	63.77±0.00a	69.14±0.38 ^a	13.74±0.47 ^b
Starch 40%	56.55±0.05 ^b	60.96±0.01 ^b	65.93±0.10 ^b	12.61±0.07°
Starch 50%	56.12±0.02 ^d	60.28±0.03 ^d	65.03±0.04°	14.80±0.19 ^a
Starch 60%	56.28±0.00 d	60.26±0.02 ^d	65.21±0.03 °	12.82±0.11 °
Starch 70%	55.49±0.01°	59.90±0.08°	64.73±0.01°	13.56±0.10 ^b

^{abc}Different letters in the same column represent significant differences according to Tukey's Test (p<0.05).

The starches evaluated in this study showed higher ΔH values than other starches, such as organic amaranth (5.92–7.17 J/g) and enzymatically treated organic rice starch (2.60–5.10 J/g), indicating denser crystalline structures and greater thermal stability.

In studies involving hydrocolloids, gelatinization onset temperature (To) either increases or remains stable, depending on molecular interactions (Chakraborty et al., 2022). For instance, interactions between corn starch and gums such as xanthan, guar, and carboxymethylcellulose can increase due to water competition and steric hindrance. Gelatinization temperature ranges for arracacha starches were narrower (7.00–7.39 °C) than those of common starches like potato (~20 °C), suggesting more uniform and stable crystalline domains (Li, 2022). This narrow range reflects improved crystal perfection and homogeneity, reinforcing the potential of ultrasound as a structural modification tool.

Field Emission Gun – Scanning Electron Microscopy (FEG-SEM)

Field Emission Gun - Scanning Electron Microscopy (FEG-SEM) was used to evaluate the morphology of native and ultrasound-treated arracacha starch granules. All samples exhibited polygonal shapes with visible concentric growth rings, typical of structured granules (Figure 4).

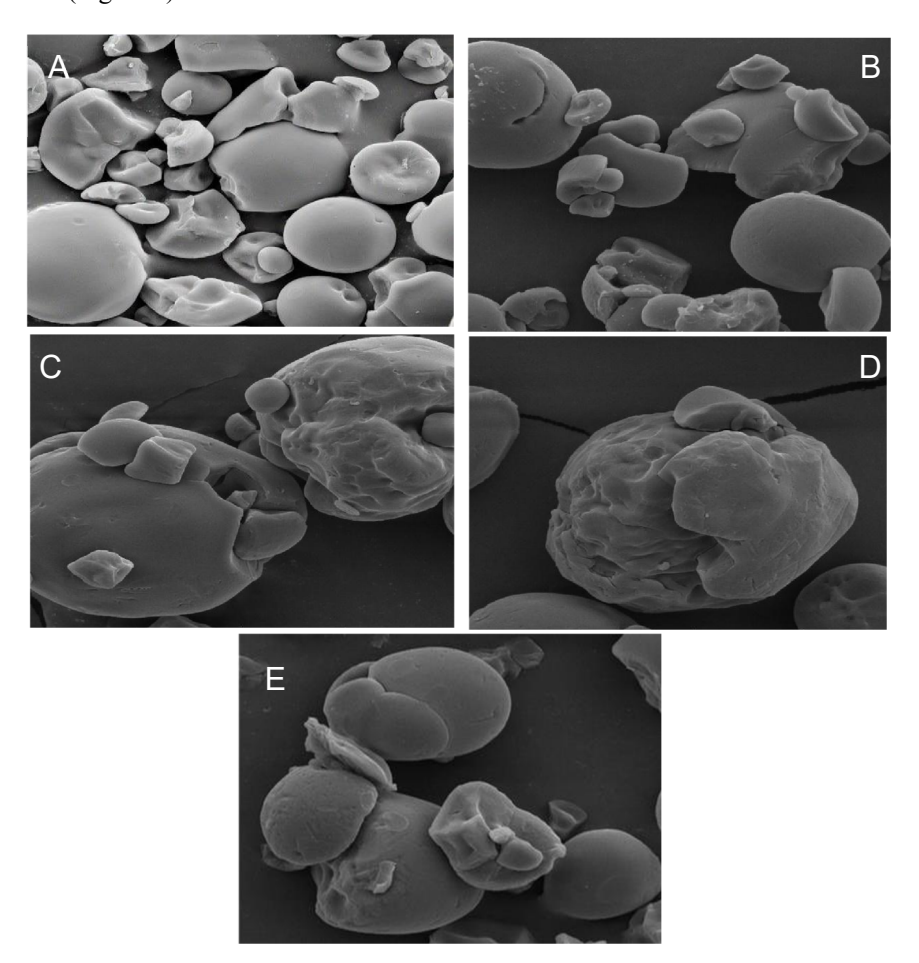


Figure 4. Scanning electron micrographs $(5,000\times)$ of native starch and starches modified by ultrasound at 40%, 50%, 60%, and 70% amplitudes:

A – Native starch, B – Starch modified at 40% amplitude; C – Starch modified at 50% amplitude; D – Starch modified at 60% amplitude; E – Starch modified at 70% amplitude.

The average granule size increased from $12.27\,\mu m$ (native) to $17.77\,\mu m$ at 50% ultrasound amplitude, followed by slight reductions at 60% and 70% amplitudes, suggesting surface erosion at higher intensities.

No granule agglomeration was observed, indicating that the ultrasound conditions applied were effective and did not compromise granule dispersion. These results are

consistent with recent findings in pea and maize starches, where ultrasound treatment caused surface roughness, microcracks, and limited swelling without loss of structural integrity (Vela et al., 2024; Wei et al., 2023b).

Ultrasound primarily disrupts amorphous regions of the starch granule, preserving crystallinity while enhancing porosity—properties that can be advantageous for applications requiring increased water interaction or enzymatic access. The observed morphological changes support the potential of ultrasonic treatment as a controlled physical modification method for starch-based systems (Jamlabadi et al., 2019; Leonel et al., 2008).

X-ray diffraction (XRD)

X-ray diffraction (XRD) analysis reveals that starch granules exhibit a lamellar structure with nanometric subunits (~9–10 nm), primarily attributed to amylopectin. This crystalline region is densely packed, hindering water and enzyme penetration and increasing resistance to hydrolysis (Zhang et al., 2023). The crystallinity patterns are classified into types A, B, and C, corresponding to the double helix packing of branched chains in amylopectin: type A is typical of cereals such as maize and rice; type B predominates in tubers and retrograded starch; and type C is an intermediate form common in roots and legumes.

The relative crystallinity index (RCI), quantified by XRD, is crucial to understanding starch structural stability (Table 4).

Crystallinity and Diffraction Pattern Peaks

Table 4

Starch	Relative crystallinity,%	Standard deviation
Native	26.34	0.0100
Starch 40%	24.03	0.0100
Starch 50%	24.71	0.0110
Starch 60%	25.67	0.0039
Starch 70%	25.86	0.0032

Crystallinity directly influences water interactions and resistance to chemical and enzymatic treatments, although excessive crystallinity may cause brittleness (Wang et al., 2021). In this study, ultrasound treatment caused changes in crystallinity depending on amplitude, with reductions at low intensity (40%) and increases at moderate amplitudes, indicating structural reorganization and a biphasic effect of ultrasound (Yu et al., 2024; Zhang et al., 2023).

Freeze-thaw cycles significantly affect starch crystalline structure, increasing amorphous regions while reducing crystalline fractions, which affects functional properties (Liu et al., 2020; Wang et al., 2019). Ultrasound primarily acts on the amorphous regions, causing localized granule disruption without altering starch polymorphs, which is beneficial for functional modification while maintaining the fundamental structure (Zheng et al., 2013).

Therefore, controlled ultrasound application emerges as a promising technique to modulate starch crystallinity and physicochemical properties, optimizing its industrial applications that require specific traits such as enhanced mechanical resistance or water absorption capacity (Vela et al., 2024).

Conclusions

The aqueous extraction of mandioquinha-salsa starch yielded results consistent with previous studies, using a simple, safe, and industrially applicable method. Ultrasonic treatment at 20 kHz significantly modified the starch properties, as confirmed by RVA, TG/DTG, DSC, FEG-SEM, and X-ray diffraction analyses. The 40% amplitude treatment showed improved shear resistance and reduced retrogradation, whereas higher amplitudes (50% and 60%) enhanced thermal stability. Morphological changes occurred without granule agglomeration, and crystallinity increased moderately but remained below that of native starch.

Overall, ultrasound proved to be an effective, sustainable, and energy-efficient method for modifying mandioquinha-salsa starch, broadening its potential in the food industry. Its low gelatinization temperature and high peak viscosity make it particularly suitable for products requiring gelation and refrigeration. This study also contributes new insights into the ultrasonic modification of this starch source, highlighting ultrasound as a clean and viable alternative for starch processing.

Acknowledgment. The authors would like to thank the Brazilian agencies CAPES and CNPq for their financial support, and the State University of Ponta Grossa (UEPG) for institutional support.

References

- Aggarwal S.L., Dollimore D. (1998), The application of thermal analysis to polymer degradation, *Journal of Thermal Analysis*, 54(1), pp. 175–190.
- Balet S., Guelpa A., Fox G., Manley M. (2019), Rapid Visco Analyser (RVA) as a tool for measuring starch-related physiochemical properties in cereals: A review, *Food Analytical Methods*, 12(10), pp. 2344–2360, https://doi.org/10.1007/s12161-019-01581-w
- Bojarczuk A., Skąpska S., Khaneghah A.M., Marszałek K. (2022), Health benefits of resistant starch: A review of the literature, *Journal of Functional Foods*, 93, 105094, https://doi.org/10.1016/j.jff.2022.105094
- Chakraborty I., Paul U.C., Rahman M.H., Mazumder N. (2022), Insight into the gelatinization properties influencing the modified starches used in food industry: A review, *Food and Bioprocess Technology*, 15(5), pp. 1234–1256, https://doi.org/10.1007/s11947-022-02761-z
- Cremasco P., Figueiredo M. (2023), Caracterização físico-química, dielétrica e reológica de amido de mandioca modificado por hidrocolóides, micro-ondas e pela combinação desses tratamentos. Tese (Doutorado) Universidade de São Paulo, Pirassununga. Disponível em, https://www.teses.usp.br/teses/disponiveis/74/74133/tde-30092024-114851/
- Daiuto E.R. (2005), Rendimento de amido em diferentes variedades de mandioca para indústria. In: Carvalho L.J.C.B. (Org.), Mandioca: fundamentos e avanços na pesquisa de melhoramento genético, pp. 209–222, Cruz das Almas, Embrapa.
- Giacomozzi J.I., Barretti B.R.V., Almeida V.S., Bet C.D., Carvalho Filho M.A.S., Lacerda L.G., Demiate I.M., Schnitzler E. (2021), Technological properties of potato starch

- treated by heat-moisture treatment with addition of organic acids, *Ukrainian Food Journal*, 10(1), pp. 90-99, https://doi.org/10.24263/2304-974X-2021-10-1-8
- Ionashiro M., Caires F.J., Gomes D. (2012), Análise térmica aplicada a biomateriais: fundamentos e aplicações, *Química Nova*, 35(1), pp. 185–190, https://doi.org/10.1590/S0100-40422012000100031
- Jamlabadi S.A., Mansouri F., Ahmadi S.A., Zarrinbandi N., Zohrei A., Nazari Z. (2019), Microstructural alterations of wheat starch caused by ultrasound: SEM analysis, *Food Science & Nutrition*, 7(3), pp. 1111–1120, https://doi.org/10.1002/fsn3.1111
- Kaur B., Arora A., Bhat Z.F., Kumar S., Kumar H. (2023), Starch: Extraction, isolation, modification, and recent applications A review, *International Journal of Biological Macromolecules*, 231, 123334, https://doi.org/10.1016/j.ijbiomac.2023.123334
- Kumar Y., Kaur M., Singh S. (2023), Ultrasound-modified starch: Structural changes and thermal degradation behaviour, *Food Chemistry*, 404, 134666, https://doi.org/10.1016/j.foodchem.2022.134666
- Leonel M., Sarmento S.B. (2008), Características físico-químicas de tubérculos e raízes tropicais e suas farinhas, *Ciência e Agrotecnologia*, 32(2), pp. 455–463, https://doi.org/10.1590/S1413-70542008000200016
- Leonel M., Cereda M.P., Sarmento S.B. (2008), Morphological characterization of arrowroot and *Canna edulis* starch granules, *Ciência e Agrotecnologia*, 3(2), pp. 455–463
- Li C. (2022), Recent progress in understanding starch gelatinization: Kinetics, water content and DSC modelling, *Carbohydrate Polymers*, 289, 119446, https://doi.org/10.1016/j.carbpol.2022.119446
- Li X., Zhang Y., Wang J., Zhao Y., Sun Q., Chen L. (2022), Structural and physicochemical changes of starches after ultrasonic treatment: A review, *Trends in Food Science & Technology*, 123, pp. 27–37, https://doi.org/10.1016/j.tifs.2022.03.013
- Liu Y., Zhao Y., Wang Y., Zhang X., Zhang J. (2020), Effects of freeze-thaw cycles on physicochemical properties of starches, *Food Chemistry*, 320, 126598, https://doi.org/10.1016/j.foodchem.2020.126598
- Liu G., Ge X., Guo C., Liu B. (2023), Effect of ultrasonic treatment on the structure and physicochemical properties of pea starch, *Foods*, 12(13), 2620, https://doi.org/https://doi.org/10.3390/foods12132620
- Nayak B., Singh J., Li L. (2022), Starch recovery and efficiency: factors influencing starch yield from plant sources, *Food Hydrocolloids*, 128, 107603, https://doi.org/10.1016/j.foodhyd.2022.107603
- Vela A.J., Villanueva M., Ronda F. (2024), Ultrasonication: An efficient alternative for physical modification of starches, flours and grains, *Foods*, 13(15), 2325, https://doi.org/10.3390/foods13152325
- Wang L., Li M., Chen Y., Zhang X., Huang J. (2021), Effects of ultrasonic treatment on the physicochemical properties of starch: A review, *Carbohydrate Polymers*, 265, 118061, https://doi.org/10.1016/j.carbpol.2021.118061
- Wei Y., Li G., Zhu F. (2023a), Impact of long-term ultrasound treatment on structural and thermal stability of quinoa and maize starches, *Ultrasonics Sonochemistry*, 80, 105850, https://doi.org/10.1016/j.ultsonch.2023.105850
- Wei Y., Li G., Zhu F. (2023b), Effect of ultrasonic treatment on physicochemical properties of pea starch, *Foods*, 12(13), 2620, https://doi.org/10.3390/foods12132620
 - Yu J., Xie F., Wang Q., Zhang L., Liu Y. (2024), Ultrasound-assisted physical modification of starch: A comprehensive review, *Ultrasonics Sonochemistry*, 92, 106227, https://doi.org/10.1016/j.ultsonch.2023.106227

—— Processes and Equipment——

- Zhang Y., Liu X., Sun Y., Wang Y. (2020), Thermal behavior and decomposition kinetics of native and modified starches, *Thermochimica Acta*, 689, 178642, https://doi.org/10.1016/j.tca.2019.178642
- Zhang H., Li G., Zhu F., Chen J., Wang S. (2023), Impact of ultrasound on starch properties and its applications: A review, *Food Hydrocolloids*, 133, 107877, https://doi.org/10.1016/j.foodhyd.2022.107877
- Zheng B., Wang J., Zhou Y., Li F., Chen X. (2013), Ultrasound treatment of starch: Effect on physicochemical properties and structure, *Food Chemistry*, 136(3-4), pp. 1435-1441, https://doi.org/10.1016/j.foodchem.2012.09.122
- Zhu F. (2015), Modification of starch by ultrasound treatment: A review, *Carbohydrate Polymers*, 122, pp. 399-416, https://doi.org/10.1016/j.carbpol.2014.11.070

Cite:

UFJ Style

dos Santos S.S.J., Bet C.D., Bisinella R.B.Z., Romko S.S., Schnitzler E. (2025), Ultrasound-assisted modification and multianalytical characterization of organic *Arracacia xanthorrhiza* starch, *Ukrainian Food Journal*, 14(3), pp. 406–419, https://doi.org/10.24263/2304-974X-2025-14-3-4

APA Style

dos Santos, S.S.J., Bet, C.D., Bisinella, R.B.Z., Romko S.S., & Schnitzler E. (2025). Ultrasound-assisted modification and multianalytical characterization of organic *Arracacia xanthorrhiza* starch. *Ukrainian Food Journal*, *14*(3), 406–419. https://doi.org/10.24263/2304-974X-2025-14-3-4

Impact of tocopheryl and retinyl acetates on oxidative stability of *Hypericum perforatum* L. and *Matricaria recutita* L. macerates in corn oil during storage

Oleksandra Kunyk^{1,2}, Walter Leal¹, Vasyl Pasichniy², Andrii Marynin², Olena Stabnikova²

- 1 Hamburg University of Applied Sciences, Hamburg, Germany
- 2 National University of Food Technologies, Kyiv, Ukraine

Abstract

Keywords:

Corn
Oil
Herb
Macerates
Tocopherol
Retinol
Storage
Oxidative
stability

Article history:

Received 19.05.2025 Received in revised form 16.09.2025 Accepted 30.09.2025

Corresponding author:

Oleksandra Kunyk E-mail: kulish.aleksa@ gmail.com

DOI:

10.24263/2304-974X-2025-14-3**Introduction.** This study examined the influence of tocopheryl and retinyl acetates on the oxidative stability of *Hypericum perforatum* L. and *Matricaria recutita* L. macerates in corn oil during storage.

Materials and methods. Refined corn oil macerated with *H. perforatum* and *M. recutita* were supplemented with tocopheryl acetate (500–1500 mg/kg) or retinyl acetate (170–690 mg/kg) and stored for six weeks at 20±2 °C and 4±1 °C. Oxidative stability was evaluated by acid value (AV), radical scavenging activity (RSA) by the 1,1-diphenyl-2-picrylhydrazyl (DPPH) assay; vitamin retention by high-performance liquid chromatography, and fatty acid profile by gas chromatography.

Results and discussion. Both macerates contained \sim 60–62% linoleic acid, reflecting high oxidisability. Initial RSA was slightly higher in *H. perforatum* (\approx 40%) than in *M. recutita* (\approx 36%), consistent with its detectable vitamin A and higher β-carotene content. Baseline AV was 0.40 mg KOH/g. After six weeks at 20 °C, AV in untreated controls exceeded the deterioration threshold (\sim 1.0 mg KOH/g), reaching 1.05 (*H. perforatum*) and 1.12 (*M. recutita*) mg KOH/g. Storage at 4 °C reduced AV increase by \sim 25–35% (controls: 0.72 and 0.79 mg KOH/g, respectively), confirming temperature as a key factor in hydrolytic/oxidative change.

Antioxidant addition produced clear, dose-dependent protection. Tocopheryl acetate was most effective across both macerates and temperatures. At 1500 mg/kg, final AVs were limited to 0.65 (*H. perforatum*) and 0.68 (*M. recutita*) at 20 °C (~35–40% lower than controls), and to 0.50–0.51 mg KOH/g at 4 °C, i.e., close to baseline and well below sensory-risk thresholds. Intermediate doses (500–1000 mg/kg) also reduced AV, with effects scaling by concentration, suggesting that chain-breaking activity of α-tocopherol esters predominated over any pro-oxidant side effects at tested levels. Retinyl acetate conferred a weaker, temperature-dependent effect. At its highest dose, AVs approached ~1.00 mg KOH/g in both macerates at 20 °C, which is better than controls but near the acceptability threshold, while at 4 °C values were 0.72 (*H. perforatum*) and 0.75 mg KOH/g (*M. recutita*). Thus, retinyl acetate alone does not ensure stability under ambient storage but can complement temperature control.

Conclusion. The combination of tocopheryl acetate at 1500 mg/kg with storage at 4 °C was most effective in preserving oxidative stability in both macerates. *H. perforatum* showed inherently greater resistance to oxidation than *M. recutita*, indicating its superior suitability as a lipid carrier in cosmetic formulations.

Introduction

Lipid oxidation is a key factor influencing the quality, safety, and shelf life of vegetable oils. The accumulation of primary (hydroperoxides) and secondary (aldehydes, ketones) oxidation products impairs sensory properties, nutritional value, and functional properties of lipid raw materials and fat-containing products (Loganathan et al., 2022; Martín-Torres et al., 2023). Recent reviews highlight the multifactorial nature of this process driven by unsaturation degree, free fatty acid content, trace metals, temperature, and oxygen exposure, and the need for validated stability assessments using peroxide value, acid value, thiobarbituric acid reactive substances, and induction period (Chabni et al., 2024; Li et al., 2019).

In cosmetic technologies, edible vegetable oils are increasingly used as emulsion components due to their biocompatibility, protective barrier properties, and the content of lipophilic bioactive substances (Hantikainen and Lagerros, 2023; Kunik et al., 2022). Recent reviews in cosmetic dermatology highlight their role in skin barrier restoration and antioxidant protection (Liu et al., 2025; McMullen, 2024), which align the quality requirements of foodgrade lipids with those essential for cosmetic stability (Abdalla et al., 2024).

A particular area of interest is oil macerates obtained by infusing plant material in refined edible oils (Arellano et al., 2019). More often refined corn oil is used as the base for macerates. However, the removal of natural antioxidants during refining, together with a possible increase in free fatty acid content (introduced by plant residues), can compromise oxidative stability, thereby increasing the need for antioxidant protection (Ma et al., 2023). This correlates with data on differences in endogenous antioxidants (types and levels of tocopherols) across oils and their contribution to stability (Kim et al., 2019).

Among strategies to improve the stability of lipid systems in food and cosmetic matrices, supplementation with lipophilic antioxidants, in particular fat-soluble vitamins, plays an important role (Niki, 2014; Shahidi and Zhong, 2010; Thiele et al., 2005). Recent studies highlight the chain-breaking mechanisms of tocopherols (vitamin E) and their synergy with other antioxidants, with attention given to optimal concentrations and matrices (Athanasiadis et al., 2023; Bayram and Decker, 2023; Martínez-Senra et al., 2024). For applied purposes, accelerated antioxidant screening tests in real oil systems (Rancimat/Oxitest) remain relevant (Chabni et al., 2024).

In light of this, the present study investigates the potential to improve the oxidative stability of *Hypericum perforatum* (common name klamathweed) and *Matricaria recutita* (common name chamomile) macerates prepared in refined corn oil by supplementing them with fat-soluble vitamins. The objectives are: (i) to quantitatively assess the effect of vitamin addition on acid value dynamics and antioxidant capacity during 6 weeks of storage at 4°C and 20°C; and (ii) to establish practical parameters (concentration, storage conditions) ensuring technological reliability when incorporated into cosmetic emulsions. This approach aligns with current trends in using natural antioxidants and combines food lipid quality requirements with cosmetic stability criteria.

Materials and methods

Materials

Oil samples. Vegetable oils in the form of macerates of klamathweed (*Hypericum perforatum* L.) and chamomile (*Matricaria chamomilla* L.) were used in the study. They were prepared by infusing the plant raw material in refined, deodorised corn oil (Leko Style Ltd., Kyiv, Ukraine) (Figure 1).

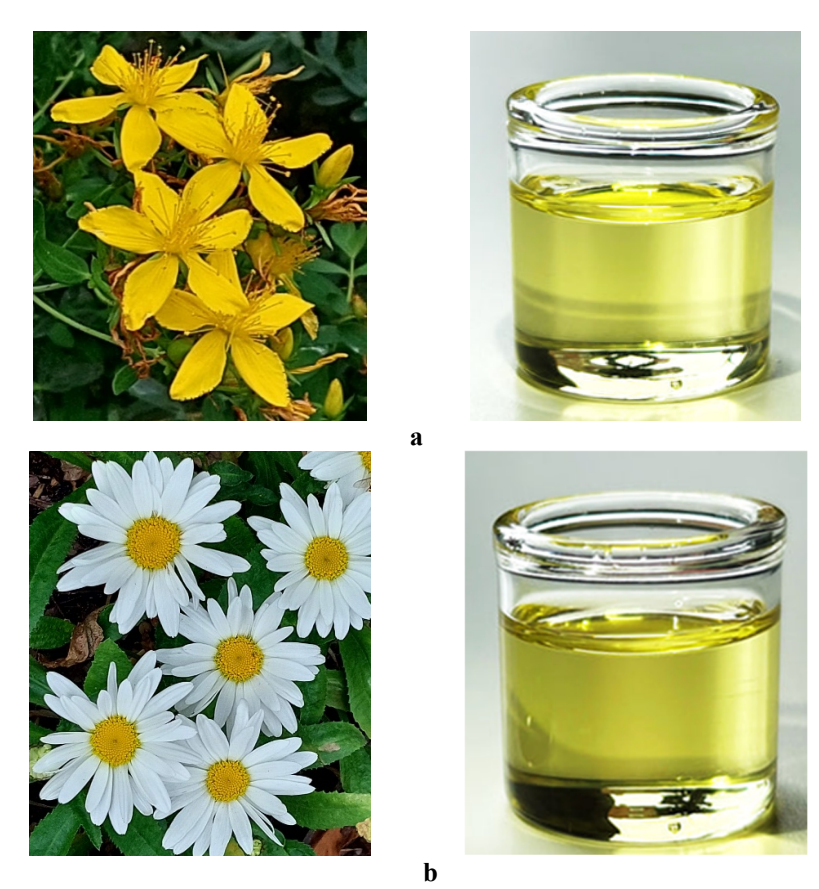


Figure 1. Images of herbs and their oil macerates: a, *Hypericum perforatum*; b, *Matricaria recutita*

The basic characteristics of macerates provided by the manufacturer is shown in Table 1.

Table 1
Characteristics of the herb oil macerates

Characteristics	H. perforatum	M. recutita
Acid value, mg KOH/g	0.4	0.4
Refractive index (at 20°C)	1.4730	1.4720
Density (at 20°C)	0.921	0.920
The number of KMAFAnM, CFU/mL	25	22

Note: KMAFAnM, the total number of mesophilic aerobic and facultative anaerobic microorganisms; CFU, colony-forming unit

According to the manufacturer's certificate, both macerates showed no acute skin toxicity, irritation, or sensitisation. Tocopheryl acetate (vitamin E, C₃₁H₅₂O₃; PrJSC Tekhnolog, Uman, Ukraine) and retinyl acetate (vitamin A, C₂₀H₃₀O; PJSC Vitaminy, Uman, Ukraine) were used as antioxidant additives, both meeting pharmacopeia quality standards.

Determination of oxidative stability of herbal oil macerates

Determination of acid value. Acid value (AV) was determined by titration according to ISO 660:2020 with minor modifications. An oil sample $(4.0-5.0 \text{ g}, \pm 0.01 \text{ g})$ was dissolved in 50 mL of ethanol–diethyl ether (1:1, v/v), and 3–5 drops of 1% phenolphthalein were added as an indicator. The mixture was titrated with 0.1 N potassium hydroxide solution (KOH) under constant stirring until a stable pale pink colour persisted for \geq 30 s. AV (mg KOH/g) was calculated as:

$$AV = 5.61 \frac{V \cdot K}{m},$$

where 5.61 is titre of 0.1 N KOH solution, mg/mL;

V is volume of 0.1 N KOH solution used for titration, mL;

K is correction factor of the titre;

m is mass of the oil sample, g.

Determination of antioxidant activity. Radical scavenging activity (RSA) was determined using the 1,1-diphenyl-2-picrylhydrazyl (DPPH) assay. A stock solution was prepared by dissolving 24 mg DPPH in 100 mL methanol and filtered to obtain a working solution with absorbance ~ 0.973 at 517 nm. For analysis, 3 mL of the DPPH working solution was mixed with 100 μ L of oil (control: 100 μ L methanol). Samples were incubated in darkness for 30 min, and absorbance was measured at 517 nm. Replicates (n = 4) showed a standard deviation ≤ 0.15 . RSA (%) was calculated as:

$$RSA = \left(\frac{A_c - A_s}{A_c}\right) \times 100\%$$

where Ac is control reaction absorbance; As is testing specimen absorbance.

Determination of quantitative composition of fatty acids. Fatty acid composition was analysed by gas chromatography (ISO 12966-1:2014) using a Crystal-2000M system with an Agilent DB-FFAP column (50 m \times 0.32 mm \times 0.50 µm). Sample volume was 1 µL; helium was used as the carrier gas. Conditions: injector 220 °C; evaporator 230 °C; detector 270 °C; isothermal programme: 60 °C (1 min), ramp to 160 °C at 20 °C/min (hold 1 min), then to 250 °C at 5 °C/min (hold 15 min). Fatty acid methyl esters were identified with a 37-component FAME Mix (Supelco), and chromatograms were processed using HP ChemStation software.

Determination of vitamin A, vitamin E and β-carotene content. The content of vitamin A (retinol and its esters), vitamin E (tocopherols), and β-carotene was determined by high-performance liquid chromatography (HPLC). Sample preparation: 0.50 ± 0.01 g of oil sample was dissolved in 10 mL of n-hexane and filtered through a 0.45 μm membrane filter. Chromatographic conditions: Agilent 1260 Infinity system (Agilent Technologies, USA); Zorbax Eclipse XDB-C18 column, 250×4.6 mm, 5 μm; mobile phase: methanol: water (95:5, v/v); isocratic elution; flow rate: 1.0 mL/min; column temperature: 25° C; injection volume: 20 μL. Detection: 325 nm for retinol (vitamin A); 292 nm for α-tocopherol (vitamin E); 450 nm for β-carotene.

Quantitative determination was carried out by the external standard method using standard samples of retinyl acetate, α -tocopheryl acetate, and β -carotene (Sigma-Aldrich, USA, purity \geq 97%). Results were expressed in mg/100 g of product.

Statistical analysis. The statistical analysis of the results was carried out using Microsoft Excel. All determinations were performed in triplicate. Values are expressed as mean±standard deviation (SD).

Results and discussion

Fatty acid composition of the corn oil macerates with *Hypericum perforatum* and *Matricaria recutita*

Fatty acid composition is a key determinant of both the nutritional and technological value of vegetable oils, as well as their oxidative stability during storage (Kim et al., 2022). Table 2 summarises the content of individual fatty acids in the corn oil macerates with *Hypericum perforatum* and *Matricaria recutita*.

Table 2 Fatty acid composition of the corn oil macerates

Fatty asid	Content,% of total amount, in	n corn oil macerates with
Fatty acid	H. perforatum	M. recutita
C14:0 Myristic	0.07±0.01	0.07±0.01
C16:0 Palmitic	6.46±0.03	6.57±0.03
C16:1 Palmitoleic	0.13±0.01	0.11±0.01
C17:0 Margaric	0.03±0.01	0.04±0.01
C17:1 Margaroleic	0.02±0.01	0.02±0.01
C18:0 Stearic	3.40±0.02	3.36±0.02
C18:1 Oleic	26.24±0.10	27.67±0.10
C18:2 Linoleic	61.99±0.15	60.11±0.15
C18:3 Linolenic	0.09±0.01	0.26±0.01
C20:0 Arachidic	0.25±0.01	0.36±0.01
C20:1n11 Gadoleic	0.20±0.01	0.32±0.01
C22:0 Behenic	0.71±0.01	0.78±0.01
C22:2 Docosadienoic	_	0.08±0.01
C24:1 Nervonic	0.26±0.01	0.26±0.01
Unidentified	0.41	0.25
SFA	10.92	11.18
USFA	88.67	88.57
USFA/SFA	8.12	7.92

Note: Indicates the standard deviation of the data, n = 3; SFA, saturated fatty acid; USFA, unsaturated fatty acid.

According to the obtained data (Table 2), both macerates were dominated by polyunsaturated fatty acids, particularly linoleic acid (C18:2), which accounted for 61.99% in *Hypericum* macerate and 60.11% in *Matricaria* macerate. A considerable proportion was also represented by monounsaturated oleic acid (C18:1) – 26.24% and 27.67%, respectively. The content of saturated fatty acids was relatively low; among them, palmitic acid (C16:0) prevailed at 6.46 - 6.57%, followed by stearic acid (C18:0) at 3.36 - 3.40%. Other saturated acids (myristic, margaric, arachidic, and behenic) were present in amounts below 1%. The *Matricaria* macerate contained a slightly higher proportion of linolenic acid (C18:3) – 0.26% compared with 0.09% in *Hypericum* macerate, and uniquely included docosadienoic acid (C22:2) at 0.08%.

Thus, both samples were characterised by a high proportion of polyunsaturated fatty acids, dominated by linoleic acid, which corresponds to the fatty acid profile of corn oil used as the maceration base (Arellano et al., 2019). The high polyunsaturated fatty acids (PUFA) content, particularly linoleic acid (\approx 60 – 62%) together with the presence of linolenic acid, indicates increased susceptibility of the studied macerates to oxidative degradation during storage (Shahidi and Zhong, 2010). This profile underlines the need for protective measures, including antioxidant supplementation and optimal storage conditions, which became the focus of the present study.

The predominance of linoleic acid confirms that both macerates inherit the lipid profile of corn oil, the solvent used for maceration. However, the presence of minor differences, such as the higher linolenic acid content and unique docosadienoic acid fraction in *Matricaria* macerate, may explain its relatively lower oxidative stability observed later in storage experiments. Similar relationships between PUFA enrichment and reduced stability have been reported for soybean and sunflower oils, where linolenic acid, even at concentrations below 1%, acts as a strong pro-oxidant trigger (Shahidi and Zhong, 2010). From a formulation perspective, this suggests that *Hypericum* macerates may serve as a more robust lipid carrier in cosmetic emulsions than *Matricaria*, unless additional antioxidant measures are applied.

Antioxidant capacity of the corn oil macerates with *Hypericum perforatum* and *Matricaria recutita*

Antioxidant activity of oil systems is an important indicator of their potential to slow oxidative processes during storage and in finished products (Abdalla et al., 2024). It reflects the ability of the lipid fraction to neutralize free radicals generated through auto-oxidation, thereby preserving the functional and sensory properties of the product (Wang et al., 2023). For the *H. perforatum* macerates, radical scavenging activity (RSA) determined by the DPPH assay was 40%, whereas the M. recutita macerate showed a lower value, approximately 36%. This difference can be attributed to variations in the composition of biologically active compounds extracted into the oil phase during maceration, particularly phenolic constituents and pigments with antioxidant properties (Harhaun et al., 2020). The higher RSA observed in the *H. perforatum* macerate indicates its greater potential to stabilize the lipid phase, making it more promising for extending the shelf life of products formulated on its basis.

This finding is consistent with the broader evidence that plant-derived antioxidants, particularly phenolic compounds and carotenoids, contribute significantly to the radical scavenging activity of herbal oils. The slightly higher RSA values in *H. perforatum* macerate suggest that its natural antioxidant profile may complement the effect of added antioxidants during storage. In contrast, the lower intrinsic RSA of *M. recutita* macerate underlines its greater susceptibility to oxidative changes and highlights the need for additional stabilisation strategies.

Vitamin A and β-carotene content in of the corn oil macerates with *Hypericum* perforatum and Matricaria recutita

The contents of fat-soluble vitamin A (retinol), β -carotene, and individual isomers of vitamin E (tocopherols) in *Hypericum perforatum* and *Matricaria recutita* macerates are shown in Table 3.

Table 3
Content of fat-soluble vitamins in the corn oil macerates

Vitamin	Corn oil macerate with			
	H. perforatum	M. recutita		
Vitamin A (retinyl acetate), mg/kg	0.78	n.a		
β-carotene, mg/kg	0.49	0.26		
Vitamin E (tocopheryl acetate), mg/kg:				
δ-tocopherol	7.33	8.09		
γ-tocopherol	15.10	15.10		
α-tocopherol	514.00	509.00		

Note: n.a., not applicable.

Vitamin A in the form of retinol was detected only in the *H. perforatum* macerate (0.78 mg/kg), whereas in the *M. recutita* macerate its concentration was below the detection limit of the method. The β -carotene content was 0.49 mg/kg in *H. perforatum* (klamathweed) and 0.26 mg/kg in *M. recutita* (chamomile), indicating a limited provitamin A potential in both macerates.

In the tocopherol profile of both samples, α -tocopherol predominated (over 500 mg/kg), while the γ - and δ -isomers were present in much smaller amounts (15.1 and 7.33 – 8.09 mg/kg, respectively).

These results suggest that the presence of β -carotene and high levels of α -tocopherol in the investigated macerates may play an important role in slowing oxidative processes and supporting quality preservation during storage. At the same time, the relatively low concentrations of γ - and δ -tocopherols indicate a potential need for additional antioxidant supplementation to prolong product shelf life (Niki, 2014).

These findings align with existing evidence that α -tocopherol is the primary antioxidant component in most refined vegetable oils and provides strong radical scavenging activity. However, the absence of detectable retinol in *M. recutita* macerate and the relatively low β -carotene levels in both samples point to a limited provitamin contribution, which may not be sufficient for long-term stabilisation under ambient storage. The predominance of α -tocopherol suggests that these macerates already possess a significant inherent antioxidant potential, but the lack of diversity in the tocopherol profile could reduce resilience against prolonged oxidative stress. Therefore, fortification with additional antioxidants or the use of controlled storage conditions may be required to ensure oxidative stability over an extended shelf life.

Changes in the acid value of the corn oil macerates with *Hypericum perforatum* and *Matricaria recutita* under the influence of fat-soluble vitamin supplementation

In this study, the effect of fat-soluble vitamin supplementation on the acid value of klamathweed (*Hypericum perforatum*) and chamomile (*Matricaria recutita*) macerates was investigated. Vitamin E was applied at concentrations of 500, 1000, and 1500 mg/kg, and vitamin A at 170, 340, and 690 mg/kg. The samples were stored under two temperature regimes $-20\pm2^{\circ}$ C (ambient) and $4\pm1^{\circ}$ C (refrigerated). Acid value was measured weekly over a period of six weeks (Figure 3, 4).

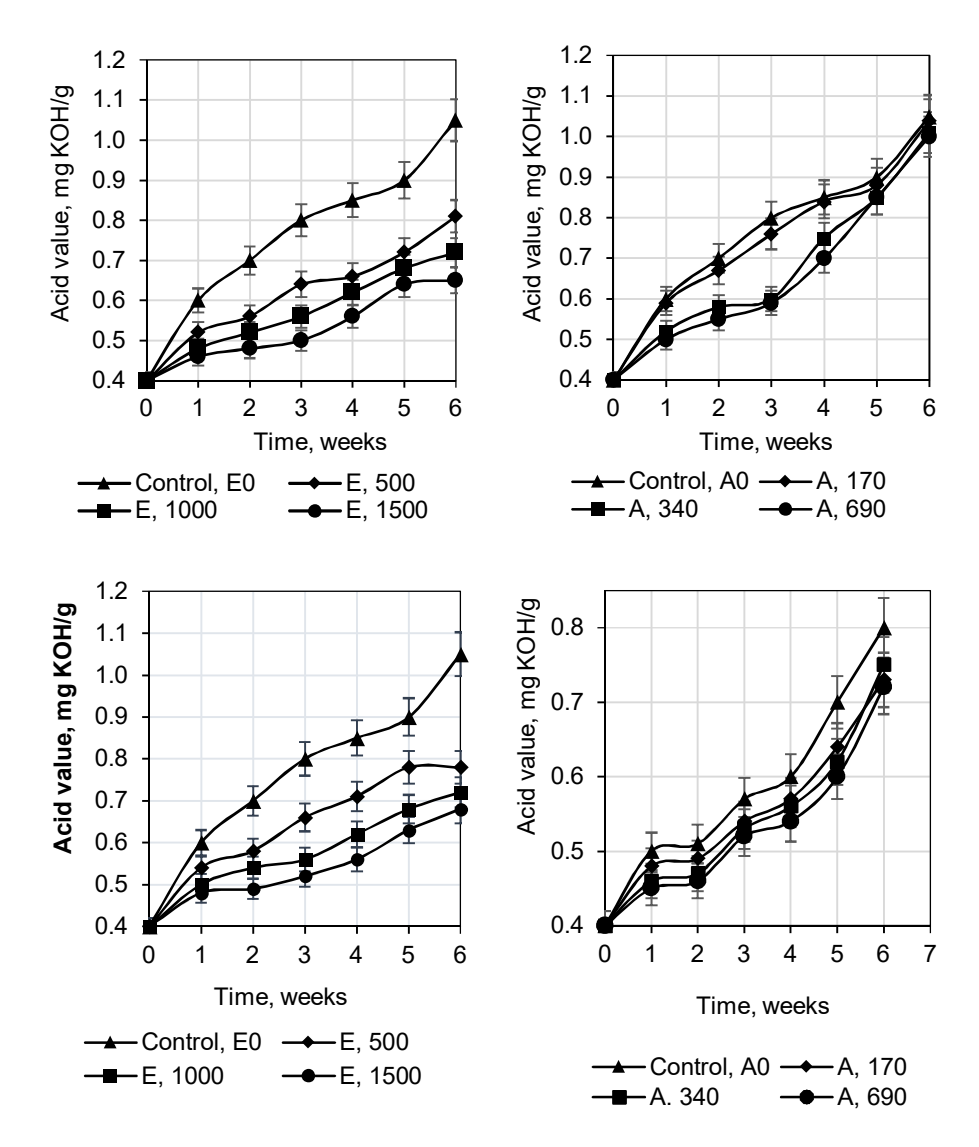


Figure 3. Changes in acid value of *Hypericum perforatum* macerates during 6-week storage with fat-soluble vitamins.

```
Vitamin E, mg/kg: \blacktriangle – 0 (control); \spadesuit – 500; \blacksquare – 100; \bullet - 1500 at 20oC (a) and 4 °C (c); Vitamin A, mg/kg: \blacktriangle – 0 (control); \spadesuit – 170; \blacksquare – 340; \bullet - 690 at 20°C (b) and 4 °C (d).
```

The selected concentration ranges were justified by previously published studies (Kunik et al., 2016) and safety considerations: the lower levels correspond to doses recommended for slowing oxidative processes in vegetable oils without affecting organoleptic properties, while the upper levels are close to the maximum permitted concentrations used in food and cosmetic fat-based products to extend shelf life (Syed, 2016). This approach allowed the evaluation of the effectiveness of vitamins as antioxidants under realistic production conditions.

Figure 3 shows the changes in the acid value of *Hypericum perforatum* macerates during six weeks of storage at 20±2°C and 4±1°C with the addition of fat-soluble vitamins E and A at different concentrations. In the control samples (without supplementation) stored at ambient temperature, acid value increased most intensively, exceeding 1.0 mg KOH/g by week six, with an average rate of 0.0964 mg KOH/g per week. Lowering the storage temperature to 4 °C significantly slowed both hydrolytic and oxidative processes across all sample groups: even in the controls, final acid values were 25–35% lower compared with those at 20°C.

The addition of vitamin E at concentrations of 500–1500 mg/kg produced a pronounced antioxidant effect, reducing the rate of acid value increase, with the greatest protection observed at 1500 mg/kg. The effect was evident at both ambient and refrigerated storage, though at 4 °C the increase in acid value remained minimal regardless of dose. Vitamin A at 170–690 mg/kg also reduced the accumulation of free fatty acids, but its protective action was less pronounced than that of vitamin E, particularly at 20°C. This may be attributed to the lower stability and weaker antioxidant capacity of vitamin A compared with tocopherols. Under refrigeration (4 °C), the differences between doses of vitamin A were marginal, and final acid values generally did not exceed 0.6 mg KOH/g.

Thus, the combination of refrigeration and supplementation with vitamin E at 1500 mg/kg proved to be the most effective strategy for slowing oxidative degradation of Hypericum perforatum macerates.

In *Matricaria recutita* macerates, acid value also increased over the six-week storage period (Figure 4) at both 20°C and 4°C, but the rate of accumulation was higher than in Hypericum perforatum. This indicates a somewhat lower inherent resistance of chamomile macerates to oxidative processes (Li et al., 2019). At ambient temperature, control samples exceeded 1.0 mg KOH/g by the end of the trial, whereas the corresponding increase in H. perforatum was less pronounced.

The addition of tocopheryl acetate at 500–1500 mg/kg significantly slowed the rise in acid value, with the strongest effect again observed at the maximum concentration. Retinyl acetate also reduced the rate of oxidative change, but its action was consistently weaker than that of tocopheryl acetate, in line with the results for *H. perforatum* (Figure 3). Lowering the storage temperature to 4°C further improved the stability of M. recutita macerates in all series; however, even under refrigeration their acid values rose faster than in the corresponding H. perforatum samples. This confirms that the chemical composition of the raw plant material – in particular, the content and profile of endogenous antioxidants – plays a decisive role in the oxidative stability of macerates (Abdalla et al., 2024).

The results clearly demonstrate that both the type of antioxidant and the storage temperature had a decisive influence on the acid value dynamics of the studied macerates. Tocopheryl acetate consistently provided the strongest protective effect, in agreement with previous findings on its chain-breaking activity in vegetable oils (Shahidi and Zhong, 2010). Its effectiveness was dose-dependent, with the highest concentration (1500 mg/kg) maintaining acid values well below the critical threshold during six weeks of storage. Retinyl acetate, although beneficial, showed weaker activity, which may be related to its lower oxidative stability and different radical scavenging mechanisms.

The greater increase in acid value in *M. recutita* compared with *H. perforatum* supports the idea that intrinsic plant-derived antioxidants, such as β -carotene and retinol (found in H. perforatum), play a significant role in lipid stability. Nevertheless, refrigeration alone already slowed acid value growth by 25–35%, emphasising temperature as a key determinant of oxidative and hydrolytic stability.

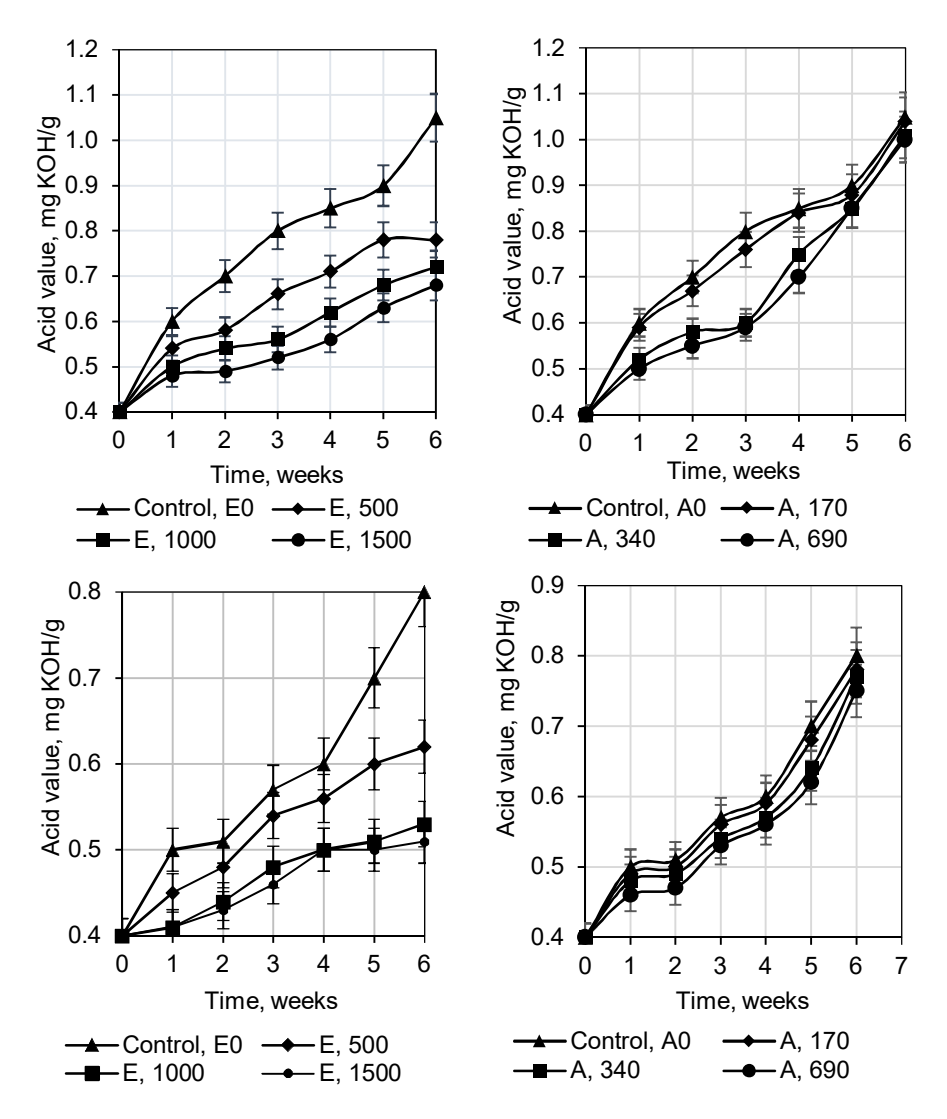


Figure 4. Changes in acid value of *Matricaria recutita* macerates during 6-week storage with fatsoluble vitamins.

Vitamin E, mg/kg: $\triangle = 0$ (control); $\blacklozenge = 500$; $\blacksquare = 100$; $\bullet = 1500$ at 20° C (a) and 4° C (c); vitamin A, mg/kg: $\triangle = 0$ (control); $\blacklozenge = 170$; $\blacksquare = 340$; $\bullet = 690$ at 20° C (b) and 4° C (d).

From a practical perspective, these results highlight that combining cold storage with tocopheryl acetate supplementation at 1500 mg/kg provides a robust strategy for prolonging the shelf life of herbal macerates. Such an approach is directly applicable to cosmetic emulsions and other formulations where oxidative stability is a prerequisite for product quality and consumer safety.

Conclusions

Macerates of *Hypericum perforatum* and *Matricaria recutita* in refined corn oil contained high levels of linoleic acid (~60–62%), rendering them highly prone to oxidation. Initial radical scavenging activity (RSA) was higher in corn oil macerate with *H. perforatum* (~40%) than with *M. recutita* (~36%), reflecting its greater β-carotene and vitamin A content. After six weeks at 20 °C, acid values in controls exceeded 1.0 mg KOH/g, while refrigeration at 4 °C reduced this increase by 25–35%. Tocopheryl acetate (500–1500 mg/kg) significantly delayed acid value increase, with the strongest effect at 1500 mg/kg, particularly at 4 °C. Retinyl acetate (170–690 mg/kg) also conferred protection but was consistently less effective, especially at 20 °C. Overall, *H. perforatum* macerates were more oxidation-resistant than *M. recutita*, and the combination of refrigeration with 1500 mg/kg tocopheryl acetate provided the most effective stabilization strategy.

Acknowledgment. This publication is connected to a research project funded by the German National Academy of Sciences Leopoldina under a Leopoldina Ukraine Distinguished Fellowship.

References

- Abdalla S., Aroua M.K., Gew L.T. (2024), A comprehensive review of plant-based cosmetic oils (virgin coconut oil, olive oil, argan oil, and jojoba oil): Chemical and biological properties and their cosmeceutical applications, *ACS Omega*, 9(44), pp. 44019–44032, http://doi.org/10.1021/acsomega.4c04277
- Arellano D., Badan-Ribeiro A., Serna-Saldivar S. (2019), Corn oil: Composition, processing, and utilization, In: S.O. Serna-Saldivar (Ed.), *Corn. Chemistry and Technology*, pp. 593–613, 3nd ed., Elsevier Inc., http://doi.org/10.1016/B978-0-12-811971-6.00021-8
- Athanasiadis V., Chatzimitakos T., Kalompatsios D., Palaiogiannis D., Makrygiannis I., Bozinou E., Lalas S.I. (2023), Evaluation of the efficacy and synergistic effect of α-and δ-tocopherol as natural antioxidants in the stabilization of sunflower oil and olive pomace oil during storage conditions, *International Journal of Molecular Sciences*, 24(2), 1113, https://doi.org/10.3390/ijms24021113
- Bayram İ., Decker E.A. (2023), Underlying mechanisms of synergistic antioxidant interactions during lipid oxidation, *Trends in Food Science & Technology*, 133, pp. 219–230, https://doi.org/10.1016/j.tifs.2023.02.003
- Chabni A., Bañares C., Torres C.F. (2024), Study of the oxidative stability via Oxitest and Rancimat of phenolic-rich olive oils obtained by a sequential process of dehydration, expeller and supercritical CO₂ extractions, *Frontiers in Nutrition*, 11, 1494091, https://doi.org/10.3389/fnut.2024.1494091
- Hantikainen E., Lagerros Y.T. (2023), Vitamin E a scoping review for Nordic Nutrition Recommendations 2023, *Food & Nutrition Research*, 67, http://doi.org/10.29219/fnr.v67.10238
- Harhaun R., Kunik O., Saribekova D., Lazzara G. (2020), Biologically active properties of plant extracts in cosmetic emulsions, *Microchemical Journal*, 154, pp. 1–5, https://doi.org/10.1016/j.microc.2019.104543

- Kantawong F., Singhatong S., Srilamay A., Boonyuen K., Mooti N., Wanachantararak P., Kuboki T. (2017), Properties of macerated herbal oil, *Bioimpacts*, 7(1), pp. 13-23. https://doi.org/10.15171/bi.2017.03
- Kim S., Jang J.E., Kim J., Lee Y.I., Lee D.W., Song S.Y., Lee J.H. (2017), Enhanced barrier functions and anti-inflammatory effect of cultured coconut extract on human skin, *Food and Chemical Toxicology*, 106(A), pp. 367–375, https://doi.org/10.1016/j.fct.2017.05.060
- Kim Y., Kim M.J., Lee J. (2022), Physicochemical properties and oxidative stability of corn oil in infrared-based and hot air-circulating cookers, *Food Science and Biotechnology*, 31, pp. 1433–1442, https://doi.org/10.1007/s10068-022-01127-7
- Kunik O.M., Saribiekova D.H., Salieba L.V., Ivakhnenko H.O. (2016), Biologically active properties of plant extracts in cosmetic emulsions, *Scientific Bulletin of the National Technical University of Ukraine "Kyiv Polytechnic Institute*", 6, pp. 107–114, http://nbuv.gov.ua/ujrn/nvkpi_2016_6_15
- Kunik O., Saribekova D., Lazzara G., Cavallaro G. (2022), Emulsions based on fatty acid from vegetable oils for cosmetics, *Industrial Crops and Products*, 129, 115776, http://doi.org/10.1016/j.indcrop.2022.115776
- Li X., Li Y., Yang F., Liu R., Zhao C., Jin Q., Wang X. (2019), Oxidation degree of soybean oil at induction time point under Rancimat test condition: Theoretical derivation and experimental observation, *Food Research International*, 120, pp. 756–762, http://doi.org/10.1016/j.foodres.2018.11.036
- Liu X., Zheng Z., Liu Y. (2025), Lipophilic antioxidants in edible oils: Mechanisms, applications and interactions, *Food Research International*, 200, 115423, http://doi.org/10.1016/j.foodres.2024.115423
- Loganathan R., Ahmad Tarmizi A.H., Vethakkan S., Teng K. (2022), A review on lipid oxidation in edible oils, *Malaysian Journal of Analytical Sciences*, 26(6), pp. 1378–1393.
- Ma Y., Wang G., Deng Z., Zhang B., Li H. (2023), Effects of endogenous anti-oxidative components from different vegetable oils on their oxidative stability, *Foods*, 12(11), 2273, http://doi.org/10.3390/foods12112273
- Martín-Torres S., González-Casado A., Medina-García M., Medina-Vázquez M.S., Cuadros-Rodríguez L. (2023), A comparison of the stability of refined edible vegetable oils under frying conditions: Multivariate fingerprinting approach, *Foods*, 12(3), 604, https://doi.org/10.3390/foods12030604
- Martínez-Senra T., Maciolek U., Losada S., Bravo-Díaz C. (2024), Synergystic effects of binary mixtures of Δ-tocopherol and gallic acid derivatives on peroxidation of soybean oil-in-water emulsions, *LWT*, 213, 117014, https://doi.org/10.1016/j.lwt.2024.117014
- McMullen R.L. (2024), The benefits and challenges of treating skin with natural oils, *International Journal of Cosmetic Science*, 46(4), pp. 553–565, http://doi.org/10.1111/ics.12960
- Niki E. (2014), Role of vitamin E as a lipid-soluble peroxyl radical scavenger: In vitro and in vivo evidence, *Free Radical Biology and Medicine*, 66, pp. 3–12, https://doi.org/10.1016/j.freeradbiomed.2013.03.022
- Shahidi F., Zhong Y. (2010), Lipid oxidation and improving the oxidative stability, *Chemical Society Reviews*, 39, pp. 4067–4079, https://doi.org/10.1039/b922183m
- Syed A. (2016), Oxidative stability and shelf life of vegetable oils, In: M. Hu, C. Jacobsen (Eds.), *Oxidative Stability and Shelf Life of Foods Containing Oils and Fats*, pp. 187–207, Elsevier Inc., http://doi.org/10.1016/B978-1-63067-056-6.00004-5

—— Processes and Equipment——

- Thiele J.J., Hsieh S.N., Ekanayake-Mudiyanselage S. (2005), Vitamin E: Critical review of its current use in cosmetic and clinical dermatology, *Dermatologic Surgery*, 31(s1), pp. 805–813, https://doi.org/10.1111/j.1524-4725.2005.31724
- Wang D., Xiao H., Lyu X., Chen H., Wei F. (2023), Lipid oxidation in food science and nutritional health: A comprehensive review, *Oil Crop Science*, 8(1), pp. 35–44, https://doi.org/10.1016/j.ocsci.2023.02.002

Cite:

UFJ Style

Kunyk O., Leal W., Pasichniy V., Marynin A., Stabnikova O. (2025), Effect of tocopheryl and retinyl acetates on oxidative stability of *Hypericum perforatum* L. and *Matricaria recutita* L. macerates in corn oil during storage, *Ukrainian Food Journal*, 14(3), pp. 420–432, https://doi.org/10.24263/2304-974X-2025-14-3-5

APA Style

Kunyk, O., Leal, W., Pasichniy, V., Marynin, A., & Stabnikova, O. (2025). Effect of tocopheryl and retinyl acetates on oxidative stability of *Hypericum perforatum* L. and *Matricaria recutita* L. macerates in corn oil during storage. *Ukrainian Food Journal*, 14(3), 420–432. https://doi.org/10.24263/2304-974X-2025-14-3-5

Volatile profile of white wines produced from grape varieties cultivated under the soil-climatic conditions of Kyustendil, Southwestern Bulgaria

Dimitar Dimitrov¹, Iliyan Simeonov¹, Simeon Krumov²

- 1 Agricultural Academy, Institute of Viticulture and Enology, Pleven, Bulgaria
- 2 Agricultural Academy, Institute of Agriculture, Kyustendil, Bulgaria

Abstract

Keywords:

White wine Volatile compounds Terroir Grapevine Varieties

Article history:

Received 23.03.2025 Received in revised form 21.05.2025 Accepted 30.09.2025

Corresponding author:

Dimitar Dimitrov E-mail: dimitar_robertov@ abv.bg

DOI: 10.24263/2304-974X-2025-14-3-6

Introduction. The aim of this study is to define the volatile composition of white wines from Slava, Droujba and Tamyanka grapevine varieties, grown in the terroir conditions of the town of Kyustendil, Southwestern Bulgaria.

Materials and methods. White wines from three varieties and several harvests were studied – Slava (three harvests – 2021, 2023 and 2024), Droujba (four harvests – 2021, 2022, 2023 and 2024), Tamyanka (three harvests – 2021, 2022 and 2024). Volatile compounds were analyzed by gas chromatography (GC-FID). Climatic characterization was performed for the study period. Descriptive statistics were applied to determine mean values and standard deviation of identified main volatile compounds.

Results and discussion. The highest amounts of total volatile compounds were found in wines from the last studied harvest (2024) -Slava (1879.92 mg/l), Droujba (1539.40 mg/l) and Tamyanka (1762.51 mg/l). The main aldehyde was acetaldehyde. Its levels in almost all studied wines were at the optimum for positive influence (up to 240.00 mg/l). The highest total content of higher alcohols was found in wines of Slava variety, where they ranged from 101.04 mg/l (harvest 2023) to 597.75 mg/l (harvest 2024). The main identified higher alcohols were 2methyl-1-butanol, 3-methyl-1-butanol (the alcohol with the highest concentration in all experimental variants) and 1-butanol with the first two being identified in all the wines studied. The highest content of 3methyl-1-butanol was found in Slava wines. In them, it varied between harvests from 42.95 mg/l (2023) to 250.63 mg/l (2024). In Droujba wine, this higher alcohol varied from 33.87 mg/l (2023) to 124.00 mg/l (2022), and in Tamyanka, a variation from 61.60 mg/l (2024) to 97.80 mg/l (2022) was found. The main ester was ethyl acetate. The highest total terpene content was found in the two harvests of Slava wines – 2021 (1.92 mg/l) and 2024 (1.45 mg/l). Slava also showed the greatest species diversity of terpenes with 5 individual representatives identified – linalool oxide, linalool, α-terpineol, β-citronellol and geraniol. Methanol was identified in all studied wines in normal concentrations, which ranged in Droujba - from 0.92 mg/l (2023) to 50.27 mg/l (2021), in Slava - from 1.90 mg/l (2023) to 60.23 mg/l (2021) and in Tamyanka - from 6.15 mg/l (2022) to 98.92 mg/l (2021).

Conclusions. The conducted comprehensive study proved that the terroir of the town of Kyustendil is promising for growing the studied varieties, providing favorable conditions for the development of their potential, which was reflected in the production of white wines with optimal and complex aromatic quality.

Introduction

Studies on the wines volatile profile determine chemical components of the composition, which are an indicator of quality. The accumulation of volatile compounds is strongly dependent from the terroir of the region where the vines are grown (Kazimova et al., 2024; Ostapenko, 2016). According to Clingeleffer (2014), the concept of terroir is based on the complex interactions between biological and physical environmental factors, specific to a particular region, with the additional participation of the applied agrotechnical measures. Thus, the terroir influence determines specific characteristics of grapes and wine, directly related to the region. Han et al. (2022) analyzed the volatile profiles of 12 white wines from various regions (France, Germany, Italy, New Zealand, Spain, USA) and vintages (2015-2018), identifying 33 volatile compounds, with the highest concentrations found for acetaldehyde (16.00-57.00 mg/L), 1-hexanol (3.75-23.88 μg/L), isoamyl acetate (1.86-39.70 μg/L), hexyl acetate (1.21–10.89 μg/L), phenylethanol (16.92–77.73 μg/L), octanoic acid (4.32–25.41 µg/L), ethyl octanoate (11.60–142.47 µg/L), and ethyl isopentyl succinate (13.01–100.02 ug/L). Bayram and Kayalar (2018) determined the volatile composition of white wines of the Narince variety grown in two different regions of Turkey – Emiseyit and Erbaa and found that wines from the second studied region accumulated higher amounts of volatile compounds (205605.32 µg/l) compared to those from the first one (179547.85 µg/l). Vilanova et al. (2013) identified 46 volatile compounds in white wines from the varieties Albariño, Treixadura, Torrones, Blanco lexitimo and Loureira, grown in Northwestern Spain and 20 of the identified volatile compounds varying significantly between variants and being determinants of the so-called "varietal aroma". Mikulikova et al. (2009) determined the volatile composition of 29 white wines (harvests 2003 – 2006) of the varieties Riesling, Pinot Gris, Sauvignon Blanc, Gewürztraminer and Grüner Valtiner from different regions of the Czech Republic and found that the highest content was presented by the higher alcohols 3methyl-1-butanol (214.00 \pm 35.00 mg/l - 257.00 \pm 15.00 mg/l), followed by the ester ethyl lactate (17.80±6.90 mg/l - 29.80±5.60 mg/l), the aromatic alcohol 2-phenylethanol $(5.80\pm1.20 \text{ mg/l} - 19.20\pm8.90 \text{ mg/l})$ and octanoic acid $(4.80\pm0.90 \text{ mg/l} - 11.60\pm4.40 \text{ mg/l})$. The team (Mikulikova et al., 2009) identified 5 terpenes in the analyzed white wines – linalool, terpineol, citronellol, geraniol and nerol, with linalool and terpineol being present in the highest levels. Kalbach et al. (2024) studied the volatile profile of 5 white wines (harvest 2018) of the Riesling, Gewürztraminer, Sémillon, Sauvignon Blanc and Chardonnay varieties from the Campanha Gaúcha region, Brazil and in the higher alcohols fraction they found a quantitative dominance of 1-hexanol (897.30 – 1316.50 mg/l), 3-methyl-1-butanol (118.90 – 157.30 mg/l) and 1-propanol (21.30 - 43.50 mg/l); The dominant esters were isoamyl acetate (646.00 – 3000.90 mg/l), diethyl succinate (573.70 – 817.30 mg/l), ethyl decanoate (468.80 -1177.80 mg/l), ethyl octanoate (238.70 -1860.00 mg/l), ethyl hexanoate (346.90 -1209.40mg/l) and ethyl butanoate (332.30 – 720.80 mg/l). Barrio-Galán et al. (2021) investigated the volatile profile of white wines (varieties - Verdejo, Sauvignon Blanc, Godello, Malvasia castellana and Albillo) from several PDO (Protected Designation of Origin) regions of Spain (Rueda, Cigales, Toro, Ribera del Duero, Bierzo) and found that wines from the Ribera del Duero and Bierzo regions accumulated high levels of terpenes, while those from Cigales, Toro and Rueda were characterized by high concentrations of alcohol acetates and ethyl esters. Weldegegris et al. (2011) determined the volatile content of white wines from South Africa, obtained from the Sauvignon Blanc, Chardonnay and Pinotage varieties, harvest 2005, from the Paarl, Stellenbosch, Worcester, Robertson, Olifants River and Swartland regions and found that the quantitatively dominant higher alcohols were isoamyl alcohol (3methyl-1-butanol) ($123.00\pm14.5 \text{ mg/l} - 133.00\pm29.20 \text{ mg/l}$), 1-propanol ($17.70\pm13.10 \text{ mg/l}$ -31.80 ± 18.30 mg/l) and isobutanol (2-butanol) (23.20 ±14.50 mg/l -30.00 ± 10.40 mg/l), and from the ester fraction, ethyl acetate was found in the highest concentration (115.00±29.50

mg/l – 130.00±23.60 mg/l). Piras et al. (2020) studied the volatile profile of three white Portuguese wines from the Malvasia, Verdelho and Galego Dourado varieties (two harvests – 2017 and 2018) and found that the higher alcohols were quantitatively dominated by 3-methyl-1-butanol (isoamyl alcohol), which ranged from 46.035±6.510 mg/l to 168.256±0.706 mg/l and phenylethyl alcohol (phenyl ethanol) with a quantitative variation from 16.634±0.10 mg/l to 47.700±2.229 mg/l; the ester fraction was dominated by ethyl lactate (2.330±0.040 mg/l – 32.908±6.573 mg/l) and monomethyl succinate (6.375±0.419 mg/l – 19.743±6.290 mg/l), and 4 terpenes have also been identified – linalool, hotrineol, 2-terpineol and 2,6-dimethyl-3,7-octadiene-2,6-diol. Gómez-Miguez et al. (2007) studied the volatile composition of white wines from the autochthonous Zalema variety from the Huelva region (Southern Spain) and found that the strongest aromatic influence was exerted by fatty acids and ethyl esters.

The aim of this study is to define the volatile composition of white wines from the Slava, Droujba and Tamyanka varieties, grown in the terroir conditions of the town of Kyustendil, Southwestern Bulgaria.

Materials and methods

Varieties, plantation and agrotechnical measures. The study was conducted during the period 2021-2024 in an experimental vineyard plantation of the Institute of Agriculture - Kyustendil, Bulgaria. The terrain is located in the eastern part of Kyustendil Valley with an altitude of 450 m. The soil in the experimental plot is a highly leached, medium-textured sandy clay, slightly to moderately stony cinnamon forest soil (Chromic Luvisol) with a neutral pH reaction. The objects of the study were white wines produced from the grape varieties Slava and Droujba, developed at the Institute of Viticulture and Enology, Pleven (IVE) (Roychev, 2012; Simeonov et al., 2017), and Tamyanka, an autochthonous grapevine variety belonging to the Oriental ecogeographical group (Figure 1).

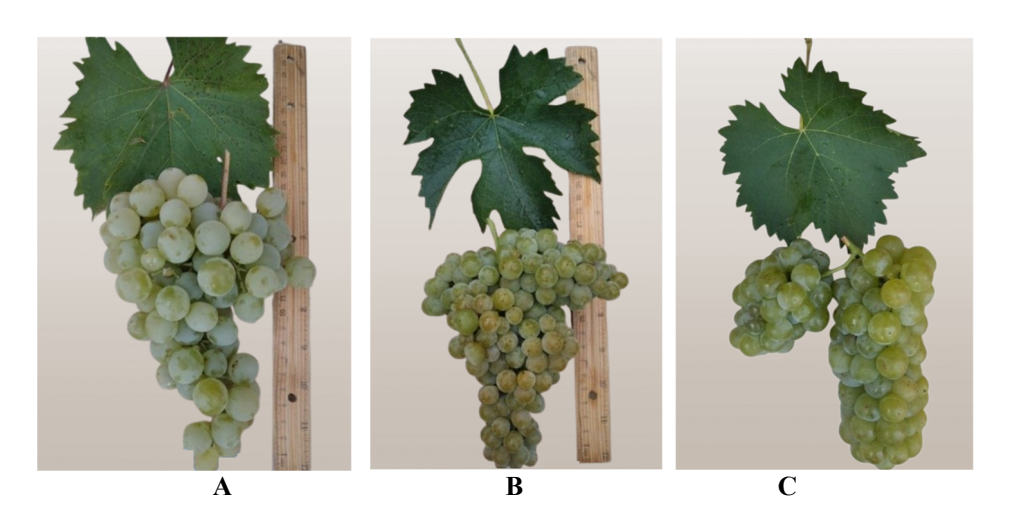


Figure 1. Grapevine varieties for white wines: A – Slava; B – Droujba; C – Tamyanka

The vines were planted in the spring of 2015, grafted onto the Berlandieri x Riparia SO4 rootstock and trained using the Guyot stem system. The planting distances were 2.50 m

between rows and 1.30 m within the row. The rows were oriented east west, in accordance with the prevailing southwestern and western winds in the area. The load during the study period was realized with 18 winter buds per vine (3 scions x 2 winter buds + 1 fruiting cane x 12 buds).

Climatic characteristics and vinification. The climate in the region is moderately continental, characterized by cold winters and conditions for late spring frosts. The average annual temperature is 10.5°C (multi-annual norm). The highest average monthly temperature is in July (21.8°C), and the lowest in January (- 0.8°C). The annual temperature amplitude is relatively large (22.4°C) and is an indicator of a prevailing moderately continental climate (Table 1).

Table 1 Average monthly air temperature and monthly precipitation amounts in the Kyustendil region

Meteorological		Month									Average		
element	I	II	III	IV	V	VI	VII	VIII	IX	X	XI	XII	Ave
Average			Pere	nnial n	orm fo	r the K	yusten	dil reg	ion, 1	904-20	08.		
monthly air	-0.8	1.2	6.0	11.2	15.4	19.1	21.8	21.2	12.2	11.2	6.2	0.9	10.5
temperature,						200	09-201	9					
t, °C	-0.5	2.6	6.3	11.1	15.4	19.1	21.5	21.1	16.6	10.4	6.1	1.0	10.9
Average			Per	ennial r	norm fe	or the	Kyuste	ndil re	gion, I	904-2	00		
monthly	43	38	36	53	65	64	60	37	42	59	57	54	608
precipitation,		2009-2019											
mm	44	41	54	43	57	61	49	32	38	56	44	47	566

During the study period, the main elements of the climate in the Kyustendil region were measured, which were directly related to the development of the vines and the quality of the grapes. The absolute minimum air temperature during the complete dormancy of the plants, in two of the years, decreased to the critical values for the regenerative organs (-18.0°C), but due to the interspecific origin of the studied varieties, no damage to the buds in the winter eyes was recorded (Ivanov et al., 2016). The average starting date of stable retention of the air temperature above 10.0°C was April 11, which is 2 days later than the multi-annual norm for the period 1956-2020 (Table 1). In autumn, the values of the average daily temperature of +10.0°C were maintained on average until October 29. The duration of the period between the two dates was 197 days with a total temperature sum of 3530.0 °C

The average multi-year date of the last spring frost in Kyustendil was April 8. According to this criterion, in 82.0% of cases, the danger of late spring frosts in the region has passed. The average monthly temperature in July, which is decisive for the technological qualities of grapes, was 22.9 °C. The established value was 2.0 °C higher than that established for the period 1956 - 2020. The last two years of the study (2023 and 2024) were the warmest since meteorological measurements have been conducted in the Kyustendil region (1904). In 2024, 46 days with absolute maximum air temperatures between 35.1-40.0°C and 6 days with above 40.0°C were recorded. For comparison, the average values of these indicators for the period 1904-2020 are 6 and 0.3 days respectively. The hydrothermal coefficient (HTC) reflecting the heat and moisture security for June, July and August was on average 0.96, which characterized the period as well-moistened (Table 2).

Agroclimatic parameters for the period 2021–2024

Table 2

year	of period with the state of the		perature for	coefficient /I - VIII hs)	une, July Ist	num air rage), °C				
Kyustendil, year	Average start date	Average end date	t > 10°C	Frost-free	Total temperature	Average air tempe July, °C	Average air temperature August ,°C	Hydrothermal co (HTC) for VI (months)	Precipitation in June, and August	Absolute minimum a temperature (average),
1956-2020*	08.IV	23.X	198	192	3391	20.9	21.1	0.77	146.0	-16.7
2021	25.IV	23.X	182	179	3153	21.2	22.2	0.38	72.9	-18.0
2022	21.IV	28.X	187	186	3197	21.5	19.0	1.23	228.8	-18.0
2023	11.IV	07.XI	208	206	3827	24.0	23.2	1.60	324.5	-13.0
2024	27.III	21.X	209	208	3943	25.0	23.9	0.61	135.6	-13.0
Average	11.IV.	29.X.	197	195	3530	22.9	22.1	0.96	190.5	-15.5

^{*} Perennial norm for the Kyustendil region of Bulgaria

The established values of the individual climate elements are a prerequisite for successful harvesting of early and mid-ripening grape varieties (Stoev, 1960)

30 kg of grapes were used for each variety. The grapes were vinified in the Experimental Wine Cellar of IVE according to a classic technological scheme for the obtaining of dry white wines (Yankov, 1992).

GC-FID analysis for determination of the volatile compounds. The content of the main volatile compounds was determined based on a stock standard solution prepared in accordance with IS 3752:2005 method. The method describes the preparation of a standard solution of one congener, but the preparation step was followed to prepare a solution of more compounds. The standard solution in the present study included the following compounds (purity > 99.0%): acetaldehyde, ethyl acetate, methanol, 2-propanol, isopropyl acetate, 1propanol, 2-butanol, propyl acetate, 1-butanol, isobutyl acetate, ethyl butyrate, 2-butyl acetate, 2-methyl-1-butanol, 3-methyl-1-butanol, 4-methyl-2-pentanol, 1-pentanol, pentyl acetate, 1-hexanol, ethyl hexanoate, hexyl acetate, 1-heptanol, linalool oxide, dimethyl succinate, phenyl acetate, linalool, ethyl caprylate, 2-phenylethanol, α-terpineol, nerol, βcitronellol, geraniol, ethyl decanoate. The prepared standard solution containing all compounds was injected in an amount of 2 µl into a gas chromatograph Varian 3900 (Varian Analytical Instruments, Walnut Creek, California, USA) with a capillary column VF max MS (30 m, 0.25 mm ID, DF= 0.25 μ m), equipped with flame ionization detector (FID). The carrier gas was helium. Hydrogen to support combustion was supplied to the chromatograph via a hydrogen bottle. The injection was manual, using a microsyringe. The gas chromatographic determination parameters were: injector temperature - 220 °C, detector temperature – 250 °C, initial oven temperature – 35 °C/1 min retention, rise to 55 °C with a step of 2 °C/min for 11 min, rise to 230 °C with a step of 15 °C/min for 3 min. Total chromatography time – 25.67 min. After the retention times of the compounds in the standard solution were determined, the identification and quantification of the volatile compounds in the wines were conducted. The volatile composition was determined based on the injection of wine distillates. Samples were injected in an amount of $2 \mu l$ into a gas chromatograph and identification and quantification of volatile compounds was performed.

Statistical analysis. Descriptive statistics were applied, with standard deviation (± SD) determined as the mean value of all harvests for the compounds found in the highest amount. The program Excel (MS Office, Microsoft Corporation, USA) was used for the analysis. Student's t-test was used to compare the values between grape varieties and five main identified volatile compounds (2-methyl-1-butanol, 3-methyl-1-butanol, Ethyl acetate, Acetaldehyde, Methanol).

Results and discussion

The results obtained for the identified volatile compounds are presented in Table 3. Wines of the Slava variety from three harvests -2021, 2023 and 2024, Droujba, which includes four consecutive harvests -2021-2024 and Tamyanka, for which wines from three harvests -2021, 2022 and 2024 were analyzed.

Table 3
Volatile compounds (mg/l) identified in white wines of Slava, Droujba and Tamyanka grapevine
varieties within different studied harvests

Identified					White	e wines				
compounds,	Slava			Droujba				Tamyanka		
mg/l		Harvest	S	Harvests				Harvests		
IIIg/1	2021	2023	2024	2021	2022	2023	2021	2022	2024	
Ethyl alcohol, vol.%	10.81	11.10	11.37	11.94	12.43	11.50	12.50	11.18	12.90	12.65
Acetaldehyde	57.78	225.22	219.87	81.81	297.66	200.00	304.00	14.56	147.28	1011.00
Methanol	60.23	1.90	8.84	50.27	36.18	0.92	8.04	98.92	6.15	7.94
2-methyl-1- butanol	62.71	7.46	150.70	52.22	38.68	5.28	26.52	47.54	21.42	13.10
3-methyl-1- butanol	120.25	42.95	250.63	121.06	124.00	33.87	110.69	74.92	97.80	61.60
4-methyl-2-	ND	ND	11.82	ND	1.29	0.46	ND	ND	ND	ND
pentanol										
1-propanol	ND	ND	2.24	8.22	ND	ND	ND	ND	ND	ND
2-propanol	13.10	ND	2.22	9.88	ND	ND	3.03	ND	ND	8.50
1-butanol	ND	34.92	18.63	ND	33.99	24.49	33.80	14.92	6.70	ND
1-pentanol	ND	ND	9.13	ND	ND	ND	0.87	ND	ND	7.34
2-butanol	30.30	6.32	77.16	ND	ND	ND	25.28	32.16	ND	5.55
1-hexanol	ND	9.39	75.22	ND	ND	9.05	5.00	ND	ND	8.23
2-henylethanol	ND	ND	ND	ND	ND	ND	41.32	ND	ND	65.57
Total content	226.36	101.04	597.75	191.38	197.96	73.15	246.51	169.54	125.92	169.89
of higher alcohols										
Ethyl acetate	33.07	22.85	495.82	142.85	46.83	19.26	759.49	211.82	71.25	127.81
Isobutyl acetate	ND	ND	75.47	7.02	ND	ND	218.88	ND	211.61	16.94
Butyl acetate	ND	ND	15.81	ND	ND	ND	ND	ND	11.32	ND
Propyl acetate	ND	ND	5.17	ND	3.94	ND	ND	ND	ND	5.42

I.J.,4:6:J					White	wines				
Identified compounds,		Slava		Droujba				Tamyanka		
mg/l		Harvest	ts		Har	vests		Harvests		
IIIg/1	2021	2023	2024	2021	2022	2023	2024	2021	2022	2024
Isopropyl	ND	ND	4.91	24.79	ND	ND	2.48	ND	ND	0.98
acetate										
Isopentyl	ND	ND	ND	ND	ND	ND	ND	39.56	ND	ND
acetate										
Pentyl acetate	ND	ND	ND	ND	ND	15.74	ND	12.25	ND	307.14
Phenyl acetate	ND	ND	179.72	ND	40.84	ND	ND	ND	ND	66.39
Ethyl caprylate	6.99	ND	ND	15.82	ND	ND	ND	33.78	ND	ND
Hexyl acetate	ND	ND	265.62	ND	ND	ND	ND	ND	310.34	ND
Dimethyl	ND	ND	ND	ND	ND	ND	ND	ND	ND	48.25
succinate										
Ethyl butyrate	ND	ND	9.49	ND	15.63	ND	ND	ND	19.52	ND
Ethyl decanoate	ND	ND	ND	ND	ND	35.49	ND	ND	ND	ND
Total content	40.06	22.85	1052.01	190.48	107.24	70.49	980.85	297.41	624.04	572.93
of esters										
Linalool oxide	0.84	ND	0.20	ND	ND	ND	ND	ND	ND	0.43
Linalool	ND	ND	0.23	ND	ND	ND	ND	ND	ND	ND
α-terpineol	ND	ND	0.27	ND	ND	ND	ND	ND	ND	0.32
Nerol	0.37	ND	ND	0.36	ND	0.69	ND	ND	0.10	ND
β – citronellol	0.16	ND	0.17	0.11	ND	ND	ND	ND	ND	ND
Geraniol	0.55	ND	0.58	0.50	0.15	ND	ND	ND	0.39	ND
Total content	1.92	0.00	1.45	0.97	0.15	0.69	0.00	0.00	0.49	0.75
of terpenes										
Total content	386.35	351.01	1879.92	514.91	639.19	345.25	1539.40	580.43	903.88	1762.51

^{*}ND – Not detected

Total volatile compounds, identified aldehydes and higher alcohols

It was found that the highest total content of volatile compounds was accumulated in the wines of the last harvest (2024). The quantitative variation of total volatile compounds in the wines of each individual variety between harvests was as follows: Slava (351.01 mg/l - 1879.92 mg/l), Droujba (345.25 mg/l - 1539.40 mg/l) and Tamyanka (580.43 mg/l - 1762.51 mg/l). According to Jackson (2020) the aromatic matrix of wines consists of over 1000 identified volatile compounds, which occupy average concentrations up to 800.00 - 1200.00 mg/l.

The aldehyde fraction was represented by acetaldehyde. This compound occupies 90% of all fatty aldehydes in wines by concentration (Chobanova, 2012). Its variation in the wines of the Slava variety ranged from 57.78 mg/l (harvest 2021) to 225.22 mg/l (harvest 2023), followed by those of the Droujba variety – 81.81 mg/l (harvest 2021) to 297.66 mg/l (harvest 2022), and Tamyanka showed a variation of the aldehyde from 14.56 mg/l (harvest 2021) to 1011.00 mg/l (harvest 2024). In dry white wines, aldehyde could vary from 7.00 to 240.00 mg/l, but could also reach 800.00 mg/l (Coetzee and du Toit, 2015; Lachenmeier and Sohnuis, 2008). Its formation is related to the yeasts activity, which synthesize it metabolically, but also to its chemical formation, which is related to oxidation processes (Nykanen, 1986). When the must is presulphated, before fermentation, the yeast synthesizes it in significant quantities, which increases its final concentration in the wine. At low

concentrations (within the norm) it gives a pleasant fruity aroma, and above the permissible levels it forms a sharp, irritating and oxidized nuance (Guittin et al., 2025).

In the present study, high levels of this aldehyde were found in the variants of white wines of the Droujba variety - harvest 2022 (297.66 mg/l) and harvest 2024 (304.00 mg/l) and Tamyanka - harvest 2024 (1011.00 mg/l), where the amount of the aldehyde was very high, indicating a strong oxidative process or presulfited must in the initial phases of processing, before fermentation.

The total content of higher alcohols in the analyzed wines did not show any distinguishable disproportions. Their content was the highest in Slava wines - 101.04 mg/l (harvest 2023) - 597.75 mg/l (harvest 2024), followed by Droujba, where they varied from 73.15 mg/l (2023) to 246.51 mg/l (2024), and for this variety it was striking that the 2021 and 2022 harvests showed an almost similar total amount of higher alcohols. The lowest levels of this fraction were found in the wines of the Tamyanka variety, where the levels of higher alcohols between its harvests were extremely similar, and in the 2021 and 2024 harvests they were almost identical. The variation in this variety was from 125.92 mg/l (2022) to 169.89 mg/l (2024).

According to Chobanova (2012), the content of higher alcohols in white wines varied in the range of 150.00 – 400.00 mg/l. The data in the present study were in correlation with these levels, with only exception of the Slava wine variant from the 2024 harvest which accumulated a slightly higher amount (597.75 mg/l).

The main identified higher alcohols were 3-methyl-1-butanol, 2-methyl-1-butanol and 1-butanol, with the first two being identified in all the wines studied.

The highest content of 3-methyl-1-butanol was found in Slava wines. In them, it varied between harvests from 42.95 mg/l (2023) to 250.63 mg/l (2024). In Droujba wine, this higher alcohol varied from 33.87 mg/l (2023) to 124.00 mg/l (2022), and in Tamyanka, a variation from 61.60 mg/l (2024) to 97.80 mg/l (2022) was found. The data correlated with other studies that found it as a major component in various white wines from regions of the Czech Republic, Brazil, South Africa and Portugal with a variation from 46.03±6.51 mg/l to 257.00±15.00 mg/l (Mikulikova et al., 2009; Kalbach et al., 2024; Weldegegris et al., 2011; Piras et al., 2020). Characteristic aromas that this alcohol had the potential to impart to wines were green, grassy, alcoholic, cheesy (Costello et al., 2012; Genovese et al., 2007; Torreus et al., 2010).

The next major higher alcohol was 2-methyl-1-butanol. It was found in lower concentrations. It was identified in the highest amount in Slava wines, where it varied between harvests from 7.46 mg/l (2023) to 150.70 mg/l (2024). Its variation in Droujba wines ranged from 5.28 mg/l (2023) to 52.22 mg/l (2021), and in Tamyanka, it ranged from 13.10 mg/l (2024) to 47.54 mg/l (2021). This compound is a major part of the wine aromatic matrix and present in wines in concentrations from 12.00 mg/l to 311.00 mg/l (Haenel, 1989). Our data correlated with this range. It was found that 2-methyl-1-butanol could impart citrus, green and malty aromas (Karabagias et al., 2011; Nistor et al., 2017).

The third main higher alcohol was 1-butanol. It was identified in the wines of two of the Slava harvests – 2023 (34.92 mg/l) and 2024 (18.63 mg/l), in three of the Droujba harvests (2022 to 2024), where it ranged from 24.49 mg/l to 33.99 mg/l, and in two of the Tamyanka harvests – 2021 (14.92 mg/l) and 2022 (6.70 mg/l). It was characterized by a floral aromatic influence (Alises et al., 2023).

The remaining higher alcohols were not present in all the studied wines, but were identified in individual harvests, which proved the significant influence of the climatic factor in the formation of the wine aromatic complex. The highest species diversity of higher alcohols was recorded in very hot and dry vegetation (2024). 4-methyl-2-pentanol was

identified in Slava's wine in the 2024 harvest variant (11.82 mg/l), in Droujba it was present in the 2022 harvest (1.29 mg/l) and 2023 (0.46 mg/l), and in Tamyanka's wines it was not identified; 1-propanol was identified in Slava's wines only in the 2024 harvest (2.24 mg/l), and in Droujba it was present only in the 2021 harvest (8.22 mg/l), while in Tamyanka it was not detected; 2-propanol was identified in two harvests of Slava – 2021 (13.10 mg/l) and 2024 (2.22 mg/l), in two harvests of Droujba – 2021 (9.88 mg/l) and 2024 (3.03 mg/l) and in one harvest of Tamyanka – 2024 (8.50 mg/l); 1-pentanol was found only in the 2024 harvest but in the wines of the all three varieties in concentrations respectively: Slava (9.13 mg/l), Droujba (0.87 mg/l) and Tamyanka (7.34 mg/l); 2-butanol was identified in all three Slava harvests, where it varied from 6.32 mg/l (2023) to 77.16 mg/l (2024), in Droujba it was found only in one harvest – 2024 (25.28 mg/l), and in Tamyanka it was present in two harvests – 2021 (32.16 mg/l) and 2024 (5.55 mg/l); 1-hexanol was identified in two of the Slava's harvests – 2023 (9.39 mg/l) and 2024 (75.22 mg/l), in two of the Droujba's harvests – 2023 (9.05 mg/l) and 2024 (5.00 mg/l) and in one of the Tamyanka's harvests – 2024 (8.23 mg/l); 2-phenylethanol – identified only in the 2024 harvest of Droujba (41.32 mg/l) and Tamyanka (65.57 mg/l).

Total ester content and identified individual representatives

The highest total ester levels were found in the 2024 harvest in all three studied wines. In Slava, esters varied between the three harvests from 22.85 mg/l (2023) to 1052.01 mg/l (2024). The variation in Droujba ranged from 70.49 mg/l (2023) to 980.85 mg/l (2024), and in Tamyanka the total ester content ranged from 297.41 mg/l (2021) to 624.04 mg/l (2022). According to Chobanova (2012), the total ester content in young wines varied from 200.00 to 500.00 mg/l. In the present study, the majority of the experimental variants covered this range, with the exceptions of Slava variants from the 2024 harvest (1052.01 mg/l), Druzhba variant from the 2024 harvest (980.85 mg/l) and Tamyanka variant from 2022 harvest (624.00 mg/l). The disproportion in the first two variants was due to the higher levels of ethyl acetate found, while in the third variant the increased total amount was due to the higher levels of hexyl acetate found.

The main ester that was identified in all the studied wines was ethyl acetate. High levels of this ester were found in two of the experimental variants – Slava – harvest 2024 (495.82 mg/l) and Droujba - harvest 2024 (759.49 mg/l). In the remaining wines, it was found in normal concentrations. In the other two harvests of Slava, it was present in an amount of 33.07 mg/l (2021) and 22.85 mg/l (2023), in Droujba it varied between the three harvests from 19.26 mg/l (2023) to 142.85 mg/l (2021), and in Tamyanka it varied from 71.25 mg/l (2022) to 211.82 mg/l (2021). According to Chobanova (2012), its concentration varies from 30.00 to 300.00 mg/l. The main characteristic of the ethyl acetate is its dual nature of aromatic influence. At concentrations up to 100.00 mg/l, it enhances the fruity nuances in the wine aroma, while above these values it can form aromas from the chemical group (Lasik-Kurdyś et al., 2018). Its presence in high concentrations indicates acidification processes. Its content in the three experimental variants listed above was above the permissible limits, which created the possibility of generating unpleasant aromatic notes in the wines. In the remaining studied variants, its concentration was in correlation with other studies - that of Miranda et al. (2017), who found a variation of ethyl acetate from 26.10±0.36 mg/l to 110.31±0.17 mg/l in young Madeira wines, the data were also in agreement with the study of Lasik-Kurdyś et al. (2018), who found ethyl acetate in young Chardonnay wines with a variation from 58.12±5.37 mg/l to 110.26±4.93 mg/l. It was found as the main ester in white wines from South Africa, in which it varied from 115.00±29.50 mg/l to 130.00±23.60 mg/l (Weldegegris et al., 2011).

The remaining esters were found in separate variants and harvests. Isobutyl acetate was identified only in one harvest (2024) of Slava (75.47 mg/l), in two of the Droujba's harvests - 2021 (7.02 mg/l) and 2024 (218.88 mg/l) and in two of the Tamyanka's harvests - 2022 (211.61 mg/l) and 2024 (16.94 mg/l); Butyl acetate was found in one of the Slava's harvests - 2024 (15.81 mg/l) and in one of the Tamyanka's harvests - 2022 (11.32 mg/l); Propyl acetate was detected in one of the Slava's harvests – 2024 (5.17 mg/l), in one of the Droujba's harvests – 2022 (3.94 mg/l) and in one of the Tamyanka's harvests – 2024 (5.42 mg/l); Isopropyl acetate was detected only in the 2024 harvest (4.91 mg/l) of Slava, in the 2021 harvest (24.79 mg/l) and 2024 (2.48 mg/l) of Droujba, and also in the 2024 harvest (0.98 mg/l) of Tamyanka; Isopentyl acetate was detected only in the 2021 harvest (39.56 mg/l) of Tamyanka; Pentyl acetate was detected in the 2023 harvest (15.74 mg/l) of Droujba and in the 2021 (12.25 mg/l) and 2024 (307.14 mg/l) of Tamyanka; Phenyl acetate was detected in the 2024 harvest (179.72 mg/l) of Slava, the 2022 harvest (40.84 mg/l) of Droujba and the 2024 harvest (66.39 mg/l) of Tamyanka; Ethyl caprylate was identified only in one of the harvests of Slava – 2021 (6.99 mg/l) and in the 2021 harvests of Druzhba and Tamyanka in concentrations of 15.82 mg/l and 33.78 mg/l, respectively; Hexyl acetate was identified only in the 2024 harvest (265.62 mg/l) of Slava and in the 2022 harvest (310.34 mg/l) of Tamyanka; Diethyl succinate was identified only in the 2024 harvest (48.25 mg/l) of Tamyanka; Ethyl butyrate was identified in the 2024 harvest (9.49 mg/l) of Slava, in the 2022 harvests of Droujba (15.63 mg/l) and Tamyanka (19.52 mg/l); Ethyl decanoate was detected only in the 2023 harvest (35.49 mg/l) of Droujba.

Total terpene content, individual representatives, and methanol

Terpenes were not identified in all the wines studied. The highest total terpene content was found in Slava's wines, as in the 2023 harvest they were not present, in the 2021 harvest they were present in an amount of 1.92 mg/l, and in the last harvest (2024) their total content was 1.45 mg/l. Droujba's wines rank second in terms of concentration presence. Terpenes were not detected in them only in the 2024 harvest, while in the other three harvests their content varied from 0.15 mg/l (2022) to 0.97 mg/l (2021). Tamyanka showed the lowest levels of terpenes, as in the 2021 harvest they were not identified, while in the 2022 harvest they occupied an amount of 0.49 mg/l, and in the 2024 harvest – 0.75 mg/l.

Terpenes are a major factor in the aroma formation of Muscat varieties, where they occupy concentrations of up to 2.00 mg/l on average (Chobanova, 2012). Based on the terpene content, varieties can be classified as Muscat - with a total terpene content higher than 6.00 mg/l, aromatic non-Muscat, which contains terpenes in the range of 1.00 to 4.00 mg/l and neutral, in which terpenes are present in amounts lower than 1.00 mg/l (Mateo and Jiménez, 2000). Based on this, wines of the Slava variety could be categorized as aromatic non-Muscat, and those of Droujba and Tamyanka as neutral. Terpenes are not a fermentation product, but pass from the grapes to the wine after processing and fermentation. Celik et al. (2015) investigated the total terpene content of the white aromatic variety Muscat of Bornova from three different terroirs – Kemaliye, Halibeyli and Menderes from Izmir-Manisa province, Turkey, for two harvests (2013 and 2014) and found a variation in total terpene content between the three regions for the first harvest from 1.3 mg/l (Kemaliye) to 2.1 mg/l (Menderes), and for the second harvest – from 1.3 mg/l (Halibeyli) to 2.6 mg/l (Kemaliye). The data for Slava in our study correlated with this range.

Linalool oxide was identified in two of Slava's wines – harvest 2021 (0.84 mg/l) and harvest 2024 (0.20 mg/l) and in one of Tamyanka's harvest – 2024 (0.43 mg/l). Linalool was identified in only one of Slava's harvests – 2024 (0.23 mg/l). α -terpineol was identified in Slava's 2024 harvest (0.27 mg/l) and Tamyanka's 2024 harvest (0.32 mg/l). Nerol was identified in Slava's 2021 harvest (0.37 mg/l), Druzhba's 2021 (0.36 mg/l) and 2023 (0.69 mg/l) and Tamyanka's 2022 harvest (0.10 mg/l). β -citronellol was detected in the 2021 (0.16 mg/l) and 2024 (0.17 mg/l) harvests of Slava and in the 2021 (0.11) harvest of Droujba. Geraniol was detected in the 2021 (0.55 mg/l) and 2022 (0.15 mg/l) harvests of Droujba and in the 2022 (0.39 mg/l) harvest of Tamyanka. The wine of the Slava variety from the 2024 harvest was the richest in individual terpenes.

According to Resolution OENO 19/2004 of the OIV (International Organisation of Vine and Wine), the maximum permissible levels of methanol in white wines must be up to 250.00 mg/l. In practice, the formation of methanol is a normal process in the production of alcoholic beverages, which is due to the breakdown of fruit pectin by the pectolytic enzyme complex, also present in the fruit (Han and Du, 2022). All established levels of methanol in the studied white wines of the three varieties were well below the limit of its permissible amount. Thus, in the three harvests of Slava, the amounts of methanol varied from 1.90 mg/l (2023) to 60.23 mg/l (2021). In the four harvests of Droujba, the methanol variation occupied concentrations from 0.92 mg/l (2023) to 50.27 mg/l (2021), and in the three harvests of Tamyanka, methanol ranged from 6.15 mg/l (2022) to 98.92 mg/l (2021). Our data correlated with the established methanol levels in Australian white wines, where it varied from 40.00 – 120.00 mg/l (Hodson et al., 2017), in Turkish white wines from different regions – 30.50 – 121.40 mg/l (Cabaroglu, 2005), in Georgian wines, where it varied from 85.90 mg/l to 111.30 mg/l (Khomasuridze et al., 2005).

Average value and statistical variation of the main volatile compounds in the analyzed wines

The data for the mean value (Slava – three harvests, Droujba – four harvests and Tamyanka – three harvests) and standard deviation of the main identified compounds (2-methyl-1-butanol, 3-methyl-1-butanol, ethyl acetate, acetaldehyde and methanol) are presented in Table 4.

	Table 4
Content of main identified volatile compounds in white wines (mg/l)	

Identified	White wines from					
compounds, mg/l	Slava*	Droujba**	Tamyanka*			
2-methyl-1-butanol	73.62±72.24	30.67±19.92	27.35±17.97			
3-methyl-1-butanol	137.94±104.96	97.40 ±42.73	78.10 ± 18.30			
Ethyl acetate	183.91±270.16	242.10±348.96	136.92±70.73			
Acetaldehyde	167.62±95.16	220.86±104.21	390.94 ±541.06			
Methanol	23.65±31.86	23.85±23.27	37.67 ±53.05			

^{*} Data for three harvests, Average±SD

^{**} Data for four harvests, Average±SD

^{***} Student's t-test was used to compare the values between grape varieties for each of the compounds. No statistically significant differences were found (p>0.05).

2-methyl-1-butanol was present (as an average amount of all studied harvests) in the highest concentration in Slava (73.62 \pm 72.24 mg/l). The other two wines – Droujba and Tamyanka showed very close average content of this higher alcohol, respectively 30.37 ± 19.92 mg/l and 27.35 ± 17.97 mg/l.

3-methyl-1-butanol, which was the higher alcohol with the highest concentration, showed an average value of all studied harvests, which is the highest (137.94±104.96 mg/l) again in Slava. In second place by average accumulation it was found in Droujba (97.40±42.73 mg/l), and its average levels were the lowest in Tamyanka (78.10±18.30 mg/l).

The highest average levels of ethyl acetate were established in the wine of the Droujba variety (242.10±348.96 mg/l), followed by Slava (183.91±270.16 mg/l), and in Tamyanka its levels were the lowest (136.92±70.73 mg/l). The large ranges of standard deviation of this compound in Slava and Droujba were due to its very high levels found in the last studied harvest – 2024.

The highest average levels of acetaldehyde were found in the wine of the Tamyanka variety (390.94±541.06 mg/l), followed by Droujba (220.86±104.21 mg/l) and the lowest, but optimal levels, were found in Slava (167.62±95.16 mg/l). Here too, a very high standard variation was reported in the wine of the Tamyanka variety, which was again due to a very high accumulated amount of acetaldehyde in the 2024 harvest (1011.00 mg/l).

In the case of methanol, the average levels for the wines of all three varieties were very close. The highest average amount was identified in Tamyanka (37.67±53.05 mg/l), and the other two wines showed almost similar average methanol concentration, respectively: Slava (23.65±31.86 mg/l) and Droujba (23.85±23.27 mg/l).

The average values of volatile compounds varied, since each harvest exerted the individual influence of many factors (soil, climate, agricultural techniques, cultivation technology, vinification technology, and yeast cultures used), which had complex and heterogeneous effects on the accumulation of each volatile compound in the wine.

Conclusions

The study demonstrated clear evidence of the influence of climatic conditions on the aromatic composition of white wines from the Kyustendil region. The 2024 harvest showed the highest total content of volatile compounds, confirming that hotter and drier seasons favor the quantitative and qualitative enrichment of wine aroma. This reflects the impact of recent climate changes marked by frequent droughts and elevated temperatures. Acetaldehyde levels were generally within acceptable limits, contributing positively to wine aroma, except in Droujba (2022 and 2024) and Tamyanka (2024) wines, where higher concentrations likely caused slight oxidative notes. The predominant higher alcohols were 2-methyl-1-butanol, 3methyl-1-butanol, and 1-butanol, while ethyl acetate was the main ester. Excessive ethyl acetate levels in Slava (2024) and Druzhba (2024) may have produced acetic tones, whereas normal levels in other wines enhanced fruity notes. The Slava wine (2024) exhibited the most diverse terpene profile, with five identified compounds (linalool oxide, linalool, α -terpineol, β-citronellol, and geraniol), indicating that drought conditions promote terpene biosynthesis in grapevines. Statistical analysis of key volatiles (2-methyl-1-butanol, 3-methyl-1-butanol, ethyl acetate, acetaldehyde, and methanol) revealed considerable variability linked to the complex interaction of soil, climate, viticultural and vinification practices, and yeast strains.

Overall, the results confirm that the Kyustendil terroir provides favorable conditions for the studied varieties, supporting the production of white wines with complex and balanced aromatic profiles. The findings enrich current knowledge on terroir-specific effects and highlight the growing impact of climate change on grapevine metabolism and wine quality.

References

- Alises M.O., Sánchez-Palomo E., González-Viñas M.A. (2023), Influence of different alcohol reduction technologies on the volatile composition of la Mancha Tempranilo rosé wines, *Beverages*, 9(3), 63, https://doi.org/10.3390/beverages9030063
- Barrio-Galán R., Valle-Herrero H., Bueno-Herrera M., López de la Cuesta P., Pérez-Magariño S. (2021), Volatile and non-volatile characterization of white and rosé wines from different Spanish protected designations of origin, *Beverages*, 7(3), 49, https://doi.org/10.3390/beverages7030049
- Bayram M., Kayalar M. (2018), White wines from Narince grapes: impact of two different grape provenances on phenolic and volatile composition, *OENO One*, 52(2), pp. 81-92, https://doi.org/10.20870/oeno-one.2018.52.2.2114
- Cabaroglu T. (2005), Methanol content of Turkish varietal wines and effect of processing, *Food Control*, 16(2), pp. 177-181, https://doi.org/10.1016/j.foodcont.2004.01.008
- Celik Z.D., Karaoğlan S.Y., Darici M., Kelebek H., Işçi B., Kaçar E., Altindişli A., Cabaroğlu T. (2015), Effects of terroir on the terpene compounds of Muscat of Bornova native white grape variety grown in Turkey, *BIO Web of Conferences*, 5, 01004, https://doi.org/10.1051/bioconf/20150501004
- Chobanova D. (2012), *Enology. Part I: Composition of wine*, Academic Press of University of Food Technologies, Plovdiv, Bulgaria.
- Clingeleffer P. (2014), Terroir: The application of an old concept in modern viticulture, *Encyclopedia of Agriculture and Food Systems*, 5, pp. 277–288, https://doi.org/10.1016/b978-0-444-52512-3.00157-1
- Coetzee C., du Toit W. J. (2015), Sauvignon blanc wine: contribution of ageing and oxygen on aromatic and non-aromatic compounds and sensory composition A review, *South African Journal of Enology and Viticulture*, 36(3), pp. 347-365, https://doi.org/10.21548/36-3-968
- Costello P.J., Francis I.L., Bartowsky E.J. (2012), Variations in the effect of malolactic fermentation on the chemical and sensory properties of cabernet sauvignon wine: Interactive influences of oenococcusoeni strain and wine matrix composition, *Australian Journal of Grape and Wine Research*, 18, pp. 287-301, https://doi.org/10.1111/j.1755-0238.2012.00196.x
- Genovese A., Gambuti A., Piombino P., Moio L. (2007), Sensory properties and aroma compounds of sweet Fiano wine, *Food Chemistry*, 103, pp. 1228-1236, https://doi.org/10.1016/j.foodchem.2006.10.027
- Gómez-Miguez M. J., Cacho J. F., Ferreira V., Vicario I. M., Heredia F. J. (2007), Volatile components of Zalema white wines, *Food Chemistry*, 100(4), 1464-1473, https://doi.org/10.1016/j.jfoodeng.2006.02.038
- Guittin C., Macna F., Perez M., Barreau A., Poitou X., Mouret J.R., Farines V. (2025), Evolution of acetaldehyde concentration during wine alcoholic fermentation: online monitoring for production balances, *Macrowine* 2025 *Bolzano* (*Italy*) 24 27 *June* 2025. *Book of abstracts*, pp. 44, https://doi.org/10.58233/macrowine2025-boa
- Han S., Yang J., Choi K., Kim J., Adhikari K., Lee J. (2022), Chemical analysis of commercial white wines and its relationship with consumer acceptability, *Foods*, 11(4), 603, https://doi.org/10.3390/foods11040603
- Han Y., Du J. (2022), Relationship of the methanol production, pectin and pectinase activity during apple wine fermentation and aging, *Food Research International*, 159, 111645, https://doi.org/10.1016/j.foodres.2022.111645

- Hodson G., Azevedo S., Battaglene T. (2017), Methanol in wine, *BIO Web of Conferences*, 9, 02028, https://doi.org/10.1051/bioconf/20170902028
- Haenel H. (1989), *IARC Monographs on the evaluation of carcinogenic risks to humans*, 44, International Agency for Research on Cancer, Lyon, France, https://doi.org/10.1002/food.19890331018
- Ivanov M., Nakov Z., Iliev A., Pachev I., Simeonov I. (2016), Low winter temperatures resistance under field conditions of wine grapevine varieties grown in Northern Bulgaria, *Journal of Mountain Agriculture on the Balkans*, 19(2), 168-183.
- Jackson R. (2020), Chemical constituents of grapes and wine, In: *Wine Science* (second edition), *Principles and Applications*, pp. 375-459, https://doi.org/10.1016/b978-0-12-816118-0.00006-4
- Kalbach S., Lemos P., Costa V., Herter F., Brunnetto G., dos Santos C., Couto J. (2024), Volatile and phenolic compounds in white wines produced at Campanha Gaúcha, Brazil, *Ciência Rural*, 54(10), e20220596, https://doi.org/10.1590/0103-8478cr20220596
- Kazimova I., Omarova E., Nabiyev A., Gasimova A. (2024), Comparative analysis of the composition of Bayan Shirey, Rkatsiteli and Cabernet Sauvignon grape varieties for production of brandy wine materials, *Ukrainian Food Journal*, 13(4), 694-707, https://doi.org/10.24263/2304-974x-2024-13-4-5
- Karabagias I.K., Karabagias V.K., Badeka A.V. (2021), Volatilome of white wines as an indicator of authenticity and adulteration control using statistical analysis, *Australian Journal of Grape and Wine Research*, 27, pp. 269-279, https://doi.org/10.1111/ajgw.12486
- Khomasuridze M., Kiladze M., Tatulashvili S. (2025), Quantitative analysis of oak barrel aging effects on methanol content and volatile acidity in traditional Qvevri Amber wines, *World Journal of Engineering Research and Technology*, 11(6), pp. 1-11.
- Lachenmeier D. W., Sohnius E. M. (2008), The role of acetaldehyde outside ethanol metabolism in the carcinogencity of alcoholic beverages: Evidence from a large chemical survey, *Food and Chemical Toxicology*, 46(8), pp. 2903-2911, https://doi.org/10.1016/j.fct.2008.05.034
- Lasik-Kurdyś M., Majcher M., Nowak J. (2018), Effects of different techniques of malolactic fermentation induction on diacetyl metabolism and biosynthesis of selected aromatic esters in cool-climate grape wines, *Molecules*, 23, 2549, https://doi.org/10.3390/molecules23102549
- Mateo J.J., Jiménez M. (2000), Monoterpenes in grape juice and wines. *Journal of Chromatography A*, 881, pp. 557-567, https://doi.org/10.1016/s0021-9673(99)01342-4
- Mikulikova R., Golias J., Mrazova V. (2009), SPME-GC-MS analysis of volatile compounds in Czech white wines from five grape varieties, *Mitteillungen Klosterneuburg*, 59, 159-165.
- Miranda A., Pereira V., Pontes M., Albuquerque F., Marques J. C. (2017), Acetic acid and ethyl acetate in Madeira wines: evolution with ageing and assessment of the odour rejection thresholds, *Ciência e Técnica Vitivinícola*, 32(1), pp. 1-11.
- Nistor A. M., Niculaua M., Luchian C. E., Cotan S. O., Teliban I., Cotea V. V. (2017), Negative influence of temperature over flavor compounds from wine, *Revista Lucrări științifice Seria Horticultură*, 60(1), pp. 127-132.
- Nykanen L. (1986), Formation and occurrence of flavor compounds in wine and distilled alcoholic beverages, *American Journal of Oenology and Viticulture*, 37, pp. 84-96, https://doi.org/10.5344/ajev.1986.37.1.84

- Ostapenko V. (2016), Analysis on application of different grape varieties in the production of icewine. A review, *Ukrainian Food Journal*, 13(4), 678-694, https://doi.org/10.24263/2304-974x-2016-5-4-7
- Piras S., Brazão J., Ricardo da Silva J., Anjos O., Caldeira I. (2020), Volatile and sensory characterization of white wines from three minority Portuguese grapevine varieties, *Ciência e Técnica Vitivinícola*, 35(1), pp. 49-62, https://doi.org/10.1051/ctv/20203501049
- Resolution OENO 19/2004. Maximum content limits of methanol in wines. International Organization of Vine and Wine.
- Roychev V. (2012), Ampelography. Academic Publishing House of AU-Plovdiv.
- Simeonov I., Ivanov M., Nakov Z., Iliev A. (2017), Results of grapevine intra-species and interspecific hybridization at IVE-Pleven (overview), *Journal of Mountain Agriculture on the Balkans*, 20(3), pp. 211-220,
- Standard 3752:2005. Alcohol Drinks Methods of Test (Second Revision).
- Stoev K. (1960), Zoning of viticulture in Bulgaria. Scientific Works of the Institute of Viticulture and Enology Pleven, 3, Sofia: Zemizdat, pp. 110.
- Torreus J., Riu-Aumatell M., Vichi S., López-Tamames E., Buxaderas S. (2010), Assessment of volatile and sensory profiles between base and sparkling wines, *Journal of Agricultural and Food Chemistry*, 58, pp. 2455-2461, https://doi.org/10.1021/jf9035518
- Vilanova M., Escudero A., Cacho J. (2013), Volatile composition and sensory properties of North West Spain white wines, *Food Research International*, 54, pp. 562-568, https://doi.org/10.1016/j.foodres.2013.07.036
- Weldegergis B., Villiers A., Crouch A. (2011), Chemometric investigation on the volatile content of young South African wines, *Food Chemistry*, 128, pp. 1100-1109, https://doi.org/10.1016/j.foodchem.2010.11.157
- Yankov A. (1992), Winemaking Technology, Zemizdat Publishing House, Sofia.

Cite:

UFJ Style

Dimitrov D., Simeonov I., Krumov S. (2025), Volatile profile of white wines produced from grape varieties cultivated under the soil-climatic conditions of Kyustendil, Southwestern Bulgaria, *Ukrainian Food Journal*, 14(3), pp. 433–447, https://doi.org/10.24263/2304-974X-2025-14-3-6

APA Style

Dimitrov, D., Simeonov, I., & Krumov, S. (2025). Volatile profile of white wines produced from grape varieties cultivated under the soil-climatic conditions of Kyustendil, Southwestern Bulgaria. *Ukrainian Food Journal*, *14*(3), 433–447. https://doi.org/10.24263/2304-974X-2025-14-3-6

Thermal stability and technological performance of fibrefortified protein-fat emulsions for meat and fish products

Mykola Vorontsov, Oleg Galenko, Oksana Topchii

National University of Food Technologies, Kyiv, Ukraine

Abstract

Keywords:

Emulsion Fish Meat Fiber Bamboo Oat Wheat

Article history:

Received 31.03.2025 Received in revised form 12.05.2025 Accepted 30.09.2025

Corresponding author:

Oleg Galenko E-mail: galen@i.ua

DOI: 10.24263/2304-974X-2025-14-3-7

Introduction. The aim of this study was to assess and compare the effects of heat treatment on the functional and technological properties, as well as the stability, of protein–fat emulsions containing bamboo, oat, or wheat fiber for meat and fish products.

Materials and methods. Fiber, oats, and bamboo fiber were used in the study. Model emulsions were prepared based on animal and vegetable proteins, sunflower oil, carboxymethyl cellulose and water. The plasticity, water holding capacity (WHC) and stability of the emulsions were evaluated before and after heat treatment and freeze-thaw cycles using pressing and centrifugation methods.

Results and discussion. Significant differences were found in the effects of heat treatment and Freeze-thaw on emulsions with different fiber types. Samples containing bamboo fiber exhibited the highest waterholding capacity (WHC, 89.7%) and moderate plasticity (5.32 cm/g), whereas those with oat fiber showed the highest plasticity (6.04 cm/g) but significantly lower stability under heat treatment and freeze-thaw conditions. The highest initial plasticity (7.43 cm/g) was observed in the samples of emulsions with oat fiber, and after heat treatment and freezing, the greatest decrease in emulsion stability was recorded (up to 20.56% of the initial value). Samples with bamboo fiber were characterized by the smallest losses in stability - 10.16% after heat treatment and 13.06% after freeze-thaw cycles - which indicates increased resistance to thermal and mechanical stress. Samples with wheat fiber showed intermediate results in all parameters. The incorporation of oat fiber rapidly increased plasticity during heating, while bamboo fiber demonstrated slow but gradual activation. During repeated freeze-thaw cycles, samples with bamboo fiber showed minimal increase in plasticity, while samples with oat fiber showed pronounced changes in their structure and an increase in plasticity along with a decrease in moisture-binding capacity. Moreover, bamboo fiber contributed to maintaining the integrity of the emulsion matrix, preventing excessive phase separation and preserving homogeneous texture throughout storage. This gradual activation behavior suggests a delayed hydration mechanism, which could be beneficial for extended product stability. In contrast, oat fiber exhibited fast hydration but poor retention under stress, which may explain its weaker performance after thermal and freezing exposure. Wheat fiber, though less efficient than bamboo, offered a balanced response, providing moderate plasticity and stability under all test conditions.

Conclusions. Bamboo fiber provides gradual functional activation and high structural resilience, ensuring consistent emulsion stability during processing and storage. These findings highlight its strong potential as a natural, multifunctional ingredient for the formulation of pasteurized or frozen meat and fish products.

Introduction

The use of dietary fibers as functional food ingredients has expanded significantly in recent years. In addition to their well-established health benefits (Stabnikova and Paredes-Lopez, 2024), dietary fibers play important technological roles in food systems, including water binding, fat replacement, texture modification, and emulsion stabilization. Contemporary food science increasingly emphasizes the identification of natural, clean-label ingredients that provide both nutritional and structural advantages (Li et al., 2023).

Dietary fibers are generally classified into two main types: soluble and insoluble. Soluble fibers, such as β -glucans, inulins, gums, and pectins, dissolve in water to form viscous gels that delay gastric emptying and promote satiety. From a technological perspective, they enhance viscosity and contribute to emulsion stability by reducing droplet mobility. Insoluble fibers, including cellulose, wheat bran, and bamboo shoot fiber, do not dissolve in water but serve primarily as bulking agents, texturizers, and stabilizers in various food products.

Soluble fibers are commonly used in beverages, sauces, and dairy alternatives to enhance mouthfeel, whereas insoluble fibers are incorporated into bakery, meat, and plant-based products to retain water, improve texture, and act as fat replacers (Stabnikova et al., 2021; Tsykhanovska et al., 2024). By selecting appropriate fiber types, manufacturers can develop foods that satisfy both nutritional and technological objectives. One of the most notable application areas includes formulations of meat (Da Silva et al., 2024) and fish products (Naghdi et al., 2025) designed to reduce fat content or improve processing tolerance.

Recent studies have explored strategies to enhance the quality, stability, and nutritional profile of meat products through the incorporation of structured plant oils and dietary fibers. It was demonstrated that sunflower oil structured with soy protein and transglutaminase can replace palm oil in fermented poultry sausages (Dreher et al., 2022). This substitution maintained color, texture, and flavor comparable to control samples, while significantly improving the fatty acid profile by increasing monounsaturated fats and reducing saturated fats. Sensory panels confirmed consumer acceptability, and emulsion stability during storage remained high.

Oyegoke et al. (2024) reviewed natural plant-derived antioxidants and antimicrobials, such as polyphenols, essential oils, spice extracts, and dietary fibers. These compounds inhibit lipid and protein oxidation and suppress spoilage and pathogenic microorganisms, aligning with clean-label trends by reducing the need for synthetic additives and phosphates. Even at low concentrations, these bioactive compounds can exert beneficial effects, and synergistic combinations may further improve product stability and sensory quality.

Engineering of dietary fibers has been shown to enhance water and fat retention in meat products, reduce cooking losses, and improve texture. Techniques include superfine grinding, agglomeration, and chemical modification (Djordjević et al., 2022). Fibers from rice, wheat, corn, orange, bamboo, carrot, and tiger nut have demonstrated improvements in juiciness, firmness, microbial stability, and shelf life in low-fat or emulsified meat products (Habiba et al., 2021). Bamboo fiber, in particular, maintained stability and plasticity during thermal and freeze-thaw treatments.

Plant oils such as argan and structured sunflower oil have been successfully used as partial replacements for animal fat, improving lipid profiles without compromising sensory properties (Mouta-Afif et al., 2024). Emulsion stabilization technologies, including cellulose nanocrystals and protein-polysaccharide systems, prevent phase separation and coalescence, ensuring homogeneous texture and facilitating the incorporation of bioactive plant compounds with antioxidant properties (Paredes-Toledo et al., 2024).

Overall, the combination of functional fibers and structured plant oils offers a promising approach to developing healthier, stable, and sensory-acceptable meat products. These strategies

enable clean-label formulations, improve nutritional quality, and provide opportunities for extending shelf life while maintaining consumer-preferred texture and flavor characteristics (Zhang et al., 2025).

Based on these results, the need for development of clean label meat products with enhanced functional-properties, that can be stable during the pasteurization and prolonged shelf-life, can be realized via the use of different sourced of plant fibers.

The use of various types of dietary fiber in meat product formulations, aimed at the partial or complete replacement of meat raw materials and animal fat, has been documented in numerous scientific studies (Aminzare et al., 2024, 2025; Du et al., 2023; Liu et al., 2024; Magalhães et al., 2020; Tsykhanovska et al., 2025). The application of bamboo fiber, in turn, is considered not only as an approach to improving the functional and technological properties of the product, but also as a component of an integrated strategy for developing products with reduced phosphate or sodium content (Pinton et al., 2024).

Emulsions are widely used in dairy products, sauces, beverages, and meat systems, but they are prone to destabilization processes including creaming, coalescence, and phase separation. Fibers interact with emulsions by altering viscosity, forming networks, and in some cases, acting as Pickering stabilizers. Soluble fibers, such as oat β -glucan, are effective viscosity builders, while insoluble fibers like wheat bran or bamboo fiber act as structuring agents. Recent studies indicate that bamboo fiber enhances gel strength and stabilizes protein matrices (Tao et al., 2024). Oat β -glucan has been shown to increase yield stress and viscosity in protein emulsions (Tao et al., 2024). Wheat fiber is commonly applied as a fat mimetic in meat emulsions, contributing to water retention and improved texture (Sampaio et al., 2024).

This paper provides a side-by-side comparison of wheat, bamboo, and oat fibers in model protein-fat emulsions, focusing on plasticity, viscosity, mechanical resilience, and freeze-thaw stability. The results offer guidance for food formulators seeking to optimize emulsion performance using natural dietary fibers. The use of bamboo fiber in the recipes of meat pates and emulsions for meat industry is still not widely presented in the scientific publications topic at the same time as the high process tolerance and possibilities to apply bamboo fiber in the recipes of meat emulsions is already known and results published (Pinton et al., 2024).

The use of high-power ultrasound in combination with bamboo fiber was evaluated as a strategy to produce phosphate-free meat emulsions. Samples were prepared with 0 or 0.25% alkaline phosphate and 0, 2.5, or 5% bamboo fiber (Pinton et al., 2024). Emulsions containing bamboo fiber but no phosphate exhibited higher stability compared to those with phosphate. The inclusion of 2.5% bamboo fiber effectively mitigated the texture changes caused by the absence of phosphate. High-power ultrasound (HPU) treatment further enhanced the effect of bamboo fiber on emulsion texture by increasing cohesiveness. Neither HPU treatment nor the addition of bamboo fiber produced notable changes in the oxidative quality of the samples. However, both instrumental analyses and sensory evaluation showed that the absence of phosphates resulted in higher lipid oxidation from the very beginning of storage.

It should also be noted that the use of bamboo fiber in emulsions has been repeatedly considered as a potential approach to replace animal proteins with high functional and technological properties, such as pork skin proteins (Dos Santos et al., 2020).

The application of bamboo fiber in low-salt meat products has been demonstrated in emulsion-type sausages at inclusion levels of 1.0–5.0% of the total raw material mass. This not only enables the development of healthier product formulations but also enhances storage stability and moisture retention (Magalhães et al., 2020).

The aim of the study was to evaluate and compare the effects of heat treatment on the functional, technological, and stability properties of protein-fat emulsions enriched with bamboo, oat, and wheat fibers for meat and fish products.

Materials and methods

Three types of dietary fibers from different raw materials were selected for the study: wheat fiber (Vitacel WF200), oat fiber (Sanacell Oat 200), and bamboo fiber (JeluCel BF200). Considering the typical applications of such products in the technology of emulsified sausages and pâtés (Ciobanu et al., 2025), several rheological and techno-functional parameters were chosen for analysis: plasticity of hydrated fibers, plasticity and stability of emulsions after cooling, after heat treatment, and under freeze-thaw conditions.

Preparation of the emulsions

Emulsions were prepared in two steps. In addition to the fibers, the formulation included a dry protein blend composed of sodium caseinate, porcine skin protein, and hydrolyzed soy protein in equal proportions, along with refined sunflower oil, guar gum, and carboxymethyl cellulose. The recipe of emulsion was designed to meet the protein: moisture: fat ratios 1:6:3 which are close to typical ranges applied in the formulations of industrial emulsions (Jin et al., 2015) with the significant content of fiber to reflect the effect of this ingredient on the estimated properties (Dos Santos et al., 2020).

The three samples of emulsions were prepared. The formulation of the emulsion samples included a protein preparation (10%), sunflower oil (35%) and fiber previously hydrated with water in 1:3 ratio (5% of fiber and 15% of water), carboxymethyl cellulose (0.5%), and additional amount of water (34.5%).

Different types of dietary fibers were used in each sample of emulsion: sample 1 contained Vitacel WF200 (15%), sample 2 contained Sanacel Oat 200 (15%), and sample 3 contained JeluCel BF200 (15%).

Emulsion preparation

The emulsion preparation involved the preliminary hydration of dietary fibers by mixing them with water at a ratio of 1:3 and stirring at 30 rpm for 5 minutes. After this initial mixing, the hydrated fibers were stirred again after 30 minutes to allow sufficient time for the fiber capillary structures to swell and/or disperse, ensuring better uniformity and a more accurate evaluation of fiber properties. The water-holding capacity (WHC) and plasticity of the hydrated fiber samples were then determined using the compression method described by Danylevych et al. (2025).

In a Bosch Kitchen Aid-type mixer, the remaining amount of water, carboxymethyl cellulose, and the protein preparation were first combined, followed by fine grinding and mixing at 800–900 rpm for 3 minutes. Subsequently, the hydrated fiber was incorporated into the mixture, and refined sunflower oil was gradually added to the primary suspension while stirring at 180 rpm. Emulsification was then performed for 5 minutes at 1200 rpm. The resulting emulsions reached a temperature of 26–27.5 °C. After cooling at room temperature for 2 hours, a portion of the emulsion was taken for plasticity and stability testing without thermal treatment, while the remaining portion was subjected to heat treatment.

Thermal treatment of emulsions

Thermal treatment of the emulsions was performed in a water bath for 30 minutes at a water temperature of 95 °C, reaching 90 °C in the emulsion mass by the end of the process. After thermal treatment, the emulsions were cooled to 25 °C in the bulk at room temperature, followed by measurement of emulsion plasticity and stability.

Determination of plasticity and rheological properties of emulsions

Emulsion plasticity was evaluated using the compression method. A $0.2-0.4\,\mathrm{g}$ sample of the prepared emulsion or hydrated fiber was placed on a laboratory glass plate and compressed under controlled conditions.

Assessment of emulsion stability during storage and after thermal treatment

Emulsion stability was determined by centrifuging the obtained samples at 3000 rpm for 10 minutes. Stability was evaluated under two treatment conditions: after pasteurization at 95 °C in a water bath for 30 minutes and without thermal treatment, followed by freezing at -24 °C for 24 hours and thawing at room temperature (18–20 °C) over the next 16 hours.

Statistical analysis

All experiments were conducted in triplicate, and statistical analyses were performed using Microsoft Excel. Analysis of variance (Anova) and Tukey's test were used to compare the means between the samples with 95% confidence (p < 0.05).

Results and discussion

Plasticity of hydrated fiber samples

According to the data presented in Table 1, the oat-based fiber samples showed the lowest plasticity, 4.76 cm/g, whereas the bamboo-based samples exhibited the highest water-holding capacity, 89.7%, and intermediate plasticity, 5.32 cm/g.

Plasticity and WHC of hydrated fiber

Table 1

Paramenter	Wheat fiber	Oat fiber	Bamboo fiber
Plasticity, cm/g	4.76±0.22 ^a	6.04 ± 0.24^{b}	5.32±0.18°
WHC,%	82.5±1.70 ^a	85.6 ± 1.10^{b}	89.7±1.20°

Note: Different letters in the same row represent significant differences according to Tukey's test (p<0.05).

Plasticity and visual assessment of protein-fat emulsions

After production and cooling, the plasticity of the emulsion samples was measured, and their texture and consistency were visually evaluated (Figure 1). The most notable difference was observed between samples 2 and 3 (oat and bamboo fibers). Sample 2 exhibited a less elastic consistency; even after cooling, the emulsion demonstrated thixotropic behavior and flowability. The consistency of sample 1, based on wheat fiber, was comparable to that of sample 3.

The plasticity of the obtained emulsions differed considerably among samples 1, 2, and 3, which corresponded to the differences in their consistency. Specifically, the oat fiber-based sample exhibited the highest plasticity (7.43 cm/g), whereas the plasticity values of samples 1 and 3 were similar (6.48 and 6.22 cm/g, respectively).

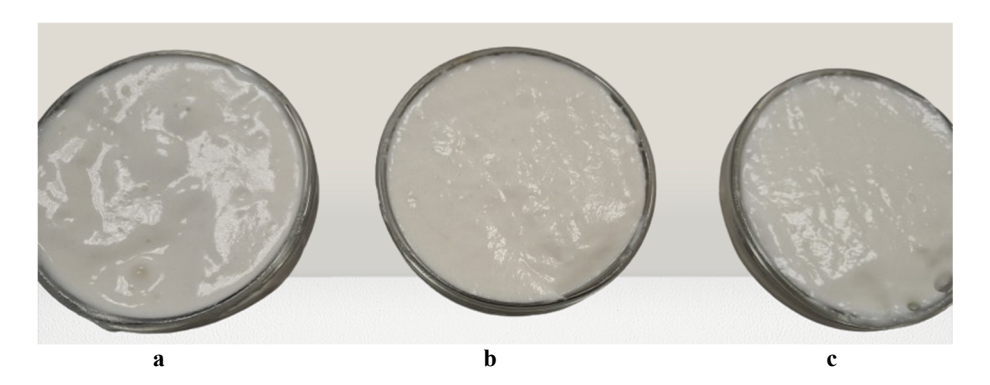


Figure 1. Emulsions based on oat (a), bamboo (b) and wheat (c) fibers

The water-holding capacities (WHC) did not show differences as pronounced as those observed in plasticity among the groups. Nevertheless, the lowest WHC value was recorded for sample 2 (78.64%), while samples 1 and 3 again demonstrated similar values (80.12% and 81.73%, respectively).

After thermal treatment and subsequent cooling, the plasticity and WHC values of the samples changed, showing a reduction in both parameters. The results are presented in Table 2.

Table 2 Characteristics of emulsion samples prior and after the thermal treatment

Characteristics	Sample 1	Sample 2	Sample 3
Characteristics	(wheat fiber)	(oat fiber)	(bamboo fiber)
Plasticity, cm/g	6.48±0.24 ^a	7.43 ± 0.20^{b}	6.22±0.20 ^a
Plasticity after thermal treatment, cm/g	5.61±0.15 ^a	6.77 ± 0.18^{b}	5.36±0.14 ^a
Δ Plasticity, cm/g	0.87 ± 0.09^{a}	0.66 ± 0.06^{b}	0.86 ± 0.08^{a}
WHC,%	80.12±1.31 ^a	78.64±1.02 ^b	81.73±1.16 ^a
WHC after thermal treatment,%	72.42±1.52 ^a	65.81±1.28 ^b	75.15±1.25 ^a
Δ WHC,%	7.70±0.42 ^a	12.83±0.59 ^b	6.58±0.45°

Note: Different letters in the same row represent significant differences according to Tukey's test (p<0.05).

The comparative assessment of emulsion characteristics before and after thermal treatment revealed distinct effects of the incorporated fibers on plasticity and water-holding capacity (WHC). The results demonstrate that the physical stability and moisture-retention behavior of the systems were highly dependent on fiber composition and structural functionality. Although all samples underwent a measurable decrease in both plasticity and WHC upon heating, the magnitude of these changes varied significantly among the fiber types, reflecting differences in their hydration potential, thermal resilience, and network-forming ability within the protein-lipid matrix.

Prior to heating, oat fiber provided the highest plasticity value (7.43 ± 0.20 cm/g), followed by wheat fiber (6.48 ± 0.24 cm/g) and bamboo fiber (6.22 ± 0.20 cm/g). This indicates that the

emulsion containing oat fiber initially exhibited the greatest structural compliance and deformation capacity, consistent with the presence of soluble β -glucans capable of increasing phase viscosity and enhancing dispersive homogeneity. The higher plasticity suggests more flexible gel-like behavior in the continuous phase, facilitating improved dispersion of lipid droplets. Wheat and bamboo fibers demonstrated comparatively lower plasticity values, implying a more compact or rigid internal network formed by the predominance of insoluble fractions such as cellulose and lignin.

After thermal processing, a reduction in plasticity was recorded for all systems, indicating structural tightening and partial dehydration of the emulsion matrix. The post-heating values decreased to 6.77 ± 0.18 cm/g for oat fiber, 5.61 ± 0.15 cm/g for wheat fiber, and 5.36 ± 0.14 cm/g for bamboo fiber. The resulting differences (Δ Plasticity) were 0.66 ± 0.06 cm/g for oat, 0.87 ± 0.09 cm/g for wheat, and 0.86 ± 0.08 cm/g for bamboo. These results indicate that oat fiber, despite its initially higher plasticity, experienced the smallest relative decrease (8.9%), suggesting that its soluble components mitigate the mechanical contraction typically caused by heat-induced protein coagulation. Wheat and bamboo fibers, in contrast, exhibited greater reductions (13.4% and 13.8%, respectively), pointing to more pronounced network compaction and reduced elasticity as heating progressed. The relatively similar Δ Plasticity values for wheat and bamboo suggest comparable rigidification kinetics, possibly due to the formation of dense, fibrous aggregates within the matrix.

Water-holding capacity (WHC) followed a similar trend, though the absolute values and the extent of changes reflected the distinct hydration properties of the fibers. Before heating, bamboo fiber displayed the highest WHC (81.73±1.16%), indicating superior ability to retain moisture within the emulsion system. Wheat fiber followed with 80.12±1.31%, while oat fiber recorded the lowest pre-heating WHC (78.64±1.02%). These differences correspond to the physicochemical composition of the fibers: bamboo fiber, rich in insoluble cellulose, possesses a highly porous structure that effectively entraps water mechanically, whereas oat fiber's solubility leads to greater hydration but less stable moisture retention under stress conditions.

After thermal treatment, all emulsions showed a notable decrease in WHC, confirming that heating promotes partial syneresis and expulsion of entrapped water. Post-heating values decreased to 72.42±1.52% for wheat fiber, 65.81±1.28% for oat fiber, and 75.15±1.25% for bamboo fiber. The magnitude of change (Δ WHC) was 7.70±0.42% for wheat, 12.83±0.59% for oat, and 6.58±0.45% for bamboo. These results indicate that bamboo fiber retained the highest proportion of water after heating, confirming its role as a thermally stable moisture-binding agent. The smallest Δ WHC in bamboo (6.58%) suggests that its dense, insoluble framework effectively immobilizes water even under thermal stress, preventing excessive phase separation. Wheat fiber exhibited an intermediate behavior, with moderate water loss consistent with its mixed soluble-insoluble composition. Oat fiber, however, demonstrated the highest water release (Δ WHC = 12.83%), reflecting the limited stability of its soluble β -glucan network when exposed to elevated temperatures.

When comparing plasticity and WHC dynamics collectively, a consistent pattern emerges. Oat fiber provided an initially flexible and hydrated structure but experienced the greatest deterioration under heat, emphasizing its transient stabilizing function. Wheat fiber maintained intermediate values across both parameters, confirming its balanced, moderate performance. Bamboo fiber, although initially less plastic, demonstrated the most stable structural response during heating, combining minimal losses in both plasticity and WHC. This dual resistance highlights the mechanical integrity and strong water-holding capability of bamboo's insoluble matrix, which consolidates over time instead of collapsing under heat-induced stress.

From a physicochemical standpoint, these results reinforce the notion that fiber solubility and microstructure dictate the emulsion's response to thermal treatment. Soluble

fibers like those in oat systems provide rapid hydration and viscosity enhancement, while insoluble fibers such as bamboo contribute to mechanical stabilization and moisture immobilization. Wheat fiber occupies an intermediate position, integrating moderate solubility with sufficient rigidity to maintain overall structural coherence.

In practical terms, these findings indicate that oat fiber can be effectively used in formulations requiring rapid hydration and high initial viscosity, especially during short thermal processes. Wheat fiber provides balanced mechanical and moisture stability for conventional processing conditions. Bamboo fiber, owing to its low plasticity loss and minimal reduction in WHC, represents the most thermally robust option, suitable for extended heat treatments or formulations that require sustained emulsion integrity and moisture retention. The combined analysis confirms that the selection of dietary fiber type critically influences both the rheological and hydration characteristics of emulsified systems before and after thermal exposure, thereby determining the final textural quality and stability of the product.

Determination of emulsion stability

Because of evaluating the stability of the obtained emulsions, the highest stability (S) prior to thermal treatment was observed in the wheat fiber-based emulsion (sample 1) at 86.28%. The values for the other two samples were similar, being 83.27% for sample 2 and 84.11% for sample 3. The losses of emuslions stability (Δ S) after thermal treatment or a freeze-thaw cycle, the stability of sample 1 decreased largely compared to the corresponding values of the other samples (Table 3).

Stability of emulsions

Table 3

Sample	ΔS after thermal treatment, %	ΔS after thawing, %
Wheat fiber	14.19±2.13 ^{ab}	18.43 ± 2.00^{a}
Oat fiber	15.08±2.03 ^a	20.56±1.91 ^a
Bamboo fiber	10.16±2.02 ^b	13.06±1.95 ^b

Note: Different letters in the same column represent significant differences according to Tukey's test (p<0.05).

The established influence of bamboo fiber on emulsion stability is comparable to the effects reported in previously published studies also including the studies for other food products (Ferreira et al., 2021). Specifically, the replacement of animal fat_and its derived emulsions, which was associated with the achievement of more optimal functional and technological properties, represents a well-known research direction (Aminzare et al., 2025). Replacement of animal fat is the technological approach allowing not only develop the products with more balanced fatty-acid compositions, but also is one of the key methods for creating the low-fat, reduced fat and functional meat products (Gumus-Bonacina et al., 2024).

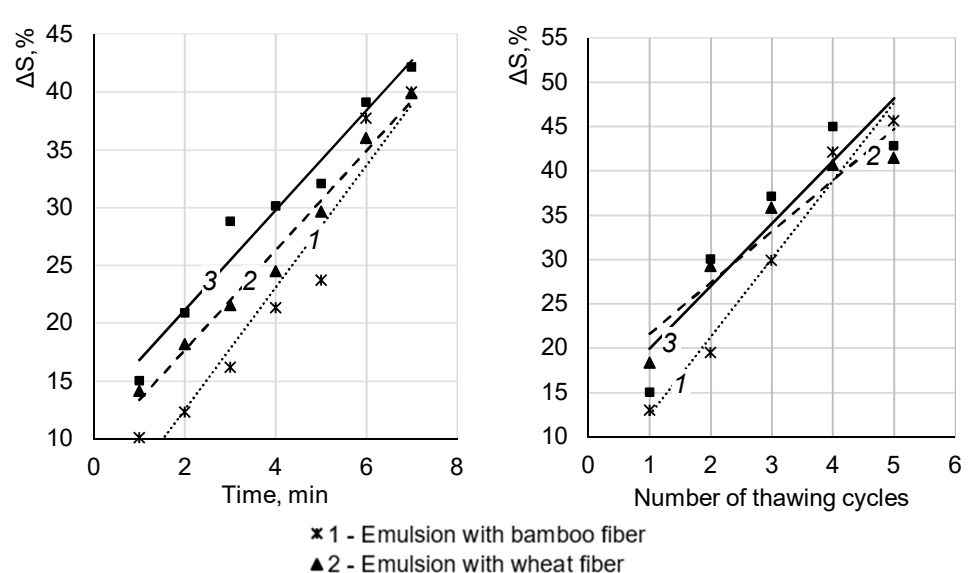
At the same time, assessing the stability of bamboo fiber allows to build the hypothesis regarding its lower susceptibility to mechanical and thermal stresses under conditions typical for the production of emulsion-type meat products and protein-fat emulsions (Dos Santos et al., 2020; Pinton et al., 2024), as observed also based on the changes in emulsion samples plasticity values.

The mechanisms by which bamboo fiber stabilizes emulsions during freez-thaw cycles remain a subject of discussion. When a clear difference in the magnitude of emulsion stability

loss exists, the distinction between samples containing bamboo fiber and other samples diminishes with the accumulation of various stress types – mechanical, thermal, or combined.

Therefore, further investigation is needed into the potential differences in soluble dietary fiber content and particle size distribution, which are key parameters of the raw material (fiber) and can influence emulsion stability due to varying levels of mechanically bound water formed during fiber hydration at the raw material preparation stage.

The emulsions were additionally subjected to a prolonged heat treatment at 95 °C for 120 min, with samples taken every 15 min. In addition, emulsion samples from another batch were subjected to multiple freeze-thaw cycles to determine the effect of these factors on emulsion stability loss (Figure 2 and Figure 3).



■ 3 - Emulsion with oat fiber

Figure 2. Decrease of emulsion stability (ΔS) Figure 3. Decrease of emulsion stability (ΔS) of the samples over time of the samples after freeze cycles

Effect of thermal treatment time and repeatable freezing on losses of emulsion stability

The data obtained during thermal processing within the range of 30–120 minutes (Table 4) indicate that all examined dietary fibers contributed to the stabilization of emulsions, although the intensity, onset, and duration of their effects varied markedly. At the initial heating stage (30–45 min), oat fiber exhibited the most pronounced stabilizing influence, outperforming both wheat and bamboo fibers. This observation is consistent with the functional role of soluble dietary fractions, especially β-glucans, which readily hydrate, increase the viscosity of the continuous phase, and consequently reduce droplet mobility. As a result, the emulsion system containing oat fiber demonstrated the lowest breakdown rate during the first 45 minutes, showing a stability decrease of 15.08–20.96%, whereas wheat fiber emulsions recorded 14.19–18.25% and bamboo fiber 10.16–12.38%. Although the absolute values for bamboo were lower, the relatively slower rate of change suggests that the stabilizing mechanism in bamboo-based systems develops more gradually and does not manifest immediately upon heat exposure.

Table 4

Decrease of stability during the thermal treatment of emulsions

	Decrease of	Decrease of emulsion stability ΔS,%							
Time	Emuslion 1 (wheat fiber)	Emuslion 2 (oat fiber)	Emuslion 3 (bamboo fiber)						
30	10.16±0.85a	14.19±0.94 ^b	15.08±0.79 ^b						
45	12.38±1.16 ^a	18.25±1.05 ^b	20.96±0.66°						
60	16.25±0.98a	21.62±1.10 ^b	28.85±0.95°						
75	21.38±0.52a	24.55±0.96 ^b	30.19±0.98°						
90	23.75±1.02 ^a	29.67±1.15 ^b	32.11±1.03°						
105	37.80±1.19ab	36.03±1.30 ^a	39.15±1.38 ^b						
120	40.02±0.91a	39.9 ± 1.11^a	42.19±1.21 ^a						

Note: Different letters in the same row represent significant differences according to Tukey's test (p<0.05).

The observed differences among the fibers can be attributed to variations in hydration kinetics and their spatial integration within the protein–lipid matrix, as also reported by Zhuang et al. (2019). Oat fiber, characterized by high solubility, interacts rapidly with the aqueous phase, increasing viscosity and forming transient gel-like networks that restrict oil droplet coalescence. However, this rapid stabilization is often temporary, as the weak networks tend to degrade under sustained thermal stress. Wheat fiber, containing both cellulose and hemicellulose, absorbs water at a moderate rate and provides a balanced stabilization profile through partial solubility and structural support. Bamboo fiber, on the other hand, composed mainly of insoluble cellulose and lignin, remains relatively inert during the initial phase but gradually swells and traps water over time, forming a mechanically robust structure as heating continues.

At 60 minutes, the overall stabilization pattern begins to shift. Oat fiber still maintains the highest stability but exhibits a steeper decline, indicating weakening of its viscosity-driven structure. Meanwhile, bamboo fiber becomes increasingly active: its emulsion stability loss rises from 16.25% at 60 minutes to 21.38% at 75 minutes, suggesting that its insoluble matrix progressively engages in structural reinforcement. The performance gap between bamboo and wheat fibers decreases from nearly 6% at 60 minutes to less than 3% by 75 minutes, showing that bamboo fiber gradually compensates for its delayed activation and starts contributing substantially to emulsion integrity.

Between 75 and 90 minutes, the stabilizing effect of bamboo fiber becomes dominant. By 90 minutes, the system containing bamboo fiber exhibits a 23.75% decrease in emulsion stability, whereas wheat and oat fibers show reductions of 29.67% and 32.11%, respectively. These results confirm that prolonged heating facilitates complete hydration and expansion of bamboo's insoluble particles, leading to the formation of a dense spatial network that minimizes droplet coalescence and enhances water-fat retention. The gradual reinforcement observed for bamboo fiber is indicative of a cumulative stabilization process, dependent on extended exposure to heat and progressive structural integration.

During the final heating phase (105–120 min), bamboo fiber achieves near-maximal stabilization efficiency. Total stability losses are 37.8–40.02% for bamboo fiber, 36.03–39.91% for wheat, and 39.15–42.19% for oat. Despite the apparent convergence of the values, the underlying mechanisms differ substantially. Oat fiber stabilization primarily results from viscosity enhancement and soluble polymer entanglement, which deteriorate

upon long-term heating. Wheat fiber, with its balanced composition, maintains moderate stability throughout, showing limited but consistent structural integrity. Bamboo fiber, in contrast, attains its peak functionality in the later stages through the densification of its fibrous matrix and immobilization of interstitial moisture, which together confer mechanical stability and prevent phase separation. The convergence of stability values after prolonged heating indicates that all systems reach a quasi-equilibrium between matrix disintegration and reorganization of the dispersed phase.

Overall, the thermal behavior of these fibers demonstrates distinct kinetic profiles: oat fiber ensures rapid but transient stabilization due to the immediate hydration of soluble fractions; wheat fiber provides a steady, balanced effect through moderate water absorption; and bamboo fiber offers delayed yet durable reinforcement because of gradual matrix activation. From a technological standpoint, this differentiation suggests that oat fiber is best suited for short-term or rapid-heat processes, wheat fiber for standard processing regimes, and bamboo fiber for extended or high-temperature applications where long-term structural integrity is required.

The demonstrated slight decrease of the bamboo fiber WHC goes align with the results obtained by Du et al. (2023). Used in this publication steam cooking demonstrates different heat transefering patters compared to the heating on the water batch, but the tendency showed in both cases give the possibility to estimate the moderate to high process tolerance of bambo fiber WHC. Jiang et al. (2019) also reported the decrease of water holding capacity of the wheat fiber applied in the dough systems, while the more representative data regarding the changes of wheat fiber WHC in emulsions are limited.

Berggren (2018) investigated the water-holding capacity and viscosity of oat fiber and various types of flour, reporting a clear relationship between β -glucan content and the heat stability of the flours studied. In our study, emulsions containing oat fiber exhibited the lowest heat stability. Therefore, to identify potential correlations, an additional assessment of β -glucan content in the investigated plant fibers is required.

Freeze-thaw stability evaluation

Under freeze-thaw conditions, the functional responses of the tested fibers deviated notably from their thermal behavior (Table 5 and Figure 3). The results presented in Table 5 clearly indicate that bamboo fiber maintained the lowest rate of emulsion destabilization across repeated cycles, confirming its superior resilience to cryogenic stress and mechanical fatigue. During the first cycle, all emulsions exhibited limited instability, but bamboo fiber demonstrated the smallest reduction in stability (13.06%), followed by oat (15.08%) and wheat (18.43%). This initial advantage can be attributed to bamboo fiber's capacity to retain mechanically bound water and resist structural deformation induced by ice crystal formation. The rigid and insoluble cellulose framework likely restricted water migration, thereby mitigating expansion and contraction forces that typically disrupt emulsified systems during freezing and thawing.

In subsequent cycles, the differences between the fiber systems became increasingly pronounced. After the second and third cycles, bamboo fiber emulsions recorded cumulative stability losses of 19.55 and 29.95%, respectively. In comparison, wheat fiber systems exhibited losses of 29.28 and 35.9%, and oat fiber systems 30.12 and 37.15%. The incremental destabilization per cycle averaged approximately 8.2% for bamboo, 8.7% for wheat, and 11.0% for oat, confirming that bamboo fiber provides superior mechanical buffering under repetitive stress conditions. These findings highlight bamboo fiber's ability to preserve the emulsion matrix despite repeated freezing-thawing transitions.

Table 5

Stability of emulsions during the freezing and thawing cycles

Number of	Decrease of emulsion stability, ΔS,%				
freeze-thawing cycles	Emuslion 1 (wheat fiber)	Emuslion 2 (oat fiber)	Emuslion 3 (bamboo fiber)		
1	13.06±0.48a	18.43±0.76 ^b	15.08±0.55°		
2	19.55±0.81a	29.28±1.05 ^b	30.12±1.03 ^b		
3	29.95±1.05a	35.9±1.18 ^b	37.15±0.98 ^b		
4	42.18±1.52 ^a	40.71±1.60 ^a	45.05±0.95 ^b		
5	45.70±1.29a	41.52±1.25 ^b	42.87±1.02 ^b		

Note: Different letters in the same row represent significant differences according to Tukey's test (p<0.05).

By the fourth cycle, all systems showed accelerated instability because of cumulative matrix fatigue and internal moisture migration. Nonetheless, bamboo fiber emulsions maintained better coherence, reaching a stability loss of 42.18%, compared to 40.71% for wheat and 45.05% for oat. Although the differences in absolute values narrowed, the failure patterns diverged: bamboo-based systems exhibited uniform, gradual degradation with minimal phase separation, whereas oat fiber systems tended to experience localized ruptures and pronounced water-fat separation due to the breakdown of soluble networks.

After the fifth cycle, the results converged further, with final stability reductions of 45.7% for bamboo, 41.52% for wheat, and 42.87% for oat. Despite bamboo showing a slightly higher absolute percentage, its overall rate of cumulative change remained the lowest across cycles, confirming its superior long-term structural endurance. The apparent convergence at later stages likely reflects exhaustion of the protein-lipid interface rather than diminished fiber efficiency, as bamboo's rigid cellulose matrix continues to preserve partial structural integrity.

From a physicochemical perspective, bamboo fiber's exceptional freeze-thaw stability can be attributed to its coarse surface morphology and rigid insoluble framework, which mechanically reinforce the protein-lipid matrix and minimize syneresis upon thawing (Sampaio et al., 2024; Zhao et al., 2023). Wheat fiber, with its intermediate composition, provides consistent yet moderate protection by combining limited solubility with structural reinforcement. Out fiber, rich in β -glucans, contributes substantially to early viscosity formation but lacks sufficient mechanical strength to prevent microstructural disruption under repeated cryogenic stress, leading to redistribution of water and lipid components (Diaz et al., 2022).

The kinetic behavior of bamboo fiber suggests a pronounced phase-stabilizing effect that delays the onset of destabilization beyond the second cycle, likely resulting from water entrapment within the cellulose network and reduced ice recrystallization. Such behavior provides technological advantages in frozen emulsion systems, where maintaining textural and structural stability over storage is critical. The data confirm that bamboo fiber effectively mitigates structural fatigue and moisture migration during repeated freezing-thawing cycles. The similar phenomena was observed in several studies investigating the freeze-thaw stability and ice recrystallization of celluloses and fibers (Xin et al., 2025; Yang et al., 2024).

From a practical and industrial perspective, these findings emphasize the necessity of tailoring fiber selection to processing and storage requirements. Bamboo fiber represents the most promising functional ingredient for formulations that undergo extended heating or

freezing-thawing cycles, such as frozen, chilled, or long-shelf-life emulsified meat products. Its delayed activation during thermal processing combined with superior structural endurance under cryogenic conditions provides a dual functional advantage. Wheat fiber offers an intermediate, cost-efficient solution with balanced stabilization properties under diverse processing conditions, while oat fiber, although less stable over time, remains advantageous in formulations requiring rapid viscosity development and short-term stabilization.

In conclusion, integration of the thermal and freeze-thaw data indicates that bamboo fiber exhibits the most favorable functional performance among the fibers investigated. Its slow activation, sustained stabilization capacity, and resistance to degradation under repetitive stress make it particularly suitable for the development of phosphate-free, high-moisture emulsions. Such characteristics are of substantial technological relevance for the production of healthier, more sustainable, and functionally stable emulsified meat products or plant-based analogues with extended shelf life and reduced additive requirements. Bamboo fiber, although slower to activate initially, demonstrates accelerated functional development over time, eventually reaching or exceeding the levels observed for wheat and approaching those of oat fiber. Crucially, it consistently yields the lowest loss of emulsion stability during thawing, especially in the early and intermediate phases, underscoring its superior protective role against freeze-thaw damage. Although this advantage lessens with prolonged exposure, bamboo fiber remains at least as effective as wheat and significantly more stable than oat fiber.

Overall, the findings suggest that bamboo fiber offers dual advantages: robust resistance to freeze-thaw destabilization and progressive functional enhancement during storage. This makes it a promising option for developing products where long-term stability and structural integrity are essential. Oat fiber, while valuable for applications requiring rapid functional improvement, is less suitable for frozen products. Wheat fiber, in turn, represents a versatile but less specialized solution, providing moderate and reliable functionality under most conditions.

Conclusions

According to the objectives set for this study, it was established that thermal treatment at 95 °C reduced the stability of emulsions containing bamboo, wheat, and oat fibers, with the slowest decline observed in the samples formulated with bamboo fiber. Furthermore, during the freezing and thawing cycles, these samples demonstrated the smallest loss of emulsion stability, confirming the superior protective capacity of bamboo fiber under thermal and freeze-thaw stress conditions. Overall, these results reinforce the conclusion that bamboo fiber provides the most robust functional performance and the highest potential for maintaining emulsion integrity in technologically demanding applications.

References

Aminzare M., Afshari A., Hashemi M., Noori S.M.A., Rezaeigolestani M. (2024), Replacement of animal fat with argan oil in Bologna-type chicken sausages, *ACS Food Science & Technology*, 4(1), pp. 1–11, https://doi.org/10.1021/acsfoodscitech.4c00753

Aminzare M., Afshari A., Hashemi M., Noori S.M.A., Rezaeigolestani M. (2025), Comparative evaluation of the effects of different dietary fibers as natural additives on the shelf life of cooked

- sausages, ACS Food Science & Technology, 5(1), pp. 1–11, https://doi.org/10.1021/acsfoodscitech.5c00144
- Berggren S. (2018), Water holding capacity and viscosity of ingredients from oats: the effect of b-glucan and starch content, particle size, pH and temperature, https://doi.org/rn:nbn:se:lnu:diva-70544
- Ciobanu M.M., Manoliu D.R., Ciobotaru M.C., Flocea E.I., Boișteanu P.C. (2025), Dietary fibres in processed meat: a review on nutritional enhancement, technological effects, sensory implications and consumer perception, *Foods*, 14(9), 1459, https://doi.org/10.3390/foods14091459
- Da Silva V.T., Mateus N., de Freitas V., Fernandes A. (2024), Plant-based meat analogues: Exploring proteins, fibers and polyphenolic compounds as functional ingredients for future food solutions, *Foods*, 13(14), 2303, https://doi.org/10.3390/foods13142303
- Danylevych I., Pasichnyi V., Shubina Y., Petryna A. (2025), Ways of improving the technology of marined semi-finished poultry meat using ultrasound, *Scientific Works of National University of Food Technologies*, 31, pp. 179–189, https://doi.org/10.24263/2225-2924-2025-31-2-16
- Diaz J.R., Kantanen K., Edelmann J.M., Suhonen H., Sontag-Strohm T., Jouppila K., Piironen V. (2022), Fibrous meat analogues containing oat fiber concentrate and pea protein isolate: Mechanical and physicochemical characterization, *Innovative Food Science & Emerging Technologies*, 77, 102954. https://doi.org/10.1016/j.ifset.2022.102954
- Djordjević M., Ambrus R., Maravić N., Vidović S., Šoronja-Simović D., Petrović J., Šereš Z. (2022), Impact of short-time micronization on structural and thermal properties of sugar beet fibre and inulin, *Food Technology and Biotechnology*, 60(4), pp. 543–555, https://doi.org/10.17113/ftb.60.04.22.7734
- Dos Santos M., Ozaki M.M., Ribeiro W.O., de Souza Paglarini C., Vidal V.A.S., Campagnol P.C.B., Pollonio M.A.R. (2020), Emulsion gels based on pork skin and dietary fibers as animal fat replacers in meat emulsions: An adding value strategy to byproducts, *LWT*, 120, 108895, https://doi.org/10.1016/j.lwt.2019.108895
- Dreher J., Knorz M., Herrmann K., Terjung N., Gibis M., Weiss J. (2022), Structuring oil to substitute palm fat in dry-fermented poultry sausages, *Food Structure*, 33, 100281, https://doi.org/10.1016/j.foostr.2022.100281
- Du J., Zhu Q., Guo J., Wu Y., Hu Z., Yang S., Jiang J. (2023), Effects of ultrasonic and steam-cooking treatments on the physicochemical properties of bamboo shoots protein and the stability of O/W emulsion, *Heliyon*, 9(9), e19825, https://doi.org/10.1016/j.heliyon.2023.e19825
- Ferreira A.R., Gianasi F., de Menezes Alves Moro T., Felisberto M.H.F., Neves E.C.A., Clerici M.T.P.S. (2021), Functional pasta: A comparative study of the use of bamboo fibers and white fibers, In: Z. Ahmad, Y. Ding, A. Shahzad (Eds.), *Biotechnological Advances in Bamboo*, pp. 431–446, Springer, Singapore, https://doi.org/10.1007/978-981-16-1310-4_18
- Gumus-Bonacina C.E., McClements D.J., Decker E.A. (2024), Replacing animal fats with plant-based lipids: Challenges and opportunities, *Current Opinion in Food Science*, 58, 101193, https://doi.org/10.1016/j.cofs.2024.101193
- Habiba U., Ali M.S., Hashem M.A., Hossain M.M., Habib M. (2021), Effect of adding different types of flour on the quality of low fat beef sausage, *Bangladesh Journal of Animal Science*, 50(1), pp. 1–11, https://doi.org/10.3329/bjas.v50i1.55562
- Jiang Y., Zhao Y., Zhu Y., Qin S., Deng Y., Zhao Y. (2019), Effect of dietary fiber-rich fractions on texture, thermal, water distribution, and gluten properties of frozen dough during storage, *Food Chemistry*, 297, 124902, https://doi.org/10.1016/j.foodchem.2019.05.176
- Jin S.K., Ha S.R., Hur S.J., Choi J.S. (2015), Effect of the ratio of raw material components on the physico-chemical characteristics of emulsion-type pork sausages, *Asian-Australasian Journal of Animal Sciences*, 29(2), 263, https://doi.org/10.5713/ajas.15.0129
- Li J., Xi Y., Wu L., Zhang H. (2023), Preparation, characterization and in vitro digestion of bamboo shoot protein/soybean protein isolate based-oleogels by emulsion-templated approach, *Food Hydrocolloids*, 136, 108310, https://doi.org/10.1016/j.foodhyd.2022.108310
- Liu X., Liu Y., Du X., Fu B., Jiang P., Qi L., Shang S. (2024), Characterization of bamboo shoots dietary fiber modified by ball milling and its role in altering the physicochemical properties of

- shrimp surimi, *International Journal of Biological Macromolecules*, 271, 131979, https://doi.org/10.1016/j.ijbiomac.2023.131979
- Magalhães I.M.C., Paglarini C.D.S., Vidal V.A.S., Pollonio M.A.R. (2020), Bamboo fiber improves the functional properties of reduced salt and phosphate-free Bologna sausage, *Journal of Food Processing and Preservation*, 44(12), e14929, https://doi.org/10.1111/jfpp.14929
- Marczak A., Mendes A.C. (2024), Dietary fibers: Shaping textural and functional properties of processed meats and plant-based meat alternatives, *Foods*, 13(12), 1952, https://doi.org/10.3390/foods13121952
- Naghdi S., Rezaei M., Kashiri M., Rezaei F., Naseri S., Nourani H., Khakpour Z. (2025), Development and evaluation of low-fat fish and chicken nuggets fortified with date seed powder and quinoa flour as agricultural dietary fiber sources, *Food Science & Nutrition*, 13(4), e4749, https://doi.org/10.1002/fsn3.4749
- Oyegoke R.A., Oladele J.O., Oladele O.T., Oladiji A.T. (2024), Role of dietary fibre and phytonutrients in human health and nutrition, In: *Nutrition and Diet in Health*, *CRC Press*, pp. 121–147, https://doi.org/10.1201/9781003361497-12
- Park S.Y., Oh T.S., Kim G.W., Kim H.Y. (2020), Quality properties of various dietary fibers as isolated soy protein (ISP) replacements in pork emulsion systems, *Journal of Animal Science and Technology*, 62(1), 94, https://doi.org/10.5187/jast.2020.62.1.94
- Paredes-Toledo J., Herrera J., Díaz-Calderón P., Robert P., Giménez B. (2024), In vitro gastrointestinal release of chlorogenic acid and curcumin co-encapsulated in double emulsions with the outer interface stabilized by cellulose nanocrystals, *Colloids and Interfaces*, 8(2), 24, https://doi.org/10.3390/colloids8020024
- Pinton M.B., Lorenzo J.M., Seibt A.C.M.D., Dos Santos B.A., da Rosa J.L., Correa L.P., Campagnol P.C.B. (2022), Effect of high-power ultrasound and bamboo fiber on the technological and oxidative properties of phosphate-free meat emulsions, *Meat Science*, 193, 108931, https://doi.org/10.1016/j.meatsci.2022.108931
- Pinton M.B., Lorenzo J.M., Dos Santos B.A., Correa L.P., Padilha M., Trindade P.C.O., Campagnol P.C.B. (2024), Evaluation of nutritional, technological, oxidative, and sensory properties of low-sodium and phosphate-free mortadellas produced with bamboo fiber, pea protein, and mushroom powder, *Meat Science*, 216, 109588, https://doi.org/10.1016/j.meatsci.2023.109588
- Sampaio U.M., Felisberto M.H.F., Campelo P.H., Clerici M.T.P.S. (2024), Bamboo fiber applications for food and feed, In: S. Jana (Ed.), *Biopolymers in Pharmaceutical and Food Applications*, pp. 293–310, Wiley-VCH GmbH, https://doi.org/110.1002/9783527848133.ch14
- Stabnikova O., Marinin A., Stabnikov V. (2021), Main trends in application of novel natural additives for food production, *Ukrainian Food Journal*, 10(3), pp. 524–551, https://doi.org/10.24263/2304-974X-2021-10-3-8
- Stabnikova O., Paredes-Lopez O. (2024). Plant materials for the production of functional foods for weight management and obesity prevention, *Current Nutrition & Food Science*, 20(4), pp. 401–422, https://doi.org/10.2174/1573401319666230705110854
- Tao J., Ma Q., Zhang Z., Hu Z., Lei L., Zhao G. (2024), Improving emulsion stabilizing capacity of sodium caseinate by colloidal lignin particles near the isoelectric point, *Food Hydrocolloids*, 151, 109813, https://doi.org/10.1016/j.foodhyd.2024.109813
- Toldra M., Taberner P., Pares D., Carretero C. (2021), Surimi-like protein ingredient from porcine spleen as lean meat replacer in emulsion-type sausages, *Meat Science*, 182, 108640, https://doi.org/10.1016/j.meatsci.2021.108640
- Tsykhanovska I., Stabnikova O., Oliinyk S., Lazarieva T., Gubsky S. (2024), Application of combined food additive based on iron oxide nanoparticles and κombu in a rye-wheat bread technology, *Ukrainian Food Journal*, 13(3), pp. 576-596, https://doi.org/10.24263/2304-974X-2024-13-3-10
- Tsykhanovska I., Stabnikova O., Dorohovich V., Lytvyn O., Hetman P. (2025), Meat cutlets with iron oxide nanoparticles and alga *Laminaria japonica*, *Ukrainian Food Journal*, 14(2), pp. 238–258, https://doi.org/10.24263/2304-974X-2025-14-2-5
- Wang X.X., Wang L.Y., Li S.M., Zhou Z.K. (2024), Amelioration of tiger nut insoluble dietary fiber as a partial substitute for fat in meat emulsions: Techno-functional properties and in vitro protein

- digestibility, Food Research International, 197, 115167, https://doi.org/10.1016/j.foodres.2022.115167
- Xin W., Zhou Y., Xiong W., Yao Y., Zhang J., Wang L. (2025), Characterisation of microcrystalline cellulose derived from wheat bran and evaluation of its ice recrystallisation inhibiting activity, *Food Research International*, 208, 116212, https://doi.org/10.1016/j.foodres.2025.116212
- Xu Y., Yan H., Xu W., Jia C., Peng Y., Zhuang X., Xu X. (2022), The effect of water-insoluble dietary fiber from star anise on water retention of minced meat gels, *Food Research International*, 157, 111425, https://doi.org/10.1016/j.foodres.2022.111425
- Yang T., Zhang Y., Guo L., Li D., Liu A., Bilal M., Xie C., Yang R., Gu Z., Jiang D., Wang P. (2024), Antifreeze polysaccharides from wheat bran: the structural characterization and antifreeze mechanism, *Biomacromolecules*, 25(7), pp. 3877-3892, https://doi.org/10.1021/acs.biomac.3c00958
- Zhang H., Zhang W., Zeng X., Zhao X., Xu X. (2022), Recent progress of fat reduction strategies for emulsion type meat products, *Food Materials Research*, 2(1), pp. 1–10, https://doi.org/10.48130/fmr-2022-0002
- Zhang Y., Wu L., Zhang F., Zheng J. (2023), Sucrose ester alleviates the agglomeration behavior of bamboo shoot dietary fiber treated via high pressure homogenization: Influence on physicochemical, rheological, and structural properties, *Food Chemistry*, 413, 135609, https://doi.org/10.1016/j.foodchem.2023.135609
- Zhao W., Zhang J., Zhang W., Yuan S., Chen H., Wu A. (2023), Effect of bamboo unit morphology on the preparation of bamboo fibers by steam explosion, *Industrial Crops and Products*, 202, 117066, https://doi.org/10.1016/j.indcrop.2023.117066
- Zhao Y., Shao Y., Fan S., Bai J., Zhu L., Zhu Y., Xiao X. (2025), Advanced modification strategies of plant-sourced dietary fibers and their applications in functional foods, *Foods*, 14(15), 2710, https://doi.org/10.3390/foods14152710
- Zhuang X., Jiang X., Zhou H., Han M., Liu Y., Bai Y., Xu X.L., Zhou G.H. (2019), The effect of insoluble dietary fiber on myofibrillar protein emulsion gels: Oil particle size and protein network microstructure, *LWT*, 101, pp. 534-542, https://doi.org/10.1016/j.lwt.2018.11.065

Cite:

UFJ Style

Vorontsov M., Galenko O., Topchii O. (2025), Thermal stability and technological performance of fibre-fortified protein-fat emulsions for meat and fish products, *Ukrainian Food Journal*, 14(3), pp. 448–463, https://doi.org/10.24263/2304-974X-2025-14-3-7

APA Style

Vorontsov, M., Galenko, O., & Topchii, O. (2025). Thermal stability and technological performance of fibre-fortified protein-fat emulsions for meat and fish products. *Ukrainian Food Journal*, *14*(3), 448–463. https://doi.org/10.24263/2304-974X-2025-14-3-7

Oxygen-driven 2-furfural accumulation and its influence on beer sensory stability

Roman Mukoid, Yurii Bulii, Serhii Kiriienko

National University of Food Technologies, Kyiv, Ukraine

Abstract

Keywords:

Beer Sensory Defects 2-furfural Thermal load Oxidation

Article history:

Received 2.04.2025 Received in revised form 10.05.2025 Accepted 30.09.2025

Corresponding author:

Roman Mukoid E-mail: Mukoid_Roman@ ukr.net

DOI: 10.24263/2304-974X-2025-14-3-8

Introduction. Key criteria for ensuring high beer quality and flavor stability include the quality of raw materials and auxiliaries, the efficiency of technological processes, and the concentration of oxidation products in the finished beer, particularly 2-furfural.

Materials and methods. The study objects were milled malt, wort, and pasteurized beer. Physicochemical parameters of beer were determined using the Anton Paar DMA 4500 analyzer; 2-furfural concentration was measured by ultraviolet spectrophotometry; alcohol and real extract by distillation; color by colorimetric titration; bitterness using spectrophotometric analysis.

Results and discussion. The concentration of 2-furfural and the intensity of its formation depend directly on the duration and degree of oxygen exposure during all stages of malt handling, wort production, and beer processing. As oxygen initiates a cascade of oxidative and thermal degradation reactions, the level of 2-furfural progressively increases, leading to deteriorated flavor, premature aging, and the development of stale, cardboard-like notes in the final product. To prevent excessive oxidation and maintain 2-furfural levels within the desirable range of 4–10 µg/l, the storage time of milled malt should not exceed 50 minutes, as prolonged exposure to air promotes early oxidative reactions already at the raw material stage. The most intensive formation of 2-furfural occurs during wort boiling with hops at elevated temperatures, where thermal degradation processes accelerate dramatically: within a 90-minute boil, its concentration increases six fold, rising from 122 to 793 µg/l. Oxygen uptake during subsequent stages also plays a crucial role. When dissolved oxygen increases from 20 to 120 µg/l during wort fermentation and green beer filtration, the concentration of 2-furfural rises accordingly – from 56.6 to 185.2 µg/l. Heat treatment further contributes to this process: even minimal pasteurization nearly doubles the level of 2-furfural (from 56 to 104 µg/l). Once its concentration reaches 150-200 µg/l, beer begins to exhibit clear oxidized notes, loses freshness, and shows noticeable sensory deterioration. Moreover, the presence of oxygen in the bottle headspace drastically accelerates this process, increasing 2-furfural content by 262% (from 107 to 388 µg/l), which severely compromises beer quality and shortens its shelf life. Ultraviolet spectrophotometry is recommended for measuring oxidation products and 2-furfural in raw materials and finished beer, as its results correlate well with chromatographic data.

Conclusions. To enhance beer sensory properties and flavor stability, it is essential to prevent oxygen exposure at all technological stages. The concentration of 2-furfural in beer should not exceed $150-200~\mu g/l$.

Introduction

As regular natural products, beer tends to age, that is, to deteriorate over time under the influence of oxygen. It is well known that oxygen negatively affects beer quality parameters at all stages of production—from malt milling to beer packaging (Bamforth, 2004). During malt storage, oxidation may occur due to contact with oxygen and moisture, altering its chemical composition and decrease quality of both the raw material and the final beer (Filipowska et al., 2021). Components the most sensitive to oxidation, such as lipids and essential oils, can cause undesirable changes in aroma, flavor, and color in finished beer (Kunz et al., 2013).

Malt is most susceptible to oxygen exposure during milling, as its protective cellulose husk is destroyed. Milling should therefore be carried out as fast as possible or in an inert gas atmosphere (e.g., CO₂). Oxidation of grain products at this stage can lead to papery and fruity-oxidized notes in fresh beer (Bettenhausen et al., 2018; Filipowska et al., 2021).

Oxidation also affects hop components, resulting in the loss of characteristic aroma and bitterness essential for beer quality (Krofta et al., 2013). Beer aging leads to the formation of compounds that impair its flavor and aroma. Oxygen promotes the formation of aldehydes that impart vinous or fruity notes; it may increase the level of diacetyl and produce a buttery flavor, and in cases of microbiological spoilage, lactic acid may form (Diaz et al., 2022).

Improper storage conditions, particularly high temperatures and light, accelerate oxidation processes. Thermal treatment intensifies melanoidin formation, sugar caramelization, and the degradation of hop volatiles, causing changes in beer color and flavor. Undesirable oxidation products such as acetaldehyde and carbonyl compounds (e.g., 2,3-butanedione) are formed (Baert et al., 2015; Pieczonka et al., 2021).

The degree of beer aging is indicated by the presence of Maillard reaction products, which can impart caramel, oxidized, papery, fruity, leathery, and other off-flavors (Carneiro and Guido, 2006; Lohinova and Petrusha, 2023). This reaction may result in the formation of heterocyclic aldehydes and ketones in beer, including 2,3-butanedione; 2-ethyl-3,5-dimethoxy-4-hydroxyhydro-2(3H)-furanone, and 5-hydroxymethyl-2-furfural. 2-furfural belongs to the group of furan aldehydes formed during thermal load of foods in the presence of atmospheric oxygen. Such processes occur during malt production (at kilning and drying stages) and during wort boiling with hops. Thermal load increases its formation and contributes to the color development of wort (Baert et al., 2012; Kunze et al., 2016). The sensory threshold of 2-furfural is $150-200~\mu g/l$. Its formation is preceded by the synthesis of 3-deoxypentosone. During the Maillard reaction, furfural is produced through a series of reactions initiated by interactions between amino acids and pentoses. Its presence in malt and wort may also result from pentose caramelization; in this case, 3-deoxypentosone is formed directly from pentoses (Rakete et al., 2014).

According to the literature, the level of 2-furfural in fresh beer is influenced by malt type (pale, caramel, dark, roasted), the thermal load on wort during boiling, and beer pasteurization (Vanderhaegen et al., 2006). When using the same wort-boiling system, specifically an internal boiler, increasing the evaporation rate from 4 to 11% decreases furfural content in cold wort from 339 to 274 μ g/l. During fermentation, yeast actively reduces this aldehyde to the corresponding alcohol (furfuryl alcohol), which further lowers its concentration in fresh beer to 20–70 μ g/l. During pasteurization, furfural content may rise again by a factor of 10–15 compared to the unpasteurized beer. Its concentration continues to increase during beer storage, with higher temperatures accelerating its accumulation. For example, after 12 weeks of storage at 20 °C, furfural concentration may increase nearly tenfold (from 25–30 to 190–200 μ g/l). This is associated with the oxidation of furfuryl

alcohol, which forms in significant amounts during wort boiling (1.8–3.0 mg/l) (Kunze, 2007; Vanderhaegen et al., 2004).

One of the commonly used methods for determining 2-furfural as a marker of beer aging is ultraviolet spectrophotometry. Absorption peaks for oxidation products, including 2-furfural, lie in the wavelength ranges of 277 nm and 310 nm. The intensity of these peaks is used to determine the degree of beer oxidation (Cuifer-Rada et al., 2015; Rico-Yuste et al., 2016).

The aim of the present study was to investigate the impact of oxidative processes occurring during wort production, fermentation, and beer storage on the quality indicators and flavor characteristics of the final product, with particular emphasis on the influence of 2-furfural concentration on the intensity and degree of beer aging.

Materials and methods

Materials

The study materials included: milled malt obtained after cold extraction with deaerated water; unhopped wort, 14 °P original extract (100% malt); hopped wort, 15 °P original extract (100% malt); pale filtered beer, 10 °P beer extract; pale filtered and pasteurized beer, 10 °P beer extract; bottled pale filtered and pasteurized beer, 10 °P beer extract.

Methods

All samples were analysed for physicochemical parameters, 2-furfural concentration, and sensory attributes according to current technical standards and established analytical protocols.

Determination of extract content (°P) by the cold extraction method. A 10.0 g sample of milled malt was placed in a 250 ml conical flask. Then, 100 ml of deaerated water at 20 °C was added, the flask was capped, and the mixture was stirred for 1 min every 5 min. After 15 min of extraction, the mixture was filtered. Oxygen content in the filtrate was determined using an Anton Paar 4500 DMA beer analyser.

For physicochemical analyses, 100 ml of beer was placed in a 100 ml cuvette and degassed on a magnetic stirrer for 5 min. Measurements were performed using the Anton Paar 4500 DMA complex beer analyser (Bamforth, 2000; Ciocan et al., 2020).

Determination of 2-furfural concentration. The concentration of 2-furfural (μ g/l) was determined by UV-VIS spectrophotometer at 277 nm and 310 nm (Olšovská et al., 202; Rico-Yuste et al., 2015).

Physico-chemical properties of the finished beer. Physico-chemical parameters in the finished beer (acidity, ml of 1 M NaOH per 100 ml of wort; color, ml of 0.1M I2 per 100 ml of water; carbon dioxide content, %) were determined using an Anton Paar analyser (Ciocan et al., 2020).

Determination of the dry matter content. The method is based on the determination of the content of extractive substances in beer by relative density (Kunze, 2007). The beer free from carbon dioxide was poured into a cylinder, which was placed on a flat surface, the temperature was measured and an areometer was immersed. The upper meniscus was used to read the areometer and determine the concentration of dry matter (DM), taking into account the correction for temperature.

Determination of the alcohol concentration. The method is based on distilling alcohol from a weighed beer sample, followed by determining the alcohol mass fraction using a refractometer and measuring the solids content by the areometric method (Kunze, 2007). In a dry distillation flask 200 ml of beer freed from carbon dioxide were taken, the flask was connected to a refrigerator through a droplet eliminator and the beer was distilled. After distillation of 1/3 of the sample volume, the rest of the distillation flask was brought to the original volume with water, mixed thoroughly, cooled to the temperature of 20 °C and the concentration of DM (actual content of the extract) was determined by areometric method. The distillate in the receiving flask was brought with water to the initial volume, mixed thoroughly and the mass fraction of alcohol in the sample was determined at 20 °C by a dip refractometer using alcohol tables.

Determination of beer bitterness. Bitterness was determined spectrophotometrically in quartz cuvettes with a 10 mm path length. Two identical 50 ml flasks were filled with 10 ml of prepared beer, 1 ml of 3 M HCl, and 20 ml of iso-octane. Flasks were capped and shaken at 750 rpm for 15 min. After phase separation for 10 min, the upper layer was measured spectrophotometrically at 275 nm (Kunze, 2007).

Determination of SO₂ content. Sulfur dioxide content was determined by distillation from an acidified beer sample, collection into a neutralized hydrogen peroxide solution (oxidizing SO₂ to sulfuric acid), and titration of the resulting solution with sodium hydroxide (Kunze, 2007).

Determination of sensory properties. Off-flavors and deviations from the brand profile were evaluated using a 25-point scale. Based on the overall sample intensity, the average score for panelists D1–D7 was calculated, an overall table of individual panelist scores was compiled, and the final score for each experimental sample was determined.

Experimental samples were categorized on the 25-point scale as follows: excellent (22–25 points), good (19–21 points), satisfactory (13–18 points) end unsatisfactory (12 points and below) (Bocharova et al., 2017).

Experimental procedures. Stage I involved examining the dependence of 2-furfural concentration on the contact time of malt grist with atmospheric oxygen. Aqueous solutions of malt grist were prepared by cold extraction. Samples were analysed after storage for 15, 30, 60, 120, 180, and 200 minutes, while the control sample had a contact time of 5 minutes.

Stage II investigated the effect of temperature on the oxidation level of unhopped wort (100% malt wort with an original extract of 14°P). The concentration of 2-furfural was measured as a function of contact time between the wort and oxygen during filtration on a filter press. Samples were taken after 15, 30, 60, 120, 180, and 200 minutes, with a 5-minute control.

Stage III studied the impact of wort boiling time on 2-furfural formation in hopped wort (15°P original extract). Contact times with oxygen were 15, 30, 45, 60, 90, and 120 minutes, with the control sample having 5 minutes of exposure.

Stage IV assessed the influence of fermentation and beer filtration on the formation and concentration of 2-furfural in the finished beer. Filtered pale beer with an original extract of $10^{\circ}P$ was artificially aerated through a sparging tube to obtain dissolved oxygen concentrations of 40, 60, 80, 100, 120, and 140 μ g/L, while 20 μ g/L was used as the control.

Stage V determined the effect of pasteurization intensity on 2-furfural levels in beer samples. The beer was subjected to pasteurization at 15, 30, 50, 100, and 300 pasteurization units (PU).

Stage VI examined changes in 2-furfural concentration during beer packaging. Beer samples with dissolved oxygen levels of 50, 80, 90, 110, 130, and 150 μ g/l were analysed, with the control being packaged pasteurized beer at 50 μ g/l oxygen.

Stage VII measured physico-chemical properties of filtered and pasteurized pale beer (10°P original extract) after packaging. The control sample consisted of pasteurized beer in 0.45 l glass bottles with minimal dissolved oxygen (50 μg/l) and 2-furfural concentration of 107 μg/l. Test samples included: Sample 1 – 140 μg/l oxygen, 211 μg/l 2-furfural; Sample 2 – 145 μg/l oxygen, 254 μg/l 2-furfural; Sample 3 – 200 μg/l oxygen, 583 μg/l 2-furfural.

Stage VIII investigated the dependence of sensory attributes on 2-furfural concentration through organoleptic evaluation of samples stored for six months. The 2-furfural concentration was determined on the day of bottling, and the samples were packaged in 0.45 I glass bottles. The sensory detection threshold for 2-furfural was 150–200 µg/l.

Data Processing: All physico-chemical parameters of wort and beer were determined in triplicate, and average values were used for analysis. The experimental error did not exceed 5%.

Results and discussion

Dependence of 2-furfural concentration on malt grist contact time with oxygen

The 2-furfural concentrations in malt grist, depending on the duration of contact with atmospheric oxygen, are presented in Figure 1.

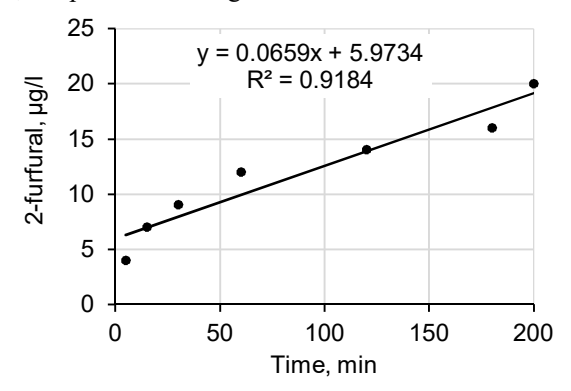


Figure 1. Dependence of 2-furfural concentration on malt grind exposure time to atmospheric oxygen

The trend illustrated in Figure 1 shows a clear linear relationship between 2-furfural concentration and exposure time. The initial concentration, measured after minimal air contact, was 4 μ g/l and increased fivefold to 20 μ g/l after 200 minutes of exposure. This finding underscores the detrimental effect of delayed processing after grinding on malt quality, leading to the accumulation of oxidation-derived secondary metabolites. To minimize the formation of undesirable compounds, it is recommended that malt grind storage time be kept below 50 minutes (Filipowska et al., 2021). The high coefficient of determination ($R^2 = 0.9184$) confirms that the linear regression model adequately describes the observed relationship.

Dependence of 2-furfural concentration on wort contact time with oxygen

Figure 2 shows the 2-furfural concentration in wort prior to hopping as a function of exposure time to atmospheric oxygen.

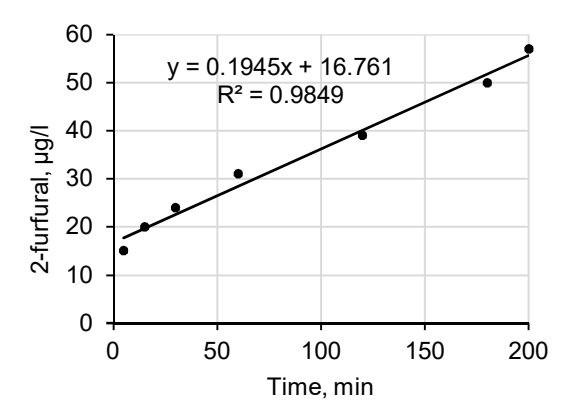


Figure 2. Dependence of 2-furfural concentration on wort exposure time to atmospheric oxygen

When the lautering step was prolonged to 200 min at 78 °C, the 2-furfural concentration in unhopped wort increased almost fourfold (from 15 to 57 μ g/l). This trend was accompanied by higher spectrophotometric readings at 310 nm and 277 nm, reflected in the rise of absorbance differences from 0.003 to 0.063.

These observations suggest an intensification of thermal carbohydrate transformation reactions and a concomitant increase in aldehyde content in the wort (Vanderhaegen et al., 2006). Prolonged exposure of wort to elevated temperatures led to the accumulation of undesirable oxidation products, negatively affecting beer aroma and taste (Ditrych et al., 2019; Krofta et al., 2013).

Dependence of 2-furfural concentration on boiling duration

The concentration of 2-furfural as a function of wort exposure to atmospheric oxygen during hopping and boiling is presented in Figure 3. Analysis revealed that increasing the exposure time from 5 to 120 min at $100\,^{\circ}\text{C}$ resulted in a 2-furfural increase from 122 to $839\,\mu\text{g/l}$. This phenomenon can be attributed to the acceleration of Maillard-type reactions between sugars and amino acids.

The highest formation of 2-furfural occurred at elevated temperatures during wort boiling with hops. Extending the boiling time from 5 to 200 min increased the 2-furfural concentration nearly eightfold, reaching $839 \mu g/l$.

Table 6 shows that the control sample, which was exposed for only 5 min, exhibited a higher content of oxidation products during boiling than the wort during lautering at 78 °C for an equivalent duration (200 min). This is explained by the fact that prolonged boiling substantially increases the wort's surface area in contact with atmospheric oxygen, thereby enhancing the formation of oxidation products, including 2-furfural (Ditrych et al., 2019).

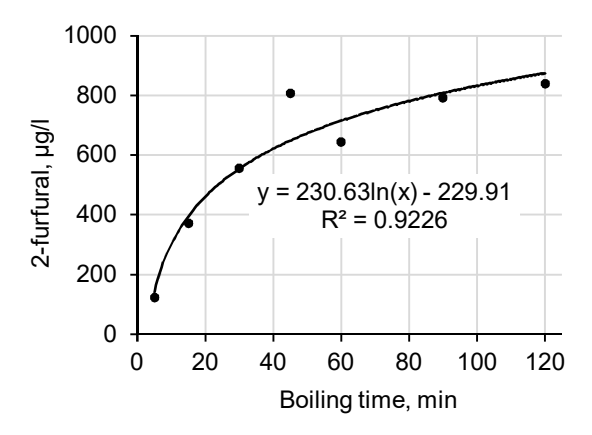


Figure 3. Dependence of 2-furfural concentration on wort exposure to atmospheric oxygen during boiling

As illustrated in Figure 3, the formation of 2-furfural is most pronounced during the initial stage of boiling (up to 30 min). During this period, 2-furfural concentration increased approximately 5.5-fold relative to the control (from 100 to 550 μ g/l). Between 40 and 120 min, the rate of formation decreased, with concentrations rising only 1.5-fold compared to the control (from 550 to 850 μ g/l). The regression model adequately describes the kinetics of this process.

Effect of wort fermentation and beer filtration on 2-furfural formation and concentration

The concentration of 2-furfural in filtered beer as a function of oxygen content is presented in Figure 4.

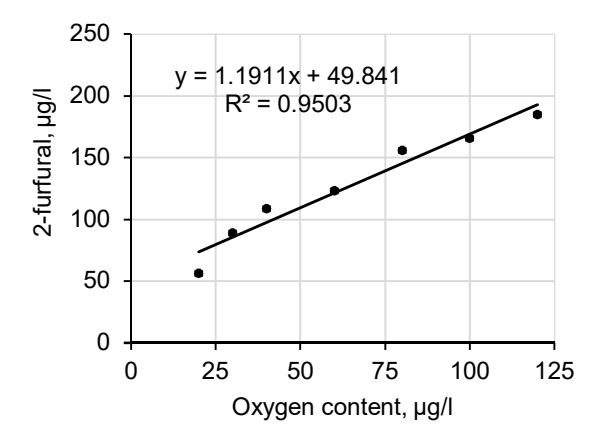


Figure 4. Dependence of 2-furfural concentration on oxygen content during wort fermentation and beer filtration

Analysis of Figure 4 reveals a linear relationship between 2-furfural concentration and dissolved oxygen in beer. The 2-furfural content in beer is markedly lower than in wort, likely

due to its reduction to furfuryl alcohol by yeast during fermentation (Dack et al., 2017). Increasing dissolved oxygen from 20 to $120\,\mu\text{g/l}$ resulted in a $127\,\%$ rise in 2-furfural concentration (from 56.6 to $185.2\,\mu\text{g/l}$). This confirms that atmospheric oxygen is a key factor driving oxidative reactions in beer, which promote accumulation of undesired aromatic compounds and reduce flavor stability (Olaniran et al., 2017). Controlling dissolved oxygen during fermentation and filtration is therefore critical for maintaining product quality. The calculated R^2 value supports the reliability of the linear model and the stepwise influence of oxygen on 2-furfural formation and accumulation.

Effect of pasteurization on 2-furfural concentration in beer

The concentration of 2-furfural in pasteurized beer as a function of pasteurization intensity is presented in Figure 5.

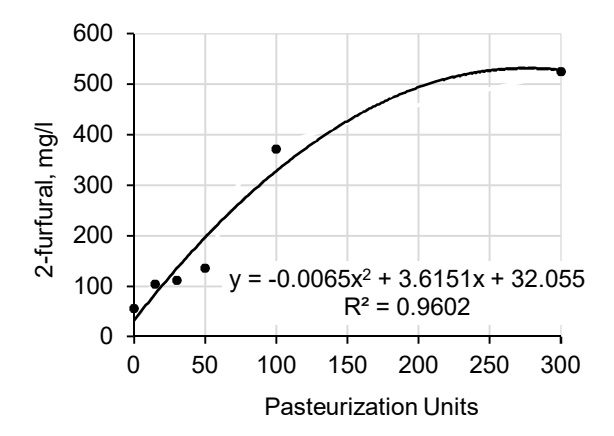


Figure 5. Dependence of 2-furfural concentration on the degree of beer pasteurization

Increasing pasteurization intensity enhances oxidative processes in beer. Even at minimal dissolved oxygen, oxidative reactions proceed rapidly under heat and with longer exposure time. At the lowest pasteurization intensity, 2-furfural concentration nearly doubled (from 56 to 104 μ g/l). Increasing pasteurization intensity to 300 PU amplified oxidation processes tenfold, raising 2-furfural concentration to 525 μ g/l.

As shown in Figure 6, increasing the pasteurization units (PU) results in a parabolic rise in 2-furfural concentration, reflecting the nonlinear nature of thermal transformations. During the initial stage of pasteurization (up to 100 PU), a sharp increase in 2-furfural content is observed, attributed to the activation of Maillard reactions and thermal stress. Further prolongation of heat treatment (beyond 200 PU) leads to a slowdown or stabilization of 2-furfural concentration, possibly due to partial decomposition of the compound or the reactions reaching equilibrium (Pieczonka et al., 2021).

The obtained regression equation is: $y = -0.0064x^2 + 3.6151x^2 + 32.055$, with a coefficient of determination $R^2 = 0.9602$, indicating high reliability of the quadratic model. This highlights the significant impact of thermal load on Maillard reaction products and underscores the need to optimize pasteurization conditions to prevent excessive formation of compounds that contribute to beer aging.

Analysis of 2-furfural concentration in finished beer

The concentration of 2-furfural in finished beer as a function of dissolved oxygen content is presented in Figure 6.

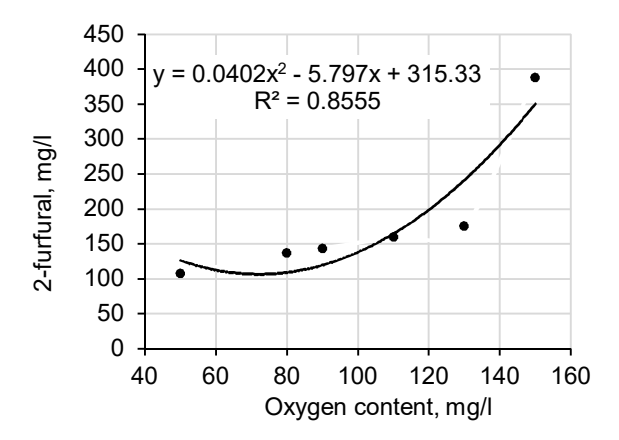


Figure 6. Dependence of 2-furfural concentration on the dissolved oxygen content in packaged beer

Figure 6 shows the relationship between 2-furfural concentration (μ g/l) and oxygen content (μ g/l). A nonlinear, parabolic dependence is observed between oxygen levels and 2-furfural concentration. The regression equation is expressed as: y=0.0402x²-5.797x+315.33. This indicates that at low oxygen concentrations, 2-furfural formation is minimal; however, as oxygen content increases from 60 to 150 μ g/l, the accumulation rate rises sharply. The calculated coefficient of determination R² demonstrates a strong correlation between the studied parameters, and the mathematical model is considered adequate.

The data indicate that oxygen present in the headspace of bottled beer after sealing promotes undesirable oxidative processes, adversely affecting beer quality. Evidence for this is the observed 262% increase in 2-furfural concentration (from 107 to 388 $\mu g/l$). Concurrently, spectrophotometric readings at 310 nm and 277 nm significantly increased, reflected in the growing difference between measurements, indicating active oxidation post-packaging. Elevated dissolved oxygen accelerated the formation of undesirable compounds, negatively impacting flavor, aroma, and stability of the beer (Wietstock et al., 2016).

Determination of physicochemical parameters of finished beer

The physicochemical parameters of filtered and pasteurized "Light" beer (10% extract content), packaged in containers, are presented in Table 1.

The physicochemical parameters of the beer comply with regulatory standards. The beer can be classified as a light, pale style with moderate bitterness, satisfactory CO₂ saturation, and typical organoleptic characteristics. However, elevated oxygen content (total 50 μ g/l) may promote the formation of oxidation products such as 2-furfural, negatively affecting flavor stability during storage (Jaskula-Goiris et al., 2019).

Table 1
Physicochemical characteristics of beer

Characteristics	Value	
Extractivity of the initial wort	10.0 % mass. extract	
Alcohol content	4.5 %/vol.	
Color	6 EBC	
Bitterness	13 mg/l	
CO ₂ content	5.0 g/l	
Dissolved O ₂	20 μg/l	
Total O ₂	50 μg/l	
pН	4.2	
Acidity	1.80 ml of 1 M NaOH per 100 ml of wort	
SO ₂ content	4 mg/l	

Dependence of sensory attributes of beer on 2-furfural concentration

The results of sensory evaluation of industrially produced beer samples are presented in Table 2.

Table 2
Dependence of sensory attributes of beer on 2-furfural concentration

	2-	Quality assessment panel members								
Beer	furfural content, µg/l	D1	D2	D3	D4	D5	D6	D7	Overall score	Comments
Control	107	24	23	24	24	24	25	24	24	No defects
1	211	20	19	20	20	21	20	20	20	Slightly oxidized, mild aging
2	254	16	16	15	16	17	16	16	16	Noticeably aged, slightly oxidized
3	583	13	12	11	12	12	12	12	12	Strongly oxidized, pronounced aging, musty aroma, Strecker aldehydes present

Data indicate dependence of sensory attributes of beer on 2-furfural concentration. During six months of storage, beer samples exhibited deterioration in sensory properties. The control beer, with the lowest 2-furfural content, received the highest overall score of 24 out of 25 and showed minimal defects, confirming excellent quality. Samples 1 and 2, with moderately elevated 2-furfural concentrations (211 and 254 µg/l, respectively), received

lower overall scores (20 and 16) and exhibited mild oxidation and aging, remaining within acceptable quality limits. Sample 3, with a markedly elevated 2-furfural concentration (583 μ g/l), received the lowest score (12) and was characterized by pronounced oxidation, evident aging, musty aroma, and the presence of Strecker aldehydes (Wietstock et al., 2016), classifying it as unsuitable or non-consumable beer.

It was established that 2-furfural concentration directly influences sensory quality deterioration, particularly in terms of oxidation, aging, and the development of undesirable aromatic notes (Jaskula-Goiris et al., 2019). Monitoring this parameter is therefore critical for preserving the organoleptic properties of the final product.

Figure 7 shows the aroma profilogram of beer samples exhibiting varying levels of oxidative deterioration. The control sample displayed a relatively balanced aroma profile, characterized by moderate overall intensity and well-defined hop- and malt-derived notes.

Sample 1 exhibited a slight increase in the "oxidized" attribute accompanied by a minor decline in malt and hop character, which is consistent with early-stage oxidative changes and the onset of staling.

In sample 2, the oxidized aroma became more pronounced, while the malt and hop notes were noticeably weakened. This deterioration correlates with the elevated concentration of 2-furfural (254 μ g/l), a key carbonyl compound associated with beer aging. Sample 3 showed the highest oxidation scores, marked by a substantial suppression of malt and hop attributes and a simultaneous rise in alcoholic and sulfur-related notes. Such changes indicate advanced oxidative degradation, intensified staling, and the presence of undesirable Strecker-derived aldehydes.

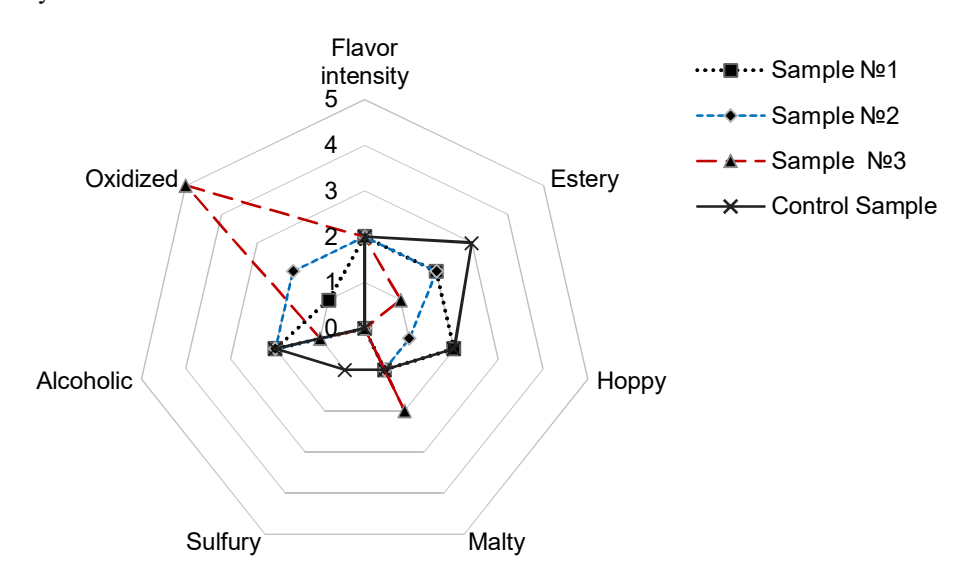


Figure 7. Aroma profile of beer samples with different degrees of oxidation

The taste profile of beer samples with varying degrees of oxidation, presented in Figure 8, demonstrates a gradual deterioration of sensory characteristics with increasing 2-furfural concentration and oxidation level. The control sample exhibited the most balanced taste, characterized by pleasant sweetness, harmonious bitterness, well-developed body, and clean aftertaste.

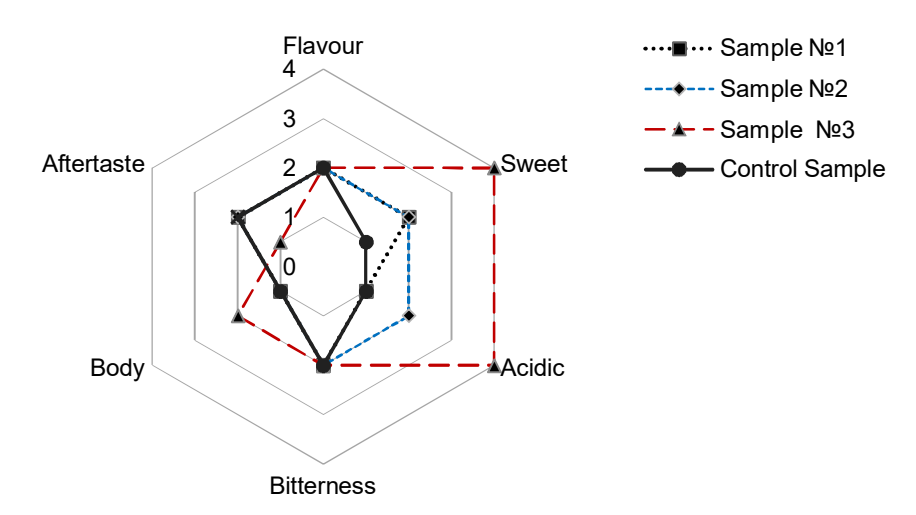


Figure 8. Taste profile of beer samples with different degrees of oxidation

Sample 1 showed a slight decrease in taste intensity and a minor increase in acidic notes, corresponding to initial stages of beer aging. Sample 2 exhibited further attenuation of body and finish, accompanied by more pronounced acidity and bitterness. Sample 3 displayed the most significant negative changes, including elevated acidity and an unpleasant lingering aftertaste, substantially impairing overall sensory perception. This was associated with a more than two times increase in 2-furfural concentration (up to $583 \mu g/l$).

Conclusions

The study demonstrates that 2-furfural, a key oxidation product, is formed at all stages of beer production and has a direct impact on beer quality. Its accumulation begins at the malt milling stage, where exposure of crushed grains to air leads to rapid increases in 2-furfural concentration. High temperatures during wort preparation, boiling with hops, and pasteurization further accelerate its formation, while elevated dissolved oxygen levels during fermentation and filtration contribute to additional accumulation. Oxygen in the bottle headspace also promotes undesirable oxidation reactions, resulting in sensory deterioration characterized by oxidized notes and loss of freshness at concentrations of 150–200 µg/l.

The results highlight the importance of controlling malt storage time, temperature, oxygen exposure, and pasteurization conditions to minimize 2-furfural formation. The proposed UV-spectrophotometric method provides a simple, rapid, and reliable approach for monitoring oxidation products throughout the brewing process, offering a practical tool for maintaining the organoleptic quality and stability of beer.

References

Bamforth C.W. (2000), Beer oxidation – A review, *Journal of the Institute of Brewing*, 106(5), pp. 327–333, https://doi.org/10.1002/j.2050-0416.2000.tb00090.x

Bamforth C.W. (2004), Analysis of critical control points for beer flavor stability, *Technical Quarterly of the Master Brewers Association of the Americas*, 41(2), pp. 97–103.

- Bettenhausen H.M., Barr L., Broeckling C.D., Chaparro J.M., Holbrook C., Sedin D., Heuberger A.L. (2018), Influence of malt source on beer chemistry, flavor, and flavor stability, *Food Research International*, 113, pp. 487–504, https://doi.org/10.1016/j.foodres.2018.07.024
- Bocharova O., Melnik I., Hnatovskaya D., Chub S. (2017), Using the profile method for evaluationthe beer quality, *Food Science and Technology*, 11(1), pp. 50–56, https://doi.org/10.15673/fst.v11i1.298
- Carneiro J.R., Guido L.F. (2006), The impact of sulphur dioxide and oxygen on the behaviour of 2-furaldehyde in beer: an industrial approach, *Journal of Food Science & Technology*, 41(5), pp. 545–552, https://doi.org/10.1111/j.1365-2621.2005.01104.x
- Ciocan M., Dabija A., Codina G. (2020), Effect of some unconventional ingredient on the production of black beer, *Ukrainian Food Journal*, 9(2), pp. 322–331, https://doi.org/10.24263/2304-974X-2020-9-2-5
- Cuifer-Rada P., Valverde-Ceralt A., Martínez-Uelamo M., Chiva-Blanch G., Hauriegi O., Estruch R., Lamuela-Raventós R. (2015), Comprehensive characterization of beer polyphenols by high-resolution mass spectrometry (LC-ESI-LTQ-Orbitrap-MS), *Food Chemistry*, 169, pp. 336–343, https://doi.org/10.1016/j.foodchem.2014.07.1
- Dack E., Black W., Koutsidis G., Usher J. (2017), The effect of Maillard reaction products and yeast strain on the synthesis of key higher alcohols and esters in beer fermentations, *Food Chemistry*, 232(1), pp. 595–601, https://doi.org/10.1016/j.foodchem.2017.04.043
- Diaz A.B., Durán-Guerrero E., Lasanta C., Castro-Mejías R. (2022), From the raw materials to the bottled product: Influence of the entire production process on the organoleptic profile of industrial beers, *Foods*, 11, 3215, https://doi.org/10.3390/foods11203215
- Ditrych M., Filipovska V., De Rouck G., Jaskula-Goiris B., Aerts G., Andersen M.L., De Cooman L. (2019), Investigation of the evolution of free staling aldehydes during wort production, *Brewing Science*, 72(1–2), pp. 10–17, https://doi.org/10.23763/BrSc18-21ditrych
- Filipowska W., Jaskula-Goiris B., Ditrych M., Bustillo Trueba P., De Rouck G., Aerts G., Powell C., Cook D., De Cooman L. (2021), On the contribution of malt quality and the malting process to the formation of beer staling aldehydes: A review, *Journal of the Institute of Brewing*, 127(2), pp. 107–126, https://doi.org/10.1002/jib.644
- Jaskula-Goiris B., De Causmaecker B., De Rouck G., Aerts G., Paternoster A., Braet J., De Cooman L. (2019), Influence of transport and storage conditions on beer quality and flavour stability, *Journal of the Institute of Brewing*, 125(1), pp. 60–68, https://doi.org/10.1002/jib.535
- Krofta K., Vrabcová S., Mikyška. (2013), The effect of hop beta acids oxidation products on beer bitterness, *Kvasny Prumysl*, 59(10), pp. 306-312, https://doi.org/10.18832/kp2013032
- Kunz T., Strähmel A., Cortés N., Kroh L.W., Methner F.J. (2013), Influence of Maillard reaction intermediates with enediol structure on the oxidative stability of beverages, *Journal of the American Society of Brewing Chemists*, 71(2), pp. 114–123, https://doi.org/10.1094/ASBCJ-2013-0429-01
- Kunze W. (2007), Technology Brewing and Malting, Berlin, VLB.
- Lohinova A., Petrusha O. (2023), Maillard reaction in food technologies, *Ukrainian Journal of Food Science*, 11(2), pp. 81-109, https://doi.org/10.24263/2310-1008-2023-11-2-4
- Olaniran A.O., Hiralal L., Mokoena M.P., Pillay B. (2017), Flavour-active volatile compounds in beer: Production, regulation and control, *Journal of the Institute of Brewing*, 123(1), pp. 13-23, https://doi.org/10.1002/jib.389
- Olšovská J., Štěrba K., Slabý M., Vrzal T. (2021), Novel method for determination of heterocyclic compounds and their impact in brewing technology, *Kvasny prumysl*, 67, pp. 417–427, https://doi.org/10.18832/kp2021.67.417
- Pieczonka S.A., Hemmler D., Moritz F., Lucio M., Zarnkow M., Jacob F., Rychlik M., Schmitt-Kopplin P. (2021), Hidden in its color: A molecular-level analysis of the beer's Maillard

—— Processes and Equipment——

- reaction network, *Food Chemistry*, 361, 130112, https://doi.org/10.1016/j.foodchem.2021.130112
- Rakete S., Klaus A., Marcus A. (2014), Glomb. Investigations on the Maillard Reaction of dextrins during aging of pilsner type beer, *Journal of Agricultural and Food Chemistry*, 62(40), pp. 9876-9884, https://doi.org/10.1021/jf503038c
- Rico-Yuste A., González-Vallejo V., Benito-Peña E., De las Casas Engel T., Orellana G., Moreno-Bondi M.C. (2016), Furfural determination with disposable polymer films and smartphone-based colorimetry for beer freshness assessment, *Analytical Chemistry*, 88(7), pp. 3959–3966. https://doi.org/10.1021/acs.analchem.6b00167
- Vanderhaegen B., Neven H., Delvaux F.R., Verstrepen K.J., Verachtert H., Derdelinckx G. (2004), Influence of the brewing process on furfuryl ethyl ether formation during beer aging, *Journal of Agricultural and Food Chemistry*, 52(22), pp. 6755-6764, https://doi.org/10.1021/jf0490854
- Vanderhaegen B., Neven H., Verstrepen K.J., Verachtert H., Derdelinckx G. (2006), The chemistry of beer aging A critical review, *Food Chemistry*, 95, pp. 357–381, https://doi.org/10.1016/j.foodchem.2005.01.006
- Wietstock P.C., Kunz T., Methner F.J. (2016), Relevance of oxygen for the formation of Strecker aldehydes during beer production and storage, *Journal of Agricultural and Food Chemistry*, 64, pp. 8035–8044, https://doi.org/10.1021/acs.jafc.6b03502

Cite:

UFJ Style

Mukoid R., Bulii Yu., Kiriienko S. (2025), Oxygen-driven 2-furfural accumulation and its influence on beer sensory stability, *Ukrainian Food Journal*, 14(3), pp. 464–477, https://doi.org/10.24263/2304-974X-2025-14-3-8

APA Style

Mukoid, R., Bulii, Yu., & Kiriienko, S. (2025). Oxygen-driven 2-furfural accumulation and its influence on beer sensory stability. *Ukrainian Food Journal*, *14*(3), 464–477. https://doi.org/10.24263/2304-974X-2025-14-3-8

Effect of bulk material mechanics on optimal packaging geometry in adaptronic dosing systems

Oleksandr Gavva, Lyudmila Kryvoplias-Volodina, Yuriy Dolomakin, Anton Kokhan, Nataliya Kulyk

National University of Food Technologies, Kyiv, Ukraine

Keywords:

Bulk product Packaging Feeding Dosing Adaptronic module

Article history:

Received 15.03.2025 Received in revised form 21.07.2025 Accepted 30.09.2025

Corresponding author:

Lyudmila Kryvoplias-Volodina E-mail: kryvoplyasvolodinalo@nuft. edu.ua

DOI: 10.24263/2304-974X-2025-14-3-9

Abstract

Introduction. The purpose of research is to substantiate the design and parameters of the feeding device of the functional module for dosing bulk products in a volumetric way with continuous operation of the rotor with measuring cups.

Materials and methods. The object of packaging is low-flux bulk products with particle sizes of 0.6–6.0 mm. The design of the feeding device is a combination of conical and cylindrical parts of the product pipeline. The analysis of the movement of bulk products in the channels of the feeding device was carried out using the methods of classical mechanics and discrete elements of Altair EDEM. Experimental studies were carried out on a packaging machine at a rotor rotation frequency of 5–20 rpm.

Results and discussion. The novelty of the conducted research is the consideration of the continuous movement of the rotor with measuring cups both at the stage of product dose formation and at the stage of bulk product feeding during the design of the effective design of the feeding device. The duration of packaging significantly affects the performance of the dosing and feeding adaptronic module of the packaging machine. With continuous rotation of the rotor with measuring cups, it is almost impossible to ensure the free movement of bulk product particles through the channels of the feeding device. To reduce the duration of interaction of particles with the inner cone surface of the feeding device, an effective method is to increase the coefficient of the cross-sectional area of the conjugation of the cone and cylindrical parts of the funnel. An eccentric arrangement of the cylindrical part of the product line relative to the conical part is proposed. An expression was obtained for determining the rational value of eccentricity at different kinematic parameters of the movement of measuring cups. In terms of the geometric construction of the cone-cylindrical feeding device, the eccentricity can be varied between 0 and 0.5 of the diameter of the cylindrical part of the funnel. To ensure the given productivity, the diameter of the base of the conical part of the feeding device is determined taking into account the kinetics of the particle's movement, geometric parameters of the rotor, kinematic and geometric parameters of the measuring cup. Using the same input data for both the theoretical and simulation models, the packaging time for a bulk product dose is 25–27% longer than that for a single characteristic particle. By increasing the cross-sectional area of the conjugation of the conical and cylindrical parts of the funnel, it is possible to reduce the duration of bulk product feeding for packaging by up to 11%.

Conclusions. By increasing the cross-sectional area of the conjugation of the conical and cylindrical parts of the funnel, it is possible to reduce the duration of of bulk product feeding for packaging to 11% and the productivity of the adaptronic module to 11%.

Introduction

Dosing and feeding is the most important and responsible operation of the process of packaging products. Bulk products, like other types of products, are characterized by different values of physical and mechanical parameters. The physical and mechanical properties of bulk products significantly affect the choice of an effective method of dosing and feeding. For easy-flux bulk products, while ensuring high productivity values, the volumetric method of dose formation is widely used.

In modern automatic machines, this method of dosing is implemented by adaptronic packaging modules, the working body of which is a cup dispenser with a continuous mode of rotation of the rotor (Gavva et al., 2023). Rotor rotation frequency and the number of cups in the rotor directly affect the performance of both the functional module and the packaging machine in general. In turn, the frequency of rotation of the rotor depends on the duration of bulk products dosing and feeding. In the rotary arrangement of the dosing and feeding module, the cycle time is the limiting packaging operation. In general, the duration of the kinematic packaging cycle includes the duration of opening the cup flap, moving products from the cup to the package, supplying and removing the container or package. Of the above cycles, the longest and most likely by definition is the cycle of moving bulk products from the cup to the package. The design of the funnel of the feeding device affects additional supports for the movement of products when it is exposed to the inner surface of the funnel and possible impact phenomena. One of the ways to minimize the duration of movement of bulk products in the product pipeline of the feeding device is to determine its rational geometric parameters.

Determining the rational parameters and geometry of the feeding device is a multiparameter problem. The duration of product movement will be affected by its physical and mechanical properties, parameters of interaction with working bodies, initial conditions of product state and aerodynamic resistance (Stypnytskyy, 2013).

Today, various methods are used to study the movement of bulk products in the product pipelines of packaging and technological machines, which were developed to model the movement of substances in liquid, quasi-liquid and gaseous states (Burmystenkov et al., 2018).

Modern dosing and feeding modules consist of several devices (bunker, dosing and feeding elements), the nature of the movement of particles in which is significantly different. Therefore, when developing mathematical models, the module and its individual links are divided into zones, the movement of products in which can be described by applying known and adapted models. Such models include models used during the mechanics of continuous systems (Bertrand et al., 2005). In general, they are called flow structure models (Behjani et al., 2019). A characteristic feature of the functional dosing module of the cup type is the separation of flows of bulk products and the chaotic movement of individual particles during the formation and separation of the product dose from its massif. Mathematical models of the flow structure for such a module make it possible only to approximate the nature of the real process, since they do not take into account the peculiarities of the real physical and mechanical process of the interaction of particles with each other and with the structural elements of the module (Burmistenkov et al., 2019). In some cases, to simplify and speed up the development of a new functional module, mathematical models of the movement of the most characteristic particles of bulk products, their interaction with the working elements of the module are created (Kafashan et al., 2019).

Regression models are effectively used for the actual design of the dosing and feeding module and a specific type of bulk product (Di Renzo and Di Maio, 2004; Dubey et al., 2011). Such models ensure high accuracy of forecasting indicators of the quality of the operation (duration, dosing accuracy) within the selected ranges of parameter variation. Along with this,

it is almost impossible to use them for other structures, since they do not take into account the nature of physical and mechanical phenomena that occur during the operation of dosing and feeding modules. This greatly complicates the use of such models in the design of dosing and feeding modules, since each design option requires the production of a prototype (Yuu and Umekage, 2011). Numerical methods, in particular, the method of discrete elements (MDE), are more universal and make it possible to analyze the phenomena that occur during the movement of bulk products in the product channels of dosing and feeding modules (Dubey et al., 2011; Munjiza, 2004). This method is based on the laws of classical mechanics used to calculate the motion of a large number of particles (Benvenuti et al., 2015).

The advantages of this method are the availability of information about the speed and position of individual particles and the ability to model breaks and pulsations in material flows. MDE does not require the creation of a physical model of equipment (Sarkar and Wassgren, 2009, 2010).

Numerical methods are also used to solve mathematical models describing the movement of individual particles of a bulk product in the field of action of mechanical forces (centered, frictional, gravitational, etc.) that arise during its movement in the working device of the dosing and feeding module and are presented in the form of differential and integral equations (Bila and Statsenko, 2012; Vera et al., 2015).

Derenivska et al. (2014) and Maslo (2013) provide data on the movement of bulk products in weight dispensers, and ways of intensifying the movement of finely dispersed bulk products under the action of vibration loads are proposed by Sholoviy et al. (2014) and Maherus (2014). However, these works separately consider the movement of bulk products in the hopper without taking into account the modes of movement of products in previously performed technological operations.

The purpose of the study is to substantiate the design and parameters of the feeding device of the functional module for dosing bulk products in a volumetric way with continuous operation of the rotor. According to the goal, the following tasks are formulated:

- analyze the kinematic parameters of the movement of the most characteristic particles of bulk products in the channels of the product pipeline of the feeding device;
- determine the effect of the displacement of the central cylindrical part of the funnel of the feeding device in relation to the cone part on the effective cross-sectional area of the movement of the product flow and the duration of movement;
- applying the method of discrete elements, to investigate the movement of the flow of bulk products in the product pipeline of the feeding device and the influence of the constructive execution of the funnel on the kinematic parameters of the packaging operation;
- check the adequacy of simulation models of the movement of bulk products in feeding devices with real processes.

Materials and methods

Research products

The object of dosing and feeding is low-flow bulk products with a size of 0.6–6 mm. Such products include cereals (rice, buckwheat, millet, oats, etc.), dry sugar and salt, small-leaf tea, etc.

Calculation model

Figure 1 shows a characteristic scheme of the functional module for dosing and feeding of bulk products of continuous action, the measuring containers of which are made in the form of telescopic cups. In such modules, unloading of measuring cups is carried out during their continuous movement. The design of the product feeding device is mostly a combination of conical and cylindrical parts of the product pipeline. The cylindrical part has the diameter of the sleeve of the film from which the package is made, or the dimensions of which are equivalent to the cross-sectional size of another type of package (pack, can, box). The conical part corresponds to a truncated cone, the larger diameter of which corresponds to the arc of movement of the cups in the packaging zone. And the smaller diameter – of the diameter of the cylindrical part. The angle of the generating side surface of the cone is taken depending on the mode of movement of bulk products (normal, hydraulic, solid). To implement a deterministic hydraulic mode of movement of bulk products, it is recommended (Statsenko et al., 2021) to take the angle of inclination of the conical surface within 60–70°. The length of the feeding device is determined by its layout depending on the diameters of the bases of the cone, the diameter of the cylindrical part, the angle of inclination of the cone surface and the location and structure of the film supply module, the formation of the package from it or the location of the supply transport system for other types of packaging.

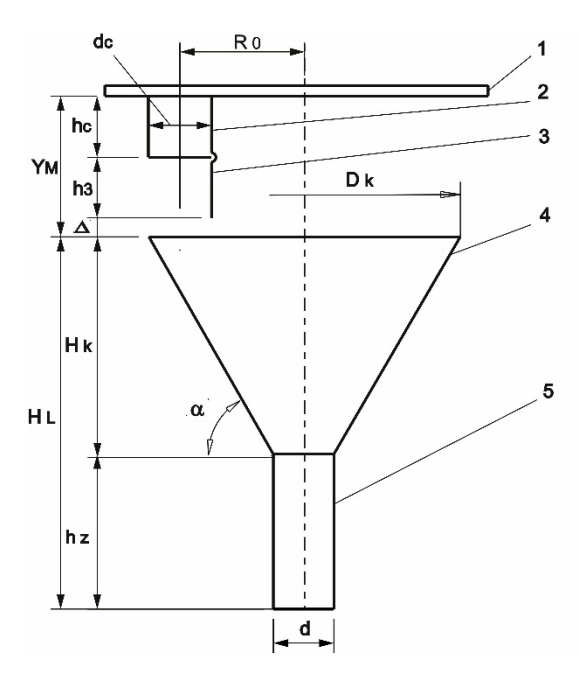


Figure 1. Scheme of dosing and feeding module for bulk products of continuous action: 1 – hopper with bulk products; 2 – cup measuring capacity; 3 – flap; 4 – conical part of funnel; 5 – cylindrical part of funnel

The technological duration of packaging is determined by the duration of the movement of products from the dosing container (cup) to the conical part of the feeding device, its movement in the conical and cylindrical part of the funnel.

In the optimal variant, regarding the minimization of the duration of product movement, it should move along the cylindrical part of the device, without contact with the inner surface of the product pipeline. However, for continuous dosing modules, it is quite difficult to achieve this type of movement.

For the most part, with the appropriate ratios of the geometric parameters of the feeding device, the frequency of rotation of the rotor with measuring cups, the physical and mechanical properties of bulk products, part of the products will move with sliding along the inner surface of the funnel cone. Along with this, force contact of the products is also possible on the inner surface of the cylindrical part of the feeding device. Such movement can lead to turbulence of movement, particle co-strikes. This increases the duration of packaging and, accordingly, reduces the performance of the module. To eliminate these negative phenomena, it is appropriate to apply several innovative proposals, one of which is the creation of a rational design of the feeding device, which involves increasing the effective cross-sectional area of the product channel and minimizing the metal capacity of the device.

In order to establish the limits of the change in the geometric parameters of the feeding device, it is appropriate to investigate the movement of characteristic particles of bulk products using the methods of classical mechanics – of the dynamics of the movement of a material particle. At the same time, the following assumptions are accepted: a particle of bulk products has mass, but its geometric dimensions can be neglected, the particle is an elastic-plastic body with a speed recovery coefficient after impact on the conical surface of the device, which is determined within $k \approx 0.1 - 0.3$, the influence of the action of the surrounding particles on the movement of the studied particle is conditionally also neglected.

To analyze the phenomena that arise during the movement of bulk products in the product channels of dosing and feeding modules, we will use numerical methods of MDE. MDE is based on the assumption that bulk products consist of discrete particles that can have different properties and surface shapes. In order to reduce the number of calculations, particles of complex shape are modeled as a set of spheres of different diameters. MDE makes it possible to simulate the movement of product particles, which is caused by the influence of gravitational and coulomb forces, as well as forces arising as a result of the action of the working bodies of functional modules on products.

The input parameters for the modeling process are the initial conditions: position (x_i, y_i, z_i) , linear $(\upsilon_{xi}, \upsilon_{yi}, \upsilon_{zi})$ and angular $(\omega_{xi}, \omega_{yi}, \omega_{zi})$ velocities of all particles. The position and parameters of the movement of the working bodies of the dosing and feeding module interacting with the products are also set.

The modeling process is iterative. Before it begins, the modeling step Δt is determined, for this we apply the Rayleigh criterion (O'Sullivan and Bray, 2004; Otsubo et al., 2017)

$$\Delta t = \frac{\pi R}{0.163\nu + 0.87766} \sqrt{\frac{\rho}{G}},\tag{1}$$

where R, ρ , G, ν are the radius, bulk mass, shear modulus, and Poisson coefficient of the particle (Zhu H. P. et al, 2006) respectively.

At the beginning of each iteration, based on the laws of classical mechanics, the total value of the forces acting on each of the particles and their moments of iteration according to differential equations is determined

$$m_{i} \frac{d^{2} x_{i}}{dt^{2}} = \sum_{i=1}^{N} F_{ij} + m_{i} g;$$
 (2)

$$J_{i} \frac{d^{2} Q_{i}}{dt^{2}} = \sum_{i=1, i \neq j}^{N} M_{ij},$$
(3)

where t is time;

m_i – particle mass;

J_i – moment of inertia of the particle;

Qi- the angle of rotation of the particle;

M_{ij} – moment of forces acting between particles;

 F_{ij} – forces acting on the particle from other particles and working bodies of the feeding device.

The sum of the forces F_i acting on the particle can be represented by the set of forces acting on the side of other particles F_{ij} and the force of gravity:

$$F_i = \sum_{i=1, i\neq j}^{N} F_{ij} + m_i g. \tag{4}$$

A similar expression can be written for a moment M_i

$$M_{i} = \sum_{i=1, i \neq j}^{N} M_{ij} = \sum_{i=1, i \neq j}^{N} (x_{i} - x_{j}) F_{ij}.$$
 (5)

At each step, the position of the particles is calculated with the working bodies of the device and with each other. In the presence of such interactions, the values of tangential and normal forces are calculated and new vectors of particle movement speeds are calculated. Based on them, the positions of the particles in the next step of modeling (after Δt time) are calculated. Then the calculation cycle is repeated.

 F_{ij} forces consist of repulsive forces and frictional forces that can be decomposed into normal and tangential.

The positions and velocities of movement of all particles after a period of time Δt , at defined forces and known initial velocities, are calculated according to Newton's second law.

$$x_i = x_{oi} + v_{xi}\Delta t + \frac{F_{xi}}{m_i} \cdot \frac{\Delta t^2}{2};$$
 (6)

$$y_i = y_{oi} + v_{yi}\Delta t + \frac{F_{xyi}}{m_i} \cdot \frac{\Delta t^2}{2}; \tag{7}$$

$$z_i = z_{oi} + v_{zi}\Delta t + \frac{F_{zi}}{m_i} \cdot \frac{\Delta t^2}{2},$$
 (8)

where F_{xi} F_{yi} F_{zi} – are the constituent sums of the forces acting on the i-th part along the x, y, z axes, respectively.

Once a new position of the particles has been determined, possible particle intersections between themselves and with surrounding objects are calculated. The values of these δ intersections are used as input parameters to determine the normal component forces acting on the particles. At each subsequent iteration, all calculation steps are repeated.

Herzen's contact theory was used to determine the normal component of the interaction force (Di Renzo and Di Maio, 2004; Zhu et al., 2007), and the tangential ratio is Midlin-Deresievich (Bertrand et al., 2005). For both of these force components, damping components determined by elasticity coefficients were calculated (Williams and O'Connor, 1999; Yan et al., 2015).

The tangential force of friction was calculated according to Coulomb's law, the force of rolling friction was calculated based on the rotational moment of the particles.

The normal component of the force was calculated according to the formula:

$$F_n = \frac{4}{3} E^* \cdot \sqrt{R^*} \delta_n^{\frac{2}{3}}, \tag{9}$$

where δ_n – is the overlap of particles;

E* is the equivalent value of Young's modulus:

$$\frac{1}{E^*} = \frac{\left(1 - v_i^2\right)}{E_i} + \frac{\left(1 - v_j^2\right)}{E_j};\tag{10}$$

R* is the equivalent value of the radius of the spheres of particles

$$\frac{1}{R^*} = \frac{1}{R_i} + \frac{1}{R_i},\tag{11}$$

 E_i , v_i R_i , E_j , v_j R_j – values of Young's modules, Poisson coefficients and radii of spheres (i-th and j-th particles) between which the interaction is calculated.

The normal component of the elastic force was determined by the formula:

$$F_n^d = -2\sqrt{\frac{5}{6}}\beta\sqrt{S_n \cdot m^*} \cdot \upsilon_n^{\overline{rel}},\tag{12}$$

where $m^* = \frac{m_i \cdot m_j}{m_i + m_j}$ the equivalent mass of the two contacting parties with the masses m_i

and mj;

 $v_{n}^{\overline{rel}}$ normal component of relative speed in the normal direction;

 β – damping coefficient, which depends on the recovery coefficient e_0 (the recovery coefficient is related to energy losses in the event of a collision);

 S_n – normal stiffness depending on Young's equivalent modulus E*, equivalent radius R* and normal overlap δ_n .

 S_n and β are calculated using formulas

$$s_n = 2E^* \cdot \sqrt{R^* \cdot \delta_n}; \tag{13}$$

$$\beta = \frac{\ln e_0}{\sqrt{\ln^2 e_0 + \pi^2}} \,. \tag{14}$$

The tangential component F_t of the interaction force was calculated based on the values of the tangential overlap δ_t t and the tangential stiffness S_t

$$F_t = -S_t \cdot \delta_t, \tag{15}$$

where

$$S_t = 8G^* \sqrt{R^* \cdot \delta_n} \; ; \tag{16}$$

G* – equivalent shear modulus.

In addition, tangential damping was defined as

$$F_t^d = -2\sqrt{\frac{5}{6}}\beta\sqrt{s_t \cdot m^*} \cdot v_t^{\overline{rel}}, \tag{17}$$

where $v_e^{\overline{rel}}$ – relative tangential velocity.

The tangential force is limited by the Coulomb friction value $\mu_s \cdot F_n$, where μ_s is the static friction coefficient.

When taking into account the force of rolling friction, calculations were performed taking into account the amount of torque of the contacting surfaces

$$T_i = -\mu_r \cdot F_n \cdot R_i \cdot \omega_i, \tag{18}$$

where μ_r is the rolling friction coefficient;

 R_i is the distance from the point of contact to the center of mass of the particle; ω_i – is the unit vector of the angular velocity of the particle at the point of contact.

To study the movement of the flow of bulk products from the telescopic cup through the product pipeline of the feeding device, a three-dimensional model of a conical-cylindrical funnel was created at Solid Works CAD and was converted into a stl-format, which was used to transfer the model to the Altair EDEM MDE calculation environment. In the stl-format, information about a three-dimensional object is stored as a list of triangular faces describing its surface and their normals.

The MDE modeling process involves determining the geometric parameters of the working bodies of the module included in the model and the parameters of their interaction. In the present case, the funnel of the device is a stationary object, so that information about the geometric dimensions is sufficient for its simulation, which is transmitted in the stl-file and the physical and mechanical properties of the material from which it is made (Table 1).

Materials parameters

Table 1

Parameter name	Particles of bulk products	Funnel body material
Poisson Coefficient	0.25	0.30
Bulk, kg/m ³	660	7800
Shear Modulus, Pa	$1.0 \cdot 10^6$	$8.0 \cdot 10^7$
Young's Modulus, Pa	$0.2 \cdot 10^6$	$1.82 \cdot 10^{11}$
Radius, mm	3.0	
Weight, kg	7.58607·10 ⁻⁶	
Volume, m ³	1.1494·10 ⁻⁸	
Moment of Inertia, kg/m ²	5.94748·10 ⁻¹²	

To carry out MDE modeling, it is necessary to set parameters for two models of interactions: particle-particle and particle-material of the funnel. For both interactions, the Herz-Mindlin elastic contact theory is used (not including slip). The parameters of the interaction models are given in Table 2.

The modeling process was performed for several variations of the change in the eccentricity of the position of the cylindrical part of the funnel in relation to the conical part (e=0; 20 mm; 50 mm; -20 mm; -50 mm) and the angular speed of rotation of the rotor with measuring cups ($\omega_p=0.525~\text{rad/s};\ 0.790~\text{rad/s};\ 1.05~\text{rad/s};\ 1.57~\text{rad/s};\ 2.10~\text{rad/s}),$ which corresponds to the following values of the performance of the automatic machine (z = 30 doses/min; 45 doses/min; 60 doses/min; 90 doses/min; 120 doses/min).

Table 2

Object interaction parameters

Parameter name	Туре	of interaction
	Particle-particle	Particle-funnel material
Coefficient of Restitution	0.08	0.2
Coefficient of Static Friction	0.7	0.4
Coefficient of Rolling Friction	0.05	0.02

Calculations were made from determining the duration of movement of the entire dose of products (m_d =0.800 kg) at three levels of the feeding device: from the measuring cup to the conical part of the feeding device; in the conical part of the funnel and in its cylindrical part.

The shape and size of the particles remained unchanged at the entire stage of movement. The angle of inclination of the side walls of the conical part of the funnel was 70° , which ensures a hydraulic mode of movement of the flow of bulk products. The diameter of the cylindrical part of the funnel is taken to be d=100 mm, its length is $H_c=450$ mm. The diameter of the base of the conical part of the funnel D_k , calculated according to the formulas and accepted $D_k=550$ mm.

Checking the adequacy of the results of analytical simulation modeling of the movement of bulk products in the product pipeline of the feeding device was carried out on a actually operating automatic machine for packaging bulk food products, in particular cereals, into a polypropylene film (Figure 2).

The functioning of the system is based on the complex use of sensor technologies, intelligent image processing and logic-program control based on a programmable logic controller.

At the initial stage of the technological process, products (rice groats) are supplied from the hopper 1 to measuring cups 3, which are fixed on the disk of the rotating rotor 2. The movement of the rotor is driven by an electric drive with frequency adjustment of the angular speed. The measuring cup, in the zone of product dose formation, is closed by a valve flap, which contacts the copier 5 through the roller 4. In the feeding zone, the roller does not come into contact with the copier, which leads to its opening and movement of bulk products into the funnel 6 of the feeding device.

The measuring cup is fixed at the opening point of the flap using an inductive positional sensor of the Pepperl+Funchs model NBB5-18GM50-E2-V1, which is installed directly in the zero position zone of the rotor. Its action is based on the principle of changing the magnetic permeability in the presence of a metal label on the rotor. When the measuring cup approaches the control position, the sensor is activated and provides a corresponding signal to the controller for further start-up of the system logic. In the next phase, the vision sensor of technical vision 9 of the BVS UR-3-10-5-E model is activated. This sensor includes a built-in CMOS camera, an LED-based backlight module and a signal processing unit. After the trigger is activated, the device captures an image of the measuring cup and performs preliminary processing, including binarization, contour extraction, and analysis of the occupied area. This allows the system to determine whether the cup contains product or is empty, preventing the formation of empty packages and ensuring the reliability of the dosing system.

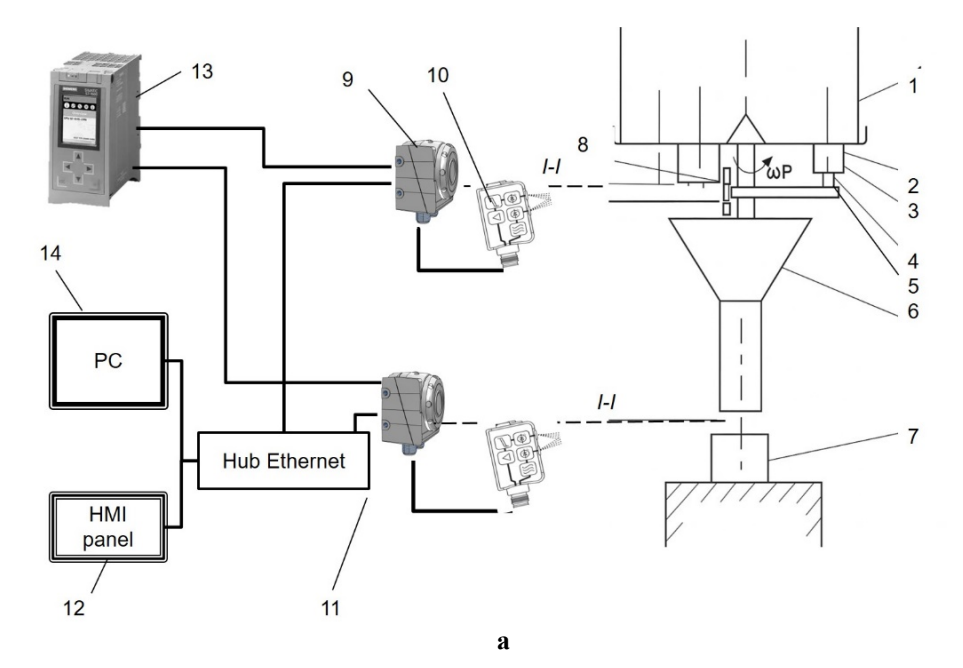




Figure 2 – Experimental installation for determining the duration of bulk products from measuring cup in a package:

 \mathbf{a} – scheme:

1 – hopper with products, 2 – rotor with measuring cups, 3 – measuring cup, 4 – roller, 5 – copier, 6 – funnel of the feeding device, 7 – packaging, 8 – position sensor inductive position, 9 – technical vision sensor, 10 – optical reflector label, 11 – Ethernet hub, 12 – HMI configuration panel, 13 – PLC S7 -1500 , 14 – PC programmer;

b – general view

b

The exact timing of product entry into funnel 6 is controlled using an optical reflector sensor 10 installed in the unloading area. This sensor operates on the photoelectric principle: a light beam emitted by the sensor is reflected from a mark or the product back to the receiver. A change in reflectivity—such as when a mark or bulk product interrupts the beam—alters the sensor output, which is recorded by the controller as an unloading event.

All sensor elements 8, 9,10 are integrated into a single automated system using a Siemens S7-1500 PLC (CPU1512SPF1PN) – position 13. Inductive and optical sensors are connected via standard discrete inputs, while the vision camera uses an Ethernet connection to transmit large amounts of data. Signal processing takes place in real time, which makes it possible to ensure accurate synchronization between mechanical events and actions of software logic. The interface of the NMI panel (Siemens SIMATIC Comfort Panel TP 700) – position 12 makes it possible to control and visualize the process, and the PC programmer 14 is used to change configurations, program or archive the results of experiments.

The method of conducting the experiment is based on the precision recording of events in the technological operation. In particular, four key time stamps are fixed:

 T_1 – the moment of activation of the inductive sensor corresponding to the filling of the measuring cup;

 T_2 – the moment when the vision sensor registers the presence of the product in the cup;

 T_3 – the moment of passage of the product through the optical mark zone (start of unloading the measuring cup);

T₄ is a signal that indicates the completion of packaging (fixed by the fact of stopping the movement of products from the cylindrical part of the funnel).

Based on these time stamps, the following intervals are calculated:

 $\Delta T_1 = T_3 - T_2$ – determines the time of movement of products to the funnel;

 $\Delta T_2 = T_4 - T_3$ characterizes the duration of bulk product feeding.

The given time intervals make it possible to determine the influence of the physical and mechanical characteristics of bulk products, geometric and kinematic parameters of the dosing module on the duration of packaging. Experiments were conducted at different values of the linear speed of movement of the measuring cup: υ_{xo1} =0.21 m/s; υ_{xo2} =0.316 m/s; : υ_{xo3} =0.42 m/s; : υ_{xo4} =0.628 m/s, which corresponds to the productivity of z_1 =30 doses/min; z_2 =45 doses/min; z_3 =60 doses/min and z_4 =90 doses/min. The number of repetitions of the experiments corresponds to a reliable probability p=0.95. The experiment was performed at e=0.0 mm. Table 3 shows the technical characteristics of the control and measurement system.

Results and discussion

Determination of rational values of eccentricity

To establish the functional dependence between the parameters of the flow of bulk products and the parameters of the feeding device of the adaptronic module, we will consider the movement of characteristic material particles in the product pipeline of the device.

It is well known that if we shift the cylindrical part of the funnel relative to the conical part, then in the conjugation zone we will get an increased effective cross-sectional area of the movement of bulk products (Statsenko et al., 2021) (Figure 3).

Table 3 Technical characteristics of control and measurement system of the experimental installation

Device name	Appointment	Error estimation
Inductive positional	Fixation of the passage of the	±0.5 mm (depending on
sensor	measuring cup through the	mounting and marking)
Pepperl+Funchs NBB5-	control position (start of the	
18GM50-E2-V1	event)	
Balluff BVS UR-3-10-	Control of the presence of	± 1 pixel, shape
5-E vision technical	products in the measuring cup by	detection error ≤3%
vision sensor	image synthesis	
Optical reflector label	Fixing the passage of the product	\pm 2 mm if the correct
with photo sensor	to record the moment of the start	mark is present
	of packaging	
PLC Siemens S7-1500	Digital processing of signals	Not determined,
CPU 1512SPF-1 PN	from all sensors, formation of	direction depends on
	the logic of the system	external sensors

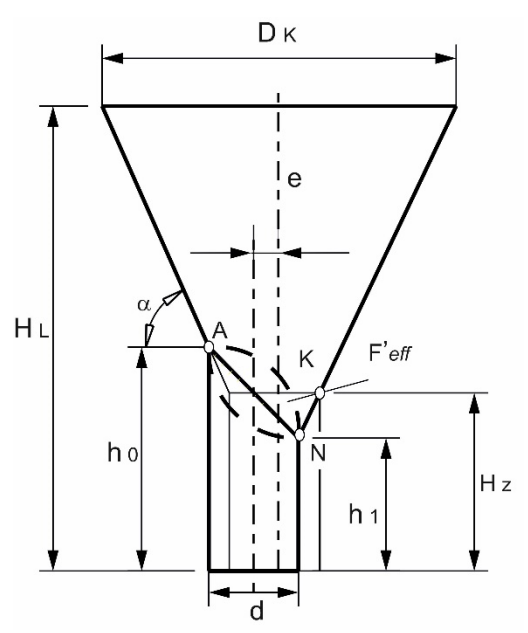


Figure 3. Scheme of the funnel of the feeding device with a shifted cylindrical part

It is known from geometric dependencies (Grewal et al., 2008) that for the cross-section of the conjugation of the conical and cylindrical parts of the funnel in the form of an ellipse, the effective area of movement of products is determined:

$$F_{\text{eff}}' = \frac{\pi d}{4} \sqrt{d + 4(e \cdot tg\alpha)^2}, \tag{19}$$

then the area increase factor will be equal to

$$k_F = \frac{F_{eff}}{F_{eff}} = \frac{4\pi d\sqrt{d + 4(e \cdot tg\alpha)^2}}{4 \cdot \pi d^2} = \frac{1}{d}\sqrt{d + 4(e \cdot tg\alpha)^2},$$
 (20)

where F_{eff} , $F_{eff}^{'}$ are the effective areas of movement of products along the circular and, accordingly, ellipsoidal conjugation;

d is an inner diameter of the cylindrical part of the funnel;

e is the eccentricity of displacement of the cylindrical part of the funnel relative to the conical part.

An increase in the value of k_F , with constant d and α , is possible with an increase in e. From the point of view of the geometric construction of the cone-cylindrical packaging device, the e-value can be varied within $0 \le e \le 0.5$ d. To determine the rational value of e, it is necessary to consider the movement of characteristic material particles of bulk products under different geometric and kinematic parameters of the dosing and feeding module.

An important design parameter of the feeding device, which ensures a continuous mode of packaging bulk products, at a given productivity, is the diameter of the base of the cone part of the funnel D_k (Gavva et al., 2023).

When determining the rational value of D_k , it is necessary to take into account the duration of movement of bulk products from the measuring cup to consumer packaging, the number of cups in the dispenser and the frequency of rotation of the rotor of the dosing module (Figure 4).

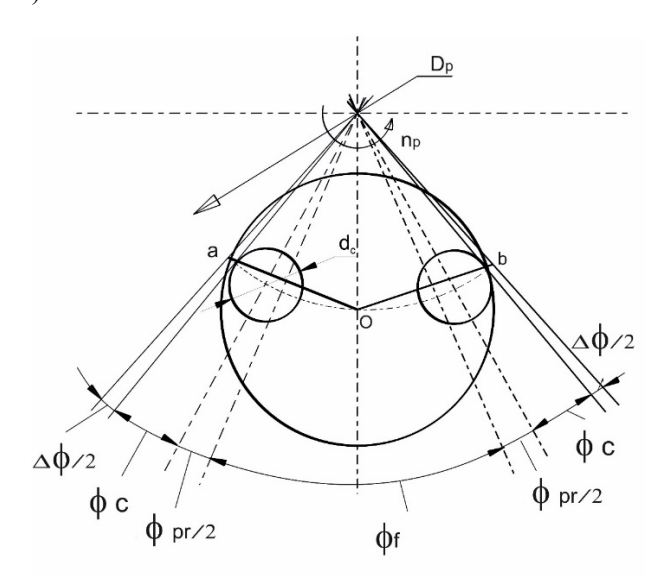


Figure 4. Scheme for determining rational value of diameter Dk of funnel cone part

The determination of the diameter of the base of the conical part of the funnel was carried out using the main provisions of the geometry, regarding the length of the chord O_a or O_B at a given diameter of the location of the measuring cups D_p and the central angle ϕ_{Σ_i} , which characterizes packaging (Grewal, 2008).

$$D_{\kappa} = 2D_{n} \cdot \sin(0.5\varphi_{\Sigma}), \tag{21}$$

where φ_{Σ} is the total central angle defined as:

$$\varphi_{\Sigma} = 0.5\varphi_f + 0.5\varphi_m + \varphi_c + 0.5, \qquad (22)$$

 φ_f – angle to which the rotor with measuring cups will return, for which all products from the cup will move to the package, $\varphi_f = \omega_r \cdot t_f$;

 $\omega_{\rm r}$ – angular speed of rotation of the rotor, $\omega_{\rm r} = \frac{\pi n_{\rm r}}{30}$;

 n_p – rotor rotation frequency, $n_r = \frac{z}{m_c}$;

z – performance of the dosing and feeding module;

m_c – the number of measuring cups in the rotor of the dosing module;

 t_p – duration of packaging – movement of bulk products from the measuring cup into the package. For project calculations, and by adopting the mode of movement of bulk products by hydraulic, the duration of t_s can be determined (Statsenko et al., 2021):

$$t_f = k_1 \cdot \lambda \sqrt{\frac{2H_{\Sigma}}{g}} \; ; \tag{23}$$

 k_1 – coefficient, which takes into account the movement of particles of bulk products on the inner surface of the funnel and possible co-impact phenomena between particles;

 λ – the coefficient of aerodynamic resistance of the movement of particles in the funnel;

 H_{Σ} the length of the path of movement of bulk products in the feeding device, $H_{\Sigma} = H_{\mu} + h_{c} + H_{\kappa} + H_{\mu}$;

 ϕ_m – rotor rotation angle corresponding to the duration of movement of the film sleeve over the length of the package or feed of the empty container

$$\varphi_m = \omega_r \cdot t_m = \omega_r \cdot L_p / v_m;$$

L_p – packaging length;

 $v_{\rm m}$ – speed of movement of welded and drawing devices (for flexible packaging);

 φ_c – is the central angle of the rotor corresponding to the radius of the measuring cup

$$\varphi_c = 2 \cdot arcsin(d_c / 2D_p);$$

 $\Delta \varphi$ is an angle adequate to the technological gap.

The obtained value of φ_{Σ} should be less than the angle of location of the measuring cups on the rotor, i.e. $2\varphi_{\Sigma} < \varphi_0$, where $\varphi_0 = 2\pi/m_c$.

The movement of a material particle in the product pipeline of the feeding device, in different periods of time, is characterized by a change in the effect of external loads on it. And therefore, according to the laws of classical mechanics, it is appropriate to consider the process of moving a particle as a set of characteristic stages (Statsenko et al., 2021).

The most unfavorable conditions of movement (interaction with the inner surface of the conical part of the funnel, impact on the cylindrical part of the funnel) will be in the particles furthest from the geometric center of the funnel, i.e. at point M (Figure 5).

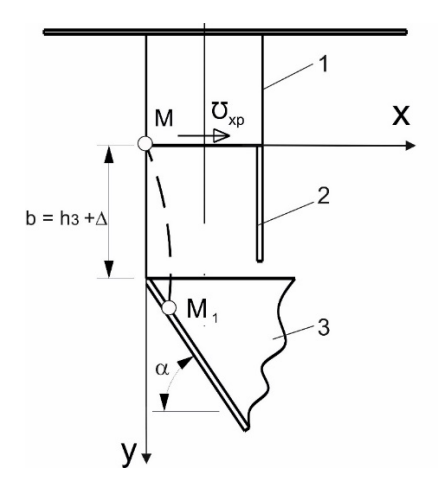


Figure 5. Scheme for calculating movement of a particle of bulk products at first stage of movement:

1 - cup; 2 - flap; 3 - cone part of funnel

To study the movement of a particle of bulk products in the product pipeline of the feeding device, the following assumptions are accepted:

- the particle has mass, but geometric parameters due to small dimensions compared to the dimensions of the funnel of the device, we neglect;
- the particle is characterized by elastic-plastic properties with a rate recovery coefficient after impact on the surface of the funnel k≈0,1–0,3;
- the influence of the action of surrounding particles on the movement of the studied particle is also neglected;
- the walls of the funnel are absolutely solid bodies, the mass of which is infinitely large;
 the coefficient of sliding of the particle on the inner surface of the funnel is a constant value;
- aerodynamic resistance to the movement of the particle is also neglected, due to small values of relative speed.

From the point of view of the action of uniform external forces on the particle, its movement in the funnel of the packaging device is given by a set of four characteristic stages:

- the first movement of the material particle from the initial position, point M, to contact with the inner cone surface of the funnel;
- the second oblique elastic-plastic impact of the particle on the inner surface of the conical part of the funnel;
- the third movement with sliding of the material particle on the inner surface of the conical part of the funnel;
- the fourth movement of the particle in the conjugation zone of the conical and cylindrical parts of the funnel and in the cylindrical part.

The duration of the packaging operation is the sum of the durations of all stages of movement of the material particle

$$T_{\Sigma} = t_1 + t_2 + t_3 + t_4 + t_5 + t_6, \tag{24}$$

where t_{1-4} is the duration of movement of the particle in the product pipeline;

t₅ duration of movement of the particle in the package;

t₆ – duration of forming, feeding new containers (packaging).

At the first stage, the movement of the particle begins at the moment of opening the flap of the measuring cup. The opening duration of the flap is insignificant compared to the movement duration of the particle in the first stage, and therefore it can be assumed that the opening of the flap occurs instantly. At the initial moment of the first stage, the particle, together with the measuring cup, moves at a linear speed $v_{x\theta}$, which is determined by v_{x0} = $\omega_p 0.5 D_p$. If we assume that the projection of the cone surface in the X0Y coordinate system is described by the equation $y = b + tg\alpha \cdot x$, where $b = H_M$ or $b = h_3 + \Delta$, then the duration of the movement of the particle before contact with the inner cone surface at the point M_1 can be determined

$$t_1 = \frac{1}{g} \left[v_{x0} \cdot tg\alpha + \sqrt{\left(v_{xo} \cdot tg\alpha\right)^2 + 2gH_{M}} \right]. \tag{25}$$

The kinematic parameters of the particle's motion at the M₁ point will be

$$x_{1K} = v_{x0} \cdot t_1$$
; $y_{1K} = 0.5g \cdot t_1^2$
 $\dot{x}_{1K} = v_{x0}$; $\dot{y}_{1K} = g \cdot t_1$.

The coordinates $x_{1\kappa}$, $y_{1\kappa}$ correspond to the coordinates of the point M_1 at which the elastic-plastic impact of the particle occurs on the inner surface of the conical part of the funnel.

In the case when the X coordinate of the particle will be within $00.5(D_\kappa - d) \le X \le 0.5(D_\kappa + d)$ at $y \le H_\kappa + H_M$, then the particle will not contact the lateral conical surface of the funnel, will further move along its cylindrical part. This type of particle movement is possible at $\omega_{D1} \le \omega_{D2}$, where

$$\omega_{p1} = \frac{D_K - d}{D_p \cdot t_{10}} ; \ \omega_{p2} = \frac{D_K + d}{D_p \cdot t_{10}}$$

$$t_{10} = \sqrt{\frac{2(H_\kappa + H_M)}{g}}.$$
(27)

If x>0.5(Dk+d), then the particle will contact the far conical surface of the funnel. The point of contact and kinematic parameters of the movement of the particle at the moment of impact are defined as (Figure 6)

$$x_{M03} = \omega_{p} \cdot 0.5D_{p} \cdot t_{1}' \qquad y_{M03} = 0.5 \left(t_{1}'\right)^{2}; \dot{y}_{M03} = gt_{1}' \qquad (28)$$

$$t_{1}' = \frac{1}{g} \left[-0.5\omega_{p} \cdot D_{p} \cdot tg\alpha + \sqrt{\left(0.5\omega_{p}D_{p}tg\alpha\right)^{2} + 2g\left(D_{\kappa} \cdot tg\alpha + H_{M}\right)} \right].$$

To determine t'_1 , an expression describing the far generating cone surface in the HOY coordinate system was used

$$y' = D_{\kappa} \cdot tg\alpha + H_{M} - tg\alpha \cdot x \tag{29}$$

Under the condition $\omega_p > \omega_{p2}$, the most unfavorable conditions regarding the duration of movement will be for the particle at the point M_0 .

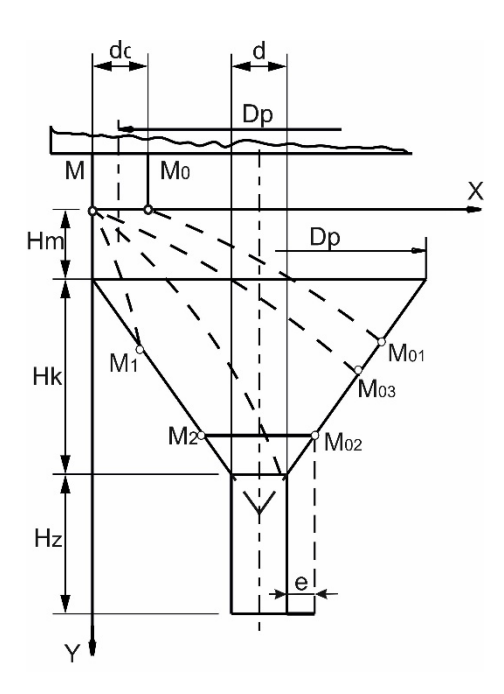


Figure 6. Scheme for calculating the movement of particle of bulk products at first stage at $\omega_n > \omega_{n2}$

The duration of movement and kinematic parameters of the movement of the particle from point M_0 to contact with the cone surface of the funnel at point M_{01} can be determined from the expressions:

$$x_{MO} = 0.5\omega_{p} \cdot D_{p} \cdot t_{1.0} + d_{c}; y_{MO} = 0.5g(t_{1.0})^{2};
\dot{x}_{MO} = 0.5\omega_{p} \cdot D_{p}; \dot{y}_{MO} = gt_{1.0}$$

$$(29)$$

$$t_{1.0} = \frac{1}{g} \left[-0.5\omega_{p} \cdot D_{p}tg\alpha + \sqrt{(0.5\omega_{p} \cdot D_{p}tg\alpha)^{2} + 2g(D_{\kappa} \cdot tg\alpha + H_{M} - d_{c}tg\alpha)} \right].$$

At point M_{01} , there will be an elastic-plastic impact of the particle on the inner conical surface of the funnel.

According to the obtained dependencies and accepted initial data: Dk=0.550 m; D_p =0.800 m; d_c =0.1 m; H_m =0.110 m; H_κ =0.618 m are given in graphic form the regions of movement of the particle without contact with the side surfaces of the conical part of the funnel (Figure 7).

According to Figure 6, all particles of the lower layer of the measuring cup will move in the cylindrical part of the funnel at only one value of angular velocity (ω_p =0.911 rad/s). To expand the range of angular speed of the dispenser rotor, it is appropriate to increase the effective cross-sectional area of the funnel at the junction of the conical and cylindrical parts due to the displacement of the cylindrical part by the appropriate eccentricity. The geometry of the funnel imposes restrictions on e_{max} =0.5d, and therefore it is important to find the rational value of e while ensuring the minimum T_{Σ} .

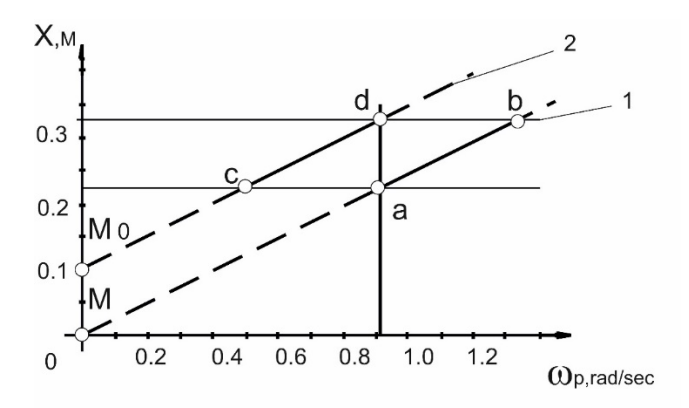


Figure 7. Nature of the movement of material particles of bulk products from points M and M_0 when condition $\omega_{p1} \le \omega_p \le \omega_{p2}$ is met

At $\omega_{p2} < \omega_p < \omega_{p1}$, at points M_1 and M_{01} , there will be a particle impact on the inner surface of the conical part of the funnel. Taking into account the trajectory of movement of a material particle and its physical and mechanical properties, it can be stated that at the second stage there will be an oblique elastic-plastic impact (Figure 8).

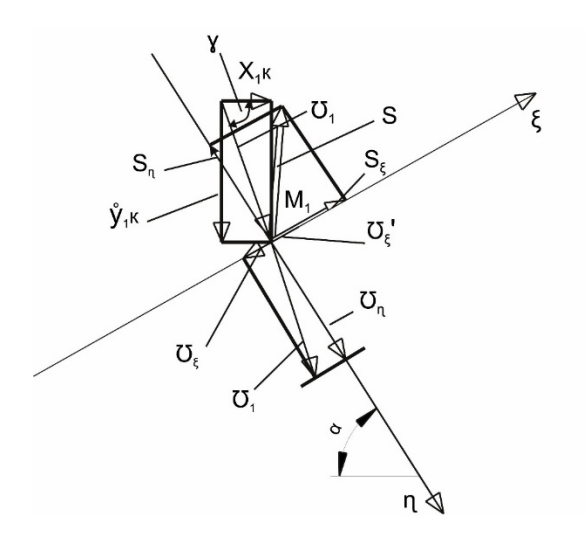


Figure 8. Scheme for determining kinematic parameters of movement of material particle of bulk products after affecting inner surface of conical part of funnel in second stage will be an oblique elastic-plastic impact

To determine the kinematic parameters of the movement of a particle of bulk products after hitting the conical part of the funnel, we use Newtonian impact theory (Lemos, 2018)

$$v_{\varepsilon} = v_1 \cdot \cos(\gamma - \alpha); \quad v_{\varepsilon} = v_{\varepsilon} \cdot k = v_1 \cdot \sin(\gamma - \alpha) \cdot k,$$
 (30)

where

$$v_1 = \sqrt{\left(\dot{y}_{1k}\right)^2 + \left(\dot{x}_{1k}\right)^2}, \quad \gamma = arctg\left(\frac{\dot{y}_{1k}}{\dot{x}_{1k}}\right);$$

k-coefficient of recovery of the particle's speed after impact.

If k > 0.5, after impact the particle may bounce off the surface of the conical part of the funnel and experience a repeated collision. However, since for many food products the coefficient k typically lies within 0.1–0.3 (Bila and Statsenko, 2012), the rebound can be neglected, and the subsequent motion of the particle can be considered as occurring solely along the surface of the conical part of the funnel. During the impact, there are power loads on both the product and the wall of the funnel. The impact load can be estimated using either the impact force or the shock pulse (S). Determination of these parameters is important during verification calculations of the thickness of the funnel material and the strength properties of the products.

The third stage is characterized by the movement of the particle on the inner surface of the cone part of the funnel with sliding, which is taken into account by the sliding resistance coefficient. At this stage, the particle moves from point M_1 to A. Point A characterizes the beginning of the cylindrical part of the funnel when it is partially shifted from the axis of symmetry of the conical part (Figure 9).

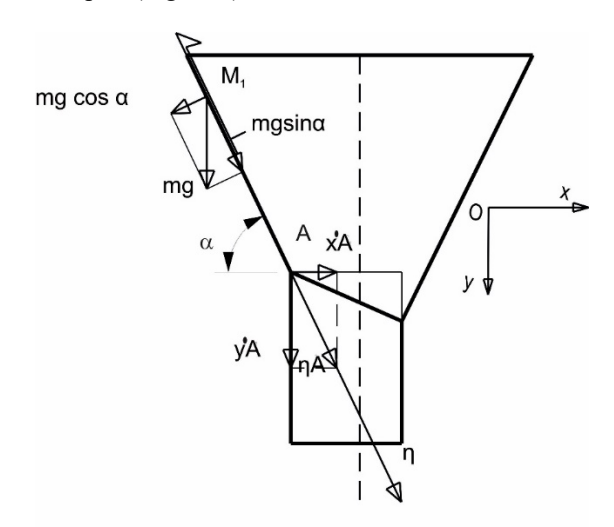


Figure 9. Scheme for determining kinematic parameters of movement of particle of bulk products on inner surface of conical part of funnel

If the distance from the point M_1 to A is taken as l_{AMI} , then the duration of movement of the particle in the third stage is determined from the expression

$$t_{3} = \left[-v_{1} \cdot cos\left(-\alpha\right) + \sqrt{\left[v_{1}cos\left(-\alpha\right)\right]^{2} + 2l_{AM1}\left(gsin\alpha - gfcos\alpha\right)} \right] \times \left[gsin\alpha - gf \cdot cos\alpha\right]^{-1}, (31)$$

where f is the coefficient of friction of the sliding of the material particle on the inner surface of the conical part of the funnel;

$$\begin{split} l_{\scriptscriptstyle AM1} = & \left\{ \frac{d^2 \cdot g^2}{\left[-\dot{y}_{\scriptscriptstyle A} + \sqrt{\left(\dot{y}_{\scriptscriptstyle A}\right)^2 + 2gh_0} \right]^2 \cdot \cos^2\alpha} - \left[v_1 \cdot \cos\left(-\alpha\right) \right]^2 \right\} \times \left[2g sin\alpha - gf \cdot \cos\alpha \right]^{-1} \\ & \dot{y}_{\scriptscriptstyle A} = & \left\{ \left[g \cdot sin\alpha - g \cdot f \cdot \cos\alpha \right] \cdot t_3 + v_1 \cdot \cos\left(-\alpha\right) \right\} \cdot sin\alpha; \\ & h_0 = H_u + etg\alpha. \end{split}$$

In the future, let's assume that at the fourth stage the particle will move in the cylindrical part of the funnel (Figure 10) (Benvenuti et al., 2015)

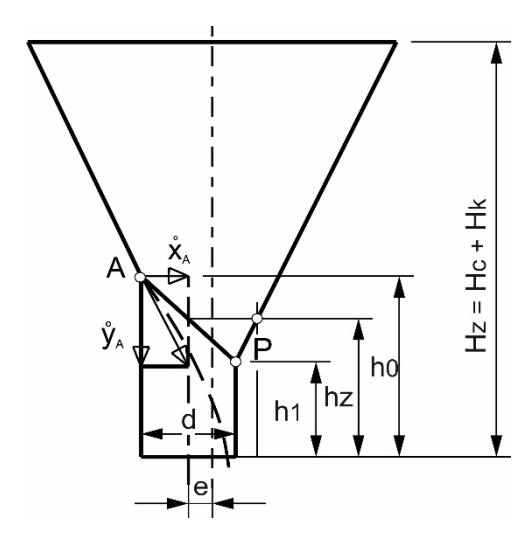


Figure 10. Scheme for determining kinematic parameters of movement of bulk product particle in cylindrical part of feeding device

The duration of movement of the material particle at the fourth stage, provided that $y_4=h_0$, $x_4\le d$ is determined by the formula

$$t_4 = \left[-\dot{y}_A + \sqrt{\left(\dot{y}_A\right)^2 + 2gh_0} \right] \cdot \frac{1}{g}.$$
 (32)

It is possible to fulfill the condition $x_4 \le d$ when choosing the rational value of the eccentricity, which is determined from the expression

$$e = \left[\frac{H_{\kappa}}{\sin \alpha} - \left[\left(\frac{\omega_{0} \cdot 0.5D \left(\omega_{0} D_{p} t g \alpha + \sqrt{\left(\omega_{p} 0.5D_{p} \cdot t g \alpha \right)^{2} + 2g H_{M}} \right)}{g \cdot \cos \alpha} \right) + l_{AM1} \right] \cdot \cos \alpha.$$
 (33)

Analysis of expression (33) shows that for all other constant geometric parameters of the feeding device, the value of the eccentricity depends on the rotation frequency of the rotor of the dosing module in parabolic dependence. The greater the value of the rotor frequency, the smaller the e value (Figure 11).

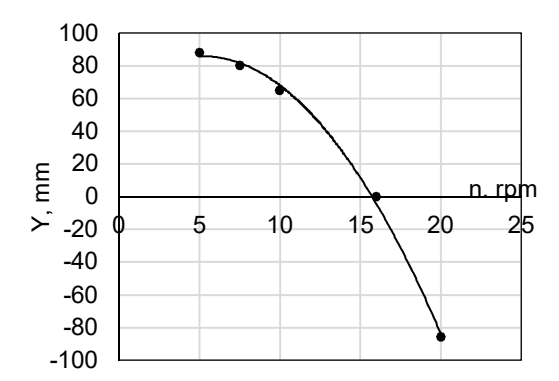


Figure 11. Changing value of eccentricity of feeding device at different values of rotation speed of dispenser rotor (estimated data: $m_0 = 6$; Dp = 0.8 m; n = 5-20 rpm)

At appropriate values of the rotor speed, the eccentricity may be negative, that is, the cylindrical portion of the funnel may be located to the right of the axis of symmetry of the conical portion of the funnel.

The movement of bulk products in the well of the hopper dispenser under the action of vibration forces is considered in the works of Sholoviy and Maherus (2014). The obtained results make it possible to determine the rational parameters of the base of the funnel cone and the value of the eccentricity. The free movement of bulk product particles is considered in the works of Maslo (2013) and Derenivska et al. (2014) in weight dispensers, but without taking into account the interaction with the working bodies of the module.

Simulation modeling

Figure 12 shows the results of simulation modeling of the movement of the dose of bulk products in the product line of the packaging device at e=0.0 mm and axial movement speeds of the measuring cup: 0.316, 0.628 and 0.84 m/s, corresponding to the performance of the dosing-feeding module: 45, 90 and 120 packs/min.

The results of the calculation are a change in the average value of the speed of movement of the flow of bulk products along the length of the feeding device and the duration of the packaging operation.

The analysis of the results of simulation modeling of the movement of bulk products makes it possible to state that at v_{x0} <0.628 m/s, a significant part of the products is slipped on the left side conical surface of the funnel, at v_{x0} >0.628 m/s – the products are mainly moved in the feeding device without contact with the conical surface of the funnel, and at v_{x0} >0.628 m/s –, the products are slipped on the right side conical surface of the funnel.

Figure 13 shows characteristic views of the path of movement of bulk products in the feeding device at e > 0.0 mm, that is, the eccentricity of the cylindrical part of the funnel

relative to the conical part.

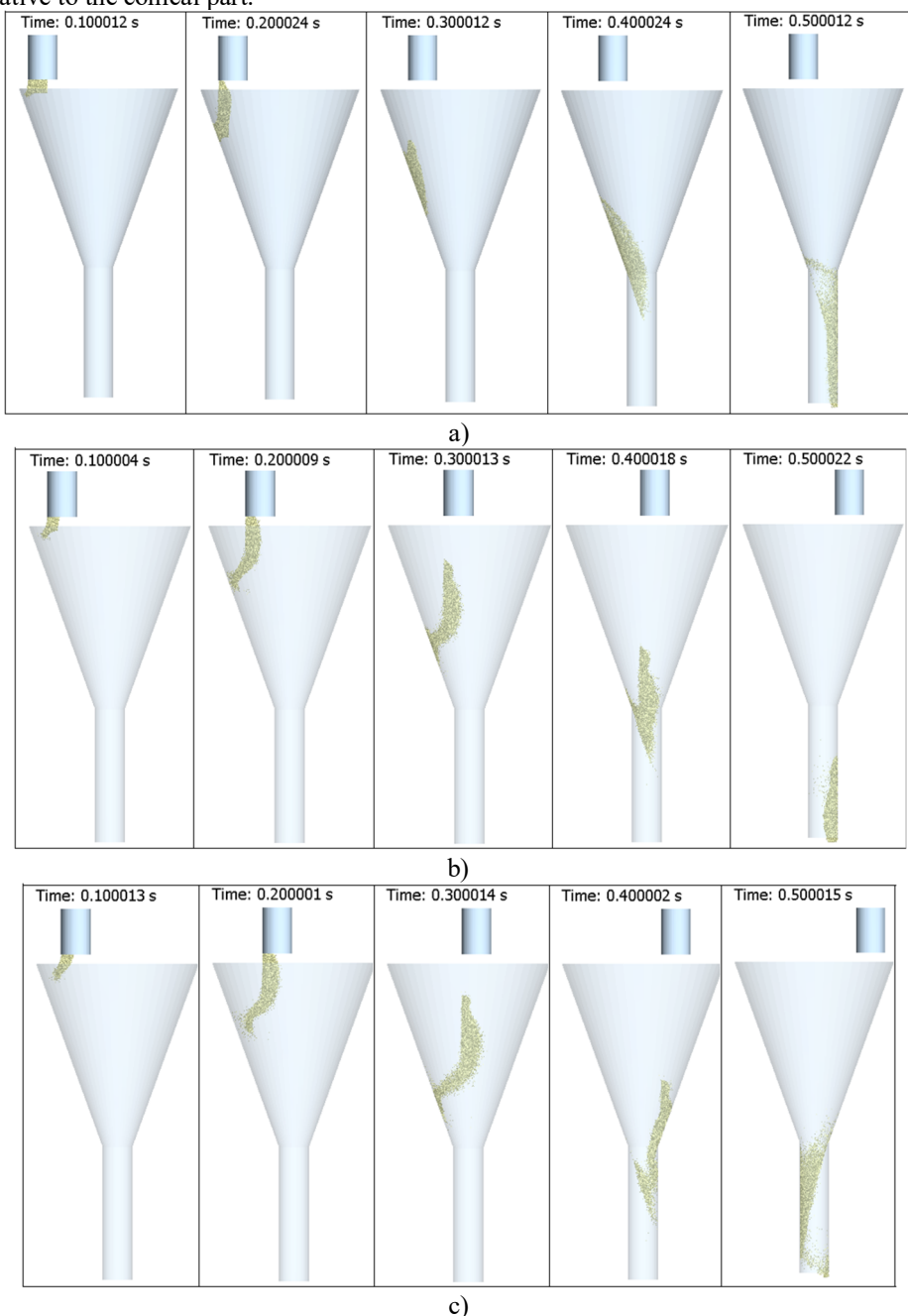


Figure 12. Characteristic views of trajectory of movement of bulk products dose in feeding device at e = 0.0 mm and axial velocities of measuring cup: $a - v_{x0} = 0.316$ m/sec; $b - v_{x0} = 0.628$ m/sec; $c - v_{x0} = 0.84$ m/sec

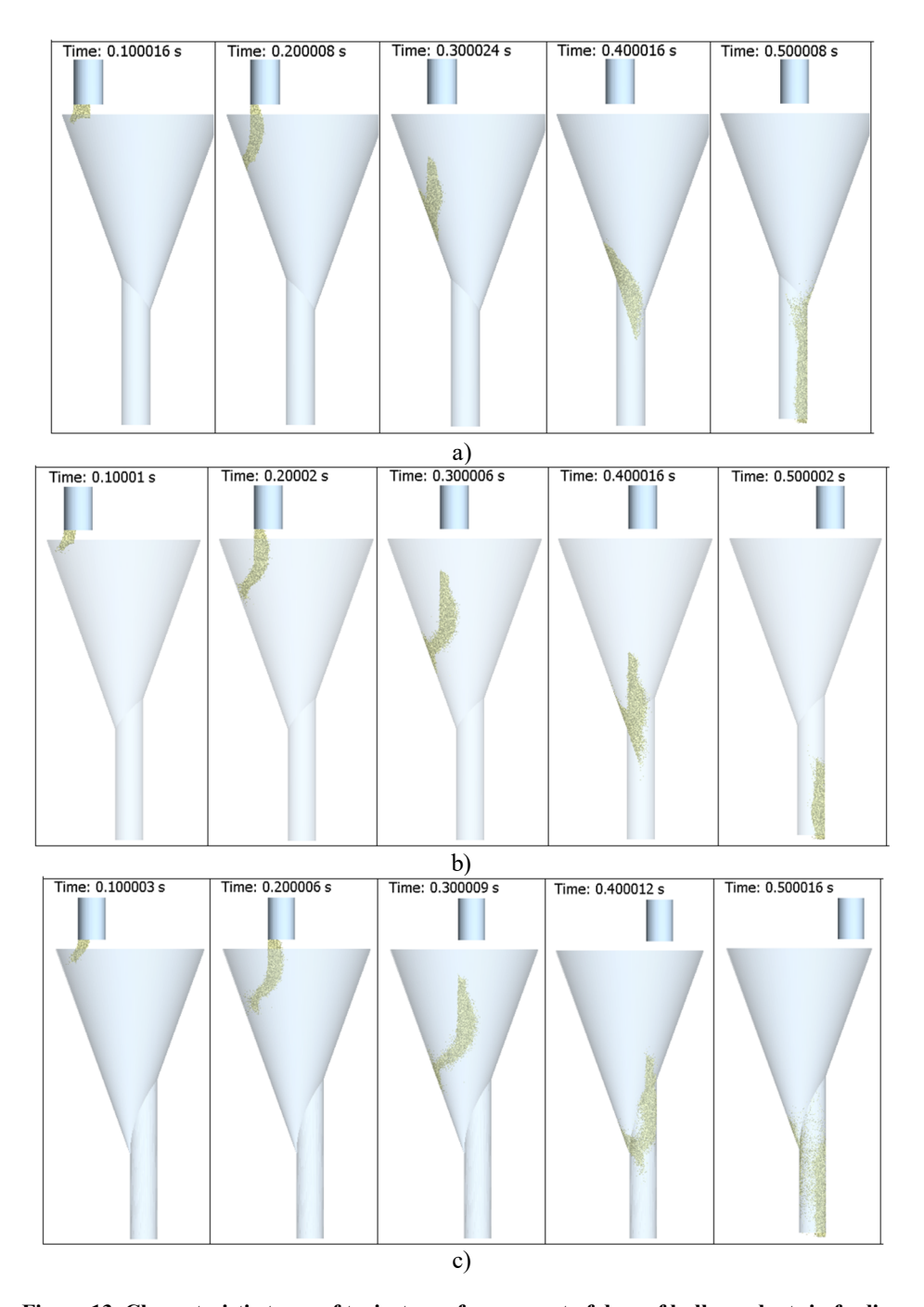


Figure 13. Characteristic types of trajectory of movement of dose of bulk products in feeding device at: a-e=-20.0 mm, $v_{x0}=0.42$ m/s; b-e=20.0 mm, $v_{x0}=0.628$ m/s; c-e=50 mm, $v_{x0}=0.84$ m/s

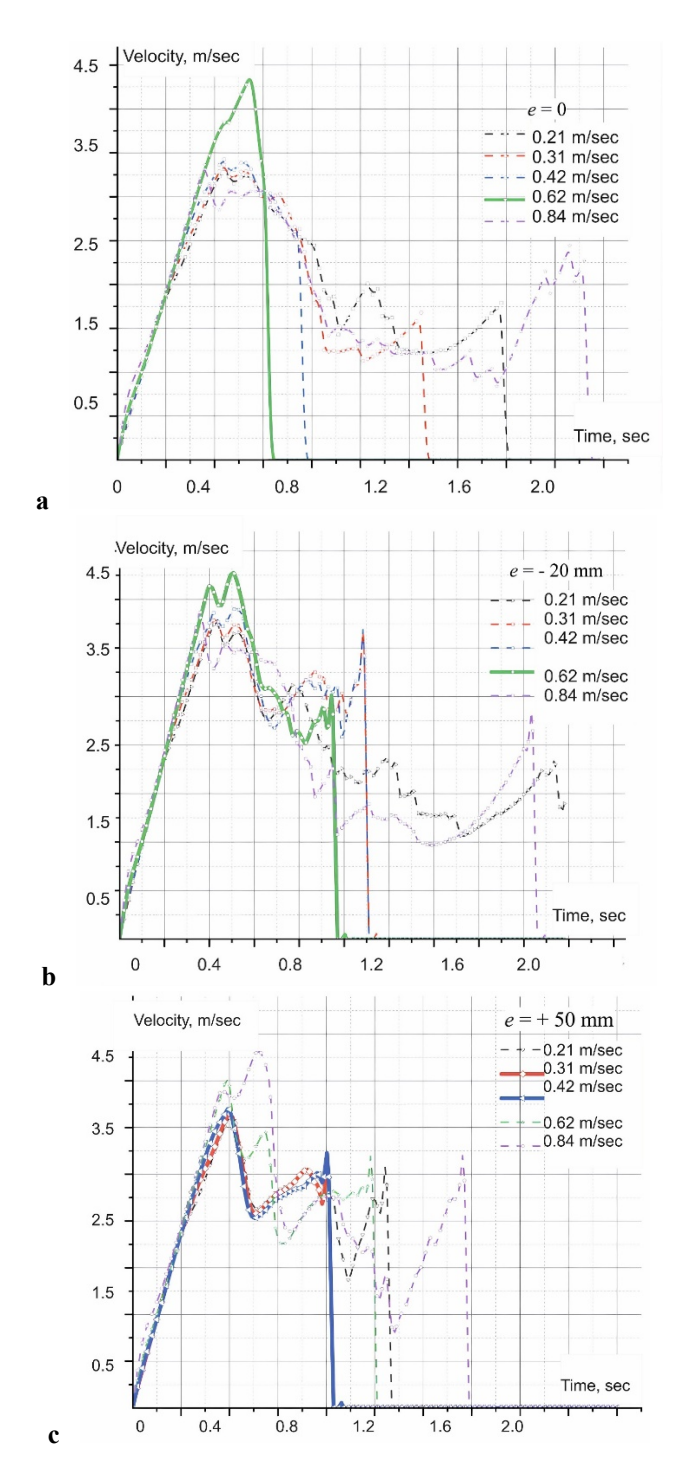


Figure 14. Change in the speed of movement of bulk products along funnel: a-e=0.0 mm; b-e=-20 mm, c-e=50 mm

The simulated trajectories of bulk product movement in the feeding device confirm the theoretical assumption that offsetting the cylindrical section of the funnel relative to the symmetry axis of its conical section makes it possible to minimize the contact time of bulk products along the conical surface. To analyze the kinetics of the movement of bulk products in the packaging device, it is appropriate to use the schedule of changes in the speed of movement of products along the length of the funnel (Figure 14).

When comparing the duration of bulk product feeding at e >= 0.0 mm and at e >0.0 mm at different values of the axial speed of movement of the measuring cup, it was established that with a rational value of e, it is possible to reduce the duration of contact of the products with the surface of the funnel and the total duration of bulk product feeding to 10-11%. These conclusions confirm the accepted assumptions in the theoretical study of the movement of a characteristic particle of the product dose. At the stages of project calculations, formula (33) can be used to determine the rational value of e.

Cundall and Strack (1979), Bertrand et al. (2004) and Burmistenkov and Statsenko (2018) investigated the movement of bulk products into a storage hopper using DEM methods. Such bulk products lack impact interactions with working surfaces and change, within wide limits, the trajectory of particle movement. Such tasks, for the most part, are of the same stage and do not require taking into account power loads of different nature. The results of the analyzed studies confirm their incompleteness and the absence of a holistic method of creating the latest samples of adaptronic modules for dosing bulk products in a volumetric way with continuous movement of the rotor with measuring cups.

Experimental studies

Checking the adequacy of the regimes of theoretical studies in comparison with experimental data established that the deviation in the duration of dose formation does not exceed 12% (Figure 15).

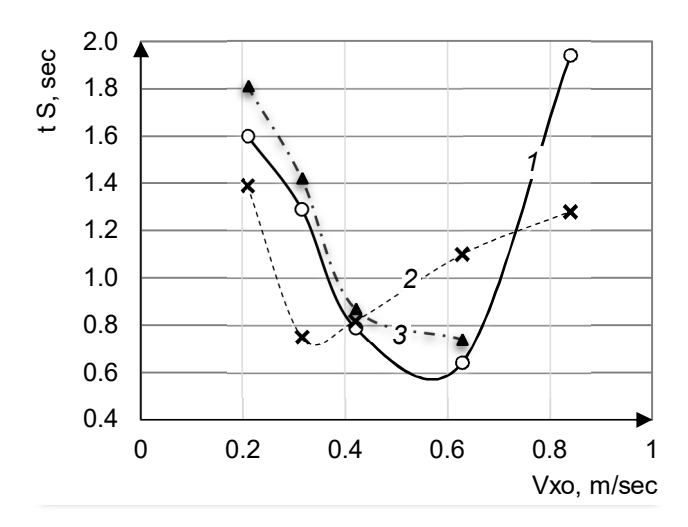


Figure 15. Effect of measuring cup axial speed on the duration of bulk product packaging: 1 - e = 0.0 mm; 2 - e = 50.0 mm; 3 - results of experimental studies

Technical offer

Analysis of the trajectory of movement of bulk products of their kinematic parameters made it possible to improve the design of the feeding device (Figure 16)

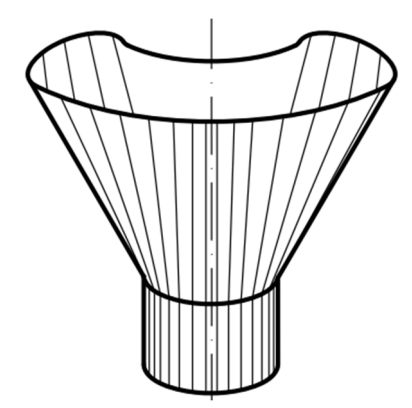


Figure 16. Improved design of feeding device for bulk products

This design of the feeding device minimizes its dimensions and metal capacity, and with a certain eccentricity of the displacement of the cylindrical part relative to the axis of the conical part of the funnel minimizes the duration of packaging.

Conclusions

- 1. The movement of characteristic particles of the dose of bulk products in feeding devices during continuous rotation of the rotor with measuring cups is characterized by a complex trajectory and interaction with the inner surface of the conical part of the funnel, which leads to an increase in the duration of product packaging.
- 2. One effective way to reduce the duration of packaging is to minimize the duration of contact of the bulk product particles with the inner conical surface of the funnel by increasing the cross-sectional area of the conjugation of the conical part of the funnel with the cylindrical part. With the geometric shape of the feeding device unchanged, this task can be solved due to the eccentric displacement of the axis of the cylindrical part relative to the axis of the conical part of the funnel.
- 3. The value and direction of the eccentricity depends on the linear speed of movement of the measuring cup and cannot be greater than $e \le 0.5$ d. The limit is set from the layout of the conical-cylindrical funnel.
- 4. To ensure the specified productivity of the dosing and feeding module, the diameter of the base of the cone part of the funnel is calculated taking into account the kinematic and geometric parameters of the rotor with measuring cups, the dimensions of the measuring cup, the diameter of the cylindrical part of the funnel and the angle of inclination of the side cone surface of the funnel.
- 5. Simulation modeling of the movement of the dose of bulk products in the feeding device confirmed the multi-stage operation and the significant influence of eccentricity on the

- duration of packaging. With a rational ratio of kinematic and geometric parameters of the movement of bulk products, when choosing a rational value of eccentricity, it is possible to reduce the duration of bulk product feeding to 11%.
- 6. The adequacy of the results of theoretical research is confirmed by experimental studies performed on a real-life automatic machine. The deviation of the duration of packaging according to theoretical calculations and experimental experiments does not exceed 10–12%.
- 7. Analysis of particle trajectories and bulk product flow allows designers of feeding devices to recommend rational values for the eccentricity of the cylindrical section's axis relative to the conical section's axis of symmetry. To minimize the device's size and weight, the conical section can be shaped like a torus.

References

- Gavva O.M., Kryvoplias-Volodina L.O. (2023), System Engineering of Automatic Packaging Machines, Kyiv, Production «Stal».
- Grewal B.S. (2008), Higher Engineering Mathematics, 43rd Edition, Khanna Publishers.
- Behjani M. A., Motlagh Y. G., Bayly A., Hassanpour A. (2019), Assessment of blending performance of pharmaceutical powder mixtures in a continuous mixer using Discrete Element Method (DEM), *Powder Technology*, 366, pp. 73–81, https://doi.org/10.1016/j.powtec.2019.10.102
- Benvenuti L., Kloss Ch., Pirker S. (2015), DEM parameter identification by means of artificial neural network for iron ore sintering. *Eleventh International Conference on CFD in the Minerals and Process Industries*, Melbourne, Australia, 7-9 December 2015.
- Bertrand F., Leclaire L.A., Levecque G. (2005), DEM-based models for the mixing of granular materials, *Chemical Engineering Science*, 60, pp. 2517–2531, https://doi.org/10.1016/j.ces.2004.11.048
- Bila T.Ya., Statsenko V.I.N. (2012), Study of the movement of mixture particles in the step rotor of a continuous centrifugal mixer, *Bulletin of the Kyiv National University of Technology and Design*, 6, pp. 17-21.
- Burmistenkov O. P., Statsenko V.V. (2018), Using the method of discrete elements to study the movement of bulk materials in bunker devices, *II International Scientific and Practical Conference Mechatronic Systems: Innovations and Engineering*, June 15, 2018, pp. 95-97, Kyiv, KNUTD.
- Burmistenkov O.P., Bila T.Ya., Statsenko V.I. (2019), Research on the energy efficiency of equipment for mixing bulk materials, *Bulletin of the Kyiv National University of Technology and Design, Series Technical Sciences*, 4, pp. 42-48, https://doi.org/10.30857/1813-6796.2019.4.4
- Cundall P.A., Strack O.D.L. (1979), A discrete numerical model for granular assemblies, *Géotechnique*, 29(1), pp. 47–65, https://doi.org/10.1680/geot.1979.29.1.47
- Derenivska A., Gavva O., Kryvoplias-Volodina, L., Kokhan O. (2014), Optimization of transportation bulk solids food products in the liner heightener of packing machine. *Journal of Food and Packaging Science, Technique and Technologies*, 3, pp. 20-23.
- Di Renzo A., Di Maio F. (2004), Comparison of contact-force models for the simulation of collisions in DEM-based granular flow codes, *Chemical Engineering Science*, 59(3), pp. 525–541, https://doi.org/10.1016/j.ces.2003.09.037

- Dubey A., Sarkar A., Ierapetritou M., Wassgren C.R., Muzzio F.J. (2011), Computational approaches for studying the granular dynamics of continuous blending processes, 1 DEM based methods, *Macromolecular Materials and Engineering*, 296(3-4), pp. 290–307, https://doi.org/10.1002/mame.201000389
- Kafashan J., Wiącek J., Abd Rahman N., Gan J. (2019), Two-dimensional particle shapes modelling for DEM simulations in engineering: A review, *Granular Matter*. 21(3), 80, https://doi.org/10.1007/s10035-023-01383-2
- Lemos N.A. (2018), Analytical Mechanics, 2nd Edition, Cambridge University Press.
- Maslo M.A. (2013), Improvement of weight dispensers, *Packaging*, 28, pp. 29-32.
- Munjiza A. (2004), *The Combined Finite-Discrete Element Method*, Wiley, https://doi.org/10.1002/0470020180
- O'Sullivan C., Bray J. (2004), Selecting a suitable time step for discrete element simulations that use the central difference time integration scheme, *Engineering Computations*, 23(21), pp. 278-303, https://doi.org/10.1108/02644400410519794
- Otsubo M., O'Sullivan C., Shire T. (2017), Empirical assessment of the critical time increment in explicit particulate discrete element method simulations, *Computers and Geotechnics*, 86, pp. 67-79, https://doi.org/10.1016/j.compgeo.2016.12.022
- Sarkar A., Wassgren C.R. (2009), Simulation of a continuous granular mixer: Effect of operating conditions on flow and mixing, *Chemical Engineering Science*, 64(11), pp. 2672–2682, https://doi.org/10.1016/j.ces.2009.02.011
- Sarkar A., Wassgren C. (2010), Continuous blending of cohesive granular material, *Chemical Engineering Science*, 65(2), pp. 5687–5698, https://doi.org/10.1016/j.ces.2010.04.011
- Sholoviy Y.P., Maherus N.I. (2014), Development of the mathematical model of the fine dispersion material behavior under vibration in the conical hole in the dispenser. Bulletin of the Lviv Polytechnic National University, Optimization of Production Processes and Technological Control in Mechanical and Instrument Engineering, 786, pp. 24-29.
- Statsenko V.V., Burmistenkov O.P., Bila T.Ya., Lischuk V. (2021), Modeling the Movement of Loose Materials in Mixing Complexes by the Method of Discrete Elements, Kyiv, KNUTD.
- Stypnytskyy V.V. (2013), Principles of functional oriented technology manufacturing products engineering production, *Bulletin of the Lviv Polytechnic National University*, *Optimization of Production Processes and Technological Control in Mechanical and Instrument Engineering*, 760, pp. 26–34.
- Vera P.M., Brøchner T., Strøm J.S., Takai H. (2015), Report 12: Flow of salt particles on a spinning spreader disk, *External influences on spray patterns (EPAS)*, https://pure.au.dk/ws/portalfiles/portal/87361608/Report12_Flow_of_salt_particles_03jun.pdf
- Williams J.R., O'Connor R. (1999), Discrete element simulation and the contact problem, *Archives of Computational Methods in Engineering*, 6(4), pp. 279–304, https://doi.org/10.1007/BF02818917
- Yan Z., Wilkinson S. K., Stitt E.H., Marigo M. (2015), Discrete element modeling (DEM) input parameters: understanding their impact on model predictions using statistical analysis, *Computational Particle Mechanics*, 2, pp. 283–299, https://doi.org/10.1007/s40571-015-0056-5
- Yuu S., Umekage T. (2011), Simulation of granular flows and pile formation in a flat-bottomed hopper and bin, and experimental verification, *Materials*, 4(8), pp. 1440–1468, https://doi.org/10.3390/ma4081440

----- Processes and Equipment-----

Zhu H.P., Zhou Z.Y., Yang R.Y., Yu A.B. (2007), Discrete particle simulation of particulate systems: Theoretical developments, *Chemical Engineering Science*, 62(13), pp. 3378–3396, https://doi.org/10.1016/j.ces.2006.12.089

Cite:

UFJ Style

Gavva O., Kryvoplias-Volodina L., Dolomakin Yu., Kokhan A., Kulyk N. (2025), Impact of bulk product mechanics in adaptronic dosing systems on optimal geometry of packaging devices, *Ukrainian Food Journal*, 14(3), pp. 478–506, https://doi.org/10.24263/2304-974X-2025-14-3-9

APA Style

Gavva, O., Kryvoplias-Volodina, L., Dolomakin, Yu., Kokhan, A., & Kulyk, N. (2025). Impact of bulk product mechanics in adaptronic dosing systems on optimal geometry of packaging devices. *Ukrainian Food Journal*, 14(3), 478–506. https://doi.org/10.24263/2304-974X-2025-14-3-9

Basic food purchasing habits of young people in dimension of price inflation

Tímea Juhasz

Budapest Business University, Budapest, Hungary Sopron University, Sopron, Hungary

Abstract

Keywords:

Food Purchasing Habits Younth Price Inflation

Article history:

Received 11.02.2025 Received in revised form 18.08.2025 Accepted 30.09.2025

Corresponding author:

Tímea Juhasz E-mail: juhasz.timea@ uni-sopron.hu

DOI: 10.24263/2304-974X-2025-14-3-10

Introduction. The aim of the research was to examine how inflation affects the basic food purchasing habits of a given consumer group and how they perceive and evaluate government measures aimed at reducing inflation.

Materials and methods. The target group examined consists of students studying at Hungary's largest economic university. The method examined is questionnaire-based research, in which the author evaluated the results using single and multiple variable methods.

Results and discussion. The analysis began with an overview of students' general food purchasing habits under the influence of recent price inflation. The findings revealed notable behavioral adjustments reflecting both economic constraints and changing consumption priorities. Many respondents reported that they now pay closer attention to prices, seek promotions more actively, and substitute more expensive products with cheaper alternatives. These adaptations suggest that young consumers are sensitive to even moderate price changes in essential food categories. The inflation had a negative impact on the purchasing habits of the young people participating in the study in the case of several basic foodstuffs. Students rated on a five-point Likert scale how their purchasing habits had changed after the introduction of inflation measures, where a score of 1 represented a decrease in overall purchasing and a score of 5 represented an increase in overall purchasing. The averages showed that purchases of the following products had decreased somewhat: homemade pork leg (M: 2.82), refined sunflower seed oil (M: 2.90), granulated sugar (M: 2.91), and plain wheat flour (BL 55) (M: 2.98). The study also confirmed that Pearson's correlation showed a very strong positive significant relationship between granulated sugar and flour (r: 0.800) and cooking oil (r: 0.726). Furthermore, there was a correlation between cooking oil and flour (r: 0.727), pork and flour (r: 0.564), and pork and oil (r: 0.572). The price trends of these foods also had an impact on the consumption and willingness to purchase foods used in combination with them. The measures introduced by the government, such as price caps and online price monitoring systems, did not have a significant positive effect on purchasing behaviour among this group of shoppers, which is due to their low awareness and infrequent use among the surveyed group.

Conclusion. Very high inflation has a negative impact on the purchases of basic foodstuffs among the young people surveyed, and that the impact of the government measures developed was not significantly noticeable for this group during the period of the study.

Introduction

In today's fast-changing world, food consumers face numerous factors that significantly influence their purchasing intentions and habits. This article presents selected results from a Hungarian study that examined the basic food purchasing habits of a group of higher-education students studying economics, focusing on their awareness of the government's inflation-control measures amid drastic price increases, and how these factors affect their food purchasing decisions.

From the early years of the second decade of the millennium onwards, Hungary's population has faced a combination of circumstances that have profoundly affected everyday life. In previous decades, such factors had never occurred simultaneously. Armed conflicts have erupted in several parts of the world, some directly impacting Hungary as a neighboring country. The effects of the Russian–Ukrainian war have been particularly significant since 2022, as rising energy and raw material prices led to a drastic increase in logistics costs. Unsurprisingly, these developments triggered an upward trend in food prices. While the average inflation rate in the European Union in October 2022 was 11.1%, Hungary's rate was nearly double that figure.

The situation was further aggravated by extremely drought-prone agricultural conditions (Szűcs-Kovács, 2023). In addition, the price of imported energy commodities almost tripled, which was reflected in the costs of numerous goods and services. These challenges emerged just as the country was recovering from the effects of the COVID-19 pandemic. Like elsewhere, COVID-19 disrupted Hungary's food supply chain by restricting the free movement of goods (Cappelli and Cini, 2020; Cullen, 2020) and triggering panic buying of many staple products, especially during the initial phase of the outbreak, when empty shelves in shops became a common sight (Power et al., 2020).

In 2023, production chains were affected to a lesser extent and in different ways, leading to a significant increase in Ukrainian exports and a consequent decline in Hungarian producer prices. Moreover, weather conditions in Hungary became much more favorable for crop production after 2022, which contributed to a decrease in food inflation to 4.8 percent by the end of 2023 (Világgazdaság, 2024). It is therefore evident that a combination of external and internal factors contributed to the emergence of high inflation in Hungary (levels that also exceeded the European Union average) and that several government measures were implemented to mitigate its effects.

The present study aimed to examine the impact of inflation on the food purchasing decisions of higher education students and to assess how well these government measures, particularly those targeting price stabilization, are known and perceived among economics students.

Factors that influence consumers' purchasing decisions. In 2019, the Hungarian National Chamber of Agriculture published a study on the factors influencing food choices. Based on this study, researchers mention sociological factors among the variables that influence consumers' purchasing decisions. In particular, the group of which the individual is already a member or to which the consumer would like to belong may be of particular importance. The closest and immediate circle is the family, which functions as a collective decision-maker on the issue in question. The other circle is that of the so-called opinion leaders, who play a decisive role in shaping and influencing opinions within a group and in the flow of information.

Other variables that emerge, according to the study, are the psychological characteristics of consumers, which play a role in whether they reject or accept certain foods. This decision may be expressed through the sensory attributes of the product, the symbols associated with the food (e.g. brand names, trademarks), or the perception of the expected

consequences. Other factors may include consumers' values, lifestyle and current trends that affect them.

Of course, the economic situation of the buyer cannot be ignored, either. However, the fact is that households' financial reserves are beginning to erode during a prolonged period of sustained high inflation, which causes people to increasingly look for bargain food products. However, Tambassur and Jabim (2020) point out that there are products for which people are willing to pay even more. For example, 44% of the consumers surveyed consented to pay an average of 9% more to buy the health and wellness food they wanted. Their regression analyses confirmed that income and education are important influencing variables when buying healthy foods. Health consciousness is the most important psychological characteristic of these shoppers, followed by product quality, taste, packaging, price, etc. in their decision to buy health and wellness foods.

Meanwhile, the research of Buglyó-Nyakas-Gál in 2023 highlighted that most households are affected by price rises. At the same time, they argue that food price rises do not always fundamentally change purchasing and consumption patterns. This can be explained by the fact that some people, known as traditionalists, cling to their old way of life even if they do not have outstanding material assets. However, it is also evident from their studies that there is a kind of action-seeking behaviour, looking for cheaper shopping opportunities, whereby consumers try to maintain the quality of food consumption and the options they were used to.

Finally, Kovács et al. (2022) point out that especially the younger generations (Millennials and Centennials) are increasingly aware of the ethical, environmental and social impacts of their food choices. In their opinion, studies on younger generations also suggest that emotional factors such as nostalgia for buying local products, entertainment, memories of old times, novelty, and the desire for experience are also included.

Government measures to curb food prices. As the author pointed out above, the inflation rate in Hungary increased significantly in 2022-2023 and was well below the EU average. Figure 1 shows the inflation rates between January 2022 and February 2024 in the EU and Hungary and demonstrates that there is a large difference between the values for the given months.

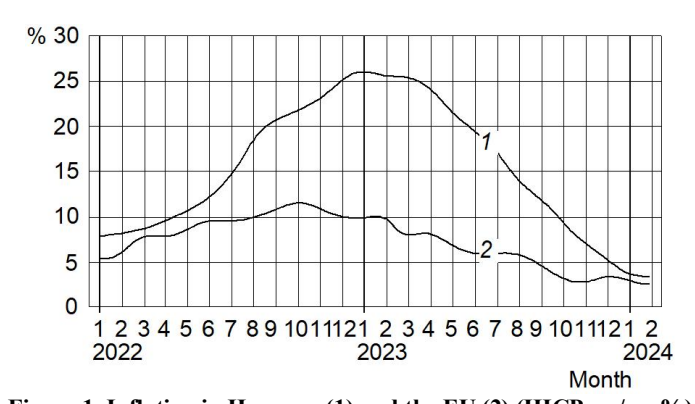


Figure 1. Inflation in Hungary (1) and the EU (2) (HICP, yr/yr, %)
Source: Eurostat, Portfolio (2024) https://www.portfolio.hu/en/economy/20240318/hungarys-inflation-remains-in-top-third-of-eu-ranking-675437

In the last three years, the Hungarian government has taken several direct measures to curb prices. These have been aimed at reducing the magnitude of inflation in the purchase of basic foodstuffs.

In the present research, the author has examined the following, without claiming completeness:

Price stop. The Hungarian government temporarily introduced a price freeze on certain staple foods in the autumn of 2021, and in November 2022 the government extended the price freeze on certain staple foods. Accordingly, the price control was extended to the following products: granulated sugar, plain wheat flour (BL 55), refined sunflower oil, domestic pork legs, chicken breast, chicken rump, chicken skin, chicken tail, chicken wings, ultra-high temperature treated cow's milk with 2.8% fat content, chicken eggs, table potatoes, excluding new potatoes. Government Decree 279/2023 (29.VI.) was related to the phasing out of the food price freeze, so the food price freeze was in force until 31 July. This intervention in market prices lasted for a total period of 1.5 years, and there is no consensus among experts on the success of its price suppressive effect. According to Balaton (2022), this measure could have a long-term negative impact on the market, distorting it and thus further worsening the competitiveness of the food industry.

Price monitoring system. To further reduce food prices and increase competition in the retail sector, the government has introduced a compulsory promotion for retail outlets from June 2023 and has agreed to the introduction of an online price monitoring database. Initially, the online price monitoring system, launched by the Office of Economic Competition, will allow consumers to find out the prices of more than 60 categories of food products. The largest retail chains with a turnover of more than HUF 100 billion were obliged to provide data, but the Hungarian government also made it possible for traders who did not have such an obligation to join voluntarily.

According to Világgazdaság (2024), the targeted government measures, the central bank's actions and the intervention of the competition authority were among the reasons why the monthly food price increase in March 2024 was only 0.7%, the lowest in almost eight years.

In the following, the author presents some results of a study conducted last year among students at a business university in Hungary. The target group was chosen deliberately. The author of the study believed that the individuals in the sample had a good basis in terms of knowledge and understanding of basic economic processes and causality, as they were students in higher education in economics, and could therefore realistically base their decisions and evaluations on this knowledge.

The aim of the research was to show how young Hungarians make decisions about purchasing basic foodstuffs in an economic environment burdened by very high inflation. It also sought to determine how aware they are of the government measures designed to curb inflation.

Materials and methods

Sample collection

The study was conducted in the second half of 2023 at the Faculty of Foreign Trade and Finance of Budapest Business University, Hungary's largest business university, and students completed a questionnaire that had not been validated before and had not been used in another research. At the beginning of the study, a test questionnaire was administered to check that all questions were understandable to the respondents. Five students participated in this process. To validate the questionnaire, after the large sample had been interviewed, a further 20 students completed the questionnaire, and the results were like those completed by the large sample. The responses were voluntary and anonymous, and the research respected

GDPR regulations. The questionnaire was posted on a social media platform and on the university's internal student platform, so it was not possible to measure the willingness to complete it. The questionnaire was eventually completed by 380 students. To determine the sufficient sample size, the author used the sample size calculator. Based on this, the institution had nearly 18,000 students at the time of the research (the university with the largest number of business students in Hungary). According to the calculator, at least 377 or more measurements/surveys are needed to get a true value within $\pm 5\%$ of the measured value at a 95% confidence level (calculator.net, 2024). Since the sample size was more than this, the author considered the sample size to be sufficient.

Sample

The sample specification is presented in Table 1.

Sample specification

Table 1

Property	Frequency (%)
No	45.5% Male
NO	54.5% Female
Place of residence	45.3% Budapest
of respondents	54.7% Rural areas
Living with parents	48.8% Living apart from parents
Living with parents	51.2% Living with parents
Personal monthly	66.9% Independent of parents
living expenses paid by	33.1% Dependent on parents

The average age of the students was 25.56 years, with a standard deviation of 11.771. Cross tabulation analyses showed that 42% of women lived in Budapest, while 42% of men did. 46.3% of girls lived apart from their parents, while the proportion for boys was 51.8%. Almost 88% of students living apart from their parents were able to support themselves. 52.5% of students living independently lived in Budapest and 68% of those living in Budapest were also able to be economically independent from their parents.

Questionnaire and statistical analysis

The questionnaire administered to students typically consisted of closed questions (18) and only 2 questions were open-ended. The questions were based on categorical variables and interval scales, including a five-point Likert scale. Following Josh et al. (2015), the author of this study interpreted the Likert scale as an interval scale. In the study, he tried to combine all the items to produce a composite score for an individual (Bone, 2012; Carifio, 2007). The author used SPSS version 29 to evaluate the questionnaire. Univariate and multivariate methods, i.e., frequency, mean, standard deviation, as well as cross tabulation analysis, correlation cluster analysis and factor analysis were used.

The questions of the questionnaire for the present study are presented by the author in three major groups (Table 2).

Table 2
Group structure of questions: Questionnaire structure

First group of questions.	Second group of questions.	Third group of questions.
Student specific questions	Trends in the purchase of	The price monitoring
	basic foodstuffs because of	system
	government measures	
No	Buying basic foodstuffs	Using the price
Age	because of online price	monitoring system
Family status?	monitoring	Factors affecting the use
Customer type	Buying basic foodstuffs	of price monitoring
Who pays the cost of living?	because of the price freeze	
Personnel costs in line with	Knowledge of government	
inflation?	measures to fight inflation	

Aims and hypothesis

In the current study, the author explores and analyses the results along the following lines:

The aim of the study is to find out how the purchase of basic foodstuffs was affected by the price freeze measure and the online price monitoring system in the sample.

The aim of the study is to find out whether gender, place of residence and who pays the cost-of-living effect perceptions of the success of the two measures.

The purpose of the survey is to find out how aware the student is of the online price monitoring system, and whether gender, place of residence, whether the student lives apart from his/her parents and who pays the living costs affect the perception of the tool. Along the above objectives, the author examines the validity of the following hypotheses:

Hypothesis 1: The willingness of the students in the study to buy basic foodstuffs was positively influenced by the price freeze and the online price monitoring system.

Hypothesis 2: For the students in the study, awareness of the government measures used is significantly influenced by gender, place of residence and who pays for the cost of living.

Hypothesis 3: The students in the study typically use the online price monitoring system, and satisfaction with the system is influenced by gender, place of residence, whether the student lives apart from their parents, and who pays their living costs.

Results and discussion

Testing the first hypothesis

The first hypothesis of the study was to examine the impact of the government's inflation-suppressing measures on the purchase of the basic foodstuffs that appeared in the regulations. The author listed a number of these for the students, who rated on a five-point Likert scale how their shopping habits changed after the measures were introduced, with a value of one indicating less shopping overall and a value of five indicating more shopping overall. The author summarised in Table 3 the general pattern of consumption of each product and the impact of the measures on the consumption of these products.

 $Table\ 3$ Effectiveness of measures affecting the purchase of consumer goods (M, SD)

Food	How have consumer price increases affected shopping?		Price stop		Online price monitoring system		Difference Mean
	Mean	SD	Mean	SD	Mean	SD	
Granulated sugar	2.91	0.741	2.98	0.777	2.03	1.174	0.95
Plain wheat flour (BL 55)	2.98	0.722	3.00	0.737	2.02	1.174	0.98
Refined sunflower seed oil	2.90	0.739	2.97	0.730	2.01	1.153	0.96
Homemade pork leg	2.82	0.762	2.88	0.725	2.03	1.181	0.84
Chicken breast, chicken tail, chicken skin, chicken tail, chicken wing ends	3.21	0.774	3.13	0.784	2.19	1.277	0.94
Ultra-high temperature treated cow's milk with 2.8% fat content	2.96	0.830	2.99	0.835	2.06	1.208	0.94
Hen's egg	3.12	0.786	3.07	0.715	2.12	1.221	0.95
Potatoes for human consumption, other than new potatoes	3.04	0.636	3.03	0.633	2.05	1.166	0.98

The data in the table show that, basically, consumer price increases had a neutral or negative effect on students' basic food purchases, i.e. they bought the same or less food. In the case of meat, pork purchases were reduced, and the situation was similar for granulated sugar, milk, flour and cooking oil. Overall, the two government measures did not have a positive impact on student purchases. The average difference between the two measures shows that the price freeze still had a more positive incentive effect than the online price monitoring system. One reason for this larger average difference may be that the online price monitoring system was a relatively recent measure at the time of the study, and therefore its awareness and impact may not yet have been as widespread and effective as that of the price freeze. The author also looked at which food purchases were strongly correlated with other consumer products. Pearson's correlation showed a very strong positive significant correlation between granulated sugar and flour (0.8), between refined oil (0.726), between refined oil and flour (0.727), between pork and flour (0.564), and between pork and oil (0.572). The price of these foods also affected the consumption and willingness to buy of the paired foods.

Overall, it can be concluded that the government measures did not have a significant positive effect on the purchasing behaviour of the students studied, and thus the first hypothesis is rejected.

Testing the second hypothesis

The second hypothesis concerned the factors that influence the visibility of government measures. On the popularity measure, respondents were asked to indicate on a five-point Likert scale the extent to which they were aware of how prices were evolving and the extent to which they were informed about government measures. Among the factors influencing awareness, the authors looked at gender, place of residence and who pays for living costs (i.e. whether the student lives with or without parents).

Table 3 presents the mean, standard deviation and independent sample T test results. The author has indicated where the groups' knowledge of a given instrument was significantly different and has noted which group had the highest mean in these cases.

Table 4
How aware are students of the extent of food inflation and the government measures to curb it?
(M, SD, T-test, significance: 0.05)

Findings			No	Residence	Cost of living
	Mean	SD	T- test	T- test	T- test
I am aware of how inflation in food is evolving in Hungary.	3.91	0.925	t: 2.584 sign: .005 Men M: 4.05	No significant difference	t: 1.818 sign: 0.035 Own M: 3.98
I am aware of the products affected by the government's price freeze.	3.88	0.958	No significant difference	No significant difference	t: 2.378 sign.: 0.009 Own M: 3.97
I am aware of the online price monitoring system that was introduced from 1 July 2023.	3.19	1.317	t: 2.597 sig.:0.005 Men M: 3.39	No significant difference	t:2.971 sig.:0.002 Own M: 3.34
I am aware of the compulsory promotion in retail shops that started on 1 June 2023.	3.39	1.253	t: 1.965 t: 0.025 Men M: 3.53	No significant difference	t: 3.599 sign. :0.001 Own M: 3.55

The average values calculated for the statements in the table show that students are familiar with both the price evolution of basic foodstuffs and the price freeze measure. However, they have less information about the price monitoring system and the compulsory action. This can be explained, among other things, by the fact that, as the author has already pointed out, this government regulation came out later than the price freeze and it is possible that more students were not yet aware of these possibilities. However, it can also be seen from the data in the table that the standard deviation values for these two measures were higher than for the price freeze, i.e. there was less unanimity among students in these cases. The author has examined whether for some factors singly significant differences in the perception of statements can be identified.

First, the writer analysed the gender gap. For almost all statements, men were more strongly aware of the issue than women, except for the dimension of the price stop.

Whether someone lived in the countryside or the capital had no significant effect on how clearly they perceived the issue. The residence variable was felt by the author to be worth investigating because living in Budapest is more expensive than in the countryside (KSH, 2023), and therefore she thought that this might be reflected in the knowledge of the measures, but this assumption was not supported.

The author of the study also looked at the livelihood situation to see who is aware of the problem and how they see it. She distinguished two groups. On the one hand, there are students who cover their own living expenses, and on the other hand, those whose parents bear the costs, either fully or partially. Many university students work while studying, primarily to pay tuition fees and support their living expenses. The institution provides several opportunities to combine work and study, organising classes as flexibly as possible to accommodate students' work schedules. For instance, many online classes are held on Fridays and can be watched at a convenient time.

The livelihood sources showed a divergence of views on several issues. This is not surprising, since students who rely only on their own resources tend to have a better understanding of the prices and trends of basic foodstuffs, since they basically buy their own products and must manage their own resources.

It can be seen, therefore, that gender and whether a student is trying to make a living on their own or with the help of their parents has an impact on their awareness of how food prices are evolving and how governments are trying to control them. Based on the results for this sample, the author only partially accepts her second hypothesis.

Testing the third hypothesis

The third hypothesis related entirely to the relatively recent introduction of online price monitoring. The research made statements about this to the students, who had to decide how true the statement was in their case. One was not true at all, while five was absolutely true. The author examined the averages and standard deviations of the students' opinions and then factorised the statements. All variables were suitable for factorization. The KMO and Barlett's test: KMO: 0.923 Khi-square: 4859.151 df: 55 sig.:0.000. Factors were constructed using Varimax rotation and three factors were constructed (Sajtos-Mitev, 2007). The explained coefficient of variance was 86.8%. In Table 5, the author presents the mean standard deviation of the variables, the factor weights and the Cronbach's alpha values of the constructed factors (Table 5).

The averages of the statements show that, in principle, the sample does not show that the online price monitoring system is used in practice by students, even via a popular device such as a mobile phone. The question arises whether this could be due to a lack of confidence in the system, given the small number of goods that are on the system on the one hand, and the lack of confidence in the authenticity of the information on the other. At the same time, price is more important than quality for most of the sample under consideration.

Three factors were created from the items by the author, which were found to have high reliability values (Cronbach's alpha). These factors were related to the use of and satisfaction with the online price monitor. For further analysis, the author of the study formed homogeneous groups or clusters using the three factors. Three clusters were created using a K-means procedure. The final cluster centres are shown in Table 6.

Table 5 Factors associated with online price monitoring, Cronbach alpha, and components

Factors	Claims	M	SD	Cronbach	Component		ent
				alpha	1	2	3
	I also use the price monitoring system while shopping.	1.78	1.09	0.97	0.905		
Using the online	I also use the shop filter function on the map in the price monitoring system.	1.77	1.13		0.895		
Using the online monitoring system	I have the price monitoring system app on my phone.		1.18		0.881		
	I check the price monitoring system before buying.	1.90	1.18		0.816		
	I consciously shop at chains that are on the price watch list.	1.86			0.815		
Satisfaction with	Authentic price information is included in the price monitor.	2.38	1.23	0.94		0.840	
the online price monitoring system	I consider the use of a price monitor to be a good savings tool.	2.38	1.26			0.838	
,	The price monitor is a very convenient tool.	2.18				0.760	
	The price monitoring system is difficult to use while shopping.	2.25	1.28	0.86			0.830
Dissatisfaction with the online price monitoring	I consider the range of products that are in the price watch to be small.	2.26	1.25				0.811
system	Despite the price watchdog, quality is still important to me, not price.	2.43	1.32				0.674

Final cluster centres

Table 6

Cluster			
1	2		
-1.19598	-0.98957		
-2.16828	2.66676		
3.71067	-2.04362		
	1 -1.19598 -2.16828		

Source: author's own research

Cluster characteristics based on cluster centres:

- 1. *Cluster:* includes those who, although they do not typically use the online price monitoring system regularly, do not have a good opinion of it. 105 respondents can be classified here.
- 2. *Cluster:* those who, although not typically using the online price monitoring system regularly, consider it a good and credible tool. 275 respondents are in this group.

The author has examined how gender, place of residence, whether the student lives apart from his/her parents and who pays for his/her living expenses affect clustering. Only for place of residence was a significant association found (Chi-square 5.886 df: 1 sig.:0.015 p<0.05). 78.5% of those living in the capital belonged to the satisfied group, while 21.5% belonged to the dissatisfied group. The same proportion for rural residents: 67.3% were satisfied with the system, while 32.7% were less satisfied.

Overall, it can be concluded that many students are not yet active users of the system, which makes it difficult for them to form a reliable opinion about it, and therefore the third hypothesis is rejected.

Hypotheses and thesis

In the light of the results of the study, the following theses can be drawn from the results (Table 7).

Hypothesis-Thesis table

Table 7

Hypothesis	Decision	Thesis
The willingness of the students in	Rejection	The willingness of the
the study to buy basic foodstuffs		students in the study to buy
was positively influenced by the		basic foodstuffs was not
price freeze and the online price		affected by price freeze and
monitoring system.		online price monitoring
		systems.
For the students in the study,	Partial	For the students in the study,
awareness of the government	acceptance	gender and who pays the cost
measures used is significantly		of living significantly
influenced by gender, place of		influenced the awareness of
residence and who pays for the		the government measures
cost of living.		used.
The students in the study typically	Rejection	The students in the study do
use the online price monitoring		not typically use the online
system, and satisfaction with the		price monitoring system, and
system is influenced by gender,		satisfaction with the system is
place of residence, whether the		influenced by whether the
student lives apart from their		student lives in the capital or
parents, and who pays their living		in the countryside.
costs.		

A conscious consumer is characterised by several qualities. Among others, consumers who are well informed, know their consumer rights and can assert them can be considered as knowledgeable (Kotler-Keller, 2013). However, many factors can influence a good purchasing decision (Andreyeva et al., 2010; Stone et al. 2024).

Recently, several factors have played a role in Hungary that have had a significant impact on consumers' consumption decisions. One such factor was food price inflation, which was triggered by international, domestic structural and cyclical factors. Without being exhaustive, such factors included, for example, global increases in crop prices, increases in energy prices, the energy intensity of the Hungarian market, exchange rate fluctuations, competitiveness gaps, etc. In the author's study, too, students cited rising food production costs, uncertain international economic relations and scarce energy supplies as the main reasons for the situation.

Inflation in Hungary has been higher than the European average for two years, with prices being 30% higher than two years earlier from November 2022 until the end of 2023 (KSH, 2023). It is no coincidence that this situation, for a conscious shopper, induces a constant rethinking of purchasing decisions. During inflationary periods, consumers switch to cheaper products and do not buy items they do not consider indispensable. This was also the case in Hungary. That is, customers, under the impact of inflation, choose cheaper products and buy from retailers where they can find discounted prices (IPSOS, 2022). At the same time, Sikos et al. (2022) stress in their study that the business success of enterprises today also depends on the extent to which retailers can adapt quickly and efficiently to market and non-market changes, including the challenges induced by inflation. In other words, whether they can move quickly ahead of their competitors, even in terms of action, whether they can develop innovative and digital solutions to reduce their production and logistics costs (Csekő, 2018), and whether they can manage and compensate for the negative effects of mandatory government measures (price freezes, mandatory action) in the long term.

The study conducted by the author also shows that the basic food purchasing habits of the university students surveyed in the study were negatively affected by inflation, and they either bought unchanged or fewer quantities of the indicated basic food items.

Molnár-Hajdú's (2023) study did not only cover staple foods when they looked at the impact of inflation on consumption. In the sample they analysed, they found a decrease in the frequency of purchases of vegetables/fruit, dairy products and bakery products. No significant shifts were identified for meats and alcoholic beverages, but they were found for sweets and desserts. Durable foodstuffs, and clothing in particular, tend to be hoarded and therefore less frequently purchased. This phenomenon was also confirmed during this period when purchasing these goods.

However, analysts are divided on the impact of government measures to curb inflation. The MNB's (Hungarian National Bank) 2024 study, The Factors Behind Domestic Food Inflation argues that price caps have not been effective in containing food inflation, as their market-distorting effects became evident during their period of enforcement, leading to a widening gap between domestic and regional food inflation. Moreover, companies sought to offset losses incurred on products subject to price freezes by increasing prices on other goods to recover lost revenues. In contrast, government measures aimed at enhancing competition among firms, such as the introduction of a price monitoring system, have contributed to a reduction in domestic food inflation. The author was also curious to know how successful the students she interviewed consider government measures to tackle inflation to be. On a Likert scale of one to five, respondents rated one as not at all successful and five as a complete success. Overall, measures to curb inflation were judged to be effective by 17% of respondents. The price freeze scheme was perceived by one in seven students, while the

online price monitor and compulsory sales promotion were perceived by one in five as good tools to achieve their objectives. It can be said, therefore, that student opinions on success and effectiveness were very mixed in the sample studied.

Conclusions

Current research has shown that inflation also influences students' consumption habits, as they tend to purchase less or approximately the same amount of basic foodstuffs in Hungary as before. These results are in several respects consistent with the findings of earlier and parallel studies on the topic, which were discussed in the previous section. Although students are aware of, or have heard about, government measures aimed at curbing inflation, they do not yet use, or only rarely use, the newly introduced online price monitoring system. Young people's opinions remain divided regarding the effectiveness of these governmental actions. However, this finding should be treated with caution, as many respondents had not yet experienced the system first-hand at the time of the survey. A follow-up questionnaire will therefore be distributed to assess how these measures may have influenced students' views now that their actual impact on reducing price inflation is becoming more evident. Furthermore, the next stage of the research will aim to include students with little or no background in economics, allowing for an analysis of their attitudes and experiences in comparison with those of students specializing in economics.

References

- Andreyeva T., Long M., Brownell K. (2010), The impact of food prices on consumption: A systematic review of research on the price elasticity of demand for food, *American Journal of Publich Health*, pp. 216-222, https://doi.org/10.2105/AJPH.2008.151415
- Balatoni A. (2022), Price caps and inflation: what does the past say and what does the present show? In: *Blog of the Analysts of the Magyar Nemzeti Ban*k, Available at: https://www.vg.hu/mnb-blog/2022/12/arsapkak-es-inflacio-mit-uzen-a-mult-es-mit-mutat-a-jelen
- Buglyó-Nyakas E., Gál T. (2023), Examining consumption and purchasing patterns of foods perceived as healthy, with a focus on price, *Nutrition Marketing*, 2, pp. 3-14, https://doi.org/10.20494/TM/10/2/1
- Boone H.N., Boone D.A. (2012), Analyzing Likert Data, *Journal of Extension*, 50(2), 48, https://doi.org/10.34068/joe.50.02.48
- Cappelli A., Cini E. (2020), Will the COVID-19 pandemic make us reconsider the relevance of short food supply chains and local productions? *Trends in Food Science & Technology*, 99, pp. 566-567, https://doi.org/10.1016/j.tifs.2020.03.041
- Carifio J., Perla R.J. (2007), Ten common misunderstandings, misconceptions, persistent myths and urban legends about Likert scales and Likert response formats and their antidotes, *Journal of Social Sciences*, 3(3), pp. 106-116, https://doi.org/10.3844/jssp.2007.106.116
- Csekő K. (2018), Digital business models, In: L. Csonka, K. Csekő (Eds.), *Digitalization and Innovation Impacts on International Transactions and Logistics Budapest*, pp. 21-31, Hungary, Budapest University of Economics.
- Cullen M. (2020), COVID-19 and the risk to food supply chains: How to respond? *Food and Agricultural Organization Technical Paper*, Available at: http://www.fao.org/3/ca8388en/CA8388EN.pdf
- IPSOS. (2022), *How inflation is changing consumer behaviour*, Available at: https://www.ipsos.com/en-us/knowledge/consumer-shopper/how-inflation-is-changing-consumer-behavior

---- Economics and Management----

- Joshi A., Kale S., Chandel S., Pal D. (2015), Likert scale: Explored and explained, *British Journal of Applied Science & Technology*, 7 pp. 396-403, https://doi.org/10.9734/BJAST/2015/14975
- Kotler P., Keller K. L. (2013), Marketing Management (14th ed.), Pearson Education.
- Kovács I., Lendvai M., Beke J. (2022), The importance of food attributes and motivational factors for purchasing local food products: Segmentation of young local food consumers in Hungary, Sustainability, 14(6), 3224, https://doi.org/10.3390/su14063224
- KSH. (2023), *Hungarian Central Statistical Office*, Available at: https://www.ksh.hu/gyorstajekoztatok#/hu/home
- Molnár L., Hajdú N. (2023), Changes in consumers' food purchasing behaviour under the impact of inflation, *Marketingkaleidoscope*, 2023, pp. 134-150.
- MNB. (2023), Available at: https://www.mnb.hu/letoltes/mnb-melyelemzes-a-hazai-elelmiszerinflacio-mogott-meghuzodo-tenyezok.pdf
- NAK. (2019), Factors influencing food purchases, available at: https://www.researchgate.net/publication/338293665_elelmiszer-valasztast befolyasolo tenyezok 2019.
- Power M., Doherty B., Pybus K., Pickett K. (2020), How Covid-19 has exposed inequalities in the UK food system: The case of UK food and poverty, *Emerald Open Research*, 2(11), 11, https://doi.org/10.1108/EOR-10-2023-0003
- Sajtos L., Mitev A. (2007), SPSS Research and Data Analysis Manual, Alinea Publishers.
- Sikos T.T., Papp V., Kovács A. (2021), Changes in domestic consumer behaviour during the first wave of the COVID-19 epidemic, *Regional Statistics*, 61(2), pp. 135-152, https://doi.org/10.15196/TS610201
- Stone A., Brown A., Douglas F., Green M, Hunter E., Lonnie M., Johnstone M., Charlotte A., FIO. (2024), The impact of the cost of living crisis and food insecurity on food purchasing behaviours and food preparation practices in people living with obesity, *Appetite*, 2024, Available at: https://osf.io/preprints/osf/pikhd v1
- Tambassur A., Jabim A. (2020), Factors affecting the consumers' willingness to pay for health and wellness food products, *Journal of Agriculture and Food Research*, Available at: https://doi.org/10.1016/j.jafr.2020.100076
- Tileva T. (2023), Consumer behaviour during times of inflation and how to save, Available at: https://kogod.american.edu/news/consumer-behavior-during-times-of-inflation-and-how-to-save

Cite:

UFJ Style

Juhasz T. (2025), Basic food purchasing habits of young people in dimension of price inflation, *Ukrainian Food Journal*, 14(3), pp. 507–520, https://doi.org/10.24263/2304-974X-2025-14-10

APA Style

Juhasz, T. (2025). Basic food purchasing habits of young people in dimension of price inflation. *Ukrainian Food Journal*, 14(3), 507–520. https://doi.org/10.24263/2304-974X-2025-14-3-10

Biotechnology approaches and improvement strategies in biocement production

Viktor Stabnikov¹, Iryna Kovshar¹, Dmytro Stabnikov^{1,2}

- 1 National University of Food Technologies, Kyiv, Ukraine
- 2 University of Wroclaw, Poland

____Abstra

Keywords:

Biocement Biological agent Plant urease Biosafety Intensification Ecology

Article history:

Received 23.04.2025 Received in revised form 1.06.2025 Accepted 30.09.2025

Corresponding author:

Viktor Stabnikov E-mail: vstabnikov1@ gmail.com

DOI: 10.24263/2304-974X-2025-14-3-11

Abstract

Introduction. This review summarizes existing research focused on overcoming the key limitations of the biocementation process.

Materials and methods. Biocement was used as a main key term in combination with terms related to its production and applications.

Results and discussion. Among environmentally friendly building materials, biocement is of special importance as an alternative to traditional cement, since it possesses valuable properties, its production does not require significant energy consumption, and it helps reduce the environmental burden by lowering carbon dioxide emissions. The precipitation of calcite due to the activity of urease producing bacteria (UPB) can be used to improve the geotechnical properties of soils and to restore concrete structures.

Obstacles to the large-scale use of biocement include its relatively high cost and the release of ammonia and ammonium during the biocementation process, the levels of which in the environment are strictly regulated.

Biocement production requires a calcium source, urea, and the enzyme urease to enable calcite precipitation. Bacteria adhere to soil particles, adsorb Ca²⁺, and act as nucleation sites, improving soil strength and concrete repair. Safety can be enhanced by using biosafe or inactivated cels of microbial urease producers, applying plant urease, or alternative bioagents such as microalgae or cyanobacteria. Costs may be reduced by applying industrial wastes and replacing expensive chemicals.

Several methods help reduce ammonium and ammonia emissions during biocementation, such as replacing CaCl₂ with calcium acetate, adding zeolite to adsorb ammonium, or using electrobiocementation with graphite electrodes. Other approaches include cation-enriched injections, ammonium recovery as struvite, and modified nutrient solutions that both strengthen soil and cut ammonia release. Additionally, captured ammonia can be adsorbed with sulfuric acid. A promising eco-friendly alternative is calcium phosphate-based biocementation.

Conclusions. Using industrial waste, plant-based urease, and safer or inactivated microorganisms can reduce costs and enhance the biosafety of biocementation.

Introduction

Concrete is the most widely used man-made material on Earth, but it is also among the most energy-intensive. In 2022, carbon dioxide emissions from cement manufacturing totaled 1.6 billion metric tons (Statista, 2023), and global emissions are projected to reach 2.34 billion metric tons of CO₂ by 2050. Meanwhile, the release of greenhouse gases into the atmosphere contributes to global warming, and climate change is recognized as one of the most urgent global challenges.

In recent years, the use of microorganisms for the production of building materials, a new direction in biotechnology, has been developing rapidly (Achal and Chin, 2021; Ivanov and Stabnikov, 2023). Among these innovations, biocement production holds a special place. The advantages of biocementation include not only the low viscosity and high permeability of biocement into concrete or soil, but also it's relatively low cost and energy consumption, along with a significant reduction in greenhouse gas emissions compared to conventional cement production.

To produce biocement, at least three components are required: (1) a source of soluble calcium, (2) a compound such as urea that alters the pH to facilitate calcium carbonate precipitation and supplies CO₂ for carbonation, and (3) microbial cells with urease activity or the urease enzyme that catalyze urea hydrolysis. The most widely used biocementation process is known as microbially induced calcite precipitation (MICP). The enzymes urease (EC 3.5.1.5) and carbonic anhydrase (EC 4.2.1.1) play crucial roles in this process:

$$(NH_2)_2CO + 2 H_2O (+ urease) \rightarrow CO_2 + 2 NH_4^+ + 2 OH^ CO_2 + H_2O (+ carbonic anhydrase) \leftrightarrow H_2CO_3 \leftrightarrow H^+ + HCO_3^- \leftrightarrow 2 H^+ + CO_3^2$$
 $CaCl_2 + (NH_2)_2CO + 2 H_2O + (+ urease + carbonic anhydrase) \rightarrow CaCO_3 \downarrow + 2 NH_4Cl_2$

Bacterial cells adhere to soil particles, and since bacterial cells have a negative surface charge, they can easily adsorb Ca²⁺ cations and serve as nucleation sites for crystallization. The precipitation of calcite due to the activity of urease producing bacteria (UPB) can be used to improve the geotechnical properties of soils and to restore concrete structures (DeJong et al., 2013; De Muynck et al., 2010; Ivanov and Chu, 2008; Van Paassen et al., 2010; Wang Z. et al., 2017).

However, the production of biocement obtained by MICP has certain drawbacks that limit its widespread practical application. These include economic challenges, such as high production costs, and ecological concerns, mainly the introduction of a large number of live bacterial cells into the environmen and, the release of toxic ammonia into the atmosphere, as well as ammonium ions into ground and surface waters when MICP is used for soil stabilization (Ivanov et al., 2019a, b) (Figure 1).



Figure 1. Main obstacles for large-scale biocement application: biosafety concerns, high cost, and ammonia emissions

To improve biocement production technology and make its manufacturing and application safer and more cost-effective, two main directions are being pursued, focusing on its key components: (a) the source of urease and (b) the source of calcium ions. This review is devoted to analyzing the research conducted in these areas.

Materials and methods

The literature search was performed using the Scopus, Web of Science and Google Scholar databases. Biocement was used as a main key term in combination with terms related to its production and applications, such as microbial urease producers, biological agents, biosafety, replacement of chemicals, intensification, cost, ecology, ammonia release, and others. Full texts of relevant articles were obtained for further evaluation. Additional publications were identified by examining the reference lists of relevant journal publications and review articles.

Results and discussion

Ways to increase the safety and reduce the cost of the microbial component of biocement

Selection of microbial urease producer

Microbial urease is a high-molecular-weight, nickel-containing multi-subunit enzyme that hydrolyzes urea to ammonia and carbon dioxide, resulting in an increase in pH. Urease-producing bacteria used for biocementation must be active in geotechnical environments characterized by high salt concentrations and alkaline pH levels. Therefore, halophilic or halotolerant and alkaliphilic UPB are preferred for biomement production. For effective biocementation, microbial urease must function at inorganic salt (CaCl₂) concentrations of 1.0–1.5 M and at pH values above 8.5.

Constitutive synthesis of urease is a common property of many strains of soil bacteria. Urease-producing bacteria are widely distributed in soils, especially in areas where urea is constantly present either as a product of nitrogen metabolism in mammals or because of the use of ammonium-containing fertilizers in agriculture. The possibility of strengthening soil by activating indigenous urease-producing bacteria through the addition of nutrients and forced aeration has been demonstrated (Burbank et al., 2012). The addition of molasses or yeast extract to coastal sand from a semi-arid environment to activate native URB, resulting in a change in the composition of the natural microbial population, its enrichment with representatives of the genus *Bacillus*, and a significant increase in urease activity (Gat et al., 2016). Strengthening the soil by activating of URB present in it was also used in the works (Gomes et al., 2018; Rajasekar et al., 2017). However, the use of artificially activated natural microflora with urease activity may be limited by several factors: (1) a low concentration of UPB in deep soil layers and their absence in mountains breeds; (2) negligible urease activity at high salt concentrations or at pH levels above 8.5; (3) potential pathogenicity; and (4) unpredictable and unstable bioactivity during the MICP process.

To carry out MICP, the use of mixed or enrichment bacterial cultures has been proposed (Al-Thawadi, 2012; Hammes et al., 2003). For example, the use of a mixed culture of ureolytic and non-ureolytic bacteria increased the efficiency of CaCO₃ precipitation, possibly due to the formation of additional crystallization centers facilitated by the adhesion of non-ureolytic bacteria (Gat et al., 2014). In addition, the cost of biocement production can be

reduced by using an enrichment microbial culture with urease activity instead of a pure culture of URB. The fact that bacterial strains used for biocementation or soil strengthening are alkaliphilic and halotolerant makes them highly competitive, enabling their cultivation in batch or even continuous processes under non-sterile conditions (Cheng and Cord-Ruwisch, 2013). However, along with UPB, undesirable microorganisms, including opportunistic pathogens, may also develop. Some studies propose using activated sludge from wastewater treatment plants (WWTP) for biocementation. This sludge can be artificially enriched with UPB through non-sterile cultivation at an initial pH of 10.0, with the addition of ammonium chloride (5 g/l) and urea (10 g/l) to the nutrient medium (Yang et al., 2020). Using this method, the cost of UPB biomass can be reduced by up to 30%; however, biosafety concerns are not addressed. Therefore, the use of pure cultures of UPB with well-characterized properties may offer a safer alternative for implementing MICP than the use of activated indigenous urease-producing bacteria or enrichment cultures.

To ensure safety in biotechnologies involving the release of microorganisms into the environment, it is preferable to work with bioagents classified as Risk Group 1 (RG1) under the European Union Directive 2000/54/EC, which includes microorganisms that do not potentially cause diseases in humans and animals. Strains of Sporosarcina pasteurii, which belong to Risk Group 1 microorganisms, are among the most widely used URB recommended for biocementation, especially the strain S. pasteurii ATCC 11859, which has been commonly employed in MICP research (Eryürük et al., 2015; Mortensen and DeJong, 2011; Whiffin and van Paassen, 2007). In addition, many biocementation studies utilize the strain Bacillus sp.VS1 (Chu et al., 2012; Stabnikov et al., 2016), whose 16S rRNA gene sequence shares 99% identity with Bacillus pasteurii, a species also classified within Risk Group 1 (Figure 2c1).

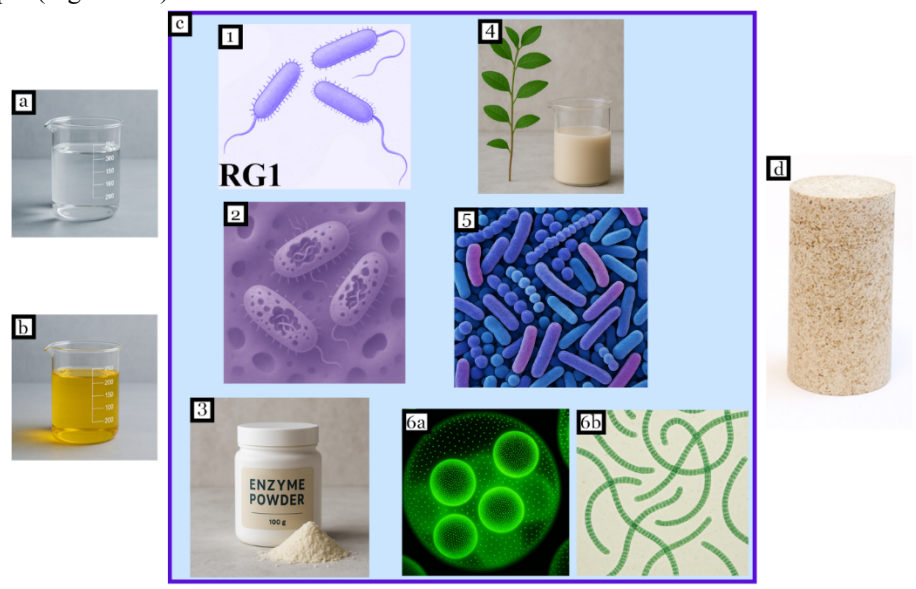


Figure 2. Biosafety of biocementation:

- (a) calcium ion solution; (b) urea solution; (c) safe sources of urease: (1) bacteria belonging to Risk group1; (2) inactivated bacterial cells; (3) pure enzyme; (4) extract of plant material with urease activity; (5) lactic acid bacteria;
- (6) photosynthetic microorganisms microalgae (6a) and cyanobacteria (6b); (d) biocement

Currently, many studies on biocementation have used strains from the genus *Lysinibacillus*, Gram-positive, rod-shaped, motile, endospore-forming bacilli belonging to RG1 group and isolated from soil (Chen M., 2021; Ekprasert et al., 2020; Gowthaman et al., 2019; Leeprasert et al., 2022; Sreekala et al., 2024; Vashisht et al., 2018), or industrial sources (Han et al., 2014; Jeong et al., 2017). Additionally, strains *Bacillus megaterium* (Andalib et al., 2016; Sun et al., 2019; Wani et al., 2024) and *Cytobacillus horneckiae* (Moqsud and Gochi, 2024), both classified within RG1, have also been successfully applied in biocementation research.

However, many halotolerant and alkaliphilic bacterial strains having significant urease activity belong to opportunistic and even pathogenic species. Numerous studies have proposed the use of urease-producing bacteria classified as RG2 group, which may cause disease in humans, for biocementation. Examples include opportunistic pathogens such as *Bacillus cereus* (Brasileiro et al., 2020), *Bacillus mycoides* (Elmanama, and Alhour, 2013), *Proteus* sp. (Khanafari et al., 2011), *Staphylococcus aureus, Klebsiella pneumoniae* (Varalakshmi and Devi, 2014), and even the pathogen *Helicobacter pylori* (Dosier, 2014) as potential biological agents for biocementation.

Non-pathogenic microbial urease producers can be isolated from extreme environments considered unfavorable for microbial growth, such as speleothems from limestone caves (Garcia et al., 2016; Omoregie et al., 2018), calcareous soil (Dhami et al., 2013) or highly alkaline cement samples (Achal et al., 2010). Meanwhile, active UPB isolated from activated sludge from WWTP have also been proposed for biocementation (Al-Thawadi, 2012; Varalakshmi and Devi, 2014; Xu G. et al., 2017), although the risk of isolating opportunistic bacteria remains high. Recently, research has focused on using mutant strains of UPB for biocementation, including mutants of *Sporosarcina pasteurii* ATCC 11859 (Han et al., 2021) and strains from the genus *Bacillus* (Li H. et al., 2014; Tayyem et al., 2021).

There is an opinion that all bacteria on Earth are natural, so transferring them to new habitats will not cause environmental changes or risks (Fritzges, 2005). However, it has been shown that it is impossible to predict the behavior of bacterial populations introduced into soil, so generalizations are unwarranted. Instead, each case requires a specific analysis of the introduction pattern and potential risks (Almajed et al., 2019). Given these biorisk concerns, the selection of bacteria for use in MICP must be grounded in a thorough biosafety analysis.

To ensure biological safety when introducing large quantities of foreign microbial cultures into soil, inactivation of bacterial cells can be employed, if the cells retain their functional activity (Fig. 2c2). For example, the use of UPB *Yaniella* sp. cells, inactivated by soaking in a 0.5% (w/v) sodium dodecyl sulfate solution, was demonstrated for constructing a model aquaculture pond through biocementation (Stabnikov et al., 2016). Some studies have explored the direct use of urease enzyme (Fig. 2c3) for repairing cracks in building materials (De Muynck et al., 2010) or for biogrouting (Almajed et al., 2019; Neupane et al., 2015). However, the high cost of urease remains a major obstacle to its practical application. Therefore, reducing the cost of urease is crucial for its practical application in biocementation (Khodadadi Tirkolaei et al., 2017).

Summarizing the above, it can be concluded that urease-producing bacteria are the basis of the biocementation process. These bacteria should be harmless to humans and the environment; capable of forming aggregates and adhering effectively to treated surfaces; tolerant to high salt concentrations, as they need to remain active in saline environments; and able to synthesize urease that functions efficiently in alkaline conditions (pH 8.5–9.2) (Stabnikov et al., 2013).

Reducing the cost for microbial urease producer

Obtaining biomass of URB includes the preparation of an expensive nutrient medium, sterile cultivation, biomass separation, and, in the case of storage, freeze-drying to preserve bacterial cell viability. To reduce the cost of the nutrient medium for growing bacteria, it is proposed to use various wastes, including activated sludge hydrolysates (Whiffin 2004; Stabnikov, 2016), liquid dairy waste, lactose-containing mother syrup (Achal et al., 2009), whey from cheese production (Chaparro et al., 2021), whey powder (Kahani et al., 2020), enzymatically hydrolyzed kitchen waste (Meng et al., 2021), effluent from biogas production using chicken manure (Yoosathaporn et al., 2016), and cheap soybean flour instead of yeast extract. The use of urine sterilized with ultraviolet light as a component of the medium for URB cultivation has been reported (Yang et al., 2022).

Plant urease instead of microbial enzyme for biocementation

Plants for urease production

In biocementation, bacterial urease can be replaced by plant urease (Fig. 2c4) (Dilrukshi et al., 2015; Ivanov et al., 2019a). Urease is found in the leaves, stems, and roots of many higher plants, allowing them to use urea as a nitrogen source. It is present in relatively high amounts in the seeds of beans, melons, and pumpkins (Das et al., 2002). The production of urease from jack beans (*Canavalia ensiformis* and *Canavalia adans*) was patented by Kakimoto and coauthors (1992). Each plant-derived urease has its own optimal conditions for catalytic activity. For example, urease from chickpea seeds shows maximum activity at a temperature of 48°C and pH 7.2 (Pervin et al., 2013), while urease from pea seeds is most active at 40°C and pH 7.5 (EL-Hefnawy et al., 2014), urease from mulberry leaves at 30°C and pH around 9.0 (Hirayama, 2000), and urease from dehusked seeds of pigeonpea had an optimum pH of 7.3, with activity over a pH range of 5.0 to 8.5 (Das et al., 2002).

It is preferable to use local plant materials or food processing waste to obtain extracts for subsequent applications in biocementation. Thus, the application of extracts from watermelon seeds (Al Imran et al., 2021; Dilrukshi et al., 2018), cabbage, wheat, or soybean leaves, and soybean pulp (Baiq et al., 2020; Hogan et al., 1983) has been shown. The technique for extracting urease from plant raw materials is extremely simple and allows one to easily obtain a solution with urease activity for its later use in the biocementation process. The plant raw material is cleaned, washed, and crushed. An extractant, which is most often distilled, deionized or tap water (Al Imran et al., 2021; Cui et al., 2023; Dilrukshi et al., 2018; Stabnikov et al., 2022), but sometimes it is 20 mM phosphate buffer (Park et al., 2014), 20 mM phosphate buffer containing 2 mM ethylenediaminetetraacetic acid Tirkolaei et al., 2020), 0.025 M Tris-acetate containing 50 μg/ml leupeptin (Das et al., 2022) or chilled 50 mM phosphate buffer containing 10 mM β-mercaptoethanol (Hamzah, 2014), is added to the crushed raw material. Chemicals such as 20-30% (v/v) ethanol solution (Lai et al., 2023; Weng et al., 2024) or 20% chilled acetone (EL-Hefnawy et al., 2014; Pervin et al., 2013) are also used as extractants to obtain crude urease extracts. The ratio of raw material to extractant varies across different studies, more commonly being 1:3, but sometimes 1:4, 1:10 or even 1:20 (Table 1).

Table 1 Urease activity of crude extracts from various plant sources

Extract from	Plant, g, to extractant,	Urease activity	Units	Reference
	ml	activity		
Germinated chickpea	1:4	0.011	mM	Pervin et al.,
(Cicer arietinum) seeds			NH ₃ /min·mg	2013
777	1.00	0.04	protein	
Watermelon (Citrullus	1:20	0.01	mM	Al Imran et al.,
lanatus) seeds	1:20	0.00	NH ₃ /min·ml	2021
Watermelon (C.	1:20	0.08	mM NH ₃ /min·g	Dilrukshi et
lanatus) seeds Dehusked watermelon	1:4	0.01	mM	al., 2018 Khodadadi
(C. lanatus) seeds	1:4	0.01	NH ₃ /min·mg of	Tirkolaei et al.,
Dehusked jack bean	1:4	0.03	protein	2020
(Canavalia enformis)	1.7	0.03	protein	2020
Jack bean (Canavalia	1:4	0.024	1	
enformis) meal	1	0.021		
Soybeans (Glycine	1:4	0.004	1	
max)				
Germinated soybean	1:20	0.70	mM urea/min·g	Stabnikov et
(Glycine max)				al., 2022
Soybean	1:10	3.90	mM urea/min·l	Weng et al., 2024
Soybean	n/a	0.14	mM urea /min·g	Gao et al.,
Soyocan	11/ 4	0.14	inivi di ca / inini g	2020
Mulberry (Morus alba)	1:3	0.076	nkat/mg protein	Hirayama et
leaves				al., 2000
Sword bean (Canavalia	n/a	0.70	mM urea/min·g	Liu L. et al.,
gladiata)				2024
Germinated pea (Pisum	1:4	0.46	mM	EL-Hefnawy
sativum) seeds			NH ₃ /min·mg	et al., 2014
D 1 1 /IV:	1:3	0.02	protein	Bedan 2020
Broad beans (Vicia faba)	1:3	0.03	mM	Bedan 2020
Dehusked pigeonpea	n/a	0.032	NH ₃ /min·ml mM NH ₃ /	Das et al., 2002
(Cajanus cajan) seeds	11/ a	0.032	min·mg protein	Das et al., 2002
Syrian mesquite	1:2	0.125	mM NH ₃ /min	Hamzah 2014
(Prosopis farcta) seeds	1.2	0.123	mM	1141112411 2017
(ocopio jan eta) seeds		0.007	NH ₃ /min·mg	
			protein	
Indian sweet-clover	1:2	0.015	mM NH ₃ /min	Hamzah 2014
(Melilotus indicus)		0.007	mM	
seeds			NH ₃ /min·mg	
			protein	

Note: n.a. – not applicable.

The extraction time and temperature vary across different studies. The resulting suspension is filtrated, and the filtrate is then centrifuged to remove suspended pulp. The solution with urease activity is referred to as the crude extract, which is often used for biocementation. Sometimes, the crude urease is further purified by the precipitation using acetone, ethanol, or ammonium sulphate (Bedan, 2020; EL-Hefnawy et al., 2014; Hirayama et al., 2000). For example, 50 g of dehusked watermelon seeds were soaked in 200 ml of an extractant at pH 7.5 for 12 h at 4°C. The mixture was then homogenized to disrupt plant cells for urease extraction, followed by filtration and centrifugation. The crude extract obtained was used to isolate purified enzyme via a two-step acetone precipitation. However, the highest strength was observed for sand treated with the crude urease rather than with urease with a higher degree of purification (Khodadadi Tirkolaei et al., 2020). Urease activity of some crude extracts from different plants is shown in Table 1.

The efficiency of extraction is influenced by the particle size of the plant material. It was shown that extract from soybean powder with particle sizes of 0.075-0.25 mm exhibited urease activity of 4.92 mM urea/min, whereas larger particles (1-2 mm) showed significantly lower activity, 2.95 mM urea/min (Shu et al., 2022). The enzymatic activity of the crude extract also depends on the concentration of plant powder used for extraction. Thus, extracts prepared from soybean powder at concentrations of 20, 40, 60, and 80 g/l exhibited urease activities of 2.15, 4.86, 6.62, and 8.17 mM urea/min, respectively (Shu et al., 2022). It is well known that during seed germination, metabolic processes are intensified due to the activation of enzymes (Guzman-Ortiz et al., 2019; Nkhata et al., 2018; Stabnikova et al., 2019; Wunthunyarat et al., 2020). In some studies, the authors carry out preliminary seed germination to enhance enzymatic activity prior to obtaining urease-containing extracts (EL-Hefnawy et al., 2014). The specific urease activity of soybean seeds reached a peak at 24 hour of germination, 0.24 mM/g·min, and then gradually declined, decreasing by 45% at 96 hours of germination (Stabnikov et al., 2022). The highest urease activity of the extract from germinated peas was observed at 192 hours of germination, 0.03 mM/ml, followed by a subsequent decrease (Pervin et al., 2013). Notably, the sprouts of germinated seeds from beans, soy, watermelon, and melon exhibited 23.3–34.5% lower urease activity compared to the seeds themselves (Stabnikov et al., 2022).

Application of plant extracts with urease activity for biocementation

The use of plant extracts with urease activity offers a sustainable and environmentally friendly alternative for various biogeotechnical applications, including soil improvement, mitigation of earthquake-induced liquefaction, and coastal erosion protection. Until recently, most studies have relied on commercially available urease with high enzymatic activity derived from jack beans. However, the successful use of ureases extracted from various plant sources for biocementation and soil biogrouting has been demonstrated. These plant-derived enzymes have proven their effectiveness, but their cost was significantly lower. Some examples of plant urease application in biocementation are given in Table 2.

Although the urease activity of plant extracts is generally lower than that of urease-producing bacteria commonly used in biocementation processes, their use is still advisanle for soil bio-strengthening and the mitigation of wind and dust erosion, as surface treatment of soil with small doses of biocement is effective in controlling wind and water erosion and significantly reduces the release of dust, bacterial contaminants, and chemical pollutants into the environment (Hao et al., 2021; Ivanov and Stabnikov, 2020; Namdar-Khojasteh et al., 2022; Stabnikov et al., 2013b). Moreover, it is believed that high urease activity is not necessary during biocementation, since the process of calcium carbonate crystal formation should proceed slowly, consistently filling the pores and cavities in the cemented material.

Table 2 Application of plant urease for biocementation

Source of	Characte	Reference	
urease and its activity	biocementation process	biocemented oil	
Crude soybean urease solution, 3.9 mM/l·min	Silica sand with a grain size of 0.425-0.6 mm; calcium chloride and urea 1M:1M; initial pH 7.5; 8 treatments	Permeability decreased from 10 ⁻³ m/s to 10 ⁻⁵ m/s, UCS 1680 kPa	Weng et al., 2024
Crude soybean extract, 0.7 mM urea/g·min	Screened river sand with a grain size of 0.0-0.6 mm (93%); calcium chloride and urea 1M:1M; 8 treatments	Permeability decreased from 6·10 ⁻⁴ m/s to 1·10 ⁻⁶ m/s	Stabnikov et al., 2022
Crude soybean extract, 6.5 mM/min	Soil prepared containing 10% clay particles (<0.005 mm), 50% silt particles (0.005–0.075 mm), and 40% sand particles (>0.075 mm); solution (calcium chloride and urea 0.5M:0.5M); 15 treatments	After 15 treatments, the soil at 100 kPa effective confining pressure had peak deviatoric stresses in the triaxial tests 250.0 kPa; for untreated soil it was 120.8 kPa	Gao et al., 2020
Jack bean extract	Sieved river sand with a grain size of 0.25- 0.075 mm, solution (CaCl ₂ and urea), 3 days of treatment	UCS of the treated sand was 317 kPa; content of precipitated calcite 6.58%	Park et al., 2014
Watermelon seed extract, 3.9 µmol urea hydrolyzed/ min	Mikawa sand with mean diameter 0.87 mm, 0.7 M calcium chloride and 0.7 M urea, 14 treatments	UCS of the treated sand was 3.0 MPa	Dilrukshi et al., 2018
Soybean extract, 13 mM/min	Sand with average particle size 0.76 mm, 1.0 M calcium chloride and 1.0 urea, 30 °C for 7 days	UCS of the treated sand was 18.5 kPa	Cui et al., 2023
Crude soybean extract, 6.62 mM urea/min	Ottawa sand with a mean size of 0.36 mm, 0.5 M urea and 0.5 M CaCl ₂ , 8 treatments at 25°C	UCS of the treated sand was 4 MPa, CaCO ₃ content 8%	Shu et al., 2022
Watermelon seed extract	Mikawa sand with a mean diameter 0.87 mm, solution (CaCl ₂ and urea)	UCS about 1.2 MPa	Al Imran et al., 2021

Note: UCS, unconfined compressive strength.

However, it has been shown that the efficiency of plant urease in producing CaCO₃ is comparable to that of bacterial urease (Cui et al., 2024). Comparison of properties of sand treated with UPB and plant urease demonstrated that, for the same amount of precipitated calcium carbonate, samples treated with plant urease exhibited higher unconfined compressive strength (Ahenkorah et al., 2020; Almajed et al., 2018). Additionally, sand treated via enzyme-induced calcium precipitation (EICP) displayed also significantly greater splitting tensile strength compared to sand with similar average CaCO₃ content treated by MICP (Ahenkorah et al., 2020).

For example, treatment using plant-derived urease and solutions of urea and calcium chloride with molar ratio of 1.5:1 was proposed to be used for mitigating fugitive dust emissions in semi-arid and arid environments (Hamdan and Kavazanjian, 2016). The successful application of jack bean and soybean ureases for surface stabilization of desert sands has also been demonstrated (Liu L. et al., 2024). Notebly, the cost of the proposed plant-based enzyme sources for biocementation was reported to be 380-1400 times lower than that of commercially available ureases.

Numerous studies have shown the effectiveness of plant-derived urease in the biocementation of desert sand through CaCO₃ precipitation to protect it against wind erosion, enhance surface strength, stabilize sloped soils prone to landslides, and combat desertification. In these studies, soybean urease was the most commonly used enzyme source (Gao et al., 2020; He et al., 2023; Liu Y. et al., 2023, 2024).

The application of mix–induced carbonate precipitation, which combines microbial and plant-derived ureases to carry out biocementation, has been investigated. Biocementation of sand foreshore slopes with a mixture of *Sporosarcina pasteurii* cell suspension and soybean powder extract proved to be more effective than using microbial and plant ureases separately (Sun et al., 2022).

The advantages of enzyme-induced calcium precipitation are undeniable: (a) there is no need to cultivate microbial producer, significantly simplifying the overall process; (b) crude extract can be prepared immediately prior to use; (c) the cost of biocementation is considerably reduced, as there is no requirement for nutrient media, electricity for aeration, or highly qualified personnel to produce microbial biomass with urease activity; (d) one of the important problems of biocementation is completely solved – no microbial cells are introduced into the environment, and the aqueous solution of homogenized plant biomass generally does not require additional biosafety assessments.

Thus, biocementation using plant-derived urease represents an environmentally friendly and sustainable approach for addressing a range of geotechnical challenges, including soil stabilization, mitigation of earthquake-induced soil liquefaction, erosion control, and dust suppression (Liu L. et al., 2022; Stabnikov et al., 2022). Additionally, EICP has been proposed for applications such as crack repair and enhancing the mechanical strength of construction materials (Nam et al., 2014; Roksana et al., 2023).

Increase of urease activity in plant materials

Several studies have investigated the influence of plant growth conditions on the urease activity in plant material. Given that urease is a nickel-containing enzyme, the effect of nickel supplementation in soil on soybean urease activity has been examined (Zhou et al., 2023). The addition of nickel to the soil contributed to an increase in urease activity in both the roots and shoots of soybeans (*Glycine max*). The introduction of NiO nanoparticles, nickel oxide (NiO), and nickel sulfate (NiSO₄), in the amount of 50 mg/kg of soil increased urease activity in both the shoots and roots of plants. It was also demonstrated that nickel supplementation

is essential when rice is cultivated in soil amended with urea-containing fertilizer, as it ensures sufficient urease activity in the plants (Gerenda et al., 1998).

The presence of urea in the soil helps to increase the activity of the plant ureolytic enzymes, which provide them with nitrogen through the decomposition of urea and the release of ammonia. This ammonia is then utilized in the synthesis of amino acids and, subsequently proteins (Ono et al., 2021). In a field experiment on soybean cultivation, addition of nitrogen-containing fertilizer to clay loam soil resulted in a significant increase in the urease activity of the harvested seeds (Achakzai et al., 2003).

Some approaches to improve biocementation process

Calcium sources and their effectiveness for biocementation

A comparative study on the application of calcium chloride, calcium acetate, and calcium nitrate in silica sand biocementation using crude soybean extract with urease activity of 3.9 mmol/l/min and the cementation solution containing 1 mol/l of calcium salt and urea revealed that CaCl₂ produced the best results, followed by calcium acetate CH₃(COO)₂Ca, while calcium nitrate was the least effective calcium source (Weng et al., 2024). For sand samples with the same calcium carbonate content of 15%, the unconfined compressive strength (UCS) was 1680 kPa for those treated with CaCl₂, while samples treated with calcium acetate exhibited a significantly lower UCS of approximately 1000 kPa. The authors attributed these differences to variations in the morphology of CaCO₃ crystals formed during precipitation, which depend on the type of calcium salt used.

However, Xiang et al. (2022), testing CaCl₂, (CH₃COO)₂Ca, and Ca(NO₃)₂ in MICP using *S. pasteurii*, concluded that the best source for biocementation is calcium acetate followed by calcium chloride and calcium nitrate. The application of calcium acetate made it possible to produce more CaCO₃, which contributed to an increase in the biocement compactness.

Application of additives to enhance biocementation

There are some studies aimed to enhance the biocementation process by incorporating various additives into the cementation solution. While this strategy benefits both microbial and plant-based urease systems, it is particularly critical for plant urease treatments, as the absence of microbial cells on sand grain surfaces reduces available nucleation sites for CaCO₃ precipitation and can diminish overall treatment efficacy (Ahenkorah et al., 2021; Miyake et al., 2022).

A biocementing solution containing $CaCl_2$, urea, plant urease was added with non-fat milk powder (Almajed et al., 2019). Silica sand was mixed with this solution, placed in an acrylic column, and left to cure at room temperature (20°C) for three days. The resulting samples then were washed, oven-dried at 40 °C to a constant weight, and subjected to unconfined compressive strength testing. The authors supposed that milk powder could stabilize the urease, and enhance the biocementation process by reducing the rate of calcium carbonate precipitation and providing additional nucleation sites for carbonate deposition. The addition of milk powder resulted in an increase of the maximum axial compressive stress (MACS) of sand from 138 ± 18 kPa to 1745 ± 83 kPa (Table 3).

Table 3 Application of additives to enhance biocementation

Source of urease	Characteristics of		Reference
and its activity	Biocementation process	Biocemented soil	
Commercial urease from jack bean, ≈3.5 mM of NH ₃ from urea/min·g Urease from jack bean (CAS 9002-	Ottawa silica sand, a mean grain size of 0.6 mm, non-fat powdered milk, 4 g/l, 1.0 M urea and 0.67 M CaCl ₂ (1:1), 2.5 g/L of urease enzyme Toyoura silica sand, a mean grain size of 0.17 mm, casein,	Increased sand strenght: MACS of sand increased from 138±18 kPa to 1745±83 kPa UCS increased to 3.58 MPa	Almajed et al., 2019 Miyake et al., 2022
Bacillus sp. MTCC 4445	64.28 g/l, 0.893 M urea and 0.581 M CaCl ₂ , 2.6 g/l urease enzyme Poorly graded silty sand, rice husk ash, 10%, 1.0 M urea and 1.0 M CaCl ₂	Reduced permiability by 22.5%	Sorum and Kalita, 2023
Pararhodobacter sp. SO1	Mikawa sand, mean diameter of 0.6 mm, particle density 2.66 g/cm ³ , 0.03% chitosan, 0.3 M urea and 0.3 M CaCl ₂ (1:1)	Increased sand strength up to 40%.	Nawarathna et al., 2020
Crude extract of soybean, ≈11 U/ml	Mikawa sand mean diameter of 0.87 mm, 0.2 – 8.0% eggshell powder, 0.5 mol/L CaCl ₂ and 0.5 mol/l urea (1:1)	Increased sand strength	Yan et al., 2024
Sporosarcina pasteurii ATCC 11859	Ottawa silica sand, the average particle diameter 0.54 mm, synthetic fibers 0.2-0.3% by weight of dry sand, 0.187 M CaCl ₂ and urea 0.187 M (1:1)	Increased the shear strength, ductility, and failure strain	Li M. et al., 2016
Bacillus sp., 3.7 mM/min	Ottawa silica sand, mean grain size of 0.73 mm, PVA fiber 0.8% by weight of sand, 0.3 M urea and 0.3 M CaCl ₂ (1:1)	Increased UCS by 138%, STS by 186%, decreased permeability by 126%, reduction in brittleness	Choi et al., 2016a
S. pasteurii ATCC 11859	Glass beads (diameter 0.05–3 mm), bentanite (5% w/w of beads), 0.5 M CaCl ₂ and 0.5 M urea (1:1)	Decreased hydraulic conductivity by 25%	Eryürük et al., 2015

Note: STS, splitting tensile strength; UCS, unconfined compressive strength.

It was shown that using casein instead of skim-milk in EICP allowed to receive biocemented sand with much higher compressive strength (Miyake et al., 2022). Under identical EICP conditions, the addition of 38.87 g/l of either milk powder or casein resulted in obtaining biocemented sand with a compressive strength of 1251 and 2439 kPa,

respectively. This improvement may be attributed to the binding of calcium ions to the phosphate and carboxyl groups of casein, leading to the formation of casein micelles, which play the role of centers for calcium carbonate nucleation (Li X. et al., 2019). The improved cohesion of sand has also been observed when casein micelles were incorporated in the MICP process (Nakano, 2024).

Positive effect of chitosan addition on the MICP initiated by *Pararhodobacter* sp. SO1was shown by (Nawarathna et al., 2020). Chitosan powder was first dissolved in 1% acetic acid, then the resulting 1% chitosan solution was neutralized to pH 6.8 using 0.1 M NaOH. Prepared solution was then added to the MICP process at a final concentration of 0.03% during the biocementation of sand. The presence of chitosan led to a higher amount of precipitate compared to the control, with the precipitate consisting of both CaCO₃ and chitosan hydrogel. As a result, the compressive strengths of cemented sand increased by up to 40% relative to sand treated without chitosan.

The addition of eggshell powder to sand treated with crude soybean extract increased the number of nucleation sites, resulting in enhanced strength of the biocemented sand compared to samples processed without the additive (Yan et al., 2024). Similarly, the incorporation of 0.25 wt.% of chitosan, a natural biodegradable linear polysaccharide derived from shrimp shells, into silica sand led to a slight improvement in the mechanical properties of the biocement after 28 days of curing (Baykara et al., 2024). It was found that the addition of fibers of different origin such as polypropylene monofilament fibers (Li M. et al., 2016), poly(vinyl alcohol) (PVA) fibers (Choi et al., 2016a), and basalt fibers (Xiao et al., 2019) increased the mechanical properties of biocemented sand (Table 3).

Positive effects on the properties of biocemented sand have been reported with the addition of various organic and biodegradable materials. These include wastepaper fibers addition to sand treated with *Lysinibacillus xylanilyticus* (Chen et al., 2021); glutinous rice powder, brown sugar, and skim milk powder in systems utilizing soybean urease (Yuan et al., 2020); and guar gum, xanthan gum, and polyol-cellulose hydrogel in treatments with jack bean urease (Hamdan et al., 2016).

Magnesium chloride has been shown to be one of the most effective additives for enhancing soil strength during EICP. The addition of 0.5 M Mg²⁺ to a solution of calcium chloride and urea resulted in biocemented sand with a maximum UCS of 6.2 MPa (Lv et al., 2022). Similar results were reported by Xu X. et al. (2020), who demonstrated that the presence of 0.01 M Mg²⁺ ions in a 0.5 M calcium acetate/urea solution enhanced the UCS of biocemented sand by 40%, while a higher Mg²⁺ concentration of 0.5 M led to a twofold improvement in strength. It was found that the presence of Mg²⁺ changes the crystal morphology of precipitates from calcite to Mg-calcite, vaterite, rosette and nesquehonite (Wang W. et al., 2024).

Cost reduction strategies for biocementation using industrial waste

One of the main chemical components used in traditional MICP biocementation is a soluble calcium salt, typically calcium chloride CaCl₂. However, its use as a chemical reagent contributes to the overall cost of the biocementation process. Moreover, while CaCl₂ is generally considered harmless to plants and soil, possible adverse effects have been noted as chloride ions increase the likelihood of corrosion of steel reinforcement (Wang Q. et al., 2024).

Thus, one approach to improving the biocementation process involves replacing calcium chloride with different calcium containing compounds. Currently, extensive research is focused on isdentifying suitable substitutes for calcium ion sources in biocementation (Yan

et al., 2025). Calcium acetate has attracted particular attention as a possible source of calcium in biocementation processes due to its ability to produce biocement with higher mechanical strength compared to that ontained using CaCl₂, while also reducing NH₃ emissions by 54.2% (Xiang et al., 2022; Zhang et al., 2014).

As possible replacer for CaCl₂, solution containing Ca²⁺ obtained by dissolving a limestone powder in acetic acid solution, a byproduct from the fast pyrolysis of lignocellulosic biomass, was proposed (Choi et al., 2017). The calcium ion was produced:

$$CaCO_3 + 2 CH_3COOH \rightarrow Ca^{2+} + 2 (CH_3COO^{-}) + CO_2 + H_2O$$

Solution used in biocementation of sand had calcium ion concentration 0.3 M, and pH, adjusted by solidum hydroxide, 7.0–7.5. The permeability of Ottawa sand treated with *S. pasteurii* reduced from 1×10^{-4} m/s to 8.2×10^{-6} m/s (Table 5).

Table 5
Replacement of calcium chloride in biocementation process

Source of urease	Characteristics of		Reference
and its activity	substitute of	biocementation	
	CaCl ₂	process	
Sporosarcina	Dissolved	Ottawa sand was treated with	Choi et
pasteurii ATCC	limestone powder	solution of urea, 0.3 M, + Ca ²⁺ ,	al., 2017
11859, 8 - 15	containg 50.7%	0.3M, for 7 days. The	
mM/min	CaO in 7% (w/v)	permeability was reduced from	
	acetic acid	1×10^{-4} m/s to 8.2×10^{-6} m/s	
Extract of soya	Eggshells treated	Poorly graded natural soil was	Hoque
bean seeds (seed	with acetic acid to	treated with solution of	and Islam,
powder, 50 g, in	obtain solution of	calcium acetate and urea in	2023
distilled water, 1	calcium acetate,	molar ratio 1:1 for 7 days to	
1)	0.39 mol/l	obtain sand with UCS of 371	
		kPa	
Sporosarcina	A limestone	Desert eolian sand with particle	Feng et
pasteurii ATCC	powder treated	sizes 0.106-0.178 mm, ratio of	al., 2023
11859	with acetic acid	Ca^{2+} : urea= 1:2.6, UCS	
		increased by 10.6%	
Extract of	Waste concrete	Compressive strength did not	He et al.,
soybean,	treated with 31.0%	differ from sand treated with	2022
6.66 mM/min	HC1	CaCl ₂ reagent	

A number of works are devoted to the use of eggshells in biocementation (Choi et al., 2016b; Kulanthaivel et al., 2022; Raheem and Jabbar, 2024). Eggshell powder was treated with an aqueous acetic acid solution for 7 days, to obtain concentration of calcium acetate, 0.39 mol/l (Hoque and Islam, 2023). Treatment using urease soybean extract and solution containing calcium acetate and urea in molar ratio 1:1 resulted in producing the biocemented sand with UCS of 371 kPa, which was by 8.5% higher than that of sand with the same calcium content, but treated with CaCl₂.

Waste concrete was treated with 31% hydrochloric acid to obtain dissolved calcium ions for further use in sand biocementation (He et al., 2022):

$$CaCO_3 + 2 HC1 \rightarrow Ca^{2+} + 2 C1^- + H_2O + CO_2\uparrow$$

A comparative study with sand treated with equimolar CaCl₂ and urea of the same concentration as a control showed no significant difference in the compressive strength of both biocemented samples (Table 4).

To obtain dissolved calcium ions, limestone powder with a particle size of about 0.282 mm was treated with acetic acid at 55°C, using a solid-to-liquid ratio of 1:14 and an acetic acid dosage of 163% (Feng et al., 2023). The UCS of sand samples treated with calcium ions derived from limestone was 10.6% higher compared to the control sand treated with CaCl₂, while the cost of MICP using Ca(CH₃COO)₂ (prepared from limestone) was reduced by 31.9%.

To replace CaCl₂ in the EICP process for treating sandy soil, it was proposed to use industrial waste calcium carbide slag powder dissolved in an acetic acid solution (Qi et al., 2022). No significant differences were observed between the properties of sand treated with reagent-grade CaCl₂ and those treated with the substitute. Therefore, utilizing waste or recycled materials in biocementation can significantly reduce the cost of soil improvement while also mitigating environmental pollution from unused industrial by-products. A replacement for both chemical reagents commonly used in the biocementation process, calcium chloride and urea, has been proposed. For example, eggshells have been used as a source of Ca²⁺ and cow urine as a source of urea (Sreekala et al., 2024). Similarly, waste carbide sludge dissolved in 0.8 M waste acid has served as a Ca²⁺ source, while urine has been used instead of urea for the cultivation of urease-producing bacteria (Yang et al., 2022).

Some studies have proposed using cheaper sources of urea to reduce the cost of the biocementation process by replacing the laboratory-grade materials with commercially available alternatives, for example, substituting urea with agricultural fertilizers and using commercially available $CaCl_2$ sold as a snow-melting agent (Moqsud and Gochi 2024). This approach has been shown to reduce the cost of materials for the biocementation process by up to 90%.

Methods for prevention of ammonium release in the environment

One of the obstacles to the large-scale application of biocementation is the release of ammonia gas into the atmosphere, along with the leaching of ammonium and hydroxide ions into groundwater and surface water (Gowthaman et al., 2021a; Ivanov et al., 2019b). During conventional MICP, the pH of the environment typically rises to 8.5 - 9.5 due to the release of ammonium ions and ammonia. It is known that at a pH \leq 7.3, approximately 99% of the released nitrogen remains in the form of ammonium ions (NH₄⁺). However, when the pH exceeds 7.5, a sharp shift occurs toward gaseous the formation of gaseous ammonia (NH₃) (Gowthaman et al., 2021a; Whiffin, 2004).

Ammonium concentrations in groundwater are typically below 0.2 mg/l. According to the European Commission (2012), the threshold value for NH₄⁺ in groundwater is 5 mg/l. Ammonia is considered as one of the five main air pollutants in the European Union, and its permissible concentration in surface waters in the United States ranges from 0.25 to 32.5 mg/l, depending on local conditions and regulations (Ammonia, 2020).

It has been estimated that biocementation or biogrouting of sandy soils requires the precipitation of at least 62 kg of calcium carbonate per one m³ of sand. This process results in the emission of approximately 10.5 kg of ammonia into the air and 11.2 kg of ammonium into ground or surface waters (Ivanov et al., 2019a). Therefore, it becomes clear that a critical challenge for the widespread adoption of biocementation is the effective limitation of ammonium and ammonia emissions into the environment.

To prevent environment contamination with ammonium ions, several methods involving additional treatments steps have been proposed including: (1) the use of calcium acetate instead of calcium chloride as calcium source. For example, replacing CaCl₂ with Ca(CH₃COO)₂ during the biocementation of sand using Sporosarcina pasteurii reduced NH₃ emission by 54.2% while also improving the strength of biocemented samples (Xiang et al., 2022); (2) the addition of zeolite, a negatively charged aluminosilicate mineral, to adsorb the resulting ammonium and produce an environmentally friendly soil stabilizer altogether with increasing of biocemented soil strength and reducing its permeability (Erdmann and Strieth, 2022; Keykha et al., 2019; Su et al., 2022); (3) the maintenance of ammonium by the graphite cathode electrode during electrobiocementation of soil to prevent the leakage of NH₄⁺ ions into the bulk of the soil (Keykha and Asadi, 2017); (4) removal of ammonium formed during soil biocementation by injection of solutions enriched with cations (Lee and Gomez, 2024; Lee et al., 2019); (5) rinsing the ammonium from the sand with subsequent its recovery by addition of Na₂HPO₄ and MgCl₂ at pH 8.5 with Mg²⁺:NH₄⁺: PO₄³⁻ molar ratio of 1.2:1:1 as struvite (NH₄MgPO₄·6H₂O) (Mohsenzadeh et al., 2022); (6) biocementation of sand with Sporosarcina pasteurii using solutions containing K₂HPO₄·3H₂O, MgCl₂, and urea led to the formation of struvite in the treated sand. UCS of the treated sand was 1.47 MPa, while ammonia gas emission was reduced by 75% compared with traditional process using CaCl₂ (Yu et al., 2021). To protect the atmosphere from ammonia release, adsorption of removed gas ammonia with sulfuric acid could be used (Ivanov and Stabnikov, 2017).

A promising and environmentally friendly alternative to reduce toxic ammonia emissions is calcium phosphate-based biocementation (Avramenko et al., 2022; Ivanov et al., 2019a). Calcium phosphate is a promising structural material with sufficient strength, while its biosafety is known (Toshima et al., 2014). Its use for soil improvement offers several advantages: (a) calcium phosphates are non-toxic and environmentally friendly materials (Kohn et al., 2002); (b) calcium phosphate present in the soil can act as a fertilizer, promoting plant growth. The formation of strong calcium phosphate crystals can be carried out from both inorganic and organic phosphate sources. Precipitation via this method can be achieved through enzymatic hydrolysis of urea, during which the pH increases from 4.4 to 7.0.

The economic advantage of hydroxyapatite biosolution lies in the possibility of using bone meal, an abundant by-product of meat processing, as a starting material. It has been found that calcium and phosphate in bone meal are present in the form of hydroxyapatite, Ca₁₀(PO₄)₆(OH)₂ (Gowthaman et al., 2021b). Acid hydrolysis of bone meal converts calcium into a soluble form and solution for biocementation with pH 3.4 and containing 8800 mg of Ca²⁺ per 1 l was received:

$$Ca_{10}(PO_4)_6(OH)_2 + 8 HC1 \rightarrow 10 Ca^{2+} + 6 HPO_4^{2-} + 8 Cl^- + 2 H_2O$$

To provide biocementation process, commercial acid urease Nagapshin, 4 g/l, was dissolved in the solution for biocementation to obtain urease activity of 2.5 mM/min at pH 4.0. Ratio of calcium: urea was 1.5, while in traditional biocementation it typicall ranges from 0.66 to 1.0. The biocemened poorly graded fine sand achieved a uniaxial compressive strength of 1.5 MPa. It was estimated that the release of ammonium ions was reduced by approximately 50%, and toxic ammonia emissions were about 90% lower compared to traditional biocementation.

An alternative biocementation process that combines the precipitation of struvite (NH₄MgPO₄) and calcium carbonate using triple superphosphate and a magnesium salt has also shown to be more environmentally friendly. This approach prevents the formation of free ammonium and the release of ammonia into the atmosphere during the biocementation process (Ivanov and Stabnikov, 2020):

$$Ca(H_2PO_4)_2 + 2 Mg^{2+} + CO(NH_2)_2 + H_2O + acid urease \rightarrow 2 NH_4MgPO_4 \downarrow + CaCO_3 \downarrow$$

To perform these types of biocementation, urease active at acidic pH is required. Commercial acid urease synthesized by *Lactobacillus fermentum* was used in the study (Gowthaman et al., 2021a), while the strain *Staphylococcus saprophyticus* AU1, isolated from acid soil, was employed in biocementation based on the calcium phosphate formation (Stabnikov et al., 2024).

Potential new bioagents for biocementation

Carbonate rocks such as calcite, aragonite, and dolomite contain large amounts of carbon in the form of calcium carbonate and represent the largest natural carbon storage sites (Zhu and Dittrich, 2016). Biodeposition of minerals is a common phenomenon in the biological world, mediated by bacteria, fungi, protozoa, and plants. Biomineralization in nature leads to the formation of more than sixty different biological minerals that exist as either extracellular or intracellular inorganic crystals. Calcium carbonate is one such mineral that naturally precipitates as a byproduct of microbial metabolic activity (Seifan and Berenjian, 2019). Carbonate precipitation can be initiated by chemotrophic and phototrophic microorganisms that produce carbonate ions through an increase in pH (Cacchio et al., 2003; Castanier et al., 1999; Wright and Oren, 2005).

There are three main groups of microorganisms responsible for carbonate precipitation in nature. These are photosynthetic microorganisms such as cyanobacteria and microalgae (Ariyanti et al., 2012); sulfate-reducing bacteria (Warthman et al., 2000), and some types of microorganisms involved in the nitrogen cycle, namely nitrogen-fixing bacteria, nitrifying bacteria, denitrifying bacteria or ureolytic bacteria (Castanier et al., 1999; Hammes and Verstraete, 2002; Stocks-Fischer et al., 1999). The formation of calcium carbonate, CaCO₃, is one of the most studied and understood biomineralization processes (Bang et al., 2010; Fernandez et al., 2018; Ronholm et al., 2014). Thus, biocement is considered an ecological material, the creation of which was inspired by nature itself (Achal et al., 2015) (Figure 3a) in contrast to artificial biocementation using urease-producing bacteria (Figure 3b).





Figure 3. A rock in the village of Pidkamin, Ukraine, an object of natural biocementation, approximately 11 million years old (Stabnikov et al., 2022) (a); 1 m³ of stone and sand mixture after biocementation (Stabnikov et al., 2015) (b)

Lactic acid bacteria

Ureases currently used in biocementation processes have optimal activity at pH values in the neutral to alkaline range, and are not only labile and prone to deactivation in an acidic environment, but also do not even catalyze the urea hydrolysis. More often, biocement is produced by precipitation of calcium carbonate at alkaline pH. However, the use of acid urease may be advantageous for biocementation in environments with a low initial pH, such as when calcium bicarbonate is used as the calcium source or during the production of calcium phosphate (Gowthaman et al., 2021a).

Lactic acid bacteria (Fig. 2c5), which are generally recognized as safe by both the US Food and Drug Administration and the European Food Safety Authority (Gowthaman et al., 2021a; Stabnikova et al., 2024), can serve as producers of acid urease (Stabnikov et al., 2025). Lactic acid bacteria can produce urease as a response to stress caused by low pH for neutralizing the acids formed. Among lactic acid bacteria producing urease there are strains of *Streptococcus thermophilus* used for production of yogurts and cheeses (Arioli et al., 2017; Scala et al., 2019), *Bifidobacterium longum* subsp. *infantis* (LoCascio et al., 2010), probiotic bacteria *Lactobacillus reuteri*, *Streptococcus thermophilus*, *S. salivarius* (Power et al., 2008; Udymovych, 2021; Wilson et al., 2014). Urease active at a pH range of 2.0–4.0 was first discovered in *Lactobacillus* sp. by Japanese researchers in 1988 (Fidaleo et al., 2006; Ough and Trioli, 1988). Commercial acid urease, Nagapshin, produced using *Lactobacillus fermentum*, was applied in the study of Gowthaman et al. (2021a) for the biocementation of sand, employing acid hydrolysate of bone meal as a source of hydroxyapatite.

Fungi

The potential use of fungal strains such as *Penicillium chrysogenum* (Fang et al., 2018; Martuscelli et al., 2020), *Aspergillus* sp. and *Fusarium oxysporum* (Dhami et al., 2017), *Pestalotiopsis* sp. and *Myrothecium gramineum* (Li et al., 2015) for calcium carbonate precipitation in soil biocementation has been shown. It was reported that the fungi *Aspergillus* sp. UF3 and *Fusarium oxysporum* UF8 synthesized carbonic anhydrase in addition to urease and produced calcite, vaterite, and aragonite during biomineralization using calcium oxalate as the calcium source (Dhami et al., 2017). Beside to the fact that the use of urease-producing fungi leads to the precipitation of calcium carbonate, the introduction of mycelial biomass into biocemented material can serve as a biological fiber additive, contributing to increased strength (Martuscelli et al., 2020). The fungal strains used for biocementation were isolated from alkaline soils (Devgon et al., 2024; Fang et al., 2018), calcareous soil (Li Q. et al., 2015) or karstic caves (Dhami et al., 2013). However, in the studies conducted, the potential biosafety risks associated with the use of fungi, including plant pathogens such as *Fusarium oxysporum*, *Myrothecium gramineum*, *Pestalotiopsis* sp., and others, in biocementation processes remain unexplored.

Microalgae

Photosynthetic organisms are considered to have played a major role in the formation of the world's carbonate deposits over the last 3 million years of Earth's history (Altermann et al., 2006). Photosynthetic microorganisms utilize carbon dioxide, which is in equilibrium with HCO₃⁻² and CO₃²⁻². When carbon dioxide is consumed by photosynthetic microorganisms, the pH increases and, in the presence of calcium ions, calcium carbonate is formed (Ariyanti et al., 2011, 2012):

$$CO_2 + H_2O \rightarrow (CH_2O) + O_2$$

 $2 \text{ HCO}_3^- \leftrightarrow CO_2 + CO_3^{2-} + H_2O$
 $CO_3^{2-} + H_2O \leftrightarrow HCO_3^- + OH^-$
 $Ca^{2+} + HCO_3^- + OH^- \leftrightarrow CaCO_3 + 2 \text{ H}_2O.$

Microalgae can promote the formation of calcium carbonate (CaCO₃) by thriving in alkaline environments saturated with Ca²⁺ ions. For instance, the formation of calcite and aragonite was observed in solutions with an initial pH 8.5, saturated with Ca²⁺ and containing the microalgae *Scenedesmus obliquus* (Santomauro et al., 2012). Currently, the application of microalgae (Fig. 2c6a) is proposed for biocement production and the self-healing of concrete cracks (Nur and Dewi, 2024).

Coccoliths, calcified haptophytes, are unicellular free-living microalgae whose cells are covered with calcified scales. They play an important role in the global carbonate cycle (Young and Henriksen, 2003). The potential use of these microalgae for biocementation is being explored as a promising approach (Al-Mardeai et al., 2024), alongside green microalgae such as *Chlorella* sp. (Ariyanti et al., 2012). Notably, the ability of microalgae *Chlorella kessleri* to produce calcium carbonate precipitates using waste cement kiln dust was demonstrated in a study (Irfan et al., 2019).

Cyanobacteria

Several studies have investigated the use of cyanobacteria (Fig. 2c6b) for biocementation (Chandra et al., 2023; Jang et al., 2023; Sidhu et al., 2022; Son et al., 2024). Cyanobacteria, commonly known as blue-green algae, are prokaryotic autotrophic algae-like bacteria that contain chlorophyll and are capable of photosynthesis, releasing molecular oxygen, which enriches the environment. Cyanobacteria inhabit diverse environments, including fresh, brackish, and saltwater ecosystems, and are active members of the soil microbiota.

A schematic illustrating the use of cyanobacteria in the manufacturing of living building materials (LBMs) is shown in Figure 4 (adopted from Son et al., 2024). The production of calcium carbonate (CaCO₃) by cyanobacteria offers the advantage that there is no CO₂ gas emissions during precipitate formation.

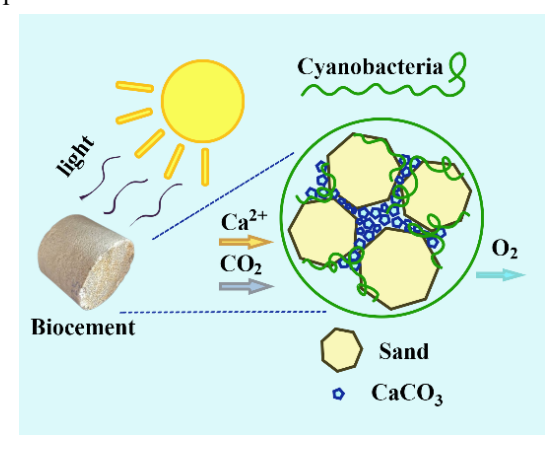


Figure 4. Schematic use of cyanobacteria for MICP formation (adopted from Son et al., 2024)

It has been suggested that cyanobacteria could enhance the mechanical properties of concrete by precipitating CaCO₃ crystals within its pores and microcracks. For example, the compressive strength of sand treated with cyanobacteria increased after 28 days of curing by 25.5% using *Synechocystis pevalekii* (Sidhu et al., 2022) and by 13% using *Leptolyngbya boryana* (Son et al., 2024) compared to control specimens without microorganisms.

Assessment of the carbon footprint for the production 1 kg of $CaCO_3$ by different methods showed that using cyanobacteria results in a lower carbon footprint of 0.815 kg CO_2/kg $CaCO_3$, compared to ureolytic bacteria at 1.51 kg CO_2/kg $CaCO_3$, and the convential carobonation process at 2.37 CO_2/kg $CaCO_3$ (Porter et al., 2021).

Conclusions

Biocementation, as a microbial-initiated calcite precipitation (MICP), presents a promising alternative to traditional cement production. It enables the creation of building materials with valuable properties while reducing energy consumption and environmental impact through lower greenhouse gas emissions. However, large scale application of biocementation faces key challenges: economically, due to relatively high production costs, and the ecologically, due to the introduction of live bacterial cells and the associated release of ammonium and ammonia into the environment.

To overcome these obstacles it is possible: (i) to reduce the cost of the biocementation process (1) by using various industrial wastes both to obtain the microbial component and to replace the chemical components of the process, namely calcium chloride and urea; (2) to use plant urease instead of urease of microbial origin; (ii) to improve the biosafety of biocementation (1) by using safe microbial urease producers or inactivated bacterial cells of urease-producing bacteria with preserved urease activity; (2) by using plant urease; (3) by using technologies that reduce the release of toxic ammonia and ammonium ions into the environment.

To improve the efficiency of the biocementation process, methods such as the introduction of additives, increasing the urease activity of plants, and the development of biocementation technologies using new bioagents are promising areas for further research.

References

- Achal V., Chin C.S. (2021), Building Materials for Sustainable and Ecological Environment, Springer, Singapore.
- Achal V., Mukherjee A., Basu P.S., Reddy M.S. (2009), Lactose mother liquor as an alternative nutrient source for microbial concrete production by *Sporosarcina pasteurii*, *Journal of Industrial Microbiology and Biotechnology*, 36(3), pp. 433–438, https://doi.org/10.1007/s10295-008-0514-
- Achal V., Mukherjee A., Reddy M.S. (2010), Characterization of two urease-producing and calcifying *Bacillus* sp. isolated from cement, *Journal of Microbiology and Biotechnology*, 20(11), pp. 1571–1576, https://doi.org/10.4014/jmb.1006.06032
- Achal V., Mukherjee A., Kumari D., Zhang Q. (2015), Biomineralization for sustainable construction A review of processes and applications, Earth-Science Reviews, 148, pp. 1-17, https://doi.org/10.1016/j.earscirev.2015.05.008

- Achakzai A.K.K., Kayani S.A., Yaqoob M., Nabi A. (2003), Effect of fertilizer and inoculation on lipase and urease activity of mature soybean cv. Williams-82 seeds, Asian Journal of Plant Sciences, 2, pp. 692-695, https://doi.org/10.3923/ajps.2003.692.695
- Ahenkorah I., Rahman M.M., Karim M.R., Teasdale P.R. (2020), A comparison of mechanical responses for microbial and enzyme-induced cemented sand, *Géotechnique Letters*, 10(4), pp. 559-567, https://doi.org/10.1680/jgele.20.00061
- Ahenkorah I., Rahman M.M., Karim M.R., Beecham S. (2021), Enzyme induced calcium carbonate precipitation and its engineering application: A systematic review and meta-analysis, *Construction and Building Materials*, 308, 125000, https://doi.org/10.1016/j.conbuildmat.2021.125000
- Al Imran M., Nakashima K., Evelpidou N., Kawasaki S. (2021), Improvement of using crude extract urease from watermelon seeds for biocementation technology, *Geomate Journal*, 20(78), pp. 142–147, https://geomatejournal.com/geomate/article/view/197
- Almajed A., Khodadadi Tirkolaei H., Kavazanjian Jr.E. (2018), Baseline investigation on enzyme-induced calcium carbonate precipitation, *Journal of Geotechnical and Geoenvironmental Engineering*, 144(11), 04018081, https://doi.org/10.1061/(ASCE)GT.1943-5606.0001973
- Almajed A., Khodadadi Tirkolaei H., Kavazanjian Jr. E., Hamdan N. (2019), Enzyme induced biocementated sand with high strength at low carbonate content, *Scientific Reports*, 9, 1135, https://doi.org/10.1038/s41598-018-38361-1
- Al-Mardeai S., El-Hassan H., Moheimani N., Hamza W., El-Maaddawy T., Al-Zuhair S. (2024), Optimization of microalgal CaCO₃ production with aim to produce biocement, *Chemical Engineering Research and Design*, 208, pp. 515-525, https://doi.org/10.1016/j.cherd.2024.07.020
- Altermann W., Kazmierczak J., Oren A., Wright D.T. (2006), Cyanobacterial calcification and its rock-building potential during 3.5 billion years of Earth history, *Geobiology*, 4(3), pp. 147–166, https://doi.org/10.1111/j.1472-4669.2006.00076.x
- Al-Thawadi S. (2012), Calcium carbonate crystals formation by ureolytic bacteria isolated from Australian soil and sludge, *International Journal of Advanced Science and Engineering Research*, 2(1), pp. 12–26.
- Ammonia. (2020), Technical bulletin Health effects information, https://www.oregon.gov/oha/ph/healthyenvironments/drinkingwater/monitoring/documents/health/ammonia.pdf, Accessed at 17 August 2025
- Andalib R., Majid M.Z.A., Hussin M.W., Ponraj M., Keyvanfar A., Mirza J., Lee H.S. (2016), Optimum concentration of Bacillus megaterium for strengthening structural concrete, *Construction & Building Materials*, 118, pp. 180-193, https://doi.org/10.1016/j.conbuildmat.2016.04.142
- Ariyanti D., Handayani N.A., Hadiyanto H. (2011), An overview of biocement production from microalgae, *International Journal of Science and Engineering*, 2(2), pp. 30-33, https://doi.org/10.12777/ijse.2.2.31-33
- Ariyanti D., Handayani N.A., Hadiyanto H. (2012), Feasibility of using microalgae for biocement production through biocementation, *Journal of Bioprocessing and Biotechniques*, 2(111), pp. 1–4, https://doi.org/10.4172/2155-9821.1000111
- Arioli S., Della Scala G., Remagni M.C., Stuknyte M., Colombo S., Guglielmetti S., De Noni I., Ragg E., Mora D. (2017), *Streptococcus thermophilus* urease activity boosts *Lactobacillus delbrueckii* subsp. bulgaricus homolactic fermentation, *International Journal of Food Microbiology*, 17(247), pp. 55-64, https://doi.org/10.1016/j.ijfoodmicro.2016.01.006
- Avramenko M., Nakashima K., Kawasaki S. (2022), State-of-the-art review on engineering uses of calcium phosphate compounds: An eco-friendly approach for soil improvement, *Materials*, 15(19), 6878, https://doi.org/10.3390/ma15196878

- Baiq H.S., Yasuhara H., Kinoshita N., Putra H., Johan E. (2020), Examination of calcite precipitation using plant derived urease enzyme for soil improvement, *Geomate Journal*, 19(72), pp. 231-237, https://doi.org/10.21660/2020.72.9481
- Bang S.S., Lippert J.J., Yerra U., Mulukutla S., Ramakrishnan V. (2010), Microbial calcite, a biobased smart nanomaterial in concrete remediation, *International Journal of Smart and Nano Materials*, 1(1), pp. 28–39, https://doi.org/10.1080/19475411003593451
- Baykara H., Riofrio A., Garcia-Troncoso N., Cornejo M., Tello-Ayala K., Rada J.F., Caceres J. (2024), Chitosan-cement composite mortars: Exploring interactions, structural evolution, environmental footprint and mechanical performance, *ACS Omega* 9, pp. 24978-24986, https://doi.org/10.1021/acsomega.4c02040
- Bedan D.S. (2020), Extraction, precipitation and characterization of urease from *Vicia faba* L. *Al-Mustansiriyah Journal of Science*, 31(1), pp. 9–14, https://doi.org/10.23851/mjs.v31i1.555
- Burbank M., Weaver T., Lewis R., Williams T., Williams B., Crawford W. (2012), Geotechnical tests of sands following bioinduced calcite precipitation catalyzed by indigenous bacteria, *Journal of Geotechnical & Geoenvironmental Engineering*, 139(6), pp. 928-936, https://doi.org/10.1061/(ASCE)GT.1943-5606.0000781
- Cacchio P., Ercole C., Cappuccio G., Lepidi A. (2003), Calcium carbonate precipitation by bacterial strains isolated from a limestone cave and from a loamy soil, Geomicrobiology Journal, 20(2), pp. 85–98, https://doi.org/10.1080/01490450303883
- Castanier S., Le G., Metayer-Levrel G., Perthuisot J.P. (1999), Ca-carbonates precipitation and limestone genesis the microbiogeologist point of view, *Sedimentary Geology*, 126(1-4), pp. 9–23, https://doi.org/10.1016/S0037-0738(99)00028-7
- Chandra S., Bhattacharya S., Pandit S., Banerjee S., Roy A., Rai A.K. (2023), Cyanobacteria as an eco-friendly bioresource for EPS production with crack healing capacity in concrete, *Biocatalysis and Agricultural Biotechnology*, 54, 102909, https://doi.org/10.1016/j.bcab.2023.102909
- Chaparro S., Rojas H.A., Caicedo G., Romanelli G., Pineda A., Luque R., Martínez J.J. (2021), Whey as an alternative nutrient medium for growth of *Sporosarcina pasteurii* and its effect on CaCO₃ polymorphism and fly ash bioconsolidation, *Materials*, 14, 2470, https://doi.org/10.3390/ma14102470
- Chen M., Gowthaman S., Nakashima K., Komatsu S., Kawasaki S. (2021), Experimental study on sand stabilization using bio-cementation with wastepaper fiber integration, *Materials*, 14, 5164, https://doi.org/10.3390/ma14185164
- Cheng L., Cord-Ruwisch R. (2013), Selective enrichment and production of highly urease active bacteria by non-sterile (open) chemostat culture, *Journal of Industrial Microbiology and Biotechnology*, 40, pp. 1095–1104.
- Choi S.G., Wang K., Chu J. (2016a) Properties of biocemented, fiber reinforced sand, *Construction and Building Materials*, 120, pp. 623–629, https://doi.org/10.1016/j.conbuildmat.2016.05.124
- Choi S.G., Wu S., Chu J. (2016b), Biocementation for sand using an eggshell as calcium source, *Journal of Geotechnical and Geoenvironmental Engineering*, 142(10), 06016010, https://doi.org/10.1061/(asce)gt.1943-5606.0001534
- Choi S.G., Chu J., Brown R.C., Wang K., Wen Z. (2017), Sustainable biocement production via microbially induced calcium carbonate precipitation: Use of limestone and acetic acid derived from pyrolysis of lignocellulosic biomass, *ACS Sustainable Chemistry & Engineering*, 5(6), pp. 5183–5190, https://doi.org/10.1021/acssuschemeng.7b00521
- Chu J., Stabnikov V., Ivanov V. (2012), Microbially induced calcium carbonate precipitation on surface or in the bulk of soil, *Geomicrobiology Journal*, 29(6), pp. 544–549, https://doi.org/10.1080/01490451.2011.592929

- Cui M., Fu X., Zheng J.J., Xiong H.H., Zeng C., Han S.Y. (2023), Multivariate experimental study on soybean urease induced calcium carbonate precipitation, *Rock and Soil Mechanics*, 43(11), pp. 3027-3035, https://doi.org/10.16285/j.rsm.2021.7157
- Cui M.J., Lai H.J., Wu S.F., Chu J. (2024), Comparison of soil improvement methods using crude soybean enzyme, bacterial enzyme or bacteria-induced carbonate precipitation, *Géotechnique*, 74(1), pp. 18-26, https://doi.org/10.1680/jgeot.21.00131
- Das N., Kayastha A.M., Srivastava P.K. (2002), Purification and characterization of urease from dehusked pigeonpea (*Cajanus cajan* L.) seeds, *Phytochemistry*, 61(5), pp. 513-521, https://doi.org/10.1016/s0031-9422(02)00270-4
- DeJong J.T., Soga K., Kavazanjian E., Burns S.,van Paassen Al., Qabany A., Aydilek A., Bang S.S., Burbank M., Caslake L., Chen C.Y., Cheng X., Chu J., et al (2013), Biogeochemical processes and geotechnical applications: Progress, opportunities and challenges, *Geotechnique*, 63(4), pp. 287–301, https://doi.org/10.1680/geot.SIP13.P.017
- De Muynck W., De Belie N., Verstraete W. (2010), Microbial carbonate precipitation in construction materials: A review, *Ecological Engineering*, 36(2), pp. 118–136, https://doi.org/10.1016/j.ecoleng.2009.02.006b
- Devgon I., Sachan R.S.K., Rajput K., Kumar M., Al-Tawaha A.R.M.S., Karnwal A., Malik T. (2024), Exploring fungal potential for microbial-induced calcite precipitation (MICP) in bio-cement production, *Frontiers Materials*, 11, https://doi.org/10.3389/fmats.2024.13960811
- Dhami N.K., Reddy M.S., Mukherjee A. (2013), Biomineralization of calcium carbonate polymorphs by the bacterial strains isolated from calcareous sites, *Journal of Microbiology and Biotechnology*, 23(5), pp. 707-714, https://doi.org/10.4014/jmb.1212.11087
- Directive 2000/54/ec of the European Parliament and of the Council. (2019), Official Journal of the European Union, L 279, 54, https://eur-lex.europa.eu/legal-content/EN/TXT/PDF/?uri=CELEX:02000L0054-20191120&rid=1
- Dosier G.K. (2014), Methods for making construction material using enzyme producing bacteria, Patent US 8728365 B2.
- Dilrukshi R.A.N., Watanabe J., Kawasaki S. (2015), Sand cementation test using plant-derived urease and calcium phosphate compound, *Materials Transactions*, 56(9), pp. 1565-1572, https://doi.org/10.2320/matertrans.m-m2015818
- Dilrukshi R.A.N., Nakashima K., Kawasaki S. (2018), Soil improvement using plant-derived urease-induced calcium carbonate precipitation, *Soils and Foundations*, 58(4), pp. 894-910, https://doi.org/10.1016/j.sandf.2018.04.003
- Elmanama A.A., Alhour M.T. (2013), Isolation, characterization and application of calcite producing bacteria from urea rich soils, *Journal of Advanced Science and Engineering Research*, 3(4), pp. 388–399.
- EL-Hefnawy M.E., Sakran M., Ismail A.I., Aboelfetoh E.F. (2014), Extraction, purification, kinetic and thermodynamic properties of urease from germinating *Pisum sativum* L. seeds, *BMC Biochemistry*, 15, 15, https://doi.org/10.1186/1471-2091-15-15
- Ekprasert J., Fongkaew I., Chainakun P., Kamngam R., Boonsuan W. (2020), Investigating mechanical properties and biocement application of CaCO₃ precipitated by a newly-isolated *Lysinibacillus* sp. WH using artificial neural networks, *Scientific Reports*, 10, 16137, https://doi.org/10.1038/s41598-020-73217-7
- Erdmann N., Strieth D. (2022), Influencing factors on ureolytic microbiologically induced calcium carbonate precipitation for biocementation, *World Journal of Microbiology and Biotechnology*, 39, 61, https://doi.org/10.1007/s11274-022-03499-8
- European Union. (2012), Statistical and Economic Information. Report 2012. Directorate-General for Agriculture and Rural Development, http://ec.europa.eu/agriculture/statistics/agricultural/2012/pdf/full-report_en.pdf, Accessed at 17 August 2025

- Eryürük K., Yang S., Suzuki D., Sakaguchi I., Katayama A. (2015), Effects of bentonite and yeast extract as nutrient on decrease in hydraulic conductivity of porous media due to CaCO₃ precipitation induced by *Sporosarcina pasteurii*, *Journal of Bioscience and Bioengineering*, 120(4), pp. 411-418, https://doi.org/10.1016/j.jbiosc.2015.01.020
- Fang C., Kumari D., Zhu X., Achal V. (2018), Role of fungal-mediated mineralization in biocementation of sand and its improved compressive strength, *International Biodeterioration and Biodegradation*, 133, pp. 216–220, https://doi.org/10.1016/j.ibiod.2018.07.013
- Feng Q., Song Y., Lu C., Fang H., Huang Y., Chen L., Song X. (2023), Feasible utilization of waste limestone as a calcium source for microbially induced carbonate precipitation (MICP), *Fermentation*, 9, 307, https://doi.org/10.3390/fermentation9030307
- Fernandez M.S., Montt B., Ortiz L., Neira-Carrillo A., Arias J.L. (2018), Effect of carbonic anhydrase immobilized on eggshell membranes on calcium carbonate crystallization in vitro, In: K. Endo, T. Kogure, H. Nagasawa (Eds.), *Biomineralization*, pp. 31–37, Springer, Singapore, https://doi.org/10.1007/978-981-13-1002-7_4
- Fritzges M. (2005), Biologically induced improvements of the response of sands to monotonic and impact loading, MS Thesis, Amherst, MA, USA.
- Gao Y.F., Meng H., He J., Qi Y.S., Hang L. (2020), Field trial on use of soybean crude extract for carbonate precipitation and wind erosion control of sandy soil, *Journal of Central South University*, 27(11), pp. 3320–3333, https://doi.org/10.1007/s11771-020-4549-x
- Garcia G.M., Marquez G.M., Moreno H.C. (2016), Characterization of bacterial diversity associated with calcareous deposits and drip-waters, and isolation of calcifying bacteria from two Colombian mines, *Microbiological Research*, 182, pp. 21-30, https://doi.org/10.1016/j.micres.2015.09.006
- Gat D., Tsesarsky M., Shamir D., Ronen Z. (2014), Accelerated microbial-induced CaCO₃ precipitation in a defined coculture of ureolytic and non-ureolytic bacteria, *Biogeosciences*, 11, pp. 2561–2569, https://doi.org/10.5194/bg-11-2561-2014
- Gat D., Ronen Z., Tsesarsky M. (2016), Soil bacteria population dynamics following stimulation for ureolytic microbial-induced CaCO₃ precipitation, *Environmental Science & Technology*, 50, pp, 616-621, https://doi.org/10.1021/acs.est.5b04033
- Gerenda J., Zhu Z., Sattelmacher B. (1998), Influence of N and Ni supply on nitrogen metabolism and urease activity in rice (*Oryza sativa* L.), *Journal of Experimental Botany*, 49(326), pp. 1545–1554, https://doi.org/10.1093/jexbot/49.326.1545
- Gomez M.G., Graddy C.M.R., DeJong J.T., Nelson D.C., Tsesarsky M. (2018), Stimulation of native microorganisms for biocementation in samples recovered from field-scale treatment depths, *Journal of Geotechnical and Geoenvironmental Engineering*, 144, 04017098, https://doi.org/10.1061/(ASCE)GT.1943-5606.0001804
- Gowthaman S., Mitsuyama S., Nakashima K., Komatsu M., Kawasaki S. (2019), Biogeotechnical approach for slope soil stabilization using locally isolated bacteria and inexpensive low-grade chemicals: A feasibility study on Hokkaido expressway soil, Japan, *Soils Foundation*, 59, pp. 484–499.
- Gowthaman S., Mohsenzadeh A., Nakashima K., Kawasaki S. (2021a), Removal of ammonium by-products from the effluent of bio-cementation system through struvite precipitation, *Materialstoday: Proceedings*, 61(Part 2), pp. 243-249, https://doi.org/10.1016/j.matpr.2021.09.013
- Gowthaman S., Yamamoto M., Nakashima K., Ivanov V., Kawasaki S. (2021b), Calcium phosphate biocement using bone meal and acid urease: An eco-friendly approach for soil improvement, *Journal of Cleaner Production*, 319, 128782, https://doi.org/10.1016/j.jclepro.2021.128782
- Guzman-Ortiz F.A., Castro-Rosas J., Gomez-Aldapa C.A., Mora-Escobedo R., Rojas-Leon A., Rodriguez-Marin M.L., Falfan-Cortes R.N., Roman-Gutierrez A. (2019), Enzyme activity

- during germination of different cereals: A review, *Food Reviews International*, 35(3), pp. 177–200, https://doi.org/10.1080/87559129.2018.151462316/j.jare.2018.01.006
- Hamdan N., Kavazanjian E. (2016), Enzyme-induced carbonate mineral precipitation for fugitive dust control, *Géotechnique*, 66(7), pp. 546-555, https://doi.org/10.1680/jgeot.15.P.168
- Hamdan N., Zhao Z., Mujica M., Kavazanjian E., He X.M. (2016), Hydrogel-assisted enzyme-induced carbonate mineral precipitation, *Journal of Materials in Civil Engineering*, 28(10), 04016089, https://doi.org/10.1061/(asce)mt.1943-5533.0001604
- Hammes F., Verstraete W. (2002), Key roles of pH and calcium metabolism in microbial carbonate precipitation, *Reviews in Environmental Science and Biotechnology*, 1(1), pp. 3–7, https://doi.org/10.1023/A:1015135629155
- Hammes F., Boon N., de Villiers J., Verstraete W., Siciliano S.D. (2003), Strain-specific ureolytic microbial calcium carbonate precipitation, *Applied and Environmental Microbiology*, 69(8), pp. 4901–4909, https://doi.org/10.1128/AEM.69.8.4901-4909.2003
- Han S.H., Kang C.H., Shin Y.J., Yeom W.S., Jeong J.H., So J.S. (2014), Sporulation of Lysinibacillus sphaericus WJ-8 isolated from concrete pavement and response to environmental stresses, Korean Society for Biotechnology and Bioengineering Journal, 29, pp. 188-192.
- Hao M., Gao Y., He J., Yongshuai Q., Lei H. (2021), Microbially induced carbonate precipitation for wind erosion control of desert soil: Field-scale tests, *Geoderma*, 383, 114723, https://doi.org/10.1016/j.geoderma.2020.114723
- He J., Mao X., Zhou Y., Tang Q. (2022), Cementation of sand with enzyme-induced carbonate precipitation (EICP) using concrete-extracted calcium, *Frontiers in Physics*, 9, 825356, https://doi.org/10.3389/fphy.2021.825356
- He J., Liu Y., Liu L., Yan B., Li L., Meng H., Hang L., Qi Y., Wu M., Gao Y. (2023), Recent development on optimization of bio-cementation for soil stabilization and wind erosion control, *Biogeotechnics*, 1(2), 100022, https://doi.org/10.1016/j.bgtech.2023.100022
- Hirayama C., Sugimura M., Saito H., Nakamura M. (2000), Purification and properties of urease from the leaf of mulberry, *Morus alba*, *Phytochemistry*, 53(3), pp. 325-330, https://doi.org/10.1016/s0031-9422(99)00521-x
- Hogan M.E., Swift I.E., Done J. (1983), Urease assay and ammonia release from leaf tissues, *Phytochemistry*, 22(13), pp. 663–667, https://doi.org/10.1016/S0031-9422(00)86958-7
- Hokkanen H.M.T., Lynch J.M. (2003), *Biological control: Benefits and risks*, Cambridge University Press.
- Hoque M.A., Islam M.H. (2023), Implementation of eggshell extracted calcium acetate in biocementation via soybean urease, 4th International Conference on Energetics, Civil and Agricultural Engineering, October 12nd - 14th 2023, Uzbekistan, Tashkent, 434, 02006, https://doi.org/10.1051/e3sconf/202343402006
- Irfan M.F., Hossain S.M.Z., Khalid H., Sadaf F., Al-Thawadi S., Alshater A., Hossain M.M., Razzak S.A. (2019), Optimization of bio-cement production from cement kiln dust using microalgae, *Biotechnology Reports*, 23, e00356, https://doi.org/10.1016/j.btre.2019.e00356
- Ivanov V., Chu J. (2008), Applications of microorganisms to geotechnical engineering for bioclogging and biocementation of soil in situ, *Reviews in Environmental Science and Biotechnology*, 7(2), pp. 139–153, https://doi.org/10.1007/s11157-007-9126-3
- Ivanov V., Stabnikov V. (2017), Construction Biotechnology: Biogeochemistry, Microbiology and Biotechnology of Construction Materials and Processes, Springer Science, Singapore.
- Ivanov V., Stabnikov V. (2020), Environmental safety of biotechnological materials and processes. In: F. Pacheco-Torgal, V. Ivanov, D.C.W. Tsang (Eds.), *Bio-based Materials* and *Biotechnologies for Eco-efficient Construction*, pp. 359–376, Woodhead Publishing, Cambridge, UK, https://doi.org/10.1016/B978-0-12-819481-2.00017-9

- Ivanov V., Stabnikov V., Stabnikova O., Kawasaki S. (2019a), Environmental safety and biosafety in construction biotechnology, *World Journal of Microbiology and Biotechnology*, 35(2), 26, http://www.doi:10.1007/s11274-019-2598-9
- Ivanov V., Stabnikov V., Kawasaki S. (2019b), Ecofriendly calcium phosphate and calcium bicarbonate biogrouts, *Journal of Cleaner Production*, 218, pp. 328–334, https://doi.org/10.1016/j.jclepro.2019.01.315
- Ivanov V., Stabnikov V., Stabnikova O., Ahmed Z. (2020), Biotechnology for construction of artificial oasis in sandy desert, *Journal of King Saud University Engineering Sciences*, 32(8), pp. 491–494, https://doi.org/10.1016/j.jksues.2019.07.003
- Jang I., Park J., Son Y., Min J., Park W., Yi C. (2023), Photosynthetic living building material: Effect of the initial population of cyanobacteria on fixation of CO₂ and mechanical properties, *Construction and Building Materials*, 396, 132218, https://doi.org/10.1016/j.conbuildmat.2023.132218
- Jeong J.H., Jo Y.S., Park C.S., Kang C.H., So J.S. (2017), Biocementation of concrete pavements using microbially induced calcite precipitation, *Journal of Microbiology and Biotechnology*, 27(7), pp. 1331-1335, https://doi.org/10.4014/jmb.1701.01041
- Kahani M., Kalantary F., Soudi M.R., Pakdel L., Aghaalizadeh S. (2020), Optimization of cost effective culture medium for *Sporosarcina pasteurii* as biocementing agent using response surface methodology: Up cycling dairy waste and seawater, *Journal of Cleaner Production*, 253, 120022, https://doi.org/10.1016/j.jclepro.2020.120022
- Kakimoto S., Sumino Y., Suzuki T. (1992), Acid urease and production thereof, United States Patent 5093255A, https://patentimages.storage.googleapis.com/5f/ef/04/787f5cfd420497/US5093255 pdf
- Keykha H.A., Asadi A. (2017), Solar powered electro-bio-stabilization of soil with ammonium pollution prevention system, *Advances in Civil Engineering Materials*, 6(1), pp. 360-371, https://doi.org/10.1520/acem20170001
- Keykha H.A., Mohamadzadeh H., Asadi A., Kawasaki S. (2019), Ammonium-free carbonate-producing bacteria as an ecofriendly soil biostabilizer, *Geotechnical Testing Journal*, 42(1), pp. 19-29, https://doi.org/10.1520/GTJ20170353
- Khanafari A., Khans F.N., Sepahy A.A. (2011), An investigation of biocement production from hardwater, *Middle-East Journal of Scientific Research*, 7(6), pp. 1990–9233.
- Khodadadi Tirkolaei H., Kavazanjian E., van Paassen L., DeJong J. (2017), Bio-grout materials: A review, *Grouting*, pp. 1–12, https://www.researchgate.net/publication/318256473
- Khodadadi Tirkolaei H., Javadi N., Krishnan V., Hamdan N., Kavazanjian E. (2020), Crude urease extract for biocementation, *Journal of Materials in Civil Engineering*, 32(12), 04020374, https://doi.org/10.1061/(asce)mt.1943-5533.0003466
- Kohn M.J., Rakovan J., Hughes J.M. (Eds.) (2002), *Phosphates geochemical, geobiological, and materials importance. Reviews in mineralogy and geochemistry*, Washington, D.C.
- Kulanthaivel P., Soundara B., Selvakumar S., Das A. (2022), Application of waste eggshell as a source of calcium in bacterial bio-cementation to enhance the engineering characteristics of sand, *Environmental Science and Pollution Research*, 29(44), pp. 66450-66461, https://doi.org/10.1007/s11356-022-20484-8
- Lai H.J., Cui M.J., Wu S.F., Yang Y., Chu J. (2023), Extraction of crude soybean urease using ethanol and its effect on soil cementation, *Soils and Foundations*, 63(3), 101300, https://doi.org/10.1016/j.sandf.2023.101300
- Lee M., Gomez M.G. (2024), Removal of ammonium by-products produced during biocementation soil improvement using rinse injection strategies, *Soil Use & Management*, 40(1), e12984, https://doi.org/10.1111/sum.12984
- Lee M., Gomez M.G., San Pablo A.C.M., Kolbus C.M., Graddy C.M.R., DeJong J.T., Nelson D.C. (2019), Investigating ammonium by-product removal for ureolytic bio-cementation

- using meter-scale experiments, *Scientific Reports*, 9, 18313, https://doi.org/10.1038/s41598-019-54666-1
- Leeprasert L., Chonudomkul D., Boonmak C. (2022), Biocalcifying potential of ureolytic bacteria isolated from soil for biocementation and material crack repair, *Microorganisms*, 10(5), 963, https://doi.org/10.3390/microorganisms10050963
- Li H., Song, Y., Li, Q., He, J. Song, Y. (2014), Effective microbial calcite precipitation by a new mutant and precipitating regulation of extracellular urease, *Bioresource Technology*, 167, pp. 269-275, https://doi.org/10.1016/j.biortech.2014.06.011
- Li Q., Csetenyi L., Paton G.I., Gadd G.M. (2015), CaCO₃ and SrCO₃ bioprecipitation by fungi isolated from calcareous soil, *Environmental Microbiology*, 17(8), pp. 3082-3097, https://doi.org/10.1111/1462-2920.12954
- Li M., Li L., Ogbonnaya U., Wen K., Tian A., Amini F. (2016), Influence of fiber addition on mechanical properties of MICP-treated sand, *Journal of Materials in Civil Engineering*, 28(4), 04015166, https://doi.org/10.1061/(asce)mt.1943-5533.0001442
- Li X., Zhao D., Qin Y. (2019), Recent progress in understanding the mechanism of the interaction between calcium and milk proteins and its influence on functional properties of milk proteins, Food Science, 40(19), pp. 340–345, https://doi.org/10.7506/spkx1002-6630-20180927-288
- Liu L., Gao Y., Geng W., Song J., Zhou Y., Li C. (2023), Comparison of jack bean and soybean crude ureases on surface stabilization of desert sand via enzyme-induced carbonate precipitation, *Geoderma*, 435,116504, https://doi.org/10.1016/j.geoderma.2023.116504
- Liu L., Gao Y., Cao X., Meng H., Wang Z., Qi Y., Li R., He J. (2024), A comparative study of low-cost crude ureases extracted from multi-species of natural plant sources in enzymeinduced carbonate precipitation, *Journal of Environmental Chemical Engineering*, 12(6), 114824, https://doi.org/10.1016/j.jece.2024.114824
- Liu L., Gao Y., Meng H., Cao X., Wang Z., Liu B., He J. (2025), Bio-reinforcement efficiency of enzyme-induced carbonate precipitation modified by sword bean crude urease combined with multiple enhancers on bio-cemented sand, *Acta Geotechnica*, 20, pp. 1193–1212, https://doi.org/10.1007/s11440-024-02436-3
- Liu Y., Gao Y., He J., Zhou Y., Geng W. (2023), An experimental investigation of wind erosion resistance of desert sand cemented by soybean-urease induced carbonate precipitation, *Geoderma*, 429, 116231, https://doi.org/10.1016/j.geoderma.2022.116231
- Liu Y., Gao Y., Liu B., Cao X., Chen J. (2024), Biocementation for desert sand against wind-induced erosion with different treatment processes, *Journal of Soils and Sediments*, 24, pp. 3265–3275, https://doi.org/10.1007/s11368-024-03888-6
- LoCascio R.G., Desai P., Sela D.A., Weimer B., Mills D.A. (2010), Broad conservation of milk utilization genes in *Bifidobacterium longum* subsp. *infantis* as revealed by comparative genomic hybridization, *Applied and Environmental Microbiology*, 76(22), pp. 7373-7381, https://doi.org/10.1128/AEM.00675-10
- Lv C., Tang C.S., Zhang J.Z., Pan X.H., Liu H. (2022), Effects of calcium sources and magnesium ions on the mechanical behavior of MICP-treated calcareous sand: Experimental evidence and precipitated crystal insights, *Acta Geotechnica*, 18, pp. 2703–2717, https://doi.org/10.1007/s11440-022-01748-6
- Martuscelli C., Soares C., Lima N., Camões A. (2020), Potential of fungi to produce biosandstone, RILEM Technical Letters, 5, pp. 157-162, https://doi.org/10.21809/rilemtechlett.2020.119
- Meng H., Shu S., Gao Y., He J., Wan Y. (2021), Kitchen waste for *Sporosarcina pasteurii* cultivation and its application in wind erosion control of desert soil via microbially induced carbonate precipitation, *Acta Geotechnica*, 16(12), pp. 4045–4059, https://doi.org/10.1007/s11440-021-01334-2

- Miyake M., Kim D., Hata T. (2022), Casein-assisted enhancement of the compressive strength of biocemented sand, *Scientific Reports*, 12, 12754, https://doi.org/10.1038/s41598-022-16879-9
- Mohsenzadeh A., Aflaki E., Gowthaman S., Nakashima K., Kawasaki S., Ebadi T. (2022), A two-stage treatment process for the management of produced ammonium by-products in ureolytic bio-cementation process, *International Journal of Environmental Science and Technology*, 19, pp. 449–462, https://doi.org/10.1007/s13762-021-03138-z
- Mortensen B.M., DeJong J.T. (2011), Strength and stiffness of MICP treated sand subjected to various stress paths, In: J. Han, D.A. Alzamora (Eds.), ASCE Geo-Frontiers 2011, Advances in Geotechnical Engineering: Geotechnical Special Publication, pp. 4012–4020, https://doi.org/10.1061/41165(397)410
- Moqsud M.A., Gochi T. (2024), Evaluation of biocementation of slope soil for erosion control with low-cost materials, *Scientific Reports*, 14, 16065, https://doi.org/10.1038/s41598-024-67185-5
- Nakano A. (2024), Sand improvement by microbially induced carbonate precipitation with casein micelles, *Géotechnique Letters*, 14, pp. 94-99, https://doi.org/10.1680/jgele.24.00029
- Nam I.H., Chon C.M., Jung K.Y., Choi S.G., Choi H., Park S.S. (2014), Calcite precipitation by ureolytic plant (*Canavalia ensiformis*) extracts as effective biomaterials, *KSCE Journal of Civil Engineering*, 19(6), pp. 1620–1625, https://doi.org/10.1007/s12205-014-0558-3
- Namdar-Khojasteh D., Bazgir M., Babaheidari S.A.H., Asumadu-Sakyi A.B. (2022), Application of biocementation technique using *Bacillus sphaericus* for stabilization of soil surface and dust storm control, *Journal of Arid Land*, 14, pp. 537–549, https://doi.org/10.1007/s40333-022-0017-9
- Nawarathna T.H.K., Nakashima K., Kawasaki S. (2020), Polymer modified microbial induced carbonate precipitation: Novel approach to densify the loose sand, *University of Jaffna*, pp. 332-336, http://repo.lib.jfn.ac.lk/ujrr/bitstream/123456789/4868/2/Polymer%20modified%20micr obial%20induced.pdf
- Neupane D., Yasuhara H., Kinoshita N., Ando Y. (2015), Distribution of mineralized carbonate and its quantification method in enzyme mediated calcite precipitation technique, *Soils and Foundations*, 55(2), pp. 447–457, https://doi.org/10.1016/j.sandf.2015.02.018
- Nkhata S.G., Ayua E., Kamau E.H., Shingiro J.B. (2018), Fermentation and germination improve nutritional value of cereals and legumes through activation of endogenous enzymes, *Food Science & Nutrition*, 6(8), pp. 2446-2458, https://doi.org/10.1002/fsn3.846
- Nur M.M.A., Dewi R.N. (2024), Opportunities and challenges of microalgae in biocement production and self-repair mechanisms, *Biocatalysis and Agricultural Biotechnology*, 56, 103048, https://doi.org/10.1016/j.bcab.2024.103048
- Omoregie A.I., Ginjom R.H., Nissom P.M. (2018), Microbially induced carbonate precipitation via ureolysis process: A mini-review, *Transactions on Science and Technology*, 5, pp. 245-256, http://tost.unise.org/pdfs/vol5/no4/5x4x245-256.pdf
- Ono Y., Fukasawa M., Sueyoshi K., Ohtake N., Sato T., Tanabata S., Toyota R., Higuchi K., Saito A., Ohyama T. (2021), Application of nitrate, ammonium, or urea changes the concentrations of ureides, urea, amino acids and other metabolites in xylem sap and in the organs of soybean plants (*Glycine max* (L.) Merr.), *International Journal of Molecular Sciences*, 22(9), 4573, https://doi.org/10.3390/ijms22094573
- Park S.S., Choi S.G., Nam I.H. (2014), Effect of plant-induced calcite precipitation on the strength of sand, *Journal of Materials in Civil Engineering*, 26(8), 06014017, https://doi.org/10.1061/(asce)mt.1943-5533.0001029
- Pervin M.S., Jahan M.G.S., Masud Rana A.Y.K.Md., Sana N.K., Rahman M.H., Shaha R.K. (2013), Effects of some environmental variables on urease in germinating chickpea (*Cicer arietinum L.*) seed, *Journal of Stress Physiology & Biochemistry*, 9(3), pp, 345-356,

- https://sciup.org/14323779
- Putra H., Yasuhara H., Kinoshita N. (2017), Applicability of natural zeolite for NH-forms removal in enzyme-mediated calcite precipitation technique, *Geosciences*, 7(3), 61, https://doi.org/10.3390/geosciences7030061
- Ronholm J., Schumann D., Sapers H.M., Izawa M., Applin D., Berg B., Mann P., Vali H., Flemming R.L., Cloutis E.A., Whyte L.G. (2014), A mineralogical characterization of biogenic calcium carbonates precipitated by heterotrophic bacteria isolated from cryophilic Polar regions, *Geobiology*, 12(6), pp. 542-556, https://doi.org/10.1111/gbi.12102
- Porter H., Mukherjee A., Tuladhar R., Dhami N.K. (2021), Life cycle assessment of biocement: An emerging sustainable solution? *Sustainability*, 13(24), 13878, https://doi.org/10.3390/su132413878
- Power D.A., Burton J.P., Chilcott C.N., Dawes P.J., Tagg J.R. (2008), Preliminary investigations of the colonization of upper respiratory tract tissues of infants using a pediatric formulation of the oral probiotic *Streptococcus salivarius* K12, *European Journal of Clinical Microbiology & Infectious Diseases*, 27(12), pp. 1261-1263, https://doi.org/10.1007/s10096-008-0569-4
- Raheem L.S., Jabbar H. (2024), Microbial-induced carbonate precipitation using eggshells and scallop shells as recycled materials, *Case Studies in Chemical and Environmental Engineering*, 10(1), 100867, https://doi.org/10.1016/j.cscee.2024.100867
- Rajasekar A., Xian J., Moy C.K.S., Wilkinson S. (2017), Stimulation of indigenous carbonate precipitating bacteria for ground improvement, *IOP Conference Series: Earth Environmental Science*, 68, 012010, https://doi.org/10.1088/1755-1315/68/1/012010
- Roksana K., Hewage S.A., Montalbo-Lomboy M., Tang C.S., Zhu C., Xue W. (2023), Bioremediation of desiccation cracking in clayey soils using enzyme induced calcite precipitation, *Geo-Congress*, pp. 603–613, https://doi.org/10.1061/9780784484708.057
- Qi Y., Gao Y., Meng H., He J., Liu Y. (2022), Biocementation via soybean-urease induced carbonate precipitation using carbide slag powder derived soluble calcium, *Geomechanics and Engineering*, 29(1), pp. 79-90, https://doi.org/10.12989/gae.2022.29.1.079
- Santomauro G., Baier J., Huang W., Pezold S., Bill J. (2012), Formation of calcium carbonate polymorphs induced by living microalgae, *Journal of Biomaterials and Nanobiotechnology*, 3(4), pp. 413-420, https://doi.org/10.4236/jbnb.2012.34041
- Scala G.D., Volontè F., Ricci G., Pedersen M.B., Arioli S., Mora D. (2019), Development of a milk-based medium for the selection of urease-defective mutants of Streptococcus thermophilus, *International Journal of Food Microbiology*, 308, 108304, https://doi.org/10.1016/j.ijfoodmicro.2019.108304
- Seifan M., Berenjian A. (2019), Microbially induced calcium carbonate precipitation: A widespread phenomenon in the biological world, *Applied Microbiology and Biotechnology*, 103, pp. 4693–4700, https://doi.org/10.1007/s00253-019-09861-5
- Sidhu N., Goyal S., Reddy M.S. (2022), Biomineralization of cyanobacteria Synechocystis pevalekii improves the durability properties of cement mortar, *AMB Express*, 12, 59, https://doi.org/10.1186/s13568-022-01403-z
- Son Y., Min J., Jang I., Park J., Yi C., Park W. (2024), Enhanced mechanical properties of living and regenerative building materials by filamentous Leptolyngbya boryana, *Cell Reports Physical Science*, 8, 102098, https://doi.org/10.1016/j.xcrp.2024.102098
- Sorum M.G., Kalita A. (2023), Effect of bio-cementation with rice husk ash on permeability of silty sand, *Civil Engineering Journal*, 9(11), pp. 2854–2867, https://doi.org/10.28991/CEJ-2023-09-11-016
- Sreekala A.G.V., Nair S., Nathan V.K. (2024), Microbially induced calcium carbonate precipitation using *Lysinibacillus* sp.: A ureolytic bacterium from Uttarakhand for soil

- stabilization, Current Microbiology, 81(11), 387, https://doi.org/10.1007/s00284-024-03899-z
- Stabnikov V., Chu J., Ivanov V., Li Y. (2013a), Halotolerant, alkaliphilic urease-producing bacteria from different climate zones and their application for biocementation of sand, *World Journal of Microbiology and Biotechnology*, 29(8), pp. 1453–1460, https://doi.org/10.1007/s11274-013-1309-1311
- Stabnikov V., Chu J., Myo A.N., Ivanov V. (2013b), Immobilization of sand dust and associated pollutants using bioaggregation, *Water, Air, & Soil Pollution*, 224(9), pp. 1631–1700, https://doi.org/10.1007/s11270-013-1631-0
- Stabnikov V. (2016), Production of bioagent for calcium-based biocement, *International Journal of Biotechnology for Wellness Industries*, 5(2), pp. 60–69, https://doi.org/10.6000/1927-3037.2016.05.02.5
- Stabnikov V., Ivanov V., Chu J. (2015), Construction biotechnology A new area of biotechnological research and applications, *World Journal of Microbiology and Biotechnology*, 31(9), pp. 1303–1314, https://doi.org/10.1007/s11274-015-1881-7
- Stabnikov V., Ivanov V., Chu J. (2016), Sealing of sand using spraying and percolating biogrouts for the construction of model aquaculture pond in arid desert, *International Aquatic Research*, 8(3), pp. 207–216, https://link.springer.com/article/10.1007/s40071-016-0136-7
- Stabnikov V., Stabnikov D., Udymovych V. (2022), Increase the ecological safety of the soil biogrouting using plant urease, *Ukrainian Food Journal*, 11(2), pp. 302–314, https://doi.org/10.24263/2304-974X-2022-11-2-10
- Stabnikov V., Udymovych V., Kovshar I., Stabnikov D. (2024), Microbial producer of acid urease and its applications for biocementation, *Ukrainian Food Journal*, 13(2), pp. 331-350, https://doi.org/10.24263/2304-974X-2024-13-2-10
- Stabnikov V., Kovshar I., Stabnikova O. (2025), Recent advances in the study of the properties and applications of lactic acid bacteria, *World Journal of Microbiology and Biotechnology*, 41, 287, https://doi.org/10.1007/S11274-025-04499-0
- Stabnikova O., Antonuk M., Stabnikov V., Arsen'eva L. (2019), Ukrainian dietary bread with selenium-enriched malt, *Plant Foods for Human Nutrition*, 74(2), pp. 157–163, https://doi.org/10.1007/s11130-019-00731-z
- Stabnikova O., Stabnikov V., Antoniuk M., Arsenieva L., Ivanov V. (2022). Bakery products enriched with organoselenium compounds. In: O. Paredes-Lopez, V. Stabnikov, O. Shevchenko, V. Ivanov (Eds.), *Bioenhancement and Fortification of Foods for a Healthy Diet*, pp. 89 111, CRC Press, Boca Raton, https://doi.org/10.1201/9781003225287
- Stabnikova O., Khonkiv M., Kovshar I., Stabnikov V. (2023), Biosynthesis of selenium nanoparticles by lactic acid bacteria and areas of their possible applications, *World Journal of Microbiology and Biotechnology*, 39, 230, https://doi.org/10.1007/s11274-023-03673-6
- Statista. (2023), Carbon dioxide emissions from the manufacture of cement worldwide in from 1990 to 2022, by select country, https://www.statista.com/statistics/1091672/carbon-dioxide-emissions-global-cement-manufacturing/
- Stocks-Fischer S., Galinat J.K., Bang S.S. (1999), Microbiological precipitation of CaCO₃, *Soil Biology and Biochemistry*, 31(11), pp. 1563–1571, https://doi.org/10.1016/S0038-0717(99)00082-6
- Shu S., Yan B., Ge B., Li S., Meng H. (2022), Factors affecting soybean crude urease extraction and biocementation via enzyme-induced carbonate precipitation (EICP) for soil improvement, *Energies*, 15(5), 5566, https://doi.org/10.3390/en15155566
- Su F., Yang Y., Qi Y., Zhang H. (2022), Combining microbially induced calcite precipitation (MICP) with zeolite: A new technique to reduce ammonia emission and enhance soil

- treatment ability of MICP technology, *Journal of Environmental Chemical Engineering*, 10(3), 107770, https://doi.org/10.1016/j.jece.2022.107770
- Sun X., Miao L., Wu L., Chen R. (2019), Improvement of bio-cementation at low temperature based on *Bacillus megaterium*, *Applied Microbiology and Biotechnology*, 103(17), pp. 7191-7202, https://doi.org/10.1007/s00253-019-09986-7
- Sun X., Miao L., Wang H., Wu L., Fan G., Xia J. (2022), Sand foreshore slope stability and erosion mitigation based on microbiota and enzyme mix–induced carbonate precipitation, *Journal of Geotechnical and Geoenvironmental Engineering*, 148(8), 04022058, https://doi.org/10.1061/(asce)gt.1943-5606.0002839
- Tayyem N.E.S.A., Elhello K.T.M., Elmanama A.A. (2021), Isolation, identification and growth conditions of calcite producing bacteria from urea-rich soil, *African Journal of Microbiology Research*, 15(1), pp. 37-46, https://doi.org/10.5897/AJMR2020.9445
- Toshima T., Hamai R., Tafu M., Takemura Y., Fujita S., Chohji T., Tanda S., Li S., Qin G.W. (2014), Morphology control of brushite prepared by aqueous solution synthesis, *Journal of Asian Ceramic Societies*, 2, pp. 52–56, https://doi.org/10.1016/j.jascer.2014.01.004
- Udymovych V. (2021), Lactic acid bacteria as producers of urease, *Scientific Works of NUFT*, 27(3), pp. 25-31, https://doi.org/10.24263/2225-2924-2021-27-3-5
- van Paassen L.A., Ghose R., van der Linden T.J.M., van der Star W.R.L., van Loosdrecht M.C.M. (2010), Quantifying biomediated ground improvement by ureolysis: Large-scale biogrout experiment, *Journal of Geotechnical and Geoenvironmental Engineering*, 136(12), pp. 1721–1728, https://doi.org/10.1061/(ASCE)GT.1943-5606.0000382
- Varalakshmi V., Devi A. (2014), Isolation and characterization of urease utilizing bacteria to produce biocement, *IOSR Journal of Environmental Science, Toxicology and Food Technology*, 8, pp. 52-57, https://doi.org/10.9790/2402-084252
- Vashisht R., Attri S., Sharma D., Shukla A., Goel G. (2018), Monitoring biocalcification potential of *Lysinibacillus* sp. isolated from alluvial soils for improved compressive strength of concrete, *Microbiological Research*, 207, pp. 226-231, https://doi.org/10.1016/j.micres.2017.12.010.
- Wang Q., Wang Z., Li C., Qiao X., Guan H., Zhou Z., Song D. (2024), Research progress in corrosion behavior and anti-corrosion methods of steel rebar in concrete, *Metals*, 14(8), 862, https://doi.org/10.3390/met14080862
- Wang W., He X., Wu S., Chu J. (2024), Presence of Mg-calcite and its influence on MICP and EICP processes, *Journal of Rock Mechanics and Geotechnical Engineering* (Available online 12 November 2024), https://doi.org/10.1016/j.jrmge.2024.09.045
- Wang Z., Zhang N., Cai G., Jin Y., Ding N., Shen D. (2017), Review of ground improvement using microbial induced carbonate precipitation (MICP), *Marine Georesources & Geotechnology*, 35, pp. 495–503, https://doi.org/10.1080/1064119X.2017.1297877
- Wani S., Geça M.J., Selvaraj T., Priya T.S. (2024), Assessing the influence of *Bacillus megaterium* and *Bacillus sphaericus* in cementitious materials: Promoting sustainability towards strength, durability and crack repair, *Ain Shams Engineering Journal*, 15(6), 102748, https://doi.org/10.1016/j.asej.2024.102748
- Warthman R., van Lith Y., Vasconcelos C., Mckenzie J.A., Karpoff A.M. (2000), Bacterially induced dolomite precipitation in anoxic culture experiment, *Geology*, 28(12), pp. 1091–1094, https://doi.org/10.1130/0091-7613(2000)28<1091:bidpia>2.0.co;2
- Weng Y., Zheng J., Lai H., Cui M., Ding X. (2024), Biomineralization of soil with crude soybean urease using different calcium salts, *Journal of Rock Mechanics and Geotechnical Engineering*, 16, pp. 1788-1798, https://doi.org/10.1016/j.jrmge.2023.09.033
- Whiffin V.S. (2004), Microbial CaCO₃ precipitation for the production of biocement, PhD thesis, School of Biological Sciences and Biotechnology, Murdoch University, Perth.

- Whiffin V.S., van Paassen L.A., Harkes M.P. (2007), Microbial carbonate precipitation as a soil improvement technique, *Geomicrobiology Journal*, 24(5), pp. 417–423, https://doi.org/10.1080/01490450701436505
- Wilson C.M., Loach D., Lawley B., Bell T., Sims I., O'Toole P.W., Zomer A., Tannock G.W. (2014), *Lactobacillus reuteri* 100-23 modulates urea hydrolysis in the murine stomach, *Applied and Environmental Microbiology*, 80(19), pp. 6104–6113, https://doi.org/10.1128/AEM.01876-14
- Wright D.T., Oren A. (2005), Nonphotosynthetic bacteria and the formation of carbonates and evaporates through time, *Geomicrobiology Journal*, 22(1-2), pp. 27–53, https://doi.org/10.1080/01490450590922532
- Wunthunyarat W., Seo H., Wang Y. (2020), Effects of germination conditions on enzyme activities and starch hydrolysis of long-grain brown rice in relation to flour properties and bread qualities, *Journal of Food Science*, 85(2), pp. 349-357, https://doi.org/10.1111/1750-3841.15008
- Xiang J., Qiu J., Wang Y., Gu X. (2022), Calcium acetate as calcium source used to biocement for improving performance and reducing ammonia emission, *Journal of Cleaner Production*, 348, 131286, https://doi.org/10.1016/j.jclepro.2022.131286
- Xiao Y., He X., Evans T.M., Stuedlein A.W., Liu H. (2019), Unconfined compressive and splitting tensile strength of basalt fiber–reinforced biocemented sand, *Journal of Geotechnical and Geoenvironmental Engineering*, 145(9), 04019048, https://doi.org/10.1061/(asce)gt.1943-5606.0002108.
- Xu G., Li D., Jiao B., Li D., Yin Y., Lun L., Zhao Z., Li S. (2017), Biomineralization of a calcifying ureolytic bacterium *Microbacterium* sp. GM-1, *Electronic Journal of Biotechnology*, 25, pp. 21–27, https://doi.org/10.1016/j.ejbt.2016.10.008
- Xu X., Guo H., Cheng X., Li M. (2020), The promotion of magnesium ions on aragonite precipitation in MICP process, *Construction Building Material*, 263, 120057, https://doi.org/10.1016/j.conbuildmat.2020.120057
- Yan Z., Nakashima K., Takano C., Kawasaki S. (2024), Feasibility study of enhancing enzyme-induced carbonate precipitation with eggshell waste for sand solidification, Biogeotechnics, 2(4), 100108, https://doi.org/10.1016/j.bgtech.2024.100108
- Yan Z., Nakashima K., Takano C., Kawasaki S. (2025), Strategies for cost-optimized biocement production: A comprehensive review, *World Journal of Microbiology and Biotechnology*, 41, 67, https://doi.org/10.1007/s11274-025-04281-2
- Yang Y., Chu J., Cao B., Liu H., Cheng L. (2020), Biocementation of soil using non-sterile enriched urease-producing bacteria from activated sludge, *Journal of Cleaner Production*, 262, 121315, https://dx.doi.org/10.1016/j.jclepro.2020.121315
- Yang Y., Chu J., Cheng L., Liu H. (2022), Utilization of carbide sludge and urine for sustainable biocement production, *Journal of Environmental Chemical Engineering*, 10(3), 107443, https://doi.org/10.1016/j.jece.2022.107443
- Yoosathaporn S., Tiangburanatham P., Bovonsombut S., Chaipanich A., Pathom-Aree W. (2016), A cost effective cultivation medium for biocalcification of *Bacillus pasteurii* KCTC 3558 and its effect on cement cubes properties, *Microbiological Research*, 186-187, pp. 132-138, https://doi.org/10.1016/j.micres.2016.03.010
- Young J.R., Henriksen K.F. (2003), Biomineralization within vesicles: The calcite of Coccoliths, *Reviews in Mineralogy & Geochemistry*, 54(1), 189–215, https://doi.org/10.2113/0540189
- Yu X., Chu J., Yang Y., Qian C. (2021), Reduction of ammonia production in the biocementation process for sand using a new biocement, *Journal of Cleaner Production*, 286, 124928, https://doi.org/10.1016/j.jclepro.2020.124928
- Yuan H., Ren G., Liu K., Zheng W., Zhao Z. (2020), Experimental study of EICP combined with organic materials for silt improvement in the yellow river flood area, *Applied Sciences*, 10(21), 7678, https://doi.org/10.3390/app10217678

---- Microbiology, Biotechnology-----

- Zhang Y., Guo H., Cheng X. (2014), Influences of calcium sources on microbially induced carbonate precipitation in porous media, *Materials Research Innovations*, 18, S2-79-S2-84, https://doi.org/10.1179/1432891714Z.00000000038
- Zhou P., Jiang Y., Adeel M., Shakoor N., Zhao W., Liu Y., Li Y., Li M., Azeem I., Rui Y., Tan Z., White J.C., Guo Z., Lynch I., Zhang P. (2023), Nickel oxide nanoparticles improve soybean yield and enhance nitrogen assimilation, *Environmental Science & Technology*, 57(19), pp. 7547-7558, https://doi.org/10.1021/acs.est.3c00959
- Zhu T., Dittrich M. (2016), Carbonate precipitation through microbial activities in natural environment, and their potential in biotechnology: A review, *Frontiers in Bioengineering and Biotechnology*, 4, 4, https://doi.org/10.3389/fbioe.2016.00004

Cite:

UFJ Style

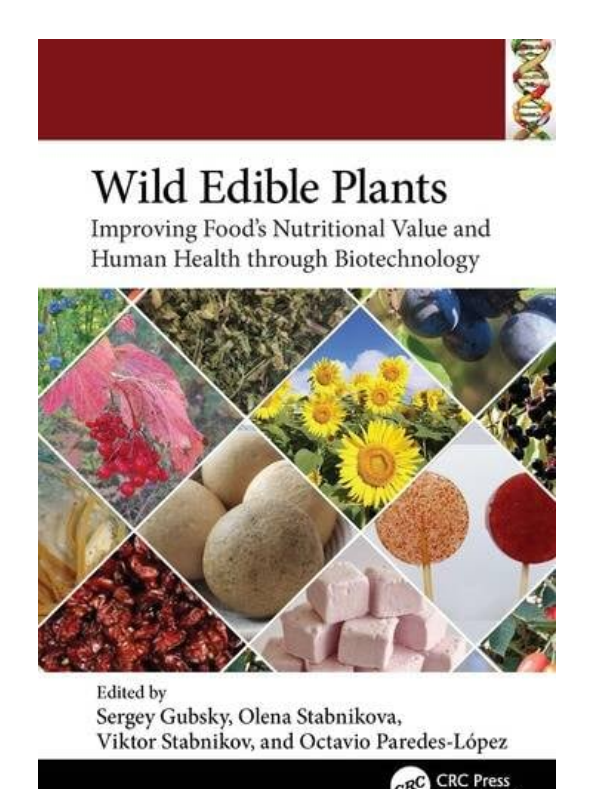
Stabnikov V., Kovshar I., Stabnikov D. (2025), Biotechnology approaches and improvement strategies in biocement production, *Ukrainian Food Journal*, 14(3), pp. 521–553, https://doi.org/10.24263/2304-974X-2025-14-3-11

APA Style

Stabnikov, V., Kovshar, I., & Stabnikov, D. (2025). Biotechnology approaches and improvement strategies in biocement production. *Ukrainian Food Journal*, *14*(3), 521–553. https://doi.org/10.24263/2304-974X-2025-14-3-11

"Wild edible plants: Improving foods nutritional value and human health through biotechnology": International Research Publications by Ukrainian Scientists

The authoritative international publishing house of scientific literature CRC Press Taylor & Francis group published the book "Wild edible plants: Improving foods nutritional value and human health through biotechnology" under the leadership of the famous biochemist and nutritionist Octavio Paredes-López, which includes the studies of Ukrainian scientists.



Wild plants have been used by humans as an important source of nutrition since ancient times. They are rich in health-promoting compounds such as phenols, flavonoids, antioxidants, vitamins, trace elements, and dietary fibers. When incorporated into food products, these materials enhance the nutritional value, functionality, and sensory qualities of traditional foods. This book explores the biotechnological approaches to developing meat, bakery, and confectionery products, as well as beverages, enriched with wild edible plants. It highlights recent advancements in the use of wild plants as natural emulsifiers, stabilizers, and thickeners in water-in-oil emulsion-based food systems. Additionally, it discusses the potential applications of edible algae and wild mushrooms in both food and medicine.

— Education and Science News —

Key Features include:

- Describes novel functional foods utilizing edible wild plant-based raw materials
- Presents innovative technologies for producing meat, bakery, and confectionery products and beverages enriched with wild plant-based ingredients
- Proposes the application of wild plants in water-in-oil emulsion-based food systems
- Explores the use of wild algae in the development of functional food products
- Covers the medicinal applications of wild edible mushrooms

This book presents recent advances in food biotechnology and serves as a visual educational tool, providing comprehensive knowledge about wild edible plants, algae, and mushrooms, along with their applications in food production. It is designed for students, educators, researchers, and professionals in the food industry and biotechnology sectors. Moreover, it offers a valuable resource for developers of innovative food technologies.

The book "Wild edible plants: Improving foods nutritional value and human health through biotechnology" is the third publication by Ukrainian scientists published in the series of books and collections "Food Biotechnology and Engineering". The first book, "Bioenhancement and fortification of foods for a healthy diet", was published in 2022, followed by the second, "Bioconversion of waste to value - added products" in 2023.

Detailed information about the Book: https://doi.org/10.1201/9781003486794

https://doi.org/10.24263/2304-974X-2025-14-3-12

Instructions for authors

Dear colleagues!

The Editorial Board of scientific periodical

Ukrainian Food Journal

invites you to publish your research findings in our journal



Manuscripts should present original research that has not been previously published and is not under consideration for publication elsewhere. Submission of the manuscript implies that its publication has been approved by all co-authors and by the appropriate institutional authorities at the organization where the research was conducted.

A cover letter to the editor is mandatory and should include a brief description of the research topic, its novelty and significance. The letter must also confirm that all authors agree to submit the manuscript to the Ukrainian Food Journal and that the work is original and authored solely by the listed contributors.

Manuscript requirements

Authors must prepare the manuscript according to the guide for authors. Editors reserve the right to adjust the style to certain standards of uniformity.

Language – English

Manuscripts should be submitted in Word.

Use 1.0 spacing and 2 cm margins.

Use a normal font 14-point Times New Roman for text, tables, and in the figure captions.

Present tables and figures in the text of manuscript.

Consult a recent issue of the journal for a style check.

Number all pages consecutively.

Abbreviations should be defined on first appearance in text and used consistently thereafter. No abbreviation should be used in title and section headings.

Please submit math equations as editable text and not as images (It is recommend software application MathType or Microsoft Equation Editor).

Minimal size of the article (without the Abstract and References) is 10 pages. For review article is 25 pages (without the Abstract and References).

Manuscript should include:

Title (should be concise and informative). Avoid abbreviations in it.

Authors' information: the name(s) of the author(s); the affiliation(s) of the author(s), city, country. One author has been designated as the corresponding author with e-mail address. If available, the 16-digit ORCID of the author(s) information on the title page.

Declaration of interest

Author Contribution Statement

Abstract. The **abstract** should contain the following mandatory parts:

Introduction provides a rationale for the study (2–3 lines).

Materials and methods briefly describe the materials and methods used in the study (3–5 lines).

Results and discussion describe the main findings (20–26 lines).

Conclusions provides the main conclusions (2–3 lines).

The abstract should not contain any undefined abbreviations or references to the articles.

Keywords. Immediately after the abstract provide 4 to 6 keywords.

Text of manuscript

References

Manuscripts should be divided into the following sections:

Introduction
Materials and methods
Results and discussion
Conclusions
References

Introduction. Provide a background avoiding a detailed review of literature and declare the aim of the present research. Identify unexplored questions, prove the relevance of the topic. The Introduction section should not exceed 1.5 pages in length.

Materials and methods. Provide sufficient detail to enable an independent researcher to replicate the study. For methods that are already published, cite the original source and summarize the procedure briefly. Detailed descriptions are required only for new techniques or significant modifications of existing methods.

Results and discussion. Results should be presented clearly and concisely, supported by appropriate tables and/or figures. The significance of the findings should be discussed in the context of existing literature, highlighting similarities, differences, and potential implications.

Conclusions. Conclusions should be clearly derived from the study's findings and summarized briefly in a separate Conclusion section.

Acknowledgments (if necessary). Acknowledgments of individuals, grants, or funding sources should be included in a separate section. List all persons who contributed assistance during the research. Names of funding organizations must be written in full.

Organize your article into clearly defined sections and, if necessary, subsections. Each subsection should have a concise and descriptive heading.

References

Please, check references carefully.

The list of references should include works that are cited in the text and that have been published or accepted for publication.

All references mentioned in the reference list are cited in the text, and vice versa.

Cite references in the text by name and year in parentheses. Some examples:

(Drobot, 2008); (Qi and Zhou, 2012); (Bolarinwa et al., 2019; Rabie et al., 2020; Sengev et al., 2013).

Reference list should be alphabetized by the last name of the first author of each work. If available, please always include DOIs links in the reference list.

Reference style

Journal article

Please follow this style and order: author's surname, initial(s), year of publication (in brackets), paper title, *Journal title (in Italic)*, volume number (issue), first and last page numbers. If available, please always include DOIs as full DOI links in your reference list (e.g. "https://doi.org/abc").

Journal names should not be abbreviated.

Popovici C., Gitin L., Alexe P. (2013), Characterization of walnut (*Juglans regia* L.) green husk extract obtained by supercritical carbon dioxide fluid extraction, *Journal of Food and Packaging Science*, *Technique and Technologies*, 2(2), pp. 104–108, https://doi.org/11.1016/22-33-85

Book

Deegan C. (2000), Financial Accounting Theory, McGraw-Hill Book Company, Sydney.

Book chapter in an edited book

Kochubei-Lytvynenko O., Kuzmyk U., Yushchenko N. (2022), Spices for dairy products. In: O. Paredes-López, O. Shevchenko, V. Stabnikov, V. Ivanov (Eds.), *Bioenhancement and Fortification of Foods for a Healthy Diet*, pp. 157–178, CRC Press, Boca Raton, https://doi.org/10.1201/9781003225287-11

Online document

Mendeley J.A., Thomson, M., Coyne R.P. (2017), *How and When to Reference*, Available at: https://www.howandwhentoreference.com

Conference paper

Arych M. (2018), Insurance's impact on food safety and food security, *Resource and Energy Saving Technologies of Production and Packing of Food Products as the Main Fundamentals of Their Competitiveness: Proceedings of the 7th International Specialized Scientific and Practical Conference, September 13, 2018*, NUFT, Kyiv, pp. 52–57, https://doi.org/11.1016/22-33-85

Figures

All figures must be created using a graphic editor with Arial font.

The font size on the figures and the text of the article should be the same.

Black and white graphic with no shading should be used.

The figure elements (lines, grid, and text) should be presented in black (not gray) colour.

Figure parts should be denoted by lowercase letters (a, b, etc.).

All figures are to be numbered using Arabic numerals.

Figures should be cited in text in consecutive numerical order.

Place figure after its first mentioned in the text.

Figure captions begin with the term Figure in bold type, followed by the figure number, also in bold type.

Each figure should have a caption describing what the figure depicts in bold type.

Submit all figures along with the corresponding Excel files containing the graph data as separate attachments.

If your manuscript includes figures previously published elsewhere, you must obtain permission from the copyright owner(s) prior to submission.

Tables

Number tables consecutively in accordance with their appearance in the text.

Place footnotes to tables below the table body and indicate them with superscript lowercase letters.

Place table after its first mentioned in the text.

Ensure that the data presented in tables do not duplicate results described elsewhere in the article.

Suggesting / excluding reviewers

Authors may suggest reviewers and/or request the exclusion of certain individuals when submitting their manuscripts.

When suggesting reviewers, authors should make sure they are totally independent and not connected to the work in any way. When suggesting reviewers, the Corresponding Author must provide an institutional email address for each suggested reviewer. Please note that the Journal may not use the suggestions, but suggestions are appreciated and may help facilitate the peer review process.

Submission

Email for all submissions and other inquiries:

ufj nuft@meta.ua

Шановні колеги!

Редакційна колегія наукового періодичного видання «**Ukrainian Food Journal**» запрошує Вас до публікації результатів наукових досліджень.

Вимоги до оформлення статей

Мова статей – англійська.

Мінімальний обсяг статті — 10 сторінок формату A4 (без врахування анотацій і списку літератури).

Для всіх елементів статті шрифт — **Times New Roman**, кегль — **14**, інтервал — 1. Всі поля сторінки — по 2 см.

Структура статті:

- 1. Назва статті.
- 2. Автори статті (ім'я та прізвище повністю, приклад: Денис Озерянко).
- 3. Установа, в якій виконана робота.
- 4. Анотація. Обов'язкова структура анотації:
 - Вступ (2–3 рядки).
 - Матеріали та методи (до 5 рядків)
 - Результати та обговорення (пів сторінки).
 - Висновки (2–3 рядки).
- 6. Ключові слова (3–5 слів, але не словосполучень).

Пункти 2-6 виконати англійською і українською мовами.

- 7. Основний текст статті. Має включати такі обов'язкові розділи:
 - Вступ
 - Матеріали та методи
 - Результати та обговорення
 - Висновки
 - Література.

За необхідності можна додавати інші розділи та розбивати їх на підрозділи.

- 8. Авторська довідка (Прізвище, ім'я та по батькові, вчений ступінь та звання, місце роботи, електронна адреса або телефон).
- 9. Контактні дані автора, до якого за необхідності буде звертатись редакція журналу.

Рисунки виконуються якісно. Скановані рисунки не приймаються. Розмір тексту на рисунках повинен бути **співрозмірним** (!) тексту статті. **Фотографії можна використовувати** лише за їх значної наукової цінності.

Фон графіків, діаграм – лише білий. Колір елементів рисунку (лінії, сітка, текст) – чорний (не сірий).

Рисунки та графіки EXCEL з графіками додатково подаються в окремих файлах.

Скорочені назви фізичних величин в тексті та на графіках позначаються латинськими літерами відповідно до системи СІ.

У списку літератури повинні переважати англомовні статті та монографії, які опубліковані після 2010 року.

Оформлення цитат у тексті статті:

Кількість авторів статті	Приклад цитування у тексті	
1 автор	(Arych, 2019)	
2 автора	(Kuievda and Bront, 2020)	
3 і більше авторів	(Bazopol et al., 2022)	

Приклад тексту із цитуванням: It is known (Arych, 2019; Bazopol et al., 2022), the product yield depends on temperature, but, there are some exceptions (Kuievda and Bront, 2020).

У цитуваннях необхідно вказувати джерело, звідки взято інформацію.

Список літератури сортується за алфавітом, літературні джерела не нумеруються.

Правила оформлення списку літератури

В Ukrainian Food Journal взято за основу загальноприйняте в світі спрощене оформлення списку літератури згідно стандарту Garvard. Всі елементи посилання розділяються лише комами.

1. Посилання на статтю:

Автори А.А. (рік видання), Назва статті, *Назва журналу (курсивом)*, Том (номер), сторінки, DOI.

Ініціали пишуться після прізвища.

Всі елементи посилання розділяються комами.

Вказуються всі автори.

Назву журналу скорочувати не можна.

Приклад:

Popovici C., Gitin L., Alexe P. (2013), Characterization of walnut (*Juglans regia* L.) green husk extract obtained by supercritical carbon dioxide fluid extraction, *Journal of Food and Packaging Science, Technique and Technologies*, 2(2), pp. 104–108, https://doi.org/5533.935-3.

2. Посилання на книгу:

Автори (рік), Назва книги (курсивом), Видавництво, Місто.

Ініціали пишуться після прізвища.

Всі елементи посилання розділяються комами.

Приклад:

Deegan C. (2000), Financial Accounting Theory, McGraw-Hill Book Company, Sydney.

3. Посилання на розділ у редагованій книзі:

Автори (рік), Назва глави, Іп: Редактори, *Назва книги (курсивом)*, Сторінки, Видавництво, Місто.

Приклад:

Kochubei-Lytvynenko O., Kuzmyk U., Yushchenko N. (2022), Spices for dairy products, In: O. Paredes-López, O. Shevchenko, V. Stabnikov, V. Ivanov (Eds.), *Bioenhancement and Fortification of Foods for a Healthy Diet*, pp. 157–178, CRC Press, Boca Raton, https://doi.org/10.1201/9781003225287-11

4. Тези доповідей конференції:

Arych M. (2018), Insurance's impact on food safety and food security, *Resource and Energy Saving Technologies of Production and Packing of Food Products as the Main Fundamentals of Their Competitiveness: Proceedings of the 7th International Specialized Scientific and Practical Conference, September 13, 2018*, NUFT, Kyiv, pp. 52–57, https://doi.org/5533.935-3.

5. Посилання на електронний ресурс:

Виконується аналогічно посиланню на книгу або статтю. Після оформлення даних про публікацію пишуться слова **Available at:** та вказується електронна адреса.

Приклад:

Cheung T. (2011), *World's 50 most delicious drinks*, Available at: http://travel.cnn.com/explorations/drink/worlds-50-most-delicious-drinks-883542

Список літератури оформлюється лише латиницею. Елементи списку українською та російською мовою потрібно транслітерувати. Для транслітерації з українською мови використовується паспортний стандарт.

Зручний сайт для транслітерації з української мови: http://translit.kh.ua/#lat/passport

Стаття надсилається за електронною адресою:

ufj nuft@meta.ua

Ukrainian Food Journal публікує оригінальні наукові статті, короткі повідомлення, оглядові статті, новини та огляди літератури.

Тематика публікацій в Ukrainian Food Journal:

Харчова інженерія Процеси та обладнання

Харчова хімія Нанотехнології

Якість та безпека харчових продуктів Упаковка для харчових продуктів

Періодичність виходу журналу 4 номери на рік.

Результати досліджень, представлені в журналі, повинні бути новими, мати чіткий зв'язок з харчовою наукою і представляти інтерес для міжнародного наукового співтовариства.

Ukrainian Food Journal індексується наукометричними базами:

- Index Copernicus (2012)
- EBSCO (2013)
- Google Scholar (2013)
- UlrichsWeb (2013)
- CABI full text (2014)
- Online Library of University of Southern Denmark (2014)
- Directory of Open Access scholarly Resources (ROAD) (2014)
- European Reference Index for the Humanities and the Social Sciences (ERIH PLUS) (2014)
- Directory of Open Access Journals (DOAJ) (2015)
- InfoBase Index (2015)
- Chemical Abstracts Service Source Index (CASSI) (2016)
- FSTA (Food Science and Technology Abstracts) (2018)
- Web of Science (Emerging Sourses Citaton Index) (2018)
- Scopus (2022)

Рецензія рукопису статті. Матеріали, представлені для публікування в «Ukrainian Food Journal», проходять «Подвійне сліпе рецензування» двома вченими, призначеними редакційною колегією: один ϵ членом редколегії і один незалежний науковець.

Авторське право. Автори статей гарантують, що робота не ε порушенням будь-яких авторських прав, та відшкодовують видавцю порушення даної гарантії. Опубліковані матеріали ε правовою власністю видавця «**Ukrainian Food Journal**», якщо не узгоджено інше.

Детальна інформація про Журнал, інструкції авторам, приклади оформлення статті та анотацій розмішені на сайті:

http://ufj.nuft.edu.ua

Ukrainian Food Journal

Редакційна колегія

Головний редактор:

Олена Стабнікова, д.р., Національний університет харчових технологій, Україна

Члени міжнародної редакційної колегії:

Агота Гедре Райшене, д-р., Литовський інститут аграрної економіки, Литва В. І. Вернадського НАН України

Бао Тхи Вуронг, д-р., Університет Меконгу, В'єтнам

Годвін Д. Ндоссі, професор, *Меморіальний університет Хуберта Кайрукі, Дар-ес-*Салам, Танзанія

Дора Марінова, професор, Університет Кертіна, Австралія

Егон Шніцлер, д-р, професор, Державний університет Понта Гросси, Бразилія

Ейрін Марі Скйондал Бар, д-р., професор, *Норвезький університет науки і техніки, Тронхейм, Норвегія*

Йорданка Стефанова, д-р, Пловдівський університет "Паісій Хілендарскі", Болгарія **Кірстен Бранд**т, професорр, Університет Ньюкасла, Великобританія

Крістіна Луїза Міранда Сілва, д-р., професор, *Португальський католицький університет – Біотехнологічний коледж, Португалія*

Крістіна Попович, д-р., доцент, Технічний університет Молдови

Лелівельд Хуб, асоціація «Міжнародна гармонізаційна ініціатива», Нідерланди

Марія С. Тапіа, професор, *Центральний університет Венесуели, Каракас, Венесуела* **Мойзес Бурачик**, д-р., *Інститут сільськогосподарської біотехнології Покапіо* (INDEAR), Покапіо, Аргентина

Октавіо Паредес Лопес, д-р., проф, *Центр перспективних досліджень Національного політехнічного інституту, Мексика*.

Олександр Шевченко, д.т.н., проф., *Національний університет харчових технологій,* Україна

Рана Мустафа, д-р., Глобальний інститут продовольчої безпеки, Університет Саскачевана, Канада

Семіх Отлес, д-р., проф. Університет Еге, Туреччина

Соня Амарей, д-р., проф, Університет «Штефан чел Маре», Сучава, Румунія

Станка Дам'янова, д.т.н., проф., *Русенський університет «Ангел Канчев»*, філія *Разград*, *Болгарія*

Стефан Стефанов, д.т.н., проф., Університет харчових технологій, Болгарія

Тетяна Пирог, д.б.н., проф., *Національний університет харчових технологій, Україна* **Умезуруйке Лінус Опара**, професор, *Стелленбошський університет*, *Кейптаун, Південна Африка*

Шейла Кілонзі, Університет Каратіна, Кенія

Юлія Дзязько, д-р. хім. наук, с.н.с., *Інститут загальної та неорганічної хімії імені В. І. Вернадського НАН України*

Юн-Хва Пеггі Хсі, д-р, професор, Університет Флориди, США

Юрій Білан, д-р., проф., Університет Томаша Баті в Зліні, Чехія

Ясміна Лукінак, д.т.н., професор, Університет Осієка, Хорватія

Ясміна Лукінак, д-р, проф., Осієкський університет, Хорватія.

Члени редакційної колегії:

Агота Гедре Райшене, д-р., Литовський інститут аграрної економіки, Литва **Бао Тхи Вуронг**, д-р., Університет Меконгу, В'єтнам

Валерій Мирончук, д-р. техн. наук, проф., *Національний університет харчових технологій*, *Україна*

Володимир Ковбаса, д-р. техн. наук, проф., *Національний університет харчових технологій, Україна*

Галина Сімахіна, д-р. техн. наук, проф., *Національний університет харчових технологій, Україна*

Годвін Д. Ндоссі, професор, *Меморіальний університет Хуберта Кайрукі, Дар-ес-*Салам, Танзанія

Дора Марінова, професор, Університет Кертіна, Австралія

Егон Шніцлер, д-р, професор, Державний університет Понта Гросси, Бразилія

Ейрін Марі Скйондал Бар, д-р., професор, *Норвезький університет науки і техніки, Тронхейм, Норвегія*

Йорданка Стефанова, д-р, Пловдівський університет "Паісій Хілендарскі", Болгарія **Кірстен Бран**дт, професорр, Університет Ньюкасла, Великобританія

Крістіна Луїза Міранда Сілва, д-р., професор, *Португальський католицький університет – Біотехнологічний коледж, Португалія*

Крістіна Попович, д-р., доцент, Технічний університет Молдови

Лада Шерінян, д-р. екон. наук, професор., *Національний університет харчових технологій, Україна*

Лелівельд Хуб, асоціація «Міжнародна гармонізаційна ініціатива», Нідерланди

Марія С. Тапіа, професор, *Центральний університет Венесуели, Каракас, Венесуела* **Мойзес Бурачик**, д-р., *Інститут сільськогосподарської біотехнології Покапіо (INDEAR), Покапіо, Аргентина*

Октавіо Паредес Лопес, д-р., проф, Центр перспективних досліджень Національного політехнічного інституту, Мексика.

Олександр Шевченко, д.т.н., проф., *Національний університет харчових технологій,* Україна

Ольга Рибак, канд. техн. наук, доц., *Тернопільський національний технічний* унівреситет імені Івана Пулюя, Україна

Рана Мустафа, д-р., Глобальний інститут продовольчої безпеки, Університет Саскачевана, Канада

Семіх Отлес, д-р., проф. Університет Еге, Туреччина

Соня Амарей, д-р., проф. Університет «Штефан чел Маре», Сучава, Румунія

Станка Дам'янова, д.т.н., проф., *Русенський університет «Ангел Канчев», філія Разград, Болгарія*

Стефан Стефанов, д.т.н., проф., Університет харчових технологій, Болгарія

Тетяна Пирог, д-р. біол. наук, проф., *Національний університет харчових технологій,* Україна

Умезуруйке Лінус **Опара**, професор, *Стелленбошський університет, Кейптаун,* Південна Африка

Шейла Кілонзі, Університет Каратіна, Кенія

Юлія Дзязько, д-р. хім. наук, с.н.с., *Інститут загальної та неорганічної хімії імені В. І. Вернадського НАН України*

Юн-Хва Пеггі Хсі, д-р, професор, Університет Флориди, США

Ясміна Лукінак, д-р, проф., Осієкський університет, Хорватія.

Олексій Губеня (відповідальний секретар), канд. техн. наук, доц., *Національний університет харчових технологій*, *Україна*.

Наукове видання

Ukrainian Food Journal

Volume 14, Issue 3 2025

Tom 14, № 3 2025

Підп. до друку 30.09.2025 р. Формат 70х100/16. Обл.-вид. арк. 15.42. Ум. друк. арк. 15.54. Гарнітура Times New Roman. Друк офсетний. Наклад 100 прим. Вид. № 39н/24.

НУХТ. 01601 Київ-33, вул. Володимирська, 68

Свідоцтво про державну реєстрацію друкованого засобу масової інформації KB 18964—7754Р видане 26 березня 2012 року.